The Circumstellar Environments of Late Type Stars

A Thesis submitted for the Degree

of

Doctor of Philosophy of the University of London

by

Ian Paul Griffin

Department of Physics & Astronomy

University College London

University of London

1991

Abstract

In this thesis a comprehensive model for the thermal emission from dust associated with the circumstellar environments of late type stars has been developed. The model fully takes into account the effects of non-isotropic scattering, absorption and thermal re-emission, and can calculate the radiative equilibrium temperature distributions consistent with the radiation field for a multiple grain size, multiple grain component dust distribution.

The model is applied to a number of well studied late type stars, with both optically thin and optically thick dust shells whose chemistry reflects the either oxygen or carbon-rich nature of the underlying stellar photosphere. Published laboratory measurements of optical constants are used to investigate which of a variety of proposed dust condensates best fit the observations; in oxygen rich environments this is found to be amorphous olivine whilst in carbon-rich envelopes it is provided by amorphous carbon, sometimes in conjunction with silicon carbide grains.

Results from a multiple wavelength observing programme of late type stars with anomalous dust shells are presented, and are compared with published models. The radiative transfer model developed for red giants with normal dust shells is used to show that a binary model for carbon stars observed to have oxygen rich dust shells has severe problems. A new model is developed for these anomalous stars by comparing their observed dust shells with those of S stars.

Acknowledgements

This thesis would not have been possible without the help, patience, support and encouragement of many people. Above them all must be Mum and Dad, who I hope feel that at least some of the trouble was worth it. Thanks!

Aunty Rose, Mike, Jon, Helen, Uncle Brian and Aunty Doris also helped out at crucial stages in my attempts to learn some astronomy, although they probably didn't know it at the time.

Chris Skinner certainly taught me how to find Uncle Billy's bar, and what to do with a tropical itch, but I suppose I ought to thank him as well for all of the help when observing and for providing the initial idea for how I could scrounge loads of money from SERC to travel the world. However, Chris also deserves special commendation for the Gerry Anderson tape. At UCL Mike Barlow, Melvyn, Ian Howarth, 'Jets', Raman, Linda and Dave (Monk) all helped out when I was stuck, although I would have preferred the pint of beer in my hand, rather than on my head, Linda. At Jodrell, Jim Cohen lent me his office and coffee, as well as his expertise.

Two other people deserve special mention, if only for the fact that life would have been pretty boring had I not met them. John Deacon, despite liking Dr. Feelgood, was always there when drinks were in the offing, and is still amongst the most tolerant people I know. Honest. Dave White is also acknowledged for introducing me to Rush, for his hospitality in Boston, and his concise best man's speech. Oh yes, and Adrian, Robin, Terry, Ian C., 'Barry', Bill 'Bill Bill' and Ian F. Thanks also to all in Armagh. Bruce Springsteen, Bon Jovi and Steve Earle all provided excellent light relief away from the UCL bar. Thanks to Frank Drebbin too.

Finally I would like to thank Maria, for her patience, understanding and support when finishing this thesis. This thesis is dedicated to you Maria.

To Maria

Contents

List of Figures

List of Tables

Chapter 1

Introduction

1.1 Overview

It would be true to say that this thesis could never have been written, were it not for the action of stellar mass loss. The atoms which constitute both the paper upon which it is written, and indeed the biological structure of its author, were liberated from their stellar factories by that very process.

This thesis attempts to address some of the problems associated with mass loss from stars in an evolutionary phase where a large stellar radius, compared with that of the sun, and a cool stellar surface temperature (generally lower than 3500K) commonly lends itself to the description 'red giant' (or, for stars with the very largest radii, 'red supergiant'). In particular, a numerical technique is detailed which is then used to investigate the nature of the solid phase in the mass outflows from a number of chemically divergent stars. The solid phase in such outflows is usually termed 'dust', though it in fact bears little chemical affinity to the material which will doubtless cover this volume in years to come!

The theoretical basis for the modelling technique used throughout this thesis are outlined in chapter 2 and 3, whilst in chapters 4, 5 and 6 the technique is applied to derive models for specific objects with oxygen rich, carbon-rich and chemically peculiar circumstellar envelopes respectively.

The purpose of this introductory chapter is to consider the ideas discussed in the following chapters within the broader astronomical perspective. To this end, the astronomical observations of gas and dust, which provide the ultimate test to the models presented in the following chapters will be briefly discussed, as will the evolutionary status of the stars

around which the dust shells being modelled have condensed. Finally, currently favoured suggestions as to what might drive the process of mass loss from the stars around which the circumstellar dust envelopes form will be reviewed.

1.2 Astronomical Observations of Gas and Dust

Although the determination of the precise nature of dust grains has only begun to become possible with the technological advances in astronomical instrumentation which have occurred since the end of the second world war, the obscuring effect of interstellar dust and gas clouds is obvious, even without optical aid, to any observer who chooses to look in the direction of the galactic plane on a clear moonless night. The dark rifts in the otherwise bright band of the Milky Way have been known since ancient times, but the presence of these regions of low star number density was first quantitatively studied using the method of 'star gauging' by William Herschel in 1784. The technique was extended to cover much of the celestial sphere during the early years of the 19th century by John Herschel and more particularly by the Russian astronomer Wilhelm Struve, who finally used the method of 'star counting' as he called it, to derive, in 1847, a directionally dependent light absorption of between 0.1 and 3.8 magnitudes per kiloparsec which he assumed to be a consequence of light absorbing material between the stars. These measurements added quantitative evidence to the qualitative arguments of Chèseaux in 1740 and Olbers, in 1823 (Jaki, 1970) who had already used the fact that the night sky was dark as an argument for the presence of obscuring matter between the stars, which reddened any radiation traversing the interstellar medium.

It was with the advent of the new astronomical tools of photography and spectroscopy during the late 19th century, that quantitative studies of the interstellar, and indeed circumstellar media became possible. Photography, as used by such exponents as the French Henry brothers, and culminating with the publication of E. E. Barnard's 'Atlas of selected regions of the Milky Way' in 1927, which was the result of 30 years surveying the galactic plane, dramatically demonstrated the existence of obscuration on both large and small angular scales. Barnard's earlier (Barnard 1907, 1910, 1919) photographic studies provided for the first time, direct evidence for a link between luminous diffuse nebulae and the clouds of obscuring matter.

The idea of absorbing clouds of matter distributed along the galactic plane was used by a number of astronomers early in the 20th century to explain the so called 'zone of avoidance', whereby globular clusters and spiral nebulae were rarely observed in the galactic plane. Curtis (1917) assumed that the Milky Way was a spiral nebula, and reasoned by analogy that the dark matter observed in equatorial bands of other spiral nebulae during long exposure photographs was also present in our own galaxy, and was therefore responsible also for the observed zone of avoidance and for Barnard's dark clouds. This speculation was not however authoritative, since at the time, there was no definite proof that the spiral nebulae were comparable with our own galaxy.

Photographic spectroscopy provided the key evidence for the existence of interstellar matter, with the discovery of the interstellar CaII line in the spectrum of the spectroscopic binary system δ Ori by Hartmann (1904), although the importance of this observation was really only realised with the discovery by Slipher (1909) that the stationary line observed by Hartmann was not confined only to spectroscopic binary systems, nor indeed were these 'interstellar lines' observed in only one ionic species. Working with an extremely efficient spectrograph at the Lowell Observatory (that was later to play a key role in identifying the large scale expansion of the universe by measuring the radial velocities of many faint galaxies), Slipher also obtained spectra of the nebulosity associated with the Pleiades open cluster in 1912 (Seeley & Berendzden, 1972), which indicated the need for a solid phase in the nebulosity, since the spectrum obtained was identical with that of the foreground stars (a reflection nebula). Subsequent studies of such reflection nebulae at a variety of wavelengths have begun to offer an insight into the sizes of dust 'grains' in the interstellar medium, such studies are discussed in more detail in Chapter 3.

The work of Trumpler (1930) which involved studying the angular sizes of galactic open clusters, was particularly important in demonstrating the fact that for these clusters, concentrated as they are in the galactic plane, the geometric size derived from the angular size of the cluster on the sky was different to the photometric distance derived from the cluster stars, and it was therefore conclusively shown that the light intensity for radiation moving in the galactic plane fell off more sharply than an inverse square law, thereby implying the existence of an absorbing medium in that plane. Trumpler's observations implied that an interstellar absorption coefficient of $0^M.67$/Kpc for photographic magnitudes eliminated the discrepancy between distances determined by photometric and

angular diameter studies.

With the conclusive evidence for the existence of an interstellar absorptive medium presented by Trumpler, the search began to identify the precise nature of this material. The variation of extinction with wavelength was found to have a λ^{-1} dependance in the optical, with considerable curvature in the UV and near-IR, and the fact that this differed from the λ^{-4} extinction expected from Rayleigh scattering provided no small clue to the nature of the absorbing material responsible for the optical obscuration.

The first suggestion that some late type stars lost mass, and could therefore input some material into the interstellar medium also occurred at about this time, when Adams & MacCormack (1935) discovered narrow blueshifted atomic lines in the spectra of some of the more luminous cool giant stars, which indicated a mass outflow from the underlying stellar photosphere at a velocity of some 5 km s^{-1}. However it was not until the work of Deutsch (1956) who studied the giant star α Her, that it was realised that stellar material could actually reach velocities high enough to escape the gravitational attraction from a parent star. This work marked the birth of the study of circumstellar as opposed to interstellar material.

The advances in technology made during and in the years immediately following the second world war enabled the development of new astronomical instrumentation which in turn began to supply high quality observations of interstellar and circumstellar material. These new observations enabled great advances to be made in the study of this material, both by making more sensitive observations of a wider variety of objects and by extending these studies outside of the optical spectroscopic regime to which most pre-war astronomers had been confined. One of the first post war advances was the discovery of interstellar polarization, which provided an observational method to study possible grain composition, especially when studied as a function of wavelength, a field which really opened up late in the 1960's when further advances in detector technology, and the availability of launch vehicles capable of putting astronomical instrumentation above the Earth's atmosphere provided observations at mid-IR and short-UV wavelengths. These further advances in technology also revolutionized the study of circumstellar material, since although the early optical studies of circumstellar mass loss enabled the accurate determination of the outflow velocities from late type stars, in reality the observations provided very little information about the composition and structure of any associated circumstellar envelope. Also, optical

studies of red giant stars were confined to 'optically bright' stars, and, as was discovered later, as a result of IR and radio studies, excluded the majority of stars with high mass loss rates.

1.2.1 IR Studies of Dust

Dust grains of most plausible compositions can not exist at temperatures higher than around 1500K, and therefore if they are to be studied on the basis of their emissive rather than their absorptive properties, Wien's law indicates that the IR spectral region is where they should be investigated.

The first large scale IR survey, at a wavelength of 2.2μm (Neugebauer & Leighton, 1969) revealed that a large number of stars possessed IR emission in excess of that expected from their photospheric temperatures. This, it was soon realised, could be explained if the stars exhibiting such excesses were enveloped by thick dust shells, which absorbed the optical and UV radiation emitted by the stars, thermally re-radiating the absorbed energy at longer, IR wavelengths. Woolf & Ney (1969) discovered a well defined emission feature in the IR spectra of a number of cool stars at a wavelength of approximately 10μm, which was attributed by them to silicate dust grains present in the circumstellar outflows from the stars. This conclusion was supported by the chemical equilibrium calculations of Gilman (1969), which suggested that silicates should be the first solid particles to condense in oxygen rich outflows. The same calculations indicated that for carbon rich outflows, the initial condensates should be carbon and silicon carbide grains, and an 11.4μm feature was subsequently detected by Treffers & Cohen (1974) in the IR spectra of carbon stars. Silicate spectral features have been observed also in interstellar locations whereas, to date, no SiC feature has been observed in interstellar locations. The silicate features studied in the ISM have not always been observed in emission. Thus, as was implied from optical studies, the interstellar medium has, like the circumstellar envelopes of red giant stars, been shown to have a solid phase composed of dust grains. Investigations as to the relationship between interstellar and circumstellar dust grains have only recently become possible, with the availability of more sensitive IR detector arrays.

Infrared surveys at longer wavelengths than the original Two Micron sky survey of Neugebauer & Leighton, by the Air Force Geophysical Laboratory (AFGL) at 10 and 20μm, and most recently by the Infra Red Astronomy Satellite (*IRAS*) (Beichmann *et al.*,

1984) at 12, 25, 60 and 100μm, have located many sources which have mid and far-IR excesses, but have barely detectable optical counterparts. Follow up studies of some of these sources (e.g. IRC +10°216, Rowan-Robinson *et al.*, 1986, Martin & Rogers, 1987, Griffin, 1990) have shown that many of these sources are late type stars surrounded by extremely thick circumstellar envelopes, which can completely obscure the stars in the optical. One excellent example of this is the star IRC+10°216, mentioned above, which is the brightest extra-solar system object when observed at a wavelength of 5μm, and yet has a mean magnitude below 16, when observed in the Johnson U band at a mean wavelength of $\approx$0.35μm.

1.2.2 Radio and Millimetre studies.

Although the presence of molecules such as CH, CH^+ and CN had been identified within the ISM via optical studies from the late 1930's, it was not until the 1960's, and at radio wavelengths that the variety and distribution of molecules within the ISM and circumstellar clouds began to become widely realised. OH was the first molecule to be detected via radio studies, at a wavelength of 18cm and by 1968, both H_2O and NH_3 had also been observed in dense molecular clouds. By 1989, the list of molecules that have been detected in either interstellar or circumstellar locations has grown to a total of nearly 80 (Verschuur, 1989), ranging in complexity from the simple diatomic molecules such as OH and CO, to the 13 atom chain molecule, $HC_{11}N$. These molecules have proved to be extremely useful in both mapping the distribution of cool gas in the ISM, as well as in providing sensitive diagnostics to the environments in which they are observed.

The number of molecules that have been identified in interstellar and circumstellar environments has increased further with the advent of large, sensitive high frequency telescopes which operate in the atmospheric windows present in the wavelength range 350μm to 3mm. These 'millimetre wave' telescopes, the most recent examples of which are the 15 metre diameter dishes of the Swedish ESO Submillimetre Telescope (SEST) located at La Silla, Chile, and the James Clark Maxwell Telescope (JCMT), located at the summit of Mauna Kea in Hawaii, utilise the atmospheric windows to observe and map the distribution of molecules such as CO in locations such as circumstellar shells, and provide extremely accurate determinations of their outflow velocities. As well as detecting spectral lines from molecular emission, both radio and millimetre receivers have

been used to detect continuum emission and hence provide important measurements of dust emissivity at the longest wavelengths (e.g. Sahai *et al.*, 1989).

In 1965, the first OH masers (Microwave Amplification by Stimulated Emission of Radiation) were detected by several groups (Weaver *et al.*, 1965, Gundermann, 1965) towards a number of HII regions. The emission was unusual in that the observed relative strengths of the hyperfine components of the 18cm OH emission line were incompatible with thermodynamic equilibrium, and often the lines were observed to be highly polarized. OH Maser emission was observed towards many of the sources detected in the two micron sky survey, by Wilson & Barret (1968), and subsequent studies (e.g. Wilson, Barrett & Moran, 1970) showed that these sources exhibited a characteristic double peaked profile, with two complexes of emission lines separated by between 10 and 50 km s^{-1} in velocity. This profile has been shown to be a natural consequence of emission from a spherically symmetric expanding shell of gas in the mass outflow from a late type star (e.g. Elitzur, Goldreich & Scoville, 1976).

The detection of H_2O and SiO maser emission from circumstellar envelopes, both of which also exhibit the double peaked spectroscopic profile has provided an extremely valuable tool in the analysis of the circumstellar envelopes of red giant stars, since stellar sources often display emission from SiO, H_2O and OH simultaneously. As the 3 masing species originate in different regions of the envelope with SiO being nearest to the star, and OH furthest, (Reid & Moran, 1981) studies of the distribution of the masing regions for each of the molecular species can contribute enormously to the understanding of the envelope dynamics and conditions (such as magnetic field strength) as a function of distance from the central star. Presently, only a few stars (e.g. VX Sgr, Chapman & Cohen, 1986) have had their envelopes studied in this way, since both high angular resolution, provided using interferometric techniques, and high spectral sensitivity are required to perform a full study for an individual circumstellar envelope, and this requires a large amount of telescope time to be done comprehensively. However, the technique does provide an immense amount of physically useful information about the region under study, and it is to be hoped that the database of stars that have been probed using it will increase in years to come.

1.2.3 Ultraviolet Studies.

Owing to the complete opacity of the Earth's atmosphere at wavelengths shortwards of approximately 3000Å, the science of UV astronomy had to await the advent of rocket and satellite bourne instrumentation. Thus it was not until the 1960's that detailed photometric and spectroscopic studies became available for many stars in the UV region of the spectrum. The region of the spectrum from 912Å—3000Å is particularly rich in the resonance lines of abundant elements, and thus if the distribution of these elements, either in the ISM, or in circumstellar shells is to be fully understood, it is important to obtain observations at these wavelengths. It is also important to obtain extinction measurements at UV wavelengths, since these may be used to derive information about the size distribution of the smallest particles present in interstellar and circumstellar environments.

Particularly important results, either in obtaining photometric or spectroscopic measurements have been obtained from a series of satellites, beginning with the Orbiting Astronomical Observatory-2 satellite in the late 1960's, progressing through the Astronomy Netherlands Satellite (ANS) and Copernicus (OAO-4) during the 1970's and continuing to date with the International Ultraviolet Explorer (IUE) satellite, launched in 1978, and the Hubble Space Telescope, launched in May 1990. UV studies performed by Copernicus and IUE have enabled the survey of many interstellar sight-lines using a method directly analogous to that used in the earliest optical studies by Hartmann and Slipher, (e.g. see Howarth & Phillips, 1986) and the measured depletions along these sight-lines play an important part in constraining the composition of interstellar dust. Both interstellar and circumstellar extinction curves have also been measured in the UV spectroscopic regime, and an unexpected extinction feature has been identified at a wavelength of 2175Å (Stecher, 1965) which has played an important role in constraining the nature of the solid phase in interstellar, and some circumstellar locations. The part played by UV spectroscopy in determining the nature of dust grains is more fully reviewed in chapter three.

1.3 The Evolutionary status of AGB Stars

Having briefly reviewed some of the more important historical episodes in the discovery of the nature of circumstellar material, it is perhaps now worthwhile investigating current ideas as to the evolutionary status of the parent stars from which that material is being

Figure 1.1: The Location of AGB Stars within the HR diagram, (from Iben, 1985)

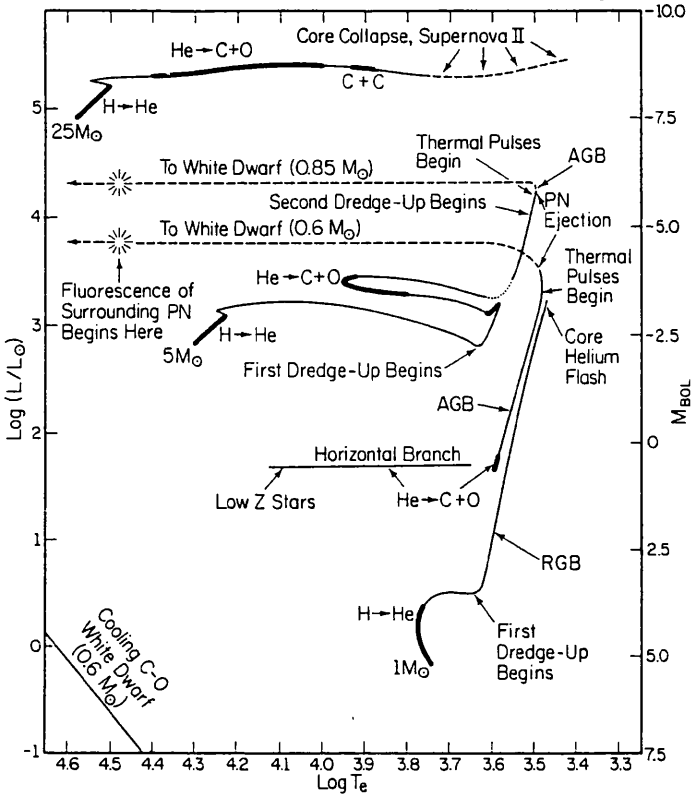

driven, before going on to discuss the theories which attempt to address the question of how these stars lose mass in the first place.

Without exception, all of the objects studied in this thesis are Asymptotic Giant Branch (AGB) stars, so called because of their location in the Hertzsprung-Russell diagram, a locus which is parallel to that occupied by stars undergoing their first ascent of the red giant branch (see Figure 1.1 for details).

Current theoretical models suggest that AGB stars have recently ceased core-helium burning (e.g. Iben & Renzini, 1983; Lattanzio, 1989). The state of hydrostatic equilibrium around the degenerate carbon-oxygen core of these stars is maintained by the combined pressure from a helium burning shell enshrouding the core, and, outside of that From a hydrogen burning shell. The structure of such a star is presented diagrammatically as Figure 1.2.

Current stellar evolution codes, such as those described above, predict that stars less massive than 8–10 solar masses will pass through the AGB region of the HR diagram, after they have exhausted initially the hydrogen and subsequently the helium in their core regions.

Figure 1.2: Core structure for an AGB star (Harwitt, 1973)

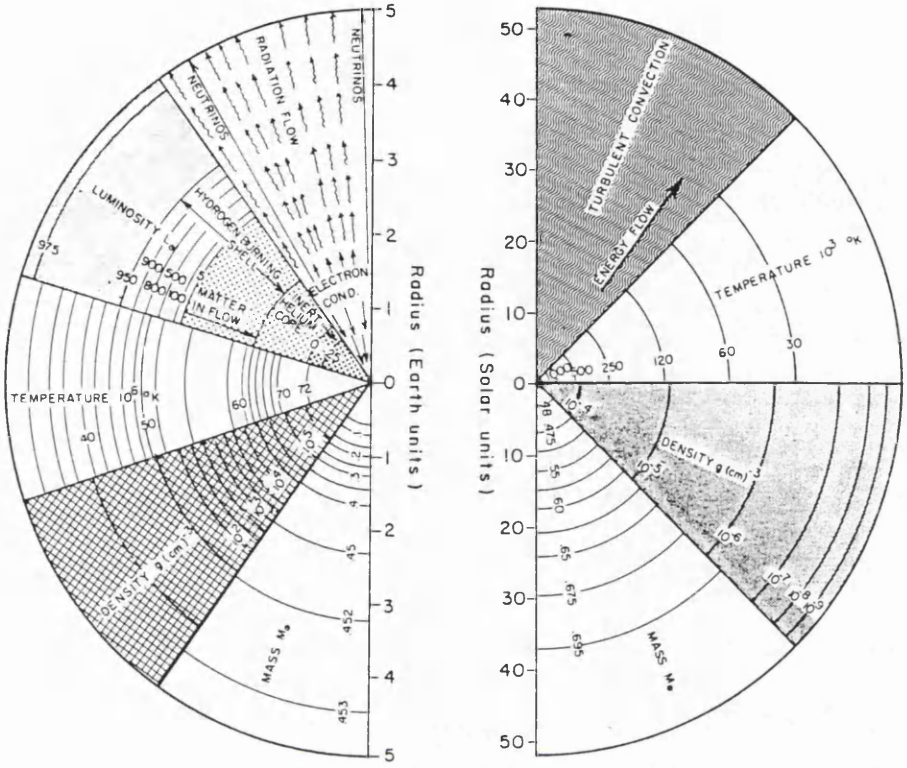

It is estimated (Iben, 1985) that shell hydrogen burning, at the base of an extended H-rich stellar envelope, provides the chief energy source for approximately 90% of the time that a star is on the AGB. However, when the mass of the helium shell, laid down during this H-shell burning phase exceeds a critical value (which is dependent upon the mass of the underlying degenerate C-O core), then He burning reactions ignite explosively in this shell, during a so called helium flash, or thermal pulse.

The reactions occurring during a He shell flash, release nuclear energy more rapidly than it can be carried away from the site of energy production by radiative transfer alone. A convective flow is initiated, which leads to an expansion in the whole stellar envelope. This in turn causes the ongoing H shell burning reactions in the envelope to be quenched, with the condition of hydrostatic equilibrium for the star then being maintained by quiescent shell He burning, until all of the He within the shell has been exhausted.

With the termination of He shell burning, and the resultant contraction of the inner envelope, the temperature climbs high enough to initiate shell H burning in a region outside of the now enlarged C-O core and helium envelope, and the whole thermal pulse cycle repeats once more.

Whilst a star is undergoing a Helium flash, as much as 20% of the helium in the shell is converted to ^{12}C and ^{16}O, whilst for stars with relatively small core masses (i.e. $M_{core} \leq 0.7M_{\odot}$) some ^{13}C may be released into the convective envelope above the shell. The ratio of ^{12}C to ^{16}O being produced during this phase is still rather uncertain, since it is dependent upon the still uncertain cross section for the reaction (Iben, 1985):

$$^{12}C + \alpha \longrightarrow ^{16} O + \gamma \tag{1.1}$$

It can be said with certainty though, that as the amount of ^{12}C produced is always greater than the amount of ^{16}O, the main effect of a Helium shell flash is a progressive enrichment of the ^{12}C content of the envelope (Lambert, 1989), which is 'dredged up' into each of the progressively higher, but overlapping, convection zones, finally reaching the stellar surface.

For stars with an appreciable heavy element abundance, the high temperatures generated in the He burning shell initiated endogenic neutron capture reactions, which can build up isotopes as heavy as ^{209}Bi. In fact, most nucleides with $24 \leq A \leq 50$ are believed to have been built up by slow neutron captures (Tayler, 1975), or the s-process, so called because the average time between captures is many years. It is thought that the neutron flux, which is necessary for the reactions to occur at all is probably derived from the exogenic reactions (e.g. Harwit, 1973, Iben & Renzini, 1983):

$$^{22}Ne + ^{4} He \longrightarrow ^{24} Mg + n \tag{1.2}$$

and

$$^{13}C + ^{4} He \longrightarrow ^{16} O + n \tag{1.3}$$

with the ^{21}Ne and ^{13}C being present in sufficient abundance to seed the neutron flux.

The s-process manufactures appreciable quantities of elements including Sr, Y, Zr, Ba, Nd and Tc, all of which have been detected in the stellar spectra of some AGB stars. These, and other elements are most probably created as the result of a series of He Shell flashes. These flashes initiate a convective behaviour during which the He-rich shell above the helium burning layer mixes with material from the carbon-rich stellar core, and eventually even with material from the hydrogen rich stellar envelope which may be convected into the core regions (Schwarzchild, 1970). In this scenario, ^{12}C and ^{1}H yield quantities of ^{13}C,

which may then produce the neutrons which power the s-process, by reacting with ^{4}He in the shell. It is interesting to note that the observed s-process elements on Earth have an abundance distribution which requires an exponential distribution of neutron exposures, which the AGB thermal pulse cycle is thought to produce.

The violent events occurring in the core of an AGB star are reflected in changes which are observed to occur in the surface chemical composition of the star. Material is dredged up to the stellar surface from the top of the shell burning regions near the stellar core, by the large scale convective motions which exist throughout the envelope.

The dominant role of the CO molecule in the dissociation equilibrium of carbon and oxygen, enables spectra of AGB stars with abundance ratios C/O<1 (oxygen-rich) to be distinguished from those with C/O>1 (carbon-rich) even at the lowest spectroscopic resolutions.

The spectra of O-rich stars (which, if on the AGB are predominantly of spectral class M) are dominated in the optical region by metal oxide bands (e.g. TiO, ZrO, YO) whilst in the near-IR (1–5μm) region, in addition to CO bands, absorption by H_2O molecular lines dominates the observed spectra. Optical spectra of the M8 star TY Dra are presented as Figure 1.3.

For C-rich stars, the observed spectra are completely different to those exhibited by the O-rich stars. The spectra are dominated by molecular bands of C_2 and CN in the optical, whilst in the IR, C_2H_2 and HCN bands are present, in addition to the omnipresent CO lines. The C-rich stellar envelopes are classified as C stars, on the AGB. A low resolution optical spectrum of the (C7,2) star WZ Cas is presented as Figure 1.4, for comparison with the O-rich spectra of TY Dra, shown in Figure 1.3.

Between the spectral types M and C lies a sequence of spectral classifications; MS, S and SC, which are broadly referred to as the 'S' stars. The C/O ratio changes through these classes from C/O$\leq$0.95 in MS stars, through 0.95$\leq$C/O$\leq$0.99 for S stars, to C=O (to better than one part in 100) for stars having the SC classification (Ake, 1979; Keenan & Boeshaar, 1980). In these S spectral classes, bands of s-process oxides, in particular ZrO and YO become particularly important in determining the nature of the emergent spectra.

The sequence M-MS-S-SC-C is thought to be one of increasing carbon-to-oxygen ratio, as well as s-process element abundance due to internal processing during evolution on the

Figure 1.3: Optical spectrum of TY Dra (M8)

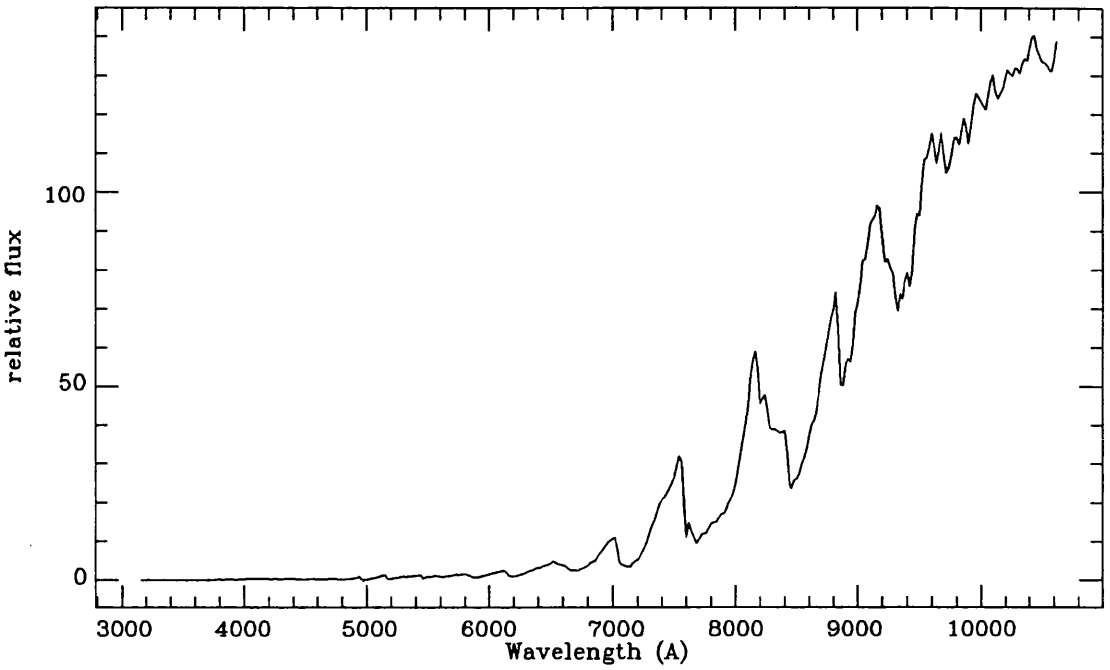

Figure 1.4: Optical spectrum of WZ Cas (C7,2)

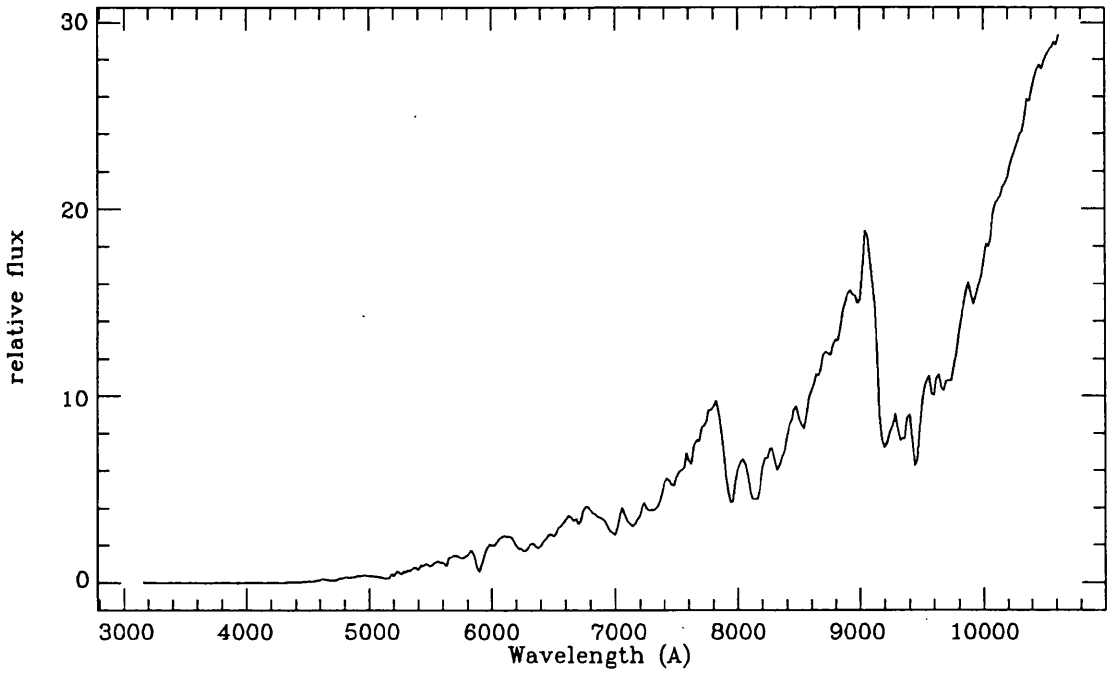

AGB. These conclusions have been drawn on the basis of spectral classification of stars in the Milky Way galaxy (Ake, 1979; Keenan & Boeshaar, 1980) as well as on the basis of observational studies of AGB stars in the Magellanic clouds (see review by Lambert, 1989).

However, the precise relationships between the various spectroscopic classes are still far from clear, and much work remains to be done before a confirmation that the spectroscopic sequence represents an evolutionary description of a star's time on the AGB. Recently, further evidence for evolutionary connections between M and C stars has come from detailed models for the circumstellar environments which attempt to match IR and mm photometric observations of the stellar dust shells (e.g. Chan & Kwok, 1988). These methods will be further discussed in chapter 6, where models are developed for some C stars which appear to exhibit 'fossil' dust shells that could have arisen during an earlier O-rich phase of mass loss.

1.4 Mass loss mechanisms & their role in AGB evolution

The AGB stars studied in this thesis posses circumstellar shells of dust because of the process of mass loss, which is responsible for driving material from the stellar photosphere in a cool outflow, or stellar wind as it is often called. The fact that many (optically classified) AGB stars exhibit circumstellar dust emission, is indicative that mass loss is commonplace amongst these stars.

The ultimate fate of a star is dependent upon competition between two physical processes; core nuclear reactions, and mass loss from the stellar envelope. If nuclear reactions manage to accumulate sufficient mass in the core to exceed the Chandrasekhar limit, then the star will explode in a supernova, which leaves either a neutron star or a black hole as the stellar remnant. If however, mass loss from the stellar surface succeeds in removing the entire envelope, then the result is the formation of a planetary nebula (PN), leaving as a remnant a white dwarf. Given that for more than 95% of all stars the effective temperatures on the main sequence are not high enough to cause radiation-driven mass loss, it can be seen that for most of a stellar lifetime, nuclear burning dominates the evolutionary process.

However, for a relatively short period, of perhaps 10^6 years or so, whilst the star is on

the AGB, its character is radically changed by the process of mass loss. Theoretically the rate at which an AGB star loses mass increases with its luminosity (Iben, 1985). In turn, the stellar luminosity increases with the mass of the degenerate C-O core, and therefore, as the star evolves along the AGB, the mass loss rate climbs to such an extent that at the end of the AGB phase, almost all of the matter in the H-rich envelope outside of the core has been stripped from the star. The remnant begins to contract, whilst remaining at the same luminosity, as the expelled envelope moves away at constant velocity. When the surface temperature of the remnant reaches approximately 30,000K, the intense UV radiation ionizes the expanding shell, and a PN is born. Eventually, the envelope disperses, and the white dwarf stellar remnant begins to cool slowly. Were it not for the process of mass loss on the AGB, every (single) star in the mass range 1.4–10$M_{\odot}$ would become a supernova; as it is, it is thought that all single stars of initial mass less than 10$M_{\odot}$ will become white dwarfs.

A comparison of observations with theoretical evolutionary calculations suggests that significant mass loss only develops after the formation of the degenerate C-O core, at the beginning of hydrogen shell burning, which initiates the AGB evolutionary phase. The end of AGB evolution has been defined (e.g. Kwok, 1987) as the point when the stellar envelope of the star begins to undergo rapid changes as a result of the depletion of the envelope mass due to mass loss. The actual value of the critical envelope mass at which this occurs, is dependent upon the core mass of the star. For a core mass of 0.6$M_{\odot}$, Schönberner (1983) estimates that the mass of the circumstellar envelope will be $\approx 10^{-3} M_{\odot}$, with the stellar effective temperature having climbed to around 5000K. At this point, AGB mass loss is expected to stop, and for a period, whilst the envelope remains un-ionised, the object is classed as a proto-planetary nebula.

Although the occurrence of copious mass loss from AGB stars is well established from observations, the actual mechanism of mass ejection is not yet fully understood. This is because the near stellar environments, from which the matter is being expelled, are complicated, and can rarely be resolved for direct study using ground based observations. The theoretical mechanisms which drive mass loss in stellar winds have been extensively reviewed, most recently by Holzer & MacGregor (1985) and Goldberg (1984), whilst Morris (1987) has reviewed the observational evidence for mechanisms which might drive stellar winds.

Although many mechanisms have been suggested, most explanations which have been presented to explain the phenomenon of mass loss may be divided into one of four groups; these involve AGB stellar winds being thermally driven, wave driven, radiation driven or shock driven.

A thermally driven stellar wind is one in which the driving force is a thermal pressure gradient. This type of wind was first described by Parker (1958), and has been subsequently discussed by a number of authors (most recently by Wantanabe, 1981). However, Holzer & MacGregor (1985) have shown that a thermal mechanism is a very inefficient way for driving a stellar outflow from cool, low gravity stars such as those on the AGB, and that a thermal mechanism alone cannot drive mass loss from these stars.

A second group of mechanisms may be broadly termed 'wave driven' since they utilise transport of a mechanical energy flux through the stellar atmosphere, usually by small amplitude waves. If the waves occur in a star with a magnetic field (and all stars on the AGB are thought to posses at least a nominal magnetic field), they may be either compressive (e.g. acoustic waves) or non-compressive (e.g. Alfvèn waves, which exert a force on a stellar atmosphere because the variation of the wave's magnetic energy density in the atmosphere creates a pressure gradient which then drives the matter away from the star).

Unfortunately, although acoustic waves driven models have proved good at extending a stellar atmosphere near its base, they have been shown to steepen quite rapidly into weak shock fronts which are dissipated within a few pressure scale heights of their initiation point, and are therefore not able to lift large quantities of stellar material out of a star's gravitational field (Hartmann & MacGregor, 1980).

Alfvèn waves, (or indeed any non compressive waves) are much less readily damped in a stellar atmosphere than the compressive waves, and may therefore extend through a stellar atmosphere over a much larger radial distance. Thus if conditions in the atmosphere are such that the non-compressional waves do occur, then it has been shown (Belcher & Olbert, 1975) that sufficient energy is available to lift photospheric material into an escape trajectory from the stellar gravitational field. The key question in determining whether Alfvèn waves are responsible for driving a stellar wind, is whether sufficient magnetic energy density is present in the atmospheres of the AGB stars to create conditions which can drive a stellar wind. It is thought that Alfvèn wave energy flux densities of some $10^5 B_0$

erg cm^{-2} s^{-1}, with B_0 being at least 10 gauss (Holzer & MacGregor, 1985) are required for this to be an effective mass loss mechanism. There are very few available measurements of the magnetic fields strengths for AGB stars, and until such measurements do become available, the role that Alfvèn wave driven winds play in mass loss will remain uncertain.

The third mechanism that has been suggested as a way of creating outflow from AGB stars is to have the outflow driven by shock waves. Many stars whose atmospheres are sufficiently dusty to have a strong coupling between the stellar radiation field and the atmosphere itself, also exhibit some degree of pulsational activity, as may be seen by inspection of the light curve of any AGB star. It has been argued (e.g. Jura, 1984) that regular pulsations could produce large-amplitude shock waves which then propagate outwards through a stellar atmosphere, eventually allowing material to escape from the stellar gravitational field simply because of the heat and momentum donated to the atmosphere by the passage of such a shock.

Pulsation driven shocks have proved, in theoretical studies, to be particularly efficient in driving mass loss from stars that exhibit regular pulsations, such as mira type variables (Wood, 1979). However, many stars on the AGB do not show regular pulsations, and there is also the fact that large amplitude shock waves are inherently non-steady (Holzer & MacGregor, 1985) which therefore necessitates modelling a stellar wind by viewing the average effect of quasi-periodic shocks as a steady process, if a steady state mass outflow from a star is to be obtained. Other uncertainties involved in modelling a pulsation driven shock stem from not knowing whether adiabatic or isothermal shocks would arise from the original pulsations.

The true description of a shock driven stellar wind probably lies somewhere between adiabatic and isothermal cases, and would require a detailed treatment of the energy balance in the moving atmosphere (Willson, 1981), which is a difficult task, that has only recently (e.g. Bowen, 1989) become feasible. However, it is clear from various theoretical treatments, that whilst the case for the involvement of stellar pulsations in the mass loss process is actually quite strong, pulsations alone can not account for the observed stellar outflows, since the mass loss rates generated by the best models (e.g. Willson & Bowen, 1986) are still much lower than those derived observationally. Skinner & Whitmore (1988a,b) have more recently suggested that radial pulsations may not be the primary mechanism in driving the mass outflow from M supergiant stars, on the basis of no corre-

lation between the derived mass loss rates for a sample of stars, and either the period or the amplitude of their optical variabilities.

Another method of driving mass away from the star is to utilise the power of the star's own radiation field to drive away matter from its envelope; schemes which attempt to do this may be grouped under the heading of 'radiatively driven' outflows. Any radiatively driven wind needs a mechanism to couple the radiation field to the stellar material. For the hot O and B stars, with high UV fluxes, and atmospheres rich in UV resonance lines, the good spectral match between the stellar radiation field and the atmospheric line opacity provide the coupling mechanism which drives the mass loss. This mechanism can not, of course apply for the cool stars on the AGB.

For such cool stars, two alternative coupling mechanisms have been suggested. A molecular coupling analogue to the hot star mechanism has been suggested by Fix & Alexander (1974) where the cool star radiation field, peaking in the near-IR couples with the molecular line opacity in the same spectroscopic region to provide the driving force, although no quantitative evidence was supplied as to how molecules could provide a sufficiently link between stellar radiation field and material in the envelope.

Another coupling mechanism for cool stars, which has gained favour recently is that radiation pressure on dust grains could prove sufficient to drive the stellar wind. As mentioned above, the envelopes of AGB stars are known to exhibit emission from solid circumstellar dust grains. A number of authors (e.g. Gehrz & Woolf, 1971, Kwok, 1975, Jura, 1984) have provided scenarios, all of which envisage grains nucleating and growing in the outer photospheric layers of the star. The grains experience an outward force from the stellar radiation field, and the friction between grains and envelope, drags the envelope along with the grains, as the radiation pressure drives them away from the star.

In order to match the (observationally derived) high mass loss rates for some AGB stars, it is necessary for the dust to condense relatively near to the photospheric surface, in order that sufficient dust 'surface area' is available to drag along the surrounding gas. Unfortunately, in the most detailed static models presented to date (e.g. Willson & Bowen, 1986) the dust condensation point occurs at a large radial distance from the stellar surface, where densities have fallen too low to allow dust to be very efficient at dragging along the surrounding gas. Thus, once again, although there is good observational evidence that dust does play a major role in the mass loss process, it cannot alone account for the mass

loss observed from cool stars.

The fact that no single mechanism has as yet been identified which can explain all of the observed aspects of mass loss from AGB stars has lead to some attempts to create models for mass loss which utilise more than one of the four methods discussed above to drive stellar outflows. For example Morris (1987) qualitatively proposed a '2 step' process, whereby pulsational shocks drive material from the stellar photosphere, to a point where dust condenses, and then radiation pressure from the central star drives the dust grains, and the coupled circumstellar gas, away from the star in a cool, low velocity wind.

Alternatively, Skinner & Whitmore (1988) propose that Alfvèn waves, generated in a turbulent photosphere may provide the necessary boost for material which allows sufficient quantities to escape, later for dusty blobs to condense, and hence a large scale mass outflow to begin. Other mechanisms have also been proposed, but, as yet, no real consensus has been reached, and most of the ideas that have been presented have been in qualitative rather than in quantitative form.

It is hoped that the models presented in chapters 4, 5 and 6 may go some way towards helping in the understanding of the chemical nature, and the quantities of dust which form around AGB stars, and that future work, incorporating these results will enable a much clearer idea to be obtained about the nature of the processes which drive stellar mass loss.

Chapter 2

Radiative transfer in circumstellar envelopes

2.1 Introduction

In this chapter, previously published techniques used to solve the equation of radiative transfer in spherically symmetric circumstellar envelopes containing dust grains are reviewed and the method adopted for use in this thesis, namely the generalised two stream Eddington approximation, is briefly described. The adopted technique allows the calculation of emergent spectra and apparent surface brightness profiles for spherically symmetric envelopes containing multiple sized dust grains composed of multiple chemical components.

2.2 The effect of dust upon radiation transfer in circumstellar environments

The presence of dust grains in a circumstellar envelope affects the transfer of radiation through that envelope in several distinct ways. Grains diminish the intensity of radiation incident upon them, both by direct absorption within the grain particle, and by scattering radiation out of the line of sight to an observer. Grains also cause a retardation in the phase of any radiation that interacts with them.

The extinction and phase retardation caused by dust grains can be attributed to a complex refractive index, $\tilde{m}$, which may be written:

$$\tilde{m} = n + ik \tag{2.1}$$

where n and k (the 'dust optical constants') are the grain refractive and absorptive indices respectively. Some workers prefer to work with the grain dielectric function, or permittivity of the material ϵ, which is given by:

$$\epsilon = \epsilon_1 + i\epsilon_2 \tag{2.2}$$

where

$$\epsilon_1 = n^2 - k^2 \tag{2.3}$$

and

$$\epsilon_2 = 2nk \tag{2.4}$$

Values for n and k, or ϵ_1 and ϵ_2, for proposed grain materials may be derived either via laboratory reflectivity measurements (e.g. Krätschmer & Huffmann, 1979) or from astronomical observations (e.g. Volk & Kwok, 1988). Various proposed grain compositions, and their derived optical constants will be discussed in chapter 3 for the different chemical environments found in the outer regions of atmospheres of red giant stars.

Once a set of optical constants has been found, by whatever means, for a grain material, they may be used to calculate the scattering and absorption cross sections (measures of the amount of radiation removed from an incident beam by the dust grain) for particles of any size composed of that material, using Mie theory. This is a classical theory which solves Maxwells' equations at the boundary of a particle, regarding the particle as a continuous medium. Usable formulae have been calculated that give the absorption and scattering cross sections ($C_{abs}(a,\nu)$ and $C_{sca}(a,\nu)$ respectively) for a variety of astronomically interesting grain shapes, including spheres, infinite cylinders and concentric spherical particles composed of different materials (Van de Hulst, 1957; Wickramasinghe, 1973).

Knowledge of $C_{abs}(a,\nu)$ and $C_{sca}(a,\nu)$ is crucial to the radiative transfer calculations involved in modelling circumstellar dust envelopes. These parameters are both functions of grain radius, a, and frequency, ν, and have units of area. They may be related to the

more often quoted efficiency factors for absorption and scattering, $Q_{abs}(a,\nu)$ and $Q_{sca}(a,\nu)$ by dividing them by the grain geometrical cross section. Thus, for spherical grains:

$$Q_{abs}(a,\nu) = \frac{C_{abs}(a,\nu)}{\pi a^2} \tag{2.5}$$

and

$$Q_{sca}(a,\nu) = \frac{C_{sca}(a,\nu)}{\pi a^2} \tag{2.6}$$

In principle, were circumstellar dust shells composed of grains whose sizes and compositions were identical, knowledge of Q_{abs} and Q_{sca} would lead directly and straightforwardly to a measurement of the total dust opacity, provided the number density of grains as a function of distance from the central star was also known. In this idealised case, and indeed generally, the total extinction caused by dust grains, $\kappa_{ext}(\nu,r)$, is given by the sum of opacities due to absorption and scattering:

$$\kappa_{ext}(\nu,r) = \kappa_{abs}(\nu,r) + \kappa_{sca}(\nu,r) \tag{2.7}$$

where

$$\kappa_{abs} = n_d(r) Q_{abs}(a,\nu)\pi a^2 \tag{2.8}$$

with n_d being the number density of grains at radial distance r from the central star.

However, as will be discussed more extensively in the following chapter, there is now strong observational (e.g. Mathis, Rumpl & Nordsieck, MRN, 1977) and theoretical (e.g. Biermann & Harwitt, 1980) evidence that dust grains in the circumstellar envelopes of red giant stars do not all have identical sizes; rather there appears to be a distribution of grain sizes. In some cases, grains of different chemical compositions may be present simultaneously in the same dust shell, and thus in the most general case, the total dust extinction opacity must be calculated in a circumstellar envelope where multiple grain sizes and components are present.

Assuming that the grain size distribution may be represented by a power law with index p, such that the number density of grains with radius a, per grain radius interval is given by, for an i component dust model, then

$$n^i(a,r) = n_g^i(r)a^{-p} \qquad a_1 \leq a \leq a_2 \tag{2.9}$$

with a_1 and a_2 being the lower and upper limits to grain radii for the size distribution being used.

Hoare & Clegg (1988) have derived the following expression for the constant n_g^i, which determines the absolute number density of dust grains at radial distance r:

$$n_g^i(r) = \frac{3m_H}{4\pi} \frac{4-p}{a_2^{(4-p)} - a_1^{(4-p)}} \frac{(m_d/m_H)n_H(r)}{\rho_d} \tag{2.10}$$

where m_d/m_H is the dust to hydrogen ratio by Mass (which is equal to 1.4 times the more commonly used dust to gas ratio, for a helium abundance of 0.1 by number relative to hydrogen), m_H is the mass of the hydrogen nucleus, and ρ_d is the density of the grain material. $n_H(r)$ is the number density of hydrogen nuclei, which may be derived from a knowledge of the expansion velocity of the stellar wind. It is given by:

$$n_H(r) = \frac{\dot{M}}{4\pi r^2 v(r) \mu m_H} \tag{2.11}$$

with $\dot{M}$ being the stellar mass loss rate, μ is the mean molecular mass of the gas in the outflow, and $v(r)$ the outflow velocity of the stellar wind at radial distance r from the star. In practice the velocity of grains in the stellar wind $v(r)$, is not known accurately as a function of radial distance for many stars, and the wind terminal velocity, v_∞ is often substituted for $v(r)$. Adoption of v_∞ as the dust outflow velocity throughout the dust shell has the advantage that its value may be fairly easily derived via observations of molecular emission lines from the stellar envelope, but its substitution into the expression used to calculate $n_H(r)$ could lead to inaccuracies in the calculated number densities, especially in the inner regions of a circumstellar envelope, where the dust grains, once they have condensed from the stellar wind, may still be being accelerated. In the few cases where the velocity fields in a stellar outflow have been studied, as a function of distance from the central star, the observations are contradictory as to the radial distance at which gas and dust in the outflow reaches terminal velocity. A detailed study of the velocities of masers in the envelope of the O-rich supergiant star VX Sgr (Chapman & Cohen, 1986) suggested that material in the envelope did not reach terminal velocity until it had reached a radial distance of several hundred stellar radii, whilst an analysis of the envelope dynamics of

the C-rich envelope associated with the C star IRC+10°216 using observations of the CO first overtone bands at 2μm (Keady, Hall & Ridgeway, 1988) found that terminal velocity was achieved by material at distances as small as ten stellar radii.

Given that dust grains are predicted to condense from stellar winds at temperatures in the range 1000–2000K, depending upon grain composition, and that these temperatures are found at radial distances of 2–5 stellar radii, depending upon the adopted model (Chan & Kwok, 1988; Rowan-Robinson *et al.*, 1986), it is important to be aware that adoption of v_∞ as the velocity throughout the stellar envelope could introduce errors into the predicted grain number densities, at least in the warmer, inner regions of the circumstellar environments under study.

With the adoption of v_∞ at the velocity at all points in the envelope, combining equations 2.10 and 2.11, and integrating 2.9 over the grain size distribution, an expression is obtained for the number density of grains at any radial distance from the star with mass loss rate $\dot{m}$, for dust component i:

$$n^i(r) = \frac{3(m_d/m_g)^i}{(4\pi)^2\rho_d^i} \frac{4-p}{a_2^{(4-p)} - a_1^{(4-p)}} \frac{\dot{m}}{r^2 v_\infty} \frac{a_2^{(1-p)} - a_1^{(1-p)}}{1-p} \tag{2.12}$$

The expression for the total absorption opacity for i dust components may then be written:

$$\kappa_{abs}(\nu, r) = \sum_i \int_{a_1}^{a_2} \pi a^2 Q_{abs}^i(a,\nu) n^i(a,r) da \tag{2.13}$$

and an analogous result may be derived for the total scattering opacity, $\kappa_{sca}(\nu,r)$ by substituting $Q_{sca}^i(a,\nu)$ for $Q_{abs}^i(a,\nu)$ into the expression.

2.3 The equation of radiative transfer

As described in the previous section, dust grains in circumstellar envelopes absorb and scatter incident radiation. Radiation absorbed by the grains increases their thermal energy, and may be re-emitted, and the effect of this thermal radiation upon other grains in the shell must be accounted for, if a realistic model for radiation transfer through the dust shell is to be developed. The ultimate goal of radiative transfer model calculations is to calculate accurately the circumstellar grain temperatures, and solve the equation of radiative transfer in order to predict the emergent flux from a circumstellar envelope.

These processes have to be done simultaneously, because it is the IR radiation from hot dust nearer the star which heats the cooler grains at larger radial distances.

The one dimensional time independent equation of radiative transfer, for a spherical dust shell may be written:

$$\mu \frac{\partial I_\nu(r,\mu)}{\partial r} + \frac{1-\mu^2}{r}\frac{\partial I_\nu(r,\mu)}{\partial \mu} = -\kappa_{ext}(\nu,r)I_\nu(r,\mu) + j(\nu,r) \tag{2.14}$$

$j(\nu,r)$ is the volume emissivity per unit solid angle. It is given by:

$$\begin{aligned} j(\nu,r) &= \sum_i \int_{a_1}^{a_2} \pi a^2 Q^i_{abs}(\nu,a) B_\nu(T^i_d(a,r)) n^i(a,r) da \\ &\quad + \sum_i \int_{a_1}^{a_2} \pi a^2 Q^i_{sca}(\nu,a) n^i(a,r) \frac{1}{2} \int_{-1}^{+1} R^i_\nu(a,\mu,\mu') I_\nu(r,\mu') d\mu' da \end{aligned} \tag{2.15}$$

Where the first summation term arises due to thermal emission from the grains, whilst the second is due to scattered light within the dust shell. $R^i_\nu(a,\mu,\mu')$ is a scattering redistribution function, which denotes the probability that a photon incident upon a grain from direction μ' will be scattered into direction μ. It is normalised in such a way that:

$$\frac{1}{2}\int_{-1}^{+1} R^i_\nu(a,cos\theta) dcos\theta = 1 \tag{2.16}$$

with θ being the angle through which the photon scattering occurred.

Unfortunately, the value of the scattering redistribution function (or the phase function) is difficult to determine from astronomical observations. Rather, workers have often attempted to measure the asymmetry parameter, or mean cosine of the scattering angle, $g(a,\nu)$, for dust in a variety of sources. It is defined by:

$$g^i(a,\nu) = \frac{1}{2}\int_{-1}^{+1} cos\theta R^i_\nu(a,cos\theta) dcos\theta \tag{2.17}$$

The quantity $g(a,\nu)$ is a measure of the amount of forward scattering, whose value varies from zero if scattering is purely isotropic in nature, to unity for the case where a phase function is such that scattering is purely in the forward direction. Values for g have been estimated from studies of dust grains in reflection nebulae in the UV and optical regions of the spectrum. For the nebulosity NGC 7023, Witt *et al.* (1984) varied in value from 0.63 at 5515Å to 0.25 at the UV wavelength of 1400Å. In the optical region, studies of other reflection nebulae, such as that associated with the star Merope in the Pleiades

(Martin, 1978 and references therein) again suggested a forward throwing phase function, with measured values all suggesting that $g \geq 0.5$. However, as pointed out by Martin (1978), the use of reflection nebulae does not provide reliable values for g, since there are uncertainties in the geometries in the systems being studied.

Better constraints have been placed upon g via studies of the surface brightness profiles of dark nebulae, such as the 'thumbprint nebula' in Chamaeleon (Fitzgerald *et al.*, 1976), where a value of ≈ 0.7 was derived for g at the wavelength of the Johnson B filter. However, such studies are few and far between, and the value of g is just not known very well for many astronomical environments.

A relationship between the phase function and asymmetry parameter may be derived, by expanding the phase function in a Legendre polynomial series (Chandrasekhar, 1960):

$$R^i_\nu(a,\mu,mu') \approx \sum_{l=0}^{L} \tilde{a}^i_l(a,\nu) P_l(\mu) P_l(\mu') \tag{2.18}$$

with $\tilde{a}^i_\nu(a,\nu)$ being coefficients in the series expansion. The observations currently available do not merit consideration of more than the first two terms in the expansion (i.e. L=1). From the normalisation condition given in the equation for $R^i_\nu(a,\mu,\mu')$, the first coefficient in the series expansion, $\tilde{a}_0$ is zero, whilst the second is related to the asymmetry parameter by $\tilde{a}_1 = 3g$ (Leung, 1975).

Thus

$$R^i_\nu(a,\mu,\mu') = 1 + 3g^i(a,\nu)\mu\mu' \tag{2.19}$$

and the expression for the volume emissivity term in the transfer equation then becomes.

$$\begin{aligned} j(\nu,r) \;=\; & \sum_i \int_{a_1}^{a_2} \pi a^2 Q^i_{abs}(\nu,a) B_\nu(T_d\ i(a,r)) n^i(a,r) da \\ & + J_\nu(r) \int_{a_1}^{a_2} \pi a^2 Q^i_{sca}(\nu,a) n^i(a,r) da \\ & + \mu H_\nu(r) \sum_i \int_{a_1}^{a_2} \pi a^2 Q^i_{sca}(\nu,a) 3g^i(a,\nu) n^i(a,r) da \end{aligned} \tag{2.20}$$

where

$$J_\nu(r) = \frac{1}{2} \int_{-1}^{+1} I_\nu(r,\mu') d\mu' \tag{2.21}$$

is the average (zero order moment) of the specific intensity over all solid angles, and is known as the mean intensity, whilst

$$H_\nu(r) = \frac{1}{2}\int_{-1}^{+1} \mu' I_\nu(r,\mu')d\mu' \tag{2.22}$$

is the first order moment, commonly called the Eddington flux. Following Hoare (1988), the terms $\bar{B}_\nu(r)$ and $\kappa_{ani}(\nu,r)$ are introduced, for the total thermal emission and anisotropic components of scattering respectively, such that:

$$\bar{B}(r) = \sum_i \int_{a_1}^{a_2} \pi a^2 Q^i_{abs}(\nu,a) B_\nu(T^i_d(a,r)) n^i(a,r) da \tag{2.23}$$

and

$$\kappa_{ani}(\nu,r) = \sum_i \int_{a_1}^{a_2} \pi a^2 Q^i_{sca}(\nu,a) 3g^i(a,\nu) da \tag{2.24}$$

with these terms, the expression for volume emissivity becomes:

$$j(\nu,r) = \bar{B}_\nu(r) + \kappa_{sca}(\nu,r) J_\nu(r) + \kappa_{ani}(\nu,r)\mu H_\nu(r) \tag{2.25}$$

which leads to a final expression for the equation of radiative transfer in a multiple grain component circumstellar envelope containing dust grains in an (as yet) arbitrary power law size distribution: This is

$$\begin{aligned} \mu\frac{\partial I_\nu(r,\mu)}{\partial r} + \frac{1-\mu^2}{r}\frac{\partial I_\nu(r,\mu)}{\partial \mu} &= -\kappa_{ext}(\nu,r) I_\nu(r,\mu) + \bar{B}_\nu(r) \\ &\quad + \kappa_{sca}(\nu,r) J_\nu(r) + \kappa_{ani}(\nu,r)\mu H_\nu(r) \end{aligned} \tag{2.26}$$

2.4 Solutions to the equation of radiative transfer

There have been many published numerical methods for solving the equation of radiative transfer, and reviews of the relative merits and approximations utilised by a variety of authors may be found in Rowan-Robinson (1982), Rowan-Robinson & Harris (1986) and Bode (1988).

To date, the most comprehensive amongst the plethora of published models, in that they have been used with some degree of success to model the emergent flux from optically thick circumstellar shells have been those derived from original work by Leung (1975),

Rowan-Robinson (1980) and Rogers and Martin (1984, 1986). Since the method of solution used in this work differs from all of these, the rationale for adoption of (yet another) method of solving the equation of radiative transfer will be justified in terms of deficiencies in each of these modelling techniques, and the need for a radiative transfer technique that overcomes these deficiencies.

Leung (1975) used a quasi-diffusion method (QDM) to determine the emergent flux from a dust shell with either a planar or spherically symmetric dust shell. The method assumed the radiation field in the dust shell to be isotropic, with a source function determined from the solution of a set of moment and energy balance equations. The derived source function was then used to solve for the angular dependence of the radiation field, using an iterative ray tracing method, which could include the effects of anisotropic scattering. The original Leung paper provided a rapid numerical method for solving the equation of radiative transfer, though as originally implemented did have a number of limitations in that it neglected the effect of radiative back-warming upon the star, and it assumed that the radiation field at the inner edge of the dust shell was isotropic (Mitchell & Robinson, 1978; Rowan-Robinson, 1980). These limitations were overcome in later adaptations of the QDM method and it has been used with some success to model the envelope of the star IRC+10°216 (Le Bertre 1987, 1988) for an envelope which was assumed to be composed of single sized grains of a single chemistry.

Rowan-Robinson (1980) described an alternative method to solve the equation of radiative transfer, and the method was applied to circumstellar shells around M-stars (Rowan-Robinson & Harris, 1983a; Rowan-Robinson *et al.* 1986) and C-stars (Rowan-Robinson & Harris, 1983b, Rowan-Robinson *et al.* 1986). The method, which Rowan-Robinson calls 'exact' (in that it does not ignore any terms in the equations, and accounts for the effect of multiple anisotropic scattering) involves calculation of the radiation field intensity as a function of frequency and direction at a grid of radial points ('depth points') throughout a dust shell, by integrating along rays through the shell, and then iterating to calculate the dust temperature distribution until conditions of radiative balance and flux conservation are satisfied. It has recently been extended to cope with axi-symmetric circumstellar geometries and a single grain size model has been presented for the disk shapes envelope of the star VY CMa (Efstathiou & Rowan-Robinson, 1990). However, the Rowan-Robinson models share at least one limitation with those of Leung, in that the

modelling process does not allow account to be taken of external heating sources (e.g. the interstellar radiation field) upon grains in the outer envelope (Bode, 1988). Also, both the Leung and Rowan-Robinson techniques use rays, in which the description of radiative transfer along each of many parallel rays provides one of the set of ordinary differential equations which are then solved. Ray techniques have been criticised by Rogers and Martin (1984) who identified some cases where a single grid being the basis of both angular and radial grids did not provide an optimum way of studying angular and radial variations of the radiation field simultaneously.

One (non ray) method of solution which does allow the effect of external heating sources to be introduced into models is the 'half range moment' method (Martin *et al.*, 1984, Rogers & Martin 1986) which has thus far only been used to model the circumstellar environment of one star, that being IRC+10°216 (Martin & Rogers, 1987). This method involves recasting the partial-differential equation of transfer into a set of ordinary differential equations for the angular moments of the intensity over two angular hemispheres. A closure relation is used to complete the set of differential equations, which when represented by finite differences result in an algebraic system of equations which may be solved to give the temperature distributions and flux throughout the dust shell via the method given in Rybicki (1971).

However, all three of the methods described above have only ever been applied to dust shells which are assumed to be composed of a single component of dust, with grains all of the same size. It will be shown in the next chapter that there is strong evidence for multiple size grains of different compositions being present in a single circumstellar envelope, and if a realistic description is to be offered of this scenario, then the radiative transfer methods adopted must be able to incorporate dust shells composed of multiple grain components comprising grains with a distribution of sizes. Admittedly, both Leung (1975) and Efstathiou & Rowan-Robinson (1990) have described how multiple size dust grains may be incorporated into their methods, although results for real stars have not been forthcoming in either case. Multiple grain component models (albeit with dust shells assumed to be composed of single sized grains) have been constructed by Sarazin (1978), Mitchell & Robinson (1978) and Tielens & de Jong (1979) in attempts to model the opacities in the HII regions associated with Orion, η Car and W3A/IRSI respectively, although in all cases, simplifications in the adopted solution techniques for the radiative

transfer made these models inapplicable to optically thick dust shells.

To date, the most comprehensive models for circumstellar environments have been those offered by Hoare (1988) for the HII region G45.13 +0.14A, by Hoare & Clegg (1988) for the O-rich planetary nebula DDDM-1, and by Hoare (1990) for the C-rich envelope around 2 further PN. These models do incorporate multiple grain components and multiple dust sizes, and utilise a numerical technique to solve the equation of radiative transfer first used by Haisch (1979). The availability of a version of the numerical code at UCL developed by Hoare (1988) from the original Haisch version, coupled with its advantageous incorporation of multi-size grains into a multiple component model led to its adoption for this thesis.

2.5 The streamed Eddington approximation

The streamed Eddington approximation assumes that a radiation field may be described by a number of directed streams, which simulate the true variation of intensity as a function of angle within a dust shell. In the simplest case, the field is assumed to consist of just two streams, one directed radially outwards, denoted by $I_\nu^+(r)$, the other directed radially inwards, denoted as $I_\nu^-(r)$. In spherical geometry this is equivalent to dividing the radiation field into two hemispheres, and assuming that the Eddington factor ($f_\nu = K_\nu/J_\nu$) has a value of one third. In this idealised case, the cosine of the angle dividing the two hemispheres measured from the outward directed normal, denoted μ_r has a value of zero. In spherical geometry, as one moves outwards through the dust shell, and the distance from the source of the radiation increases, the radiation field becomes more outward peaked (i.e. $\mu_r \rightarrow 1$, $f_\nu \rightarrow 1$).

The simple case of the so called 'two stream' Eddington approximation was generalised by Unno & Kondo (1976). The generalisation accounted for the geometrical dilution of the radiation field as a function of optical depth by allowing μ_r to be positionally dependant, with the positional dependance being determined by an approximate solution to the equation of radiative transfer.

Haisch (1979) developed the method of Unno & Kondo for model dust shell calculations in spherical geometry. The method presented by Haisch fully took into account the effects of non-isotropic scattering, absorption and thermal re-emission in shells composed

of multiple sized dust grains. The numerical code of Haisch has been further developed by Hoare (1988) to a state where it allows for a continuous (as opposed to a discrete) grain size distribution, and also incorporates multiple dust components into the modelling process.

Although the details of the numerical implementation of the generalised two stream Eddington approximation have been given by Haisch (1979) and Hoare (1988), a brief summary of the differential equations and techniques of numerical solution will be given below, since models calculated later in this thesis use an updated version of the numerical code. In any case, the version of the code described by Hoare was used specifically to model the environments of PN and HII regions, and a number of changes were made to his numerical code to bring it into a form where it could be usefully employed to model the circumstellar environments of red giant stars, and these (albeit small) changes are worthy of discussion in the light of the equations of which they aid the solution.

Unno & Kondo (1976) define the specific intensity in the two stream Eddington approximation by:

$$I_\nu(r,\mu) = \begin{cases} I_\nu^+(r) & 1 \geq \mu \geq \mu_r \\ I_\nu^-(r) & \mu_r \geq \mu \geq -1 \end{cases} \tag{2.27}$$

with μ_r being defined as the cosine of the angle dividing the two radiation streams. After taking the first four moments, J_ν, H_ν, K_ν and N_ν of the specific intensity, which were defined by integral relations of the form:

$$\frac{1}{2}\int_{-1}^{+1} \mu^n I_\nu(r,\mu')d\mu' \tag{2.28}$$

for n=0, 1, 2 and 3 respectively, yielded the relations

$$K_\nu(r) = \frac{1}{3}(J_\nu(r) + 2\mu_r(r,\mu)H_\nu(r)) \tag{2.29}$$

and

$$N_\nu(r) = \frac{1}{2}(1 + \mu_r^2(r,\mu))H_\nu(r) \tag{2.30}$$

Three differential equations may then be obtained by taking the first three moments of the equation of radiative transfer. These may be written (Hoare, 1988):

$$\frac{1}{r^2}\frac{d}{dr}(r^2 H_\nu(r)) = -\kappa_{abs}(\nu,r)J_\nu(r) + \bar{B}_\nu(r) \tag{2.31}$$

$$\frac{dJ_\nu}{dr} + \frac{2}{r^3}\frac{d}{dr}(r^3\mu_r(r,\nu)H_\nu(r)) = -3(\kappa_{ext}(\nu,r) - \frac{1}{3}\kappa_{ani}(\nu,r))H_\nu(r) \qquad (2.32)$$

and

$$\frac{d\mu_r(r,\mu)}{dr} = \frac{1-\mu_r^2(r,\nu)}{r\mu_r(r,\nu)} - \frac{2}{3}\frac{1+3\mu_r^2(r,\mu)}{4\mu_r(r,\nu)}\frac{1}{r^2H_\nu(r)}\frac{d}{dr}(r^2H_\nu(r)) - \frac{2}{3}\kappa_{ext}(\nu,r) \qquad (2.33)$$

These equations then being solved for $J_\nu(r), H_\nu(r)$ and $\mu_r(r,\nu)$ using the same boundary conditions as Haisch (1979).

The first boundary condition is that at the inner radius of the dust envelope, the outward stream is defined by the solid angle subtended by the stellar disk. i.e. (at all frequencies):

$$\mu_r(r_{in}) = \left(1 - \left(\frac{R_*}{r_{in}}\right)^2\right)^{\frac{1}{2}} \qquad (2.34)$$

As noted by Haisch, the intensity in the outward stream is that of the stellar surface; this provides a second boundary condition, as:

$$I_\nu^+(r_{in}) = I_\nu^* = J_\nu(r_{in}) + \frac{1+\mu_r(r_{in})}{1-\mu_r^2(r_{in})}2H_\nu(r_{in}) \qquad (2.35)$$

where I_ν^* can either be that given by a blackbody whose temperature is equivalent to the energy source at the centre of the dust shell, or via use of a stellar model atmosphere, should one be available.

The third boundary condition may be derived from the assumption that at the outer boundary of the dust shell, there is no external radiation field. Thus:

$$I_\nu(r_{out},\mu) = \begin{cases} I_\nu^+(r_{out}) & 1 \geq \mu \geq \mu_r \\ I_\nu^-(r_{out}) & \mu_r \geq \mu \geq 0 \\ 0 & 0 \geq \mu \geq -1 \end{cases} \qquad (2.36)$$

This effectively ignores the contribution of the interstellar radiation field, and its heating effect upon dust grains in the outer regions of the circumstellar envelope. This is obviously an approximation whose importance must be considered in the light of the results presented by Rogers *et al.* (1983) and Rogers & Martin (1984) whose models do incorporate the effect of an external radiation field upon dust in the outer regions of the envelope. However, ignoring for a moment the possible inaccuracies introduced by ignoring any external radiation field, the third boundary condition may be written:

$$J_\nu(r_{out}) = \frac{2H_\nu(r_{out})}{1+\mu_r(r_{out},\nu)} \qquad (2.37)$$

The three equations are solved numerically after initially guessing at an initial value for $\mu_r(r,\nu_1)$, the angular dependence of the radiation field at the lowest frequency and at a run of $T_d(a,r)$, the temperature of the dust grains as a function of radial distance from the star, throughout the dust shell. These initial guesses are not as difficult to make as it may seem from first inspection of the problem. At the lowest frequencies, the optical depth of the circumstellar envelope due to dust grains, and the thermal emission from the grains, diminishes, and thus stellar emission becomes the dominant contributor to the radiation field. Therefore, an initial guess as to the value of $\mu_r(\nu_1)$, the lowest frequency being modelled, may be obtained, since it is given simply by the geometrical dilution undergone by the radiation at the radial distance from the star:

$$\mu_r(r,\nu_1)_{initial} = \left(1 - \left(\frac{R_*}{r}\right)^2\right)^{\frac{1}{2}} \tag{2.38}$$

An initial guess as to a value for T_d(a,r) is obtained by calculating (approximately) the radial distance from the star at which the warmest (smallest radius) dust grains reach their condensation temperature, and then assuming that the grain temperature falls off in proportion to the half power of its radial distance from the star, throughout the radial grid.

After making initial guesses at $\mu_r(r,\nu)$ and $T_d(a,r)$, equations 2.31 and 2.32 were solved for J_{ν_1} and H_{ν_1} via matrix inversion. The values obtained were then used to solve $\mu_r(r,\nu_1)$ in equation 2.33, by using a predictor-corrector method originating at the inner boundary of the dust shell. The process is then iterated until convergence of $\mu_r(r,\nu)$ is obtained, which takes between 3 and 4 iterations.

Once values for $J_\nu(r)$, $H_\nu(r)$ and $\mu_r(r,\nu)$ have been obtained for the first frequency point, the initial guess at $\mu(r,\nu)$ for the next frequency point can be made from the previously converged value. The entire process is repeated until converged values have been obtained for all $\mu_r(r,\nu)$.

With the achievement of converged values of the three quantities $J_\nu(r), H_\nu(r)$ and $\mu_r(r,\nu)$ for all frequencies, a temperature correction procedure, developed by Haisch (1979), but extended by Hoare (1988) to incorporate multiple dust components, was used to calculate dust temperatures throughout the dust shell. This procedure utilises the conservation of frequency integrated spherical flux relies upon the fact that the 'true'

integrated flux, $H^T(r)$ may be calculated from:

$$H^T(r) = H(r) + \Delta H(r) = \left(\frac{r_{in}}{r}\right)^2 H_{r_{in}} \tag{2.39}$$

for $r_{in} \leq r \leq r_{out}$, as opposed to integrating H_ν over frequency. The value of $\Delta H(r)$ is used by the temperature correction procedure to calculate the grain temperatures as a function of radial distance. These newly calculated grain temperatures may then be used to solve for $J_\nu(r,\nu)$, $H_\nu(r)$ and $\mu_r(r,\nu)$ again, and the entire process of temperature correction is iterated until converged values of grain temperatures are obtained within the dust shell, which can take up to 5 iterations.

2.6 Surface brightness profiles

A development by Hoare (1988) of the Haisch (1979) numerical code which was not incorporated into the original work as given by Haisch, was to incorporate the ability to calculate surface brightness profiles. This technique offers an additional (and powerful) method of deriving the physical properties of circumstellar envelopes by comparing the model surface brightness profiles directly with spatially resolved observations of an astronomical source.

The method used by Hoare (1988) involves calculating the model surface brightness at a point p, $I_\nu^+(p)$, by integrating the emission along a series of rays in the line of sight direction to an observer, in a way analogous to the impact parameter technique described by Leung (1976). For an optically thick circumstellar envelope it is the source function, $S_\nu(r) = j(\nu,r)/\kappa_{ext}(r,\nu)$ which is integrated along each of a series of rays, that when taken in unison give a surface brightness profile, for a spatially resolved source.

In the case of spatially resolved observations of a source being obtained with an instrumental beam width whose size is comparable with that of the angular size of the source under observation, then the beam profile must be convolved with the model surface brightness profile in order to compare the model directly with observation. In the method described by Hoare, and adopted here, all instrumental beam profiles used to make spatially resolved observations were assumed to be two dimensional Gaussians, with a profile symmetrical in shape about the beam centre.

As well as comparing models with spatially resolved observations, the convolution technique used by Hoare is of use in correcting observed fluxes, derived from the literature,

made with finite (known) beam sizes, for the effects due to a beam being smaller than a source (if the angular diameter of the instrumental beam is smaller than the angular size of a source on the sky, then some flux from the source outside of the beam may be effectively 'lost' and an underestimate made of the actual source flux).

2.7 The accuracy of the generalised two stream approximation

Rowan-Robinson (1982) has questioned the accuracy of the generalised two stream Eddington approximation as given by Unno & Kondo (1976), since some of the true intensity distributions calculated by his 'exact' numerical models (Rowan-Robinson, 1980) did not resemble a two stream case. However, Petrosian & Dana (1980) have investigated the relative accuracies of QDM models (similar, though not identical in implementation with those used by Rowan-Robinson) and models calculated using a modified Eddington approximation for the case of radiative transfer in the case of an optically thick dusty nebula. It was found that the Eddington approximation provided results of comparable accuracy to those obtained using the QDM technique in a far shorter computational time. The work of Hoare & Clegg (1988) and Hoare (1990) in using the 2 stream Eddington approximation to model dust in the neutral regions of planetary nebulae has also proved the technique useful in obtaining self consistent models for ionised nebulae.

The neglect of the interstellar radiation field, which is implicit in the adoption of the second boundary condition for solving the moment equations is in fact a common assumption used in radiative transfer modelling of circumstellar envelopes, and to date, only Martin & Rogers (1987) have incorporated its effects into a model for the carbon star IRC+10°216. Though the component proved to have negligible effect upon the model fluxes in the wavelength region studied by Martin & Rogers (which was surprising when one considers that the interstellar radiation field ultimately constrains the outer radius of the circumstellar dust envelope), there was some evidence that it needed to be incorporated to explain surface brightness observations at wavelengths of 0.55μm. However, the actual value of the intensity of the interstellar radiation field, as a function of both frequency and of spatial location in the galaxy is far from certain, and there is some doubt that the intensity of the field measured in the solar neighbourhood (e.g. Mathis, Mezger &

Panagia, 1983) may be applied generally within the galaxy. It was therefore decided that for the purposes of this project, attempting to incorporate a model for the interstellar radiation field would introduce an unnecessary complication into an already complicated modelling process, and its quantitative effects would therefore be ignored.

2.8 Numerical implementation of the code

At the outset of this thesis, the code was available in a fortran-66 version implemented upon the University of London Computer Centre (ULCC) Cray-1S mainframe computer. This version was that adapted by Hoare (1988) from the original coding by Haisch (1979), and in practice, a typical model for a dusty nebula, comprising 200 radial grid points, 90 frequency points, and 20 grain sizes, took about 5 minutes of cpu to iterate to convergence over 4 frequency and 4 temperature iterations (Hoare, 1988).

The reason for the original implementation of the code upon the Cray was that, at the time of implementation, the speed of the UCL Starlink VAX 11-780 was such that a similar model would have taken some 2 hours of processor time. The speed of mini computers has increased dramatically over the past few years though, and the μVax 3800 computer currently installed at the UCL Starlink node is a factor 3.8 faster (A Fish, private communication) in cpu time than the 11/780. If this is coupled with the fact that the ULCC Cray is run on a batch schedule basis, where even small jobs may take as long as 12 hours to be processed and returned to the user, it can be seen that the proposition of implementing the numerical code upon the Starlink μVax became very attractive.

Thus, during late 1987, I completely re-wrote and re-optimised the code, in Vax fortran-77 and implemented it upon the Starlink μVax. In performing the transfer, a number of modifications were made to the numerical code as implemented by Hoare, which improved its usefulness in modelling circumstellar envelopes. The principal modification involved adapting the code to allow for different condensation temperatures for grains of different components. As implemented by Hoare, the code did allow for a dust shell to be composed of multiple dust components, but all dust components had to share the same radial grid, beginning and ending at identical inner and outer radii. This could, in practice, lead to some non realistic models. For example in a model comprised of a multiple component dust shell, the inner radius of the shell was determined by the condensation temperature

of the more refractory grain component, and all other dust components were assumed to condense at that point in the shell. This could lead to situations in which dust grains existed, and their effects upon radiation transport through the circumstellar shell were accounted for in models, in cases where in a 'real' dust shell the grains had not actually condensed.

In the modified version of the code, the inner radius of the shell was still determined by the condensation temperature of the most refractory grains, but the effects of the less refractory grains were only incorporated into the radial grid once the grain temperatures of the warmest grains of the most refractory grain component had reached the condensation temperatures of the less refractory component.

Of course, since the dust was assumed to be composed of a grain size distribution, there was a distribution of temperatures within a single dust component at any point in the radial grid. Once again, grains of an individual component were only allowed to affect radiative transfer once the temperature of grains of a given radius at a position within the envelope had reached that corresponding to their condensation point. It is felt that this modification provided a more realistic description of conditions within a circumstellar envelope than in the original code.

The modified code provides a model spectrum for a 100 point radial grid at 70 frequencies in $\approx$35 minutes of cpu on the μVax computer, for a 4$\times$4 grid of temperature and frequency iterations.

Chapter 3

The composition of circumstellar dust

3.1 Introduction

Dust grains that condense and grow in the winds of post-AGB stars are seeded to the interstellar medium via the process of mass loss. Thus in a very real way, the chemical and physical nature of dust in circumstellar envelopes is probed, albeit to some small degree, during the course of every astronomical observation, since the path to every celestial object is veiled to some extent by the dust grains contained within the ISM which pervade all sightlines.

The grains that comprise the solid phase of the ISM may differ from those that have recently condensed in the winds of post-AGB stars, due to physical and chemical processing that they may be subjected to. However, information derived about grain properties from observations of the ISM may be used to constrain the composition of dust in circumstellar envelopes as long as the processes undergone by these grains during their period in the ISM can be understood and accounted for within models. If the true nature of circumstellar dust grains is to be discovered, it becomes important to acknowledge the position of circumstellar grains within the broad spectrum of grains thought to occur within the ISM, by studying observations of grains located in a variety of environments.

Within this chapter, the relationships between grain models for dust in circumstellar and interstellar environments will be discussed, and an attempt will be made to better define the chemical and physical compositions of grains located in the circumstellar en-

velopes of post-AGB stars. To this end, the observed interstellar extinction curve, and its implications for both the composition and size distribution of interstellar dust grains will be used as a starting point for the development of circumstellar grain models.

3.2 The evidence for dust grains

At short wavelengths ($\lambda \leq 1\mu$m) the presence of dust may be identified by its absorption and scattering of radiation, whereas at longer wavelengths its presence in a source may be inferred by intrinsic emission and/or absorption of radiation. Dust grains may generally be seen to absorb radiation in the UV and optical regions of the spectrum, and to emit it at IR and longer wavelengths.

One method that has been used extensively to derive grain properties is to study the way in which the grains extinguish radiation in the UV, optical and near-IR spectral regions, and then attempt to identify materials whose extinction properties match those observed. In practice, deriving the extinction to an astronomical source requires a knowledge of its intrinsic energy distribution. Providing a source whose intrinsic energy distribution is known can be identified, then the extinction properties of the dust in the line of sight to that source as a function of wavelength (an 'extinction curve') may be derived.

At UV, optical and IR wavelengths, intrinsic spectra have been studied as a function of spectral type and luminosity class for a wide variety of stars, and hence intrinsic photometric 'colours' (magnitude differences measured through filters with standard bandpass) have been calculated. Thus, a multi-filter photometric, or indeed spectrophotometric observation of a dust obscured star whose spectral type and luminosity class is known yields a measure of the extinction curve towards that star, by simply comparing the observed photometric colours with those expected from an unobscured ('unreddened') star, and finding the differences. If the observations extend sufficiently far into the IR, the absolute amount of extinction, or the zero point, towards the star may be derived, since as observations go to longer wavelengths, the amount of extinction at each wavelength will tend to zero.

In order to compare the extinction curves observed along different sightlines, a normalised form of the curve has been developed. The usual normalisation chosen, is to plot

E(λ–V)/E(B–V) as a function of wavelength, where E(λ–V) is the difference (expressed in magnitudes) between the extinction measured at wavelength λ, and that measured towards the star through the Johnson 'V' filter. Extrapolation of such a plot to the longest wavelengths, where E(λ–V)=$-A_V$ gives as its intercept the ratio of total to selective extinction, $A_V/E(B-V)$, which is sometimes denoted R.

Figure 3.1 presents an average interstellar extinction curve, derived from measurements made towards stars of a wide range of spectral types in all directions within the galaxy. Though there are detectable (and sometimes substantial) variations in the shape of the extinction curve from star to star (some of these 'anomalous' sightlines are illustrated in figure 4.1), the shape of the interstellar extinction curve exhibits some common characteristics along all galactic sightlines studied to date. The first study of this type, which concentrated upon extinction in the optical spectroscopic region, was performed by Johnson (1968) who showed that the average extinction curve (or law) closely followed a theoretical curve (number 15) calculated by Van de Hulst (1946) to be appropriate for that exhibited by grains with a certain distribution in sizes and grain refractive index. Though this work provided a good first step along the road to understanding the nature of interstellar dust grains, later work, extending coverage of the extinction curve into the UV and near-IR (see reviews by Savage & Mathis, 1979; Massa & Savage, 1988) discovered features in the curve which made the Johnson model obsolete.

The most obvious feature in the interstellar extinction curve is the feature located at $\approx 4.6\mu m^{-1}$, which corresponds to a wavelength of $\approx$2175Å in the UV spectroscopic region.

3.2.1 The 2175Å feature

Since its discovery in the early UV surveys by Stecher (1965, 1969), the 2175Å extinction hump has provided a tough observational test for models of the solid phase of the ISM. A number of different mechanisms and materials have been suggested to account for the observed width, shape and spectral location of this feature, which was found by Fitzpatrick & Massa (1986) to have an average width of some 480Å, with a peak position of 2175Å, but the general consensus is now that the extinction hump is caused by some sort of dust material, and that it is entirely due to absorption (Greenberg & Chlewicki, 1983).

The profile of the 2175Å feature has been shown to be well matched by a Lorenzian (Seaton, 1979) or alternatively (and with a slightly better fit) by a Drude profile (Fitz-

Figure 3.1: An average interstellar extinction curve (after Bless & Savage, 1982)

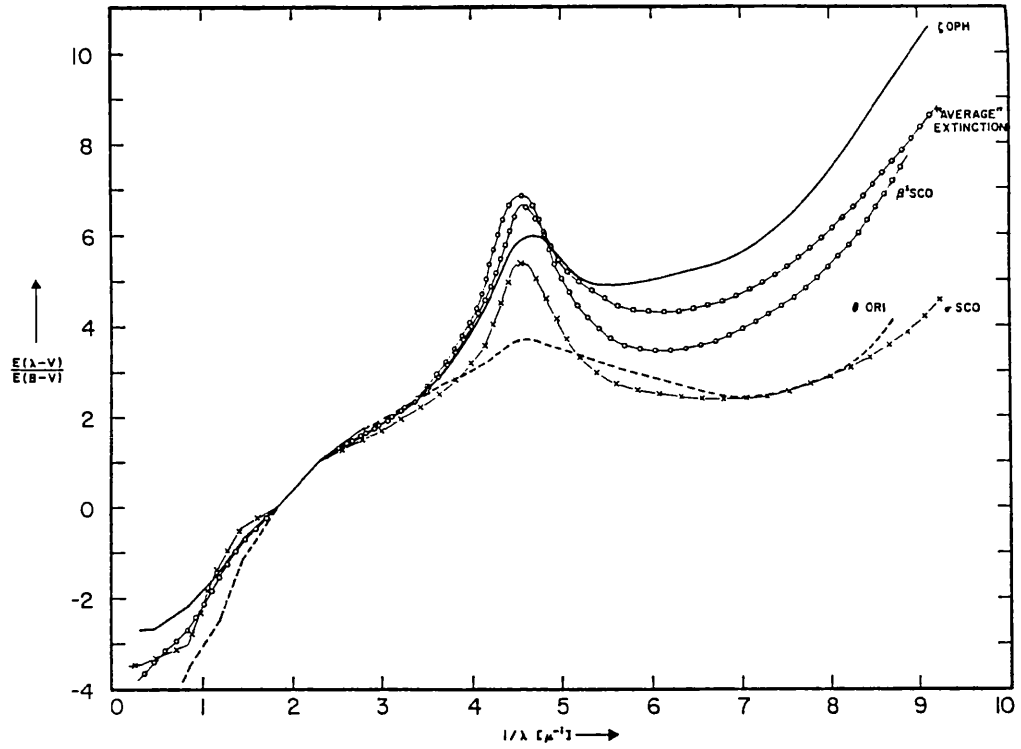

patrick & Massa, 1986) which, as noted by Massa & Savage (1989) has the advantage over the Lorenzian profile that it may be related to simple paramterizations of the optical properties of solids (e.g. Bohren & Huffman, 1983). Though parameterisations such as those of Seaton, and Massa & Savage do not explicitly identify the substance causing the 2175Å feature, they do aid in the characterisation of its strength and central position in a variety of objects using (relatively) simple analytical formulae.

The nature of the agent responsible for the 2175Å feature is the subject of much debate in the astronomical literature. Initially, graphite particles were put forward to explain the observed feature (Strecher, 1965; Donn, 1968) since bulk graphite presents an extinction peak at 2600Å in laboratory spectra, although Gilra (1972) suggested that the 2175Å feature might arise from surface plasmon oscillations in graphite grains whose radii were $\approx$ 200Å.

More recently, a number of workers have developed models for interstellar extinction which incorporate graphite grains to reproduce the 2175Å extinction hump (Mathis *et al.* 1977; Hong & Greenberg, 1980; Draine & Lee, 1984; Mathis & Whiffen, 1989). In general, it was found that the position of the extinction feature produced in these models was

strongly dependent upon both the size and shape of the graphite grains, with the best fits coming from models that assumed the grains to have small (a$\approx$0.01μm) radii.

There is however observational evidence that graphite is not a major component in circumstellar dust shells, and therefore by inference nor is it an important contributor to the ISM. This is because the 11.52μm resonance feature predicted to arise from pure graphite grains (Draine & Lee, 1984) has not been observed in C rich environments around either the mass losing star IRC+10°216 (Treffers & Cohen, 1974) nor in high resolution spectra of the Wolf-Rayet star Ve 2-45 (Glasse *et al.*, 1986) whilst Nuth (1985) also found that primitive meteorites contained little graphite. It is this lack of observational evidence for the existence of pure graphite in the ISM that has le d some workers to explore other possible grain components which could produce a 2175Å feature. The search is constrained by the fact that the uniformity of the observed feature requires a material which is well defined, whilst the observed strength of the feature, in relation to the cosmic elemental abundances requires a high absorption cross-section near 2175Å (Greenberg, 1986).

In fact a variety of alternative mechanisms and agents have been suggested to account for the 2175Å feature. Prominent amongst these is amorphous carbon (AC) (Borghesi *et al.*, 1985; Hecht, 1986) for which there is now considerable evidence for its existence in the circumstellar envelopes of C stars (Rowan-Robinson & Harris, 1983; Rowan-Robinson *et al.*, 1986; Martin & Rogers, 1987, Griffin, 1990). There are however problems with the utilization of AC grains to account for the 2175Å feature. Firstly, laboratory measurements indicate that AC particles produce an extinction feature that peaks at $\approx$ 2350Å (Borghesi *et al.*, 1983; Borghesi, Bussoletti & Colangeli, 1985; Colangeli *et al.*, 1986). Secondly, more than the measured cosmic abundance of carbon is required to account for the observed strength of the feature (Bussoletti, Colangeli & Orofino, 1987). These problems were overcome by Bussoletti *et al.* (1987) who developed an 'interstellar AC' (IAC) compound of particles whose mean radius was $\approx$10Å, and a fair match to the UV extinction hump was obtained.

Further carriers, some invoking O-rich, rather than C-rich agents, that have been suggested include magnesium silicate containing O^{2-} ions (Duley & Najdowsky, 1983), polycyclic aromatic hydrocarbons (Léger & Puget, 1984), a quenched carbonaceous material (Sakata *et al.*, 1983), charge transfer reactions between neutral hydrogen and ions on grains (Carnochan, 1988), unsaturated linear chain molecules (Hoyle & Wickramasinghe,

1977) and a carbonaceous substance photochemically formed from the mantles of solid core organic refractory particles (de Groot *et al.*, 1988). All of the proposed carriers have some problems associated with them, and at present there really exists no real agreement as to the identity of the carrier of the 2175Å feature.

Some work has been done in trying to discover the chemical nature (i.e. whether it is C-rich or O-rich) of the carrier, by deriving UV extinction curves towards regions whose chemistry is known to be either C-rich or O-rich. In practice this involves observing a serendipitous binary system where the radiation from a normal early type star is extinguished by a C or O-rich circumstellar gas cloud from a nearer evolved star. Alternatively observing a system in which stellar variability is caused entirely by a variation in the amount of circumstellar dust (e.g. R CrB stars) allows an extinction curve for the system to be derived simply by comparing spectra obtained at maximum and minimum light. The former method has been used by Snow *et al.* (1987) and Seab & Snow (1988) to investigate circumstellar extinction around M supergiants; these authors found no evidence for a 2175Å feature in any of the stars studied. The C-rich envelope around the R CrB star RY Sgr has been studied by Hecht *et al.* (1984) who found a broad shallow extinction bump in the 2300–2500Å region, but no evidence for a 2175Å extinction peak. Studies of other C-rich environments (e.g. that of the red rectangle by Sitko *et al.*, 1981) have revealed similar results, with the 'displaced' extinction hump being explained by Hecht *et al.* (1984) as being consistent with that produced by a power law size distribution of AC spheres, with radii in the range 150–500Å.

In conclusion then, it may be seen that the available evidence is inconclusive as to the true carrier of the 2175Å feature, although there are observational and theoretical reasons to suspect that its presence is associated with a C-rich chemistry.

3.2.2 Other features of the interstellar extinction curve

Although the most notable feature of the interstellar extinction curve visible in figure 3.1 is the 2175Å hump, there are several other distinctive features present in the curve from which information may be derived about the grain population contributing to the ISM.

At optical wavelengths, the curve exhibits a λ^{-1} dependance, which has been interpreted as a contribution from dust grains whose sizes are comparable with the wavelength (i.e. $2\pi a \approx \lambda$) (Martin, 1978). There is also some structure observed in the optical extinc-

tion curve; a 'knee' exists at $\approx 2.25 \mu m^{-1}$, and though this knee feature is observed in all sightlines, the ratio of the slopes on either side of the knee are found to be variable from one sightline to another (Massa & Savage, 1989).

The linear form of the extinction curve observed in the optical is seen to continue into the UV, but at the shorter UV wavelengths, a curvature appears. The strength of the far UV extinction is not correlated either with the extinction observed at visible wavelengths, or with the strength of the 2175Å feature (Seab *et al.*, 1981; Greenberg & Chlewicki, 1983). This has led some workers to suggest that the far-UV rise in extinction is due to a separate component of grains with a different chemical identity to those needed to provide the optical extinction and 2175Å feature (e.g. Martin, 1978). However, Jones *et al.* (1988) have pointed out that this need not necessarily be the case, since there are some substances (e.g. AC grains such as those described by Borghesi *et al.*, 1985; Colangeli *et al.*, 1986) that show optical properties at visual and far-UV wavelengths that are sensitive to the chemical and structural nature of the material.

It is generally agreed that the far-UV rise in extinction is due to a population of progressively smaller grains than those responsible for extinction in the optical. The uniformity of curvature observed in the far UV towards many separate sightlines was used by Greenberg & Chlewicki (1983) as an argument for very little scattering, which would be the case if the grains were small. The radii of these smaller grains would have to be less than $0.01 \mu m$ for the grain dimensions to be comparable with the wavelengths under discussion. At the shortest UV wavelengths, the observed rise in extinction necessitates particles whose dimensions are similar to those of large molecules, such as polycyclic aromatic hydrocarbons (PAHs) which have been invoked (see later) to explain unidentified emission features observed in the IR spectra of evolved objects (Léger & Puget, 1984).

Extinction in the IR region has been extensively studied, and Koornneef (1983) summarized many of the early results, and derived an average near-IR extinction curve for dust in diffuse clouds within the ISM, where a value of 3.1 for the ratio of total to selective extinction was also found to provide the best fit to a majority of the sightlines studied. A simple analytical formula for the extinction law in the IR and optical region has been derived by Howarth (1983), and may be used to parameterise extinctions in the IR and optical in a way analogous to that suggested by Seaton (1979) or Fitzpatrick & Massa (1986) for the UV region. More recent work e.g. by Whittet & Martin (1990) or Draine

(1989) shows that in the 1–5μm region, $A_\lambda \propto \lambda^{-1.8}$.

In summary then, although the interstellar extinction curve can in principle give valuable information about the dust grains which comprise the solid component of the ISM, the precise message that the available information, derived from the observations discussed above, is trying to tell is unclear. More sensitive observations are needed to better tie down the dust parameters, and the wavelength coverage of the known mean interstellar extinction curve needs to be extended further into the IR and UV/X-ray regions. In particular, observations made at the shortest X-ray wavelengths can provide particularly useful information, since it is not only possible to observe the extinction at these wavelengths, but also the halo into which the radiation has been scattered (Hayakawa, 1970; Mauche & Gorenstein, 1986). The additional constraints provided by observations of dust scattering haloes, which should become available with the next generation of high resolution and high sensitivity X-ray observatories such as AXAF, will give a greater idea as to grain compositions and properties than can be obtained presently from extinction measurements alone.

To gain further insight into the nature of dust, it becomes necessary to investigate the identities of spectroscopic features which may be related to the presence of dust. Though these features are observed in the ISM, the uncertain chemistry of the interstellar clouds means that the best places to study these spectral features is in locations where the chemistry (at least in terms of the C/O ratio) is better defined. Circumstellar envelopes provide such a location.

3.3 Spectral features and circumstellar dust envelopes

A collection of features have been observed in several spectral regions that have been attributed to, or at least associated with, the action of dust. These range from optical studies of the diffuse interstellar bands (e.g. Herbig, 1975) through the unidentified near to mid infrared features (see review by Allamandola, 1989) to the resonance features now known to be associated with the presence of C-rich or O-rich grains.

The spectral features observed in O-rich regions are very different to those found in

C-rich locations, and this has provided insights into the chemical nature of the grains in each environment. Particular advances in studies of the composition of circumstellar envelopes have been made with the publication of the *IRAS* LRS catalogue of 8–23μm spectra, obtained with the low resolution spectrometer aboard the Infra Red Astronomy Satellite (Beichmann *et al.*, 1984).

3.3.1 Dust in O-rich envelopes

Mid-IR (8–35μm) observations of the O-rich envelopes associated with M type and OH/IR stars (Gillet Low & Stein, 1968; Treffers & Cohen, 1974; Forrest *et al.*, 1979) and of planetary nebulae for which UV based abundance studies indicate an O-rich nature (i.e. C/O$\leq$1) (Aitken *et al.*, 1979; Aitken & Roche, 1982) reveal broad spectroscopic features centred at 9.7μm and $\approx$18μm, with the 18μm feature being weaker than the one at 9.7μm. In optically thin circumstellar shells, the 9.7μm feature is seen in emission, whereas in optically thick shells it is seen in absorption. The 9.7μm feature has been attributed to a Si-O bond which is observed in all silicates (Martin, 1978) whereas the 18μm feature is thought to arise from an Si-O-Si bending mode, also found in silicate molecules (Martin, 1978).

There are many different types of silicates, and much effort has been expended in identifying the type that is responsible for the silicate feature observed both in circumstellar and in interstellar sightlines. The exact wavelength and profile of a silicate feature is systematically dependent upon the crystalline structure of the grains responsible for it. Thus, by comparing the laboratory spectra of various silicates with the observed strengths and profiles of the circumstellar dust features, the nature of the silicate grains responsible for those features may be derived.

When identifying astronomical dust from IR spectra (not just those for O-rich environments), authors have often resorted to the large body of literature concerned with the infrared properties of mineral grains which have been derived using laboratory-based methods, such as the KBr pellet technique or by measuring the reflectivites of bulk mineral samples. The former technique involves deriving the bulk absorptive optical properties of powders of the substance under test with a large grain size (typically $\approx$4μm) suspended in a pellet of KBr, which has a refractive index of about 1.5 in the mid IR region of interest. This method has been criticised since it is generally accepted that interstellar

and circumstellar grains need to be much smaller than 0.1μm to account for the observed extinction towards C and O-rich stars. Also, the high refractive index of the KBr pellet must be carefully accounted for, since grains in circumstellar environments are situated in a medium whose refractive index is close to unity. Therefore, as it is known that both particle size and the refractive index of the surrounding medium can affect the shape and wavelength of absorption features (Penman, 1976), results obtained using the KBr pellet technique have to be studied very carefully if they are to be compared directly with the features observed in either circumstellar or in interstellar media.

In principle, the problems associated with the KBr pellet technique may be avoided if the reflectivity measurement method is utilised. This involves measuring the reflectivities of bulk samples of the mineral under investigation, and then using the Kramers-Kronig dispersion relations (e.g. Perry *et al.*, 1964) or alternatively a dispersion model based upon classical physics (Spitzer & Kleinmann, 1961) to give the real and imaginary parts of the materials refractive index, which may then be used to calculate the bulk absorptive properties of the material using Mie theory, as described in the previous chapter.

There are difficulties involved with the use of the reflectivity method. The principal problem is the difficulty of initially finding and then of making measurements upon samples of 'interesting' materials of sufficient purity which are not necessarily isotropic. As discussed by Penman (1976), analysis of reflectivity of unpolarised radiation from a polished surface results in average optical constants which may, or may not, give good calculated cross sections for a dust cloud composed of randomly orientated particles.

There is also evidence that Mie calculations provide results of questionable accuracy if applied to small particles, with radii in the range 0.01–0.2μm (e.g. Steyer, Day & Huffmann, 1974). For the smallest particles it was found that though Mie theory correctly predicted the wavelengths and relative strengths of features, it proved unable to correctly reproduce the observed widths or the absolute heights of the features.

Given the many difficulties in deriving accurate laboratory spectra of astronomically interesting minerals, it is perhaps not surprising that a variety of different minerals have been put forward as offering good fits to the features observed in astronomical sources. The task of matching mineral to feature is made more difficult still by the fact that there appear to be two distinct 'forms' of silicate dust feature. The first, described above and observed in the interstellar medium and in O-rich envelopes around PN and evolved

stars does appear to be relatively constant in shape (with slight variations) in all sources where it has been studied (Little-Marenin, 1986). A second, slightly broader feature, first observed towards the Trapezium in Orion (e.g. Forrest, Gillet & Stein, 1975) and also observed towards some other sources is suggested to be due to thermal processing of the grains (Nuth *et al.*, 1986) although it perhaps also involves grain size effects (Papoular & Pegourie, 1983). For both varieties of silicate feature though, the lack of observed fine structure in any of the many sightlines studied to date has been used as an argument for an amorphous as opposed to a crystalline structure for the grains.

On the basis of a chemical model, Gilman (1969) predicted that for a gas ejected from an O-rich star, with the outflowing gas exhibiting cosmic (solar) abundances, olivine, with a chemical formula $(MgFe)_2SiO_4$, would be the most likely condensate. On this basis, samples of amorphous olivine have been studied in the laboratory (e.g. Day & Donn, 1978; Stephens & Russell, 1979) and have been found to provide an excellent fit to the broad 9.7μm feature observed in circumstellar shells. However, this form of olivine was found to produce a second feature whose wavelength was closer to 20μm than to the 18μm required to match the observations. Other amorphous silicates have also been studied; Krätschmer & Huffman (1979) and Krätschmer (1980) have measured the mid-IR reflectivities for a sample of radiation damaged olivine. The samples studied were prepared by exposing them to doses of heavy ions and then collecting the condensate by burning this irradiated sample between two arcs. The optical constants calculated from the reflectivity measurements on this condensate were found by Skinner & Whitmore (1987, 1988) to provide excellent fits to the IR spectra of M giant and supergiant stars at both 9.7 and 18μm.

Other materials for which good matches have been claimed to the observed silicate features at both 9.7 and 18μm in astronomical sources have been amorphous enstatite (chemical formula $MgSiO_3$) (Day, 1979), and amorphous bronzite [$(Mg,Fe)SiO_3$] (Dorschner *et al.*, 1986), though to date, the optical constants derived for these materials have not been used to produce detailed radiative transfer models for any astronomical source. A further set of optical constants for silicate grains has been synthesized by Draine & Lee (1984) by combining measured laboratory derived optical constants with some estimated from astronomical observations of O-rich envelopes. One problem with this set of constants is that the Trapezium-type emission was used to estimate the optical constants in the 9.7μm feature, and hence these are of little use in modelling circumstellar envelopes, where, as

already noted, a different, narrower silicate feature is observed.

More esoterically, some authors have found that organic material, specifically cellulose, can provide a good match to the observed 'silicate' features at both 9.7 and 18μm (Hoyle & Wickramasinghe, 1979; Khare & Sagan, 1979). However, it has been stated by Krätschmer (1980) that correlations between strengths of a 3.1μm feature (also predicted by these models) and the observed strengths of 9.7 and 18μm features do not exist. It is not clear either how cellulose might be formed in interstellar/circumstellar environments, nor how it might survive in the physically harsh conditions located therein.

Apart from the 9.7μm and 18μm silicate features, other absorption features are observed at 3.1, 6.0 and 11.5μm in the most optically thick OH/IR and post-AGB stars such as the 'frosty Leo' nebula (Whittet, 1989). These features are attributed to the O–H stretch (3.1μm), a bending mode (6.0μm) and a libration mode (11.5μm) in the structure of pure water ice molecules contained in frost mantles which are thought to condense upon the silicate grain cores in the outermost regions of a stellar outflow.

3.3.2 Dust in C-rich envelopes

Early chemical models of the dust condensates expected in conditions where the C/O ratio was greater than unity (Gilman, 1969; Gilra, 1972) predicted that graphite and/or AC grains should be the first to condense, with silicon carbide being the next most likely condensate, although Wildt had previously suggested SiC as a possible condensate in cool stellar atmospheres as early as 1933.

As discussed previously, there is growing evidence that graphite is not a major component of interstellar or circumstellar environments, and many authors now propose that amorphous carbon (AC) particles may be the preferential condensate in C-rich conditions. Unfortunately, AC, with the possible exception of a weak feature observed in laboratory spectra at a wavelength of around 8μm (Koike *et al.*, 1980) does not exhibit any unambiguously detectable spectral features, and hence its presence in an envelope is usually inferred by lack of spectral features of other predicted condensates, rather than by its own spectroscopic features.

Mid-IR observations of C stars, and C-rich PN (Treffers & Cohen, 1974; Willner *et al.*, 1979; Aitken *et al.*, 1979) have identified an emission feature centered at $\approx$11.4μm, which has been identified as being due to SiC grains. Laboratory spectra of at least two types of

SiC have been investigated. Dorschner *et al.* (1977) suggested that a form of SiC known as 'black' or α–SiC which contains hexagonal rhomboedric polytypes could provide a good fit to the observed 11.4μm feature observed in the spectrum of the C star V Hya. Stephens (1980) investigated a second form of SiC with a cubic crystalline structure ('green' or β–SiC), although these results were not compared directly with any astronomical spectra. Samples of both α and β–SiC were studied by Friedemann *et al.* (1981) who tabulated mass absorption coefficients for both types, and produced a model for the envelope of the C star Y CVn. It was found that a better fit to the observations was obtained with the black form of SiC.

More recently, Borghesi *et al.* (1985) found that for both forms of SiC, the shape of spectroscopic features obtained in laboratory spectra was dependent upon the size and shape of the grains in the sample. Optical constants were derived by Pegourié (1988) for α–SiC grains from the measurements published by Borghesi *et al.* in the range 0.1–243μm, using the Kramers-Kronig relation, and these optical constants were used, as part of a multiple component dust model by Griffin (1990) to reproduce the observed SiC feature in the spectrum of the C star IRC+10°216.

Another feature, centered at around 30μm is also observed in the spectra of C stars and some PN (Forrest, Houck & McCarthy, 1981). The feature, which is very broad (it begins at around 24μm and may extend as far as 50μm in some objects observed by Goebel & Moseley, 1985) has been assigned to emission from MgS grains by Nuth *et al.* (1985) on the basis of comparing the observed feature with that produced in the laboratory by substances including CaS, FeS_2, SiS_2, Fe_3C as well as MgS. To date, optical constants have not been published for MgS, and this has, as yet, precluded its incorporation into radiative transfer models for C star envelopes, which would be one of the best ways to test the validity of the assignment of the 30μm feature.

What experimental laboratory measurements there are, suggest that neither MgS or SiC grains provide great sources of opacity outside the resonance features by which they are identified. Instead amorphous carbon and/or graphite grains are thought to provide the major opacity source at most wavelengths in circumstellar shells. Optical constants have been given for particles of graphite by Draine & Lee (1984, 1987) with values being given for both the perpendicular and parallel planes of the highly anisotropic crystals, whilst for AC, optical constants have been derived by Mathis & Whiffen (1989) from

the measurements of Bussoletti *et al.* (1987). Runs of optical constants for AC have been synthesised by many authors, most recently by Martin & Rogers (1987) and by Hoare (1990). Syntheses of optical constants, used in the radiative transfer modelling of circumstellar envelopes are necessary since the measurements of reflectivities used to derive the constants are rarely measured from the UV to IR by a single author; instead, measurements made at different wavelengths are published separately, and it is the work of the synthesist to derive self- consistent runs of constants for a single material. Difficulties arise when different methods may be used to prepare samples for measurements made in the different regions of the spectrum, and for this reason alone, syntheses of constants must be regarded with extreme caution when using them to construct models of mooted circumstellar dust components.

3.3.3 The UIR and ERE features

Other spectroscopic features are sometimes observed in the IR spectra of some C-rich stellar envelopes, proto-planetary and planetary nebulae, as well as in the spectra of HII regions, reflection nebulae and galaxies. The features are observed at wavelengths of 3.3, 6.2, 7.7, 8.6 and 11.3 μm and have been interpreted as being due to emission from polycyclic aromatic hydrocarbon (PAH) molecules (see for example the review by Bregman, 1989). PAH molecules are made up of benzene rings linked to each other in a plane, with H-atoms or other radical ions saturating the outer bonds of the peripheral C atoms. Léger & Puget (1984) proposed both an excitation mechanism and possible modes of emission for the observed features, by assuming that a typical PAH molecule, coronene ($C_{24}H_{12}$) was the responsible species.

In the Léger & Puget (1984) model, excitation is provided by the direct absorption of an individual UV photon by a large, isolated molecule of coronene. The 3.3, 6.2, 7.7 and 11.3μm features were then (it was proposed) identified with fundamental vibrational modes of the molecule: a =C–H stretch (3.3μm feature), the C=C stretching modes (6.2μm), an in plane =C–H bond (7.7μm) and finally an out of plane bend in the =C–H bond was identified as being the cause of the 11.3μm feature. The ratio of the strengths of the 11.3μm and 3.3μm features may be used to estimate the molecular size of the emitting species (Jourdain de Muizon *et al.*, 1989) which has been found to be typically in the range 50–130 atoms, implying that large molecules are responsible for the observed

emission bands.

Probably associated with the presence of hydrogenated amorphous carbon is the so called extended red emission (ERE) which has been observed as an excess emission in the red optical spectra of a number of reflection nebulae (e.g. Witt *et al.*, 1984; Witt & Schild, 1985). Dust luminescence, excited by mid-UV radiation from hot stars embedded in reflection nebulosity has been offered as one mechanism to explain the observed excess, on the basis of a study of 14 reflection nebulae by Witt & Schild (1986). It was found for those nebulae that the ERE was most common in sources illuminated by stars of spectral type B or early A, and that the contribution of the ERE to the surface brightness of the nebula was 15–25% in the B photometric filter, rising to 30–50% in the I filter. Witt (1989) claims that the presence or absence of the ERE band can give information as to the degree of hydrogenation of AC in the nebulae.

3.3.4 The far-IR emissivity of dust grains

Observations of dust continuum emission in the far-IR spectral region (i.e. $\lambda \geq 30\mu$m) can provide an insight into the nature of grains in circumstellar envelopes. Theoretical evidence suggests that the slope, p of the far-IR emissivity is determined by the structural composition of the dust grains. Crystalline grains are predicted to have emissivities that fall off as λ^{-p}, with p having a value of ≈ 2 (Andriesse, 1974) whereas amorphous grains are thought to exhibit a less steep fall off, with p being in the range 1–2 (Day, 1976; Koike *et al.*, 1980; Day, 1981) although Koike *et al.* (1987) have recently identified some scenarios for which the slope could be outside of this range for amorphous grains.

In fact, grain size has also been shown to play a rôle in determining the slope of the far-IR emissivity, and theoretical studies (Seki & Yamamoto, 1980) show how for small grains, a value of p close to unity arises from dominant surface vibration resonances between grain and radiation, whilst for larger grains, so called bulk mode resonances of the entire grain tend to cause an emissivity fall proportional to λ^{-2}. According to Seki & Yamamoto, the wavelength at which the turnover between λ^{-1} and λ^{-2} occurs is grain size dependant, and is directly proportional to grain radius for radii greater than 0.005μm.

Far-IR and sub mm observations have been used to derive grain emissivity, either directly from observations, or by fitting the observational data with model spectra derived from radiative transfer models. To date, only HII regions have been studied using the

former approach, which has been used by Gear *et al.* (1988) to obtain a value for p for the dust of 1.75±0.2, although considerable scatter was found for the values of p for separate HII regions from the observations. Other workers, including most recently Ericksson *et al.* (1981) found that p=1 gave a better fit to dust emissivity for the HII regions being studied, whilst Chini *et al.* (1986) identified the best fit on the basis of a model fit, as having $p \approx 2$.

For O-rich circumstellar environments around M giants, supergiants and OH/IR stars, a similar disparity of derived values for the far-IR emissivity of dust is found. For these objects, the IR emissivities have been derived from radiative transfer models by a number of workers, including Rowan-Robinson & Harris (1983) and Rowan-Robinson *et al.* (1986), who found that a value of p=1 provided good fits to observations extending out only as far as 100μm. However, Skinner & Whitmore (1987, 1988) found that the spectra of the M supergiant α Ori (Betelguese) and several other M giants and supergiant stars could be adequately represented over the range 0.5μm–10cm with a dust emissivity proportional to λ^{-2}, if free-free emission from a warm extended chromosphere was incorporated into the modelling procedure. Similarly, Hoare & Clegg (1988) obtained good fits to the observed spectrum of the halo planetary nebula DDDM1, also by using a λ^{-2} far-IR emissivity law for the dust.

In C-rich environments, a similar variation is found in the literature for published values for the far-IR emissivity of the dust grains. Of particular importance in attempts to find the far-IR emissivity of C-rich dust grains have been studies of the C star IRC+10°216 which has proved a boon to emissivity students due to its high surface brightness at all wavelengths (it has been studied in the wavelength range 4000Å–6cm). Different studies of IRC+10°216 have proposed values of p of 1.1 (Zuckerman & Dyck, 1986), 1.2 (Sopka *et al.*, 1986), 1.3 (Jura, 1983; Le Bertre, 1987, 1988) on the basis of radiative transfer 'best fits' to the observed energy distribution of the source, as well as the p value of unity, which would arise were the grains amorphous (Rowan-Robinson & Harris, 1983; Rowan-Robinson *et al.*, 1986; Martin & Rogers, 1987). All of the workers mentioned have used single grain sizes in their models for the circumstellar envelope of IRC+10°216, and hence their results may be biased if grain size and shape change the exponent of the emissivity law (Seki & Yamamoto, 1980).

Thus for both silicate and for AC grains, the precise chemical and physical compositions

Dust type	λ	C/O Ratio	Where observed
Silicate	9.7,18	$\leq$1.0	K, M, OH/IR, PN, ISM
SiC	11.4	$\geq$1.0	C stars, PN
H_2O ice	3.1, 6.0, 11.5	$\leq$1.0	OH/IR, post AGB, ISM
PAH(?)	3.3,3.4,6.2,7.7,8.6,11.3	$\geq$1.0	proto PN, PN, ISM

Table 3.1: **Spectroscopic features associated with dust**

of grains remain highly uncertain. It is hoped that during the course of the present work that these properties may be better defined, at least in the case of circumstellar envelopes. To this end, a summary of the observed spectroscopic features which have been ascribed to dust emission and discussed in this chapter are presented as Table 3.1. Any unified grain model for the grains present in the envelopes of evolved stars, or more generally within the interstellar medium must account for these observations, if it is to stand up to even the most basic of observational tests.

3.4 Models for circumstellar and interstellar dust

Taken as a whole, the observations of dust obtained at various wavelengths, in conjunction with the theoretical models used to explain the observed spectroscopic features provide a large quantity of data which may be incorporated into unified models that attempt to explain the gross solid state features observed in the interstellar environment within the framework of a single model. For circumstellar environments, or PN, which of course provide the raw material for the ISM via mass loss, the O-rich and C-rich components of a successful model may be used separately, depending upon the C/O ratio.

A number of grain models have been proposed, that attempt to match the entire interstellar extinction curve, from far-UV to sub- mm wavelengths. Amongst the more recent, and most widely discussed are those of Mathis, Rumpl & Nordsieck (MRN, 1977), Hong & Greenberg (1980), Duley (1987) and Mathis & Whiffen (1989).

MRN proposed a model with separate populations of bare silicate and graphite grains, with the grains being present in a power law grain size distribution, such that $n(a) \propto a^{-3.5}$ for $0.005\mu m \leq a \leq 0.25\mu m$, with a being the grain radius. The $a^{-3.5}$ size distribution has

been found to be a natural consequence of grain-grain collisions in the winds of red giant stars (Biermann & Harwitt, 1980) and was found by MRN to provide a good fit to the extinction curve from the IR to the far-UV. Recent extensions of the MRN model, by Draine & Anderson (1985) have extended the size distribution limits downwards to 3Å, in order to explain the observed 60 and 100μm emission detected towards interstellar clouds by the *IRAS* satellite (Low *et al.*, 1984). This extension may also provide a link between grain models and the PAH hypothesis, since the lower limits of this size distribution are beginning to approach the upper limits to sizes of PAH molecules inferred by the observations discussed earlier.

One problem with the MRN model is its inclusion of a graphitic component, which is needed to match the observed 2175Å feature. However, as discussed previously, graphite, in a pure form, may not be a major component of the ISM. This has le d some workers, starting with Mathis (1986, 1988) and Hoare (1988) to substitute amorphous carbon grains for the graphitic component in the MRN model. This substitution does have some theoretical justification in the light of the work discussed above where it was found that in some circumstances, both the strength and profile of the 2175Å feature could be matched by AC grains.

Hong & Greenberg (1980) have developed a model with grains composed of refractory silicate cores, which are enveloped by tenuous organic mantles. The core radii are $\approx$0.10μm and the mantles have a distribution of thicknesses. The Hong & Greenberg model also incorporates a population of (separate) bare silicate and graphite grains with small grain radii (a$\approx$0.01μm). Once again, the pure graphite component is invoked to match the 2175Å feature, the far-UV rise is provided by the small silicate and graphite particles, whilst the organic mantles provide the optical extinction. The Hong & Greenberg model does appear to have some severe difficulties. Firstly, both it (and indeed the MRN model) actually use more carbon than is available along most sightlines (Whittet, 1984); this problem may be overcome if the grains are allowed to be fluffy, or porous (Mathis, 1988; Jones, 1988). The second (and more important) drawback to this model is that no optical constants have as yet been offered by the authors for their core/mantle grains, which means in effect that they may not be incorporated into radiative transfer models.

The model of Duley (1987) uses small (a$\leq$0.01μm) silicate core/ hydrogenated amorphous carbon mantle grains, in conjunction with large (a$\approx$0.1μm) iron silicate grains in a

MRN size distribution. In this model, it is the small silicate grains that are responsible for giving rise to the 2175Å feature. This may be problematic, since, as discussed earlier, extinction curves derived towards O-rich circumstellar shells do not show a 2175Å feature, arguing against an O-rich carrier for it.

Most recently, Mathis & Whiffen (1989) have developed a model for interstellar grains, where the grains are assumed to be very small collections of individual particles of silicates, AC and graphite, bonded together in a loose aggregate. This model, gives a good match to the observed extinction curve in the wavelength range $0.12 \leq \lambda \leq 1500\mu$m.

However the graphite particles are again required to provide the 2175Å feature, but as discussed by Mathis & Whiffen, these small graphitic particles may be produced directly from AC by annealing during the high temperatures attained immediately after the absorption of a single UV photon. The grains are assumed to be in an MRN size distribution.

Although not directly applicable as a model for all grains in the ISM, Frenklach *et al.* (1989) have described a possible condensation sequence which may occur in the envelopes of C stars, and provide a method by which AC could be returned to the ISM. In their scenario, Frenklach *et al.* proposed that in the envelopes of C stars, the first condensate would be small particles of SiC, which, as they move away from the star acquire a mantle of AC, whose thickness grows as the particle moves out through the stellar wind. To date, the existence of these SiC core/AC mantle grains within the ISM has yet to be confirmed.

In the following chapters, some of the dust models discussed above will be incorporated into detailed radiative transfer models for the circumstellar envelopes of both O-rich and C-rich stars. In particular, the MRN and Mathis & Whiffen models will be used as starting points for model descriptions of grains in circumstellar envelopes.

For O-rich envelopes, the optical constants given by Draine & Lee (1984,1987) and Krätschmer & Huffmann(1979) will be tested, whilst for AC, the optical constant syntheses presented by Mathis & Whiffen (1989) and Hoare (1990) will be examined in the light of observational evidence. For SiC grains in C-rich envelopes, the synthesis of constants given by Pégourie (1988) will be used as a starting point.

Chapter 4

A model for the circumstellar envelope of WX Ser

4.1 Introduction

In this Chapter, the radiative transfer code described in Chapter 2 is used to develop a model for the circumstellar envelope of the M giant and Mira variable star, WX Ser, which is known to be chemically O-rich in nature.

It is argued that dust is the sole opacity source in the circumstellar envelope of this star, and that there is no observational evidence for the existence of a stellar chromosphere or corona, which might give rise to free-free emission that would contribute to the energy distribution at IR and longer wavelengths.

Optical constants for amorphous silicate grains derived from laboratory measurements of olivine grains are then tested against high signal to noise observations of WX Ser, and a coherent dust model produced for its circumstellar envelope.

4.2 Why WX Ser?

In the past, workers have preferred to model observations of large numbers of different stars, using either laboratory based optical constants (e.g. Treffers & Cohen, 1974; Onaka *et al.*, 1989) or by deriving optical constants which provide the 'best fit' to the sample of stars under study (e.g. Rowan-Robinson & Harris, 1983a; Rowan-Robinson *et al.*, 1986; Volk & Kwok, 1988).

The launch of the *IRAS* satellite in 1983, and the consequent publication of 4 colour photometry at 12, 25, 60 and 100μm, coupled with flux calibrated low resolution spectra from the Dutch Additional Experiment (Beichmann *et al.*, 1984), of a large sample of red giant stars, has provided an excellent opportunity to extend the spectroscopic range of circumstellar dust models for O-rich shells into the mid-IR spectral region.

Although observations of O-rich circumstellar dust shells had previously been published in this spectroscopic region (particularly in the 8–21μm atmospheric window where the important 9.7 and 18μm silicate reasonance features are located), it was only with the publication of the *IRAS* observations that coeval data at multiple IR wavelengths became available for the first time for a variety of dust shells exhibiting a range of optical depths.

However, it must be admitted, that not all of the *IRAS* data are of the highest signal to noise ratio, and difficulties can arise when these data are used to interpret the nature of the circumstellar dust shells. In particular, the LRS spectra for many objects are of a quality which is insufficient to provide a detailed test of, or indeed a basis for deriving, optical constants for the dust grains located in O-rich environments.

For the purposes of this project, a different approach to those described above was adopted, in attempting to test the properties of circumstellar dust grains. It was decided to select from the available photometry, a single example of a star having either an optically thin or optically thick dust shell, for which high quality photometric observations existed over a wide range of wavelengths.

Since it has been argued that some red giant stars, and most red supergiant stars have warm extended chromospheres (e.g. Skinner & Whitmore, 1987; 1988) whose presence modifies the character of a spectrum at mid-IR and longer wavelengths, it becomes important to select a source for which there is no observational evidence for chromospheric emission, if a straightforward discussion of the optical properties of dust grains is to be embarked upon.

The selected star should also have well defined parameters (distance, radius, mass loss rate etc.) and no evidence for extensive departure from spherical symmetry in its dust envelope. This would minimise the uncertainties in the modelling process, ideally confining any such uncertainties to the properties of the silicate dust grains used within the modelling process.

In order to test the optical properties of dust grains, the star WX Ser was selected for

modelling purposes, as it fulfilled at least some of the selection criteria described above.

4.3 Modelling the circumstellar dust shell

The adopted stellar parameters for WX Ser are given in Table 4.1. The star is a classical Mira with a period of 425.1 days (Kukarkin *et al.*, 1969), and has been classified as a non-radio luminous type II OH/IR star, with an IR excess which is due to a dusty mass-losing wind (Hyland *et al.*, 1972). Near-IR CVF spectra in the wavelength range 1.4–3.8μm obtained by Jones *et al.* (1988) exhibit strong photospheric absorption features that are characteristic of a Mira variable star (strong water vapour bands at 1.9μm and 2.37μm), as well as CO second overtone lines shortwards of 1.6μm. The spectra obtained by Jones *et al.* were used to assign the spectral type of VM by those authors, who were also responsible for deriving the adopted stellar effective temperature of 1960K (from the observed strengths of CO lines in the photospheric spectrum, used for WX Ser in the models calculated below).

4.3.1 Molecular line blanketing

The strong photospheric absorption features observed in the near-IR spectrum of WX Ser provide an obstacle for models of the emergent spectrum of this, and indeed any late type star. Traditionally, it is assumed that a Planck function appropriate to the given effective temperature provides a realistic description of the stellar radiation field, and this is used as the input to the radiative transfer code. However, molecular and atomic line opacities in the cool atmospheres of late type stars mean that the stellar spectrum is far removed from that of a black body, and if a realistic model is to be made, then this departure must be accounted for within the modelling process. The problem is mainly confined to the optical and near-IR spectroscopic region where much of the line-blanketing occurs; at longer wavelengths the blanketing plays a progressively lesser rôle in determining the nature of the emergent stellar spectrum.

The ideal solution to this problem would be to utilise a model stellar atmosphere, appropriate to the star in question, as the illuminating source at the centre of the circumstellar envelope, rather than a black body. The main difficulty with this is that at the moment, there exist no accurate model atmospheres for M type stars with effective temperatures lower than 2500K (see Bowen, 1989; Bessell & Scholz, 1989; Bessell *et al.*,

Parameter	Value	Reference
Distance	0.72 Kpc	Rowan-Robinson *et al.* (1986)
R_*	4×10^{13}cm	This Work
T_*	1960 K	Jones *et al.* (1988)
$\dot{M}$	$4.0\times10^{-6}M_\odot$ Yr^{-1}	This Work
V_∞	7.5 km s^{-1}	Engels (1979)

Table 4.1: Adopted stellar parameters for WX Ser

1989 for a discussion of the best recent model stellar atmospheres for late type stars).

A further problem with atmospheres of Mira stars particularly is the fact that they are non-static and for a static model of the circumstellar envelope the question would arise as to which phase in the stellar pulsational cycle would be appropriate to the dust model. Ideally of course, a dynamically linked pulsational stellar atmosphere and dust model would solve this problem, but this solution is not as yet possible, since pulsational model atmospheres have only recently become available for the shorter period (P=300-400 days) stars (e.g. Bessell *et al.*, 1989), again only for those with effective temperatures higher than 2500K.

Thus, if the effects of line blanketing are to be taken into account within the modelling process, an alternative method must be sought to quantify the departure of the emergent spectrum from that of a black body. Rowan-Robinson & Harris (1983) derived empirical relations for the intrinsic broad band colour indices for their sample of M giants and Supergiants, which were then used to calculate 'correction factors', which gave the amount by which a black body model for a star of a particular effective temperature should be decreased as a function of wavelength, due to the effects of molecular line blanketing. Unfortunately, the synthetic colours derived by Rowan-Robinson & Harris bear no resemblance to the best current model atmospheres, and correction factors derived from them can not therefore be believed.

For example, Rowan-Robinson & Harris give the intrinsic V-K index for a star of spectral type Mt, where $4 \leq t \leq 9$ and is the spectral class, as:

$$V - K = 1.6t - 1.6 \tag{4.1}$$

For a star with an effective temperature of 2800K (to which Rowan-Robinson & Harris assign spectral type M5) this equation implies a V–K index of 6.4; However, in a recent model for a Mira with an effective temperature of 2800K, the V–K index was given as 10.8 (Bessell *et al.*, 1989).

Thus although the Rowan-Robinson & Harris method does in principle give a way of estimating the inaccuracies introduced by using a black body to represent the stellar energy distribution, it requires knowledge of the intrinsic colour indices of the star, which, as was pointed out above, are just not known for cool Miras like WX Ser.

It was therefore decided not to attempt to quantify the effect of the molecular line blanketing upon the model spectra at this stage in the analysis; If reliable stellar atmospheres and/or colour indices become available at a future date, then the models presented can be recalculated with an accurate estimate as to the size of this effect. Also, since the main thrust of this project was to examine the solid state dust features in the 8–23μm region of the spectrum, where the molecular blanketing effects are very small, it was felt an unneccesary complication would be added, should an an attempt be made to estimate an (at the moment) unquantifiable effect.

4.3.2 The distance to WX Ser

To date, there have been two published estimates as to the distance of WX Ser. Hyland *et al.* (1972) calculated a distance of 0.97 Kpc for the star, on the basis of assigning it an intrinsic luminosity of $(1\pm0.5)\times10^4$ $L_\odot$.

Alternatively, Rowan-Robinson & Harris (1983) estimated the distance to WX Ser as 0.72 Kpc, on the basis of an assumed relation between bolometric magnitude and spectral type at maximum light, which, as they admitted, was only a plausible extrapolation of their data for stars of spectral type later than M7. However, a comparison of distances ascribed to other stars in the sample examined by Rowan-Robinson & Harris using their method, and distances to the same stars provided by independent methods proved favourable, and thus for this work, a distance of 0.72 Kpc will be assumed for WX Ser.

To date, the only published value for the expansion velocity of the envelope of WX Ser comes from the work of Engels (1979) who studied maser emission from the circumstellar

shell. The envelope has, as yet, not been detected in any CO transition; indeed this was used by Knapp (1985) to put an upper limit to the gas mass loss rate of $\leq 7.4 \times 10^{-7} M_{\odot} y^{-1}$, which is a factor ten lower than the estimate derived in this work (Table 4.1). It is perhaps worthwhile noting here that the stellar radius given in Table 4.1 for WX Ser is derived from the modelling process as giving the best match to the observed energy distribution for the star.

4.4 Selection of photometry

All Mira stars exhibit periodic variations in their light output, with any variation having an amplitude which decreases with increasing wavelength (see for example Sopka *et al.*, 1985 for details). If a self-consistent model is to be developed for such a star, it becomes important to select photometry from the literature which has (ideally) been obtained coevally at all wavelengths, which would then represent an unique dataset describing the stellar energy distribution at a known photometric phase.

For many stars however, especially those which are optically faint, light curves may not be available, due to lack of observations, and indeed at the longer wavelengths, the very lack of observations can sometimes mean that only a single measure of flux is available for comparision with models, and no indication as to the amplitude of any variations at that wavelength can be made, nor indeed accounted for in the modelling process.

It often becomes neccessary to use a composite photometric dataset to derive the energy distribution for a star being modelled, with the individual photometric points having being obtained at different epochs. This introduces uncertainties into the modelling process, since neither amplitude nor period of a Mira are constant from cycle to cycle. Hence any irregularities in either amplitude or period would tend to make a composite energy distribution an inaccurate representation of the true photometric phase that it is supposed to describe.

This aspect is normally ignored in attempts to model spectra for variable stars, since the size of the inaccuracies introduced is probably small compared with the other unknowns used in the modelling process. Also since the amplitude of variation decreases with increasing wavelengths, the problem is only really serious in the UV to near-IR regime, becoming unimportant at the longer wavelengths.

It was decided to develop a model for the emergent spectrum of WX Ser for an epoch corresponding to that of maximum optical brightness. Therefore, for WX Ser, a Mira, whose amplitude and variation are fairly well defined, observations were selected at epochs (as derived from the published light curve, e.g. Kukarkin *et al.*, 1969) close to that of a maximum. The epoch of maximum given in the *General Catalogue of Variable Stars (GCVS)* by Kukarkin *et al.* was JD 2433365, and using this as a starting point the literature was searched for photometry obtained within ±0.2 of the 425.1 day period of a maximum.

Johnson magnitudes for WX Ser at B, V and R, obtained by Wisniewski *et al.* (1967) were converted to absolute fluxes via the calibrations in Allen (1973).

A further photometric dataset was presented by Hyland *et al.* (1972) in the near-mid IR region. The dataset was completed by the four colour *IRAS* fluxes, and 8-21μm LRS spectrum for the star obtained during 1983 (Beichman *et al.*, 1984).

4.4.1 Interstellar extinction towards WX Ser

In developing a model for the circumstellar dust shell of WX Ser, it becomes necessary to have some estimate as to the effect that interstellar reddening has upon the observed energy distribution of the star, before any models may usefully be compared with the observations. WX Ser is located at a high galactic latitude (53 degrees above the galactic equator, which Hyland *et al.* (1972), assumed indicated a perpendicular distance of nearly 800 parsecs above the galactic plane) and consequently escapes the largest effects of extinction in the plane of the Milky Way. It was therefore decided to investigate quantitatively whether extinction towards WX Ser should be included in the models for the star.

The parameterisation of Sharov (1964), which is essentially the same as that originally developed by Parenago (1940) was used to estimate the extinction in the Johnson V band towards WX Ser, and then the interstellar extinction curve in the 1–13μm region given by Rieke & Lebofsky (1985) was used to calculate the effect that the degree of extinction calculated at V for WX Ser might have upon the stars near to mid-IR spectra.

The method of Sharov was preferred to those of other authors since it provided a quantitative estimate the directional dependance of the V band extinction over the whole sky; in this scheme, the extinction $A(r,b)$, expressed as a function of galactic latitude, b,

Filter	Reddening Factor
V	3.98
R	2.81
I	1.95
J	1.48
H	1.27
K	1.16
L	1.08
M	1.03
N	0.78
10μm	1.07

Table 4.2: Calculated interstellar reddening factor as a function of λ towards WX Ser

and distance, r, in magnitudes at the Johnson V band is given by:

$$A(r,b) = \frac{a_0\beta}{\sin b}\left(1 - e^{-\frac{r\sin b}{\beta}}\right) \tag{4.2}$$

The values of the constants a_0 and β are given by Sharov for a total of 118 different regions which cover the entire sky, one of which, region 117 contains the sightline to WX Ser, for which values of $a_0 = 2.1 \pm 0.2$ and $\beta = 83 \pm 20$ are given. For the adopted distance of 720 parsecs, the formula gives a value of the interstellar extinction towards WX Ser in the Johnson V band of $\approx 1^m.5$.

Table 4.2 gives the factor by which model spectra must be reddened to match observations of WX Ser at a number of IR wavelengths, assuming the IR extinction law of Rieke & Lebofsky (1985) applies to the sightline towards WX Ser and that the V band extinction is $1^m.5$; it can be seen from this that the effect of interstellar extinction is really confined to wavelengths shorter than 1 μm for WX Ser. The reddening factor is the amount by which the model flux must be divided to 'correct' it for the effects of interstellar extinction.

The value of 1.5 magnitudes for the extinction towards WX Ser in the Johnson V band did seem rather large, given the high galactic latitude of the star, and before adopting it, it was decided to resort to another, more accurate method of deriving the interstellar extinction towards the star, as an independent check.

Burstein & Heiles (1982) derived line of sight reddenings in the galaxy using the HI/galaxy counts method. These authors published maps giving E_{B-V} as a function of galactic latitude, which they argue vales for the selective extinction accurate to ± 0.01 mag for any given direction. For the position of WX Ser, Burstein & Heiles give a value of 0.03 magnitude for E_{B-V}.

Adopting 3.1 as a value for the total to selective extinction (e.g. Allen, 1973) the value of A_V, or the extinction at V becomes 0.093 magnitudes, much smaller than that calculated via the Sharov method. It was decided to adopt this latter value for the magnitude of the interstellar extinction towards WX Ser, and, as it was such a small value, it was decided to neglect the effect of interstellar reddening towards WX Ser (as an example of why it can be neglected, the reddening factor at V is reduced from 3.98 to 1.09 in Table 4.2, if the extinction towards WX Ser at V is 0.093 magnitudes.)

4.5 Silicate dust grain parameters

One of the major aims of this work is to utilise the comprehensive model for radiative transfer through circumstellar dust shells, which was developed in Chapter 2, to test the relative merits of different proposed grain models against the photometric dataset described above for WX Ser at maximum light.

Presently however, there exists no real concensus as to the precise chemical nature of the O-rich agent responsible for the observed 9.7 and 18μm silicate features, and a variety of different 'runs' of complex refractive indices for the proposed grain materials have been published since the first assertion that silicate material of some form was responsible for the 9.7 and 18μm features.

Day (1979) gives the complex refractive indices of amorphous fosterite (a magnesium rich olivine) in the 8–30μm region which Hoare (1988) dismissed as not giving reasonable fits to IR observations of some sources, whilst Krätschmer & Huffmann (1979) gave a different set of dielectric functions for an irradiated form of amorphous olivine in the same spectral region, which Skinner & Whitmore in a series of papers claimed gave an excellent representation for the emergent spectra for M giants and supergiants in the mid-IR spectroscopic region (Skinner & Whitmore, 1987, 1988). Yet another set of complex refractive indices, published by Dorschner *et al.* (1986) for amorphous bronzite were used

by those authors to fit the mid-IR circumstellar spectra of T Tauri and young stellar objects.

To date, the most comprehensive collation of optical constants for silicate grains, based upon published IR astronomical spectra, has been that presented by Draine & Lee, and Draine (1985, 1987a,b) which cover the wavelength range from UV all the way through to the mm region. The Draine & Lee silicate dust has been used by a number of authors (e.g. Hoare, 1988; Hoare & Clegg, 1988; Middlemass, 1990) to model the emergent spectra from O-rich envelopes around planetary nebulae.

However, Skinner & Whitmore (1987) found that when the Draine & Lee dust was incorporated into models for the circumstellar environment of the M supergiant star α Ori, and for other M supergiants (Skinner & Whitmore, 1988), it did not match the observed 9.7μm feature in those stars, being broader than the feature observed in their spectra. As described above, Skinner & Whitmore suggested that the best match to the IR spectra from the circumstellar shells of the stars they were modelling was provided by dust grains whose emissivities were derived from the dielectric functions of Krätschmer & Huffmann (1979).

In the following sections, the conclusions of Skinner and Whitmore as to the non-applicability of the Draine & Lee complex refractive indices for modelling the mid-IR spectrum of WX Ser will be tested, using the more comprehensive radiative transfer code described in Chapter 2. It should be noted that, unlike the stars being modelled by Skinner & Whitmore, WX Ser does not appear to exhibit chromospheric emission, and thus the modelling process employed here has not the additional complication of the need for a stellar chromospheric model.

At the inner edge of the circumstellar dust shell, the principal heating mechanism for the dust grains is by absorption of optical radiation from the stellar photosphere, and therefore, if a fully self-consistent model is to be produced for the emergent spectrum of WX Ser, it becomes important to have a 'run' of complex refractive indices, or dielectric functions, from ultraviolet to millimetre spectroscopic regions, for all grain materials being tested in the model. For Draine & Lee's dust, this information is already available, but for the dust composition proposed by Krätschmer & Huffmann, the dielectric functions were only measured between 8 and 30μm, and hence these must be joined to other measured dielectic functions, if the wavelength coverage is to match that of the Draine & Lee dust.

Skinner & Whitmore joined the Krätschmer & Huffmann data to the measurements of Jones & Merril (1976) for a 'dirty silicate'; The substance was termed 'dirty' because the imaginary component of the refractive index was allowed to have a finite value, which, unlike that in 'clean' silicates, which have a small or absent imaginary component of the refractive index, allowed some absorption in the optical region of the spectrum; in this model the grain refractive index has a constant value, given by:

$$\epsilon = 2.39 + 0.31i \tag{4.3}$$

at all wavelengths shorther than 8μm. However, as pointed out by Draine & Lee (1984), the more recent work of Rogers, Martin & Crabtree (1983) favoured a different (but again constant) value of:

$$\epsilon = 2.3 + 0.03i \tag{4.4}$$

in the range 0.7–4.8μm, as this gave a better match to observations made in that region.

Draine & Lee decided to adopt a dielectric function which was intermediate in absorptivity between those of Jones & Merrill and Rogers, Martin & Crabtree, in the 1–5μm region but had the advantage of smoothly joining the mid-IR data to that measured for grains at much shorther wavelengths.

Although in reality, in the 1–5μm region there is little difference between the dielectric function adopted by Skinner & Whitmore, and that derived by Draine & Lee, the latter is adopted here since the Draine & Lee data provide a way of testing observations of WX Ser obtained at wavelengths as short as 0.55μm, whilst the models of Skinner & Whitmore stopped at 1 μm.

Thus, the adopted dielectric function for Krätschmer & Huffmann dust grains in the region $\lambda \leq 8\mu$m is that for silicate grains derived by Draine & Lee (1984). At 8μm the Draine & Lee dielectric functions are then swapped for those measured by Krätschmer & Huffmann (1979), and in fact an examination of the data indicates a remarkably smooth transition between the two datasets.

4.5.1 Grain shape, size distribution and density

As discussed in Chapter 2, the bulk grain properties (emissivity, albedo and scattering asymmetry parameter) needed to specify the transfer of radiation through the circumstellar dust shell can be calculated for dust grains via Mie theory.

However, the grain properties calculated in this way are strongly dependent upon grain shape. In order to account for the observed polarization in the 9.7μm feature towards some astronomical sources, Draine & Lee (1984) assumed their grains to be oblate spheroids, with a 2:1 axis ratio. Skinner & Whitmore on the other hand assummed their grains to be spherical, and calculated their dust parameters accordingly.

In this work, it is assumed that the dust grains in the envelope of WX Ser are spherical. This is because, in the view of the author, an arbitrary assumption on grain shape, based on observations of other sources would not be warranted at this time. If observations as to the existence of polarization in the 9.7μm feature of WX Ser do come to light at some future date, it will then be time to introduce this added complexity into the models for this star.

As described in Chapter 2, the radiative transfer code used to model the emergent spectrum of the star allows for a power law distribution in dust grain sizes, whereby the number density of grains of radius a, per unit grain radius at a distance r from the central star is:

$$n_d(a,r) = n_d(r)a^{-p}, \qquad a_1 \leq a \leq a_2 \tag{4.5}$$

As a starting point for the modelling process, the Mathis, Rumpl & Nordsieck (MRN, 1977) grain size distribution is adopted, in which p=3.5, a_1 = 0.005μm and a_2 = 0.25μm. This distribution was adopted since it has been shown by Biermann & Harwitt (1980) to provide a plausible description of the relative numbers and sizes of grains resulting from grain-grain collisions in the outflows from massive cool stellar atmospheres.

More recent observational studies of dust grains in the outflow of α Sco (Seab & Snow, 1989) have implied that there is a cut off in the size distribution of the circumstellar silicate grains, and that grains smaller than 800Å are rare, or perhaps not present at all in the circumstellar envelope of this star, implying, if true, that the lower limit to the MRN distribution is a factor $\approx$10 too small for the grains in O-rich circumstellar envelopes. However, the data are confined to just one star, and this work may provide

further information as to the relevence of Seab & Snow's work to other stars.

The grain emissivity, albedo and asymmetry parameter was calculated via Mie theory for each of 20 grain sizes at each wavelength of interest. The selected grain radii linearly spanned the MRN grain size distribution, and this enabled the calculation of grain temperatures for each grain size component as a function of radial distance from the central star, during the modelling process.

The density of the adopted grain material does of course vary with the chemical composition of the grains. Olivine is a magnesium-rich silicate material, whose density may be approximated as (Deer, Howie & Zussmann, 1976):

$$\rho_{Mg} = 4.32 - 1.8[Mg^{2+}] g cm^{-3} \tag{4.6}$$

In which $[Mg^{2+}]$ is the atomic proportion of magnesium. Generally, the composition of olivine in circumstellar shells has been assumed in previous studies (e.g. Skinner & Whitmore, 1987) to be $(Fe_{0.07}Mg_{0.93})_2SiO_4$, which gives $\rho_d \approx 3.30 g cm^{-3}$.

4.5.2 Far-IR emissivity of silicate dust grains

As discussed more fully in Chapter 3, the far-IR (i.e. $\lambda \geq 20\mu$m) emissivity of circumstellar dust is dependent upon both its chemical and its physical structure, and indeed also upon the size and shape of the grains which compose it.

For silicate grains situated in circumstellar dust shells, it has generally been assumed that the grains have metallic properties (Andriesse, 1974; Aannestad, 1975) and in consequence the grain emissivity should fall off as λ^{-2}. This was indeed the claim of Skinner and Whitmore based on their analysis of a number of M stars, whilst Forrest *et al.* (1979) also obtained a λ^{-2} slope for the dust emissivities in the 16-39μm region from simple models of stars of the same spectral type.

Rowan-Robinson & Harris (1983a,b), and Rowan-Robinson *et al.* (1986) however chose to explain the observed far-IR spectra of stars of the same spectral type (including in fact WX Ser!) as those observed by Skinner & Whitmore by using a grain emissivity function which fell off as λ^{-1}, whilst Volk & Kwok (1988), in their models for circumstellar shells of M type stars prefer to use an emissivity law which was proportional to λ^{-1} in the 20–μm region, but which steepened to λ^{-2} longwards of 84μm.

The differences between these modelling schemes, and the fact that all of them managed

to fit identical spectra in a satisfactory manner, is an example of how difficult it is to obtain an unique match to an observed spectrum with any model; Skinner & Whitmore's model used a MRN distribution of grain sizes in the dust shell, and assumed a stellar chromosphere was responsible for supplying free-free emission in the far-IR, whilst Rowan-Robinson *et al.* and Volk and Kwok chose to explain the far-IR emission from the objects in terms of dust emission alone from grains of a single size in the circumstellar shells.

It was partly to examine which of these, very different models for the circumstellar environments is closer to the truth, that WX Ser was chosen for this project, since, as described above, it shows no evidence for the existence of a chromosphere, and may therefore be safely modelled as an example of a star in which dust plays the major rôle in sculpting its observed spectrum. In this work, the far-IR emissivity of dust grains will be allowed to fall off as λ^{-1} and λ^{-2} longwards of 25μm, to test which gave the best fit to the observed energy distribution of WX Ser.

4.5.3 Dust shell inner radius

The dust shell inner radius is determined by the condensation temperature of the grains. For the purposes of this project, the dust shell inner radius is defined more precisely as the radial distance from the central star at which the ambient temperature of the warmest dust grains (as calculated by the radiative transfer code) reaches the grain condensation temperature.

Once again, there exists no real concencus as to the precise coindensation temperature of silicate dust grains, with some authors favouring values as high as 1500K (Volk & Kwok, 1988), others (e.g. Skinner & Whitmore) a value of 1000K, whilst a value as low as 500K was used as the dust temperature in the shells of some stars by Rowan-Robinson *et al.*, (1986). Given such a diverse selection of proposed condensation temperatures, it was decided to construct models for the dust shell of WX Ser with grains allowed to condense at each of these temperatures, and to select the one which best fitted the observations.

4.5.4 Dust shell outer radius

If a realistic model for the emergent flux from WX Ser at the far-IR and radio regions of the spectrum is to be developed, then the choice of dust shell outer radius becomes fairly important, since most of the flux at the longer wavelengths will originate in the cooler,

outer regions of the dust shell. Rowan-Robinson *et al.* (1986) adopted a value of 1000 times the inner dust shell radius in their models for the dust shells around M stars, whilst Skinner & Whitmore (1987, 1988a,b) chose to terminate their radiative transfer models when the dust temperature reached a 'typical' interstellar value, which they decided was 30K.

Spatially resolved observations of the WX Ser dust shell are not as yet available, and hence can cast no additional light on its extent. In this work, it was decided to follow the example of Skinner & Whitmore and chose the point at which the coolest grain temperatures reached 30K as defining the outer radius of the dust shell; In reality, as there are no observations of WX Ser at wavelengths longwards of 100μm, the difference between adopting the Rowan-Robinson *et al.* outer radii, and the one chosen, was very small.

In all models discussed below, the mass loss which gives rise to the dust envelope is assumed to be spherically symmetric, and constant for the time it has taken for the dust shell to reach its present state.

4.5.5 Dust to gas ratio in the circumstellar envelope

The dust to gas ratio in the circumstellar envelope of WX Ser is not known. Studies of the dust to gas ratio in the interstellar medium (see for example J. L. Puget in Lucas *et al.*, 1985) suggest a dust to gas ratio by mass of between 1.0×10^{-3} and 1.0×10^{-2}, but there is no evidence that the value in the circumstellar shell of WX Ser should be the same.

Knapp (1985) derived a mean gas to dust ratio by mass in a sample of O-rich Mira variables of $\approx 6 \times 10^{-3}$ by comparing the gas mass loss rates calculated from her observations of the stars CO envelopes by the dust mass loss rates for the same sample of stars derived from the radiative transfer models of Rowan-Robinson & Harris (1982, 1983a,b).

Using a different dust modelling method from that of Rowan-Robinson & Harris, Skinner & Whitmore (1987, 1988a,b) discovered that a fixed value 0.002 for the gas to dust ratio could be used to successfully model the emergent spectra of a large number of O-rich envelopes around M type giants and supergiant stars, if the gas mass loss rates for the same stars were calculated from observations of circumstellar CO emission. Similarly low values for the dust to gas ratio of $\leq 1.0 \times 10^{-3}$ have been calculated from models of the dust emission from the neutral regions in envelopes of O-rich planetary nebulae by Hoare (1988) and Hoare & Clegg (1988), who, like Skinner & Whitmore adopted the MRN grain

size distribution in their modelling of the sources.

It was decided to copy Skinner & Whitmore and adopt a value of 0.002 for the dust to gas ratio in the circumstellar envelope of WX Ser. As only an upper limit to the gas mass loss rate existed, on the basis of the CO observations, this provided one way of deriving the mass loss rate for the star. Modelling the source then consisted of varying the gas mass loss rate, until a good fit could be made to the observations, once the effects of interstellar reddening had been taken into account.

4.6 Results

4.6.1 Draine & Lee models

The radiative transfer model calculated for the circumstellar envelope of WX Ser using the Draine and Lee dust parameters provides a poor fit to the mid-IR spectrum of WX Ser. The best model, presented as Figure 4.1, shows a definite difference in shape between the observed 9.7μm feature and that predicted by the model. This model, which assumed a dust condensation temperature of 1000 K and a dust to gas ratio in the envelope of 0.002 provided a fair fit to the near and far-IR observations, but was completely inappropriate to the *IRAS* LRS spectrum of WX Ser. Note that for these exploratory models, the grain emissivity was allowed to fall off as λ^{-1} at wavelengths longer than 22μm; this will be examined in more detail in a later section.

A detailed comparison of the Draine & Lee dust model with the *IRAS* LRS spectrum is given as Figure 4.2. Here it can be seen that though a fair fit to the 18μm region is obtained, the 9.7μm feature of the model is different in character to that shown in the observations.

Thus the finding by Skinner & Whitmore that the Draine & Lee dust does not fit the 9.7μm feature observed in M type stars, is confirmed here for the M type Mira WX Ser. However, the 18μm region of the WX Ser spectrum is matched quite well by the model spectrum; since Draine & Lee derived their complex refractive indices in this region in part from observations of dust shells of late type stars.

The discovery that the WX Ser 9.7μm feature is not matched by a model based upon Draine & Lee dust parameters is not at all surprising, since the aim of Draine & Lee in providing a run of complex refractive indices was to match the 9.7μm feature observed in

Figure 4.1: Model fit to WX Ser photometry, using Draine & Lee dust parameters

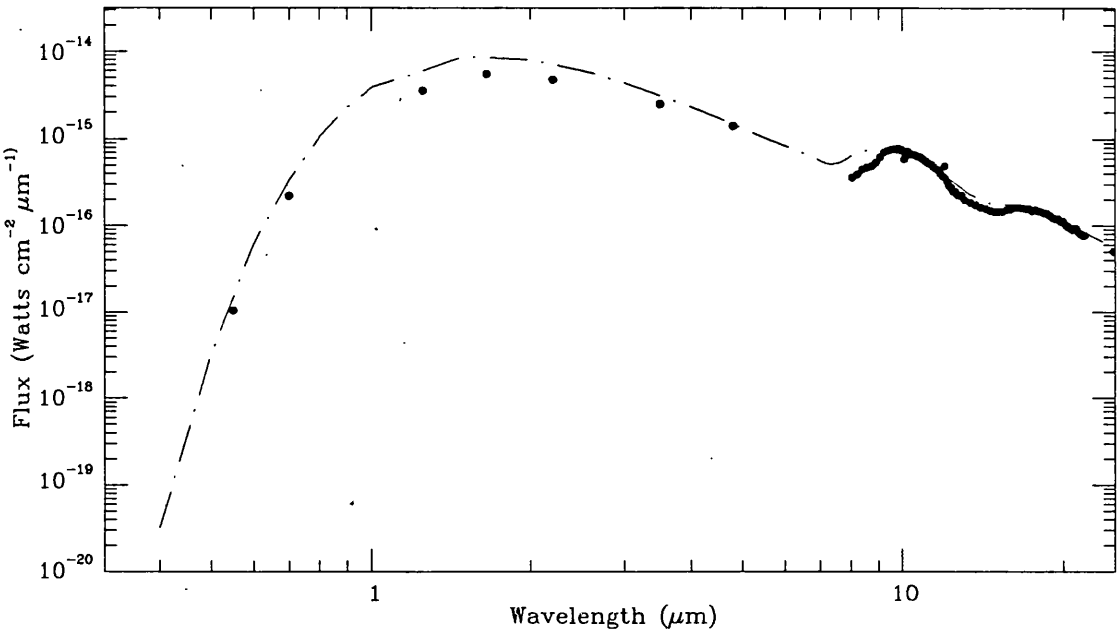

the Trapezium region of the Orion nebula. This is an HII region, where the physical and chemical environment of the dust grains is very different to that thought to occur in a circumstellar outflow, and it is not therefore surprising that grains with slightly different optical properties to those condensing in the outflows from evolved stars are observed there.

Thus, although the Draine & Lee dust provides a good match to the spectra of HII regions and PN (e.g. Hoare, 1988; Hoare & Clegg, 1988), dust with different optical properties in the 9.7μm region is required to match the observed spectrum of WX Ser. In an attempt to locate dust that does match the spectrum of WX Ser in that region, the Krätschmer & Huffmann dust, favoured by Skinner & Whitmore in their series of papers will now be examined.

4.6.2 Krätschmer & Huffmann Models

The best fit achieved to the photometry of WX Ser using a model based upon the dust parameters of Krätschmer & Huffmann (in the 8–20μm region of the spectrum) is presented as Figure 4.3. It was found that the best fit to the photometry again came by adopting

Figure 4.2: Model fit to *IRAS* LRS spectrum of WX Ser, for model using Draine & Lee dust parameters

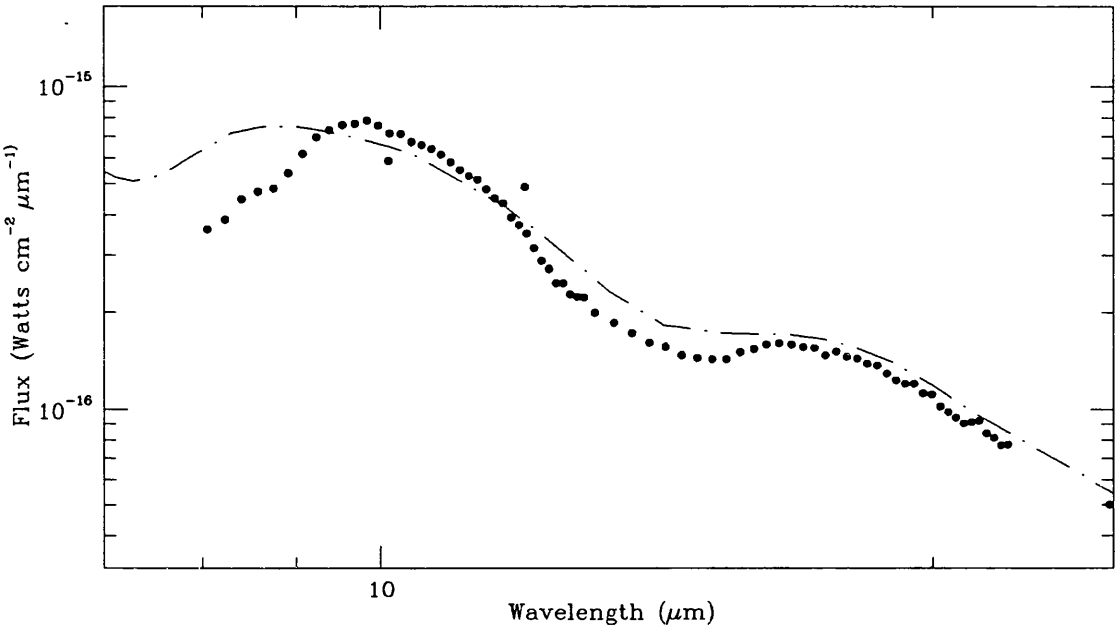

a dust to gas ratio of 0.002 in the stellar outflow, and by using a dust condensation temperature of 1000 K to determine the inner radius of the dust shell.

Generally the fit to the photometry is good, except, once again in the mid-IR region, where the fit becomes poor at wavelengths longer than $\approx 12\mu$m.

A detailed comparison between the best model and the *IRAS* LRS spectrum of WX Ser, which can be made using Figure 4.4. reveals that a superior fit to the 9.7μm feature is indeed obtained by using the Krätschmer & Huffmann data rather than those of Draine & Lee; however, the fit in the region 13-20 microns is markedly poorer.

It appears that the ratio of 9.7μm to 18μm features is too small in the Krätschmer & Huffmann models, and that the depth of the central 'trough' between the two features is too deep in the model when compared to the observations. Because Skinner & Whitmore always found that emission from a mooted chromosphere dominated in their sample of stars at wavelengths longer than $\approx 15\mu$m, they would not have discovered this effect of using the Krätschmer & Huffmann dielectric function, which will, as shown here, only become apparent for stars in which dust is the chief source of emission at $\approx 18\mu$m.

Figure 4.3: Model fit to photometry of WX Ser, for model using Krätschmer & Huffmann dust parameters

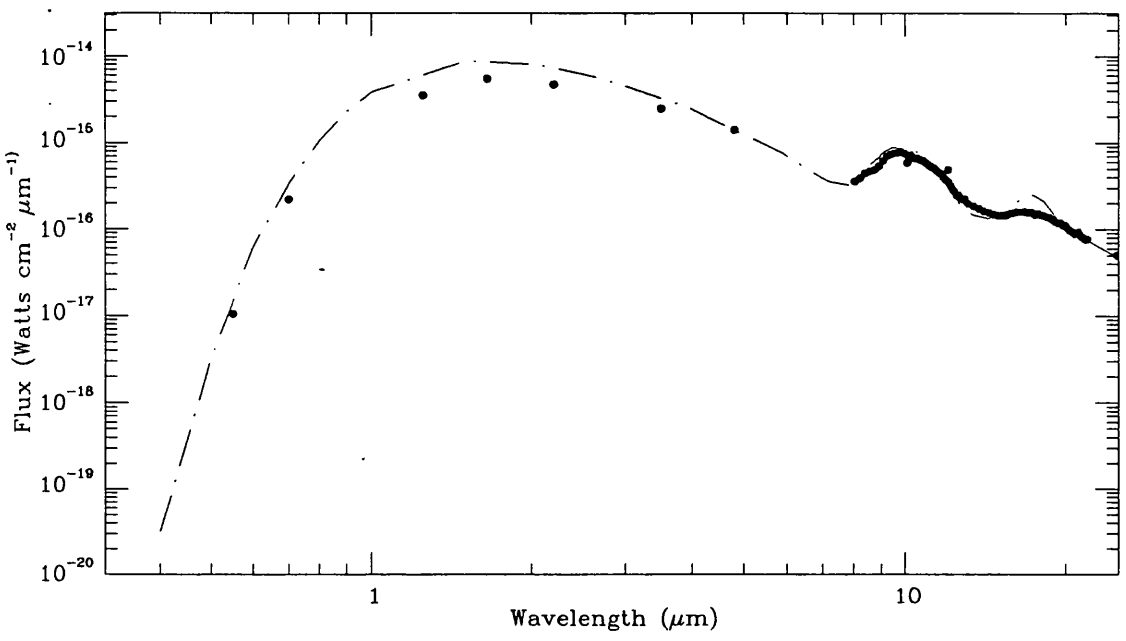

4.6.3 Production of a 'composite' dust model

It became apparent that neither the Krätschmer & Huffmann nor the Draine & Lee datasets gave a good representation of the spectrum of WX Ser in the region 8-23μm. However, it was noted, from examination of the fits of both of the best models to the photometry, that since the Krätschmer & Huffmann data provided a good fit to the observations in the wavelength range 8–12μm and the Draine & Lee data provided a better fit at the longer wavelengths, there might perhaps be some benefit in attempting to create a new 'composite' set of dielectric functions for the 8–22μm region, which utilised the 'best fitting' regions of each run of dielectric functions. To this end, the individual runs were compared, and a decision made where they could best be merged.

Table 4.3 presents the final set of dielectric functions adopted. The values of ϵ_1 and ϵ_2 from 0.3–7.93μm are those of Draine & Lee; from 7.93–11.69μm the values are derived from the measurements of Krätschmer & Huffmann, whilst longwards of 11.69μm, the values are again those of Draine & Lee. The adopted dielectric function provided for a fairly smooth join between the different datasets.

$\lambda(\mu m)$	ϵ_1	ϵ_2
0.3	3.1	0.100
0.4	3.0	0.101
0.5	2.964	0.101
0.6	2.924	0.100
0.7	2.940	0.101
0.8	2.940	0.102
0.9	2.940	0.103
1.0	2.940	0.104
1.5	2.930	0.107
2.0	2.920	0.113
2.5	2.904	0.119
3.0	2.880	0.126
4.0	2.814	0.137
4.5	2.403	3.1E-02
5.0	2.411	3.1E-02
5.2	2.381	3.1E-02
5.5	2.269	3.2E-02
5.8	2.134	2.9E-02
6.2	2.012	1.2E-02
6.6	1.912	3.2E-03
6.9	1.843	1.0E-03
7.1	1.804	4.8E-04
7.2	1.795	2.6E-03
7.3	1.782	9.1E-03
7.6	1.721	2.3E-02
7.9	1.570	4.0E-02
8.2	1.402	0.173
8.6	1.204	0.279
8.8	0.993	0.383
9.0	0.782	0.512
9.1	0.757	0.567
9.4	0.435	0.854
9.8	4.4E-02	2.055
10.1	0.282	2.607
10.4	0.882	3.128
11.6	3.898	4.465
13.3	3.928	2.396
14.2	3.539	1.829
15.3	2.898	1.848
16.6	2.423	2.264
17.3	2.259	2.604
18.1	2.179	3.022
19.0	2.230	3.500
20.0	2.470	3.990
21.0	2.783	4.305
22.2	2.097	4.593

Table 4.3: Adopted Dielectric function for 'composite' silicate dust

Figure 4.4: Model fit to *IRAS* LRS spectrum of WX Ser, for model using Krätschmer & Huffmann dust parameters

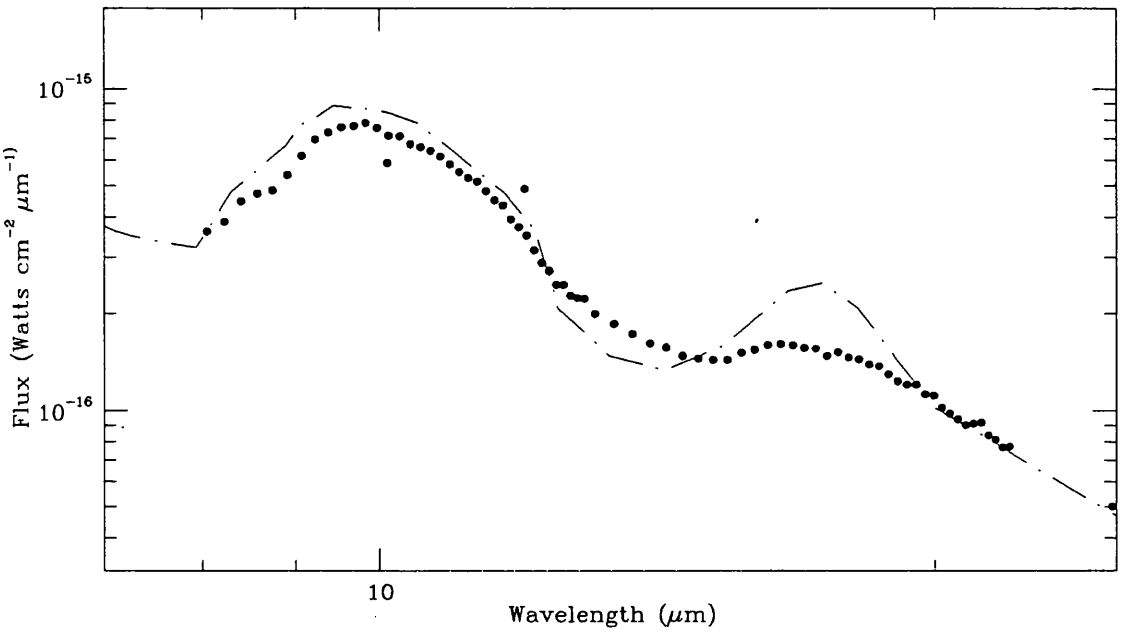

4.6.4 A composite dust model for WX Ser

The dielectric function given in Table 4.3 was used to calculate grain emissivity, albedo and scattering assymetry parameter for each of the 20 grain radii spanning the MRN grain size distribution, and then these grain parametars were used as the basis for a radiative transfer model for the dust shell of WX Ser, in exactly the same was as was done for the individual Draine & Lee and Krätschmer & Huffmann datasets.

The best fitting model, presented as Figure 4.5 does indeed appear to give a better fit to the observations than either of the two previous 'best fits', although the fit is still by no means perfect in the 12-16μm region, where the grain emissivity appears too high when it is compared with the observations. This can be better seen in the larger scale plot of the 8–23μm region given as Figure 4.6, which shows that the model emissivity is nearly 20% higher than the observations in this region of the spectrum.

The dust optical depths in the 4–22μm region of the spectrum may be compared by examining Figure 4.7, which also effectively shows the 'cross-over' regions in the composite model, where a change was made between the Draine & Lee and Krätschmer & Huffmann

Figure 4.5: Model fit to WX Ser photometry, for model using composite dust parameters of Table 4.3

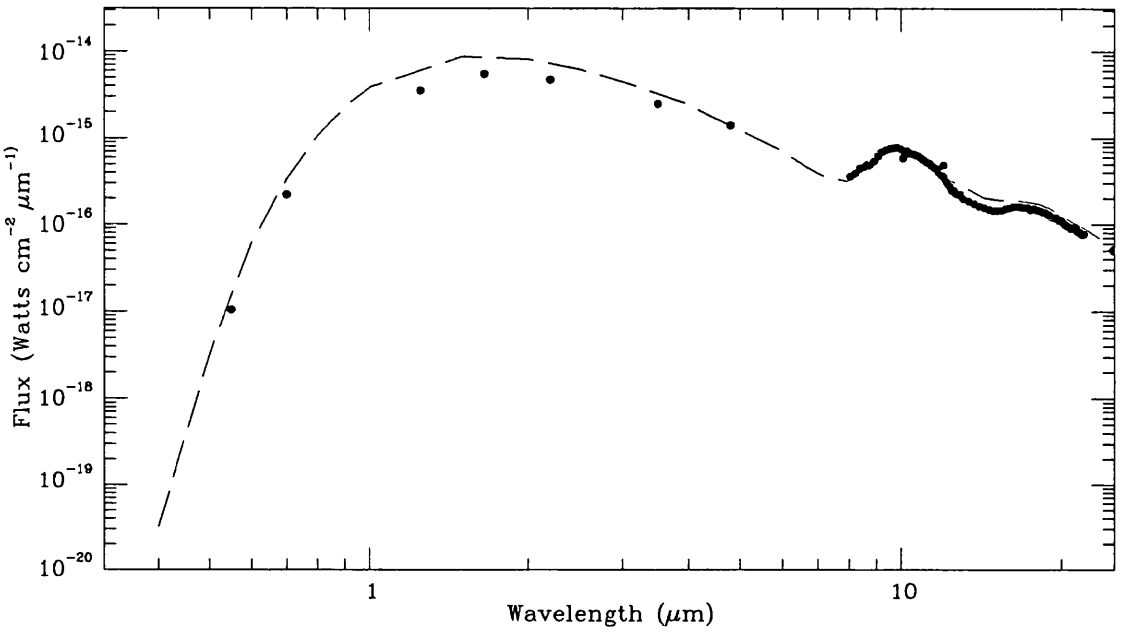

dielectric functions.

It can be seen from Figure 4.7 that for all models, the optical depth in the 9.7μm feature is just over unity, and therefore the dust shell is just becoming optically thick at this wavelength.

The parameters for this best fitting model with composite dust are identical to those for the best fits obtained with the other dust dielectric functions (i.e. stellar parameters are identical with those in Table 4.1); a dust condensation temperature of 1000K again gave the closest match to the optical photometric points. A gas mass loss rate of $4.0 \times 10^{-6} M_{\odot} y^{-1}$ is implied, for the adopted dust-to-gas ratio of 0.002. This is a factor of $\approx$5 times greater than the upper limit to the mass loss rate of the star inferred by Knapp (1985) from her non-detection of CO lines from the circumstellar shell of the star. However, the mass loss rate derived here is, rather surprisingly, given the differences in modelling techniques, in agreement with that derived by Rowan-Robinson & Harris (1983) for WX Ser.

The best model predicted that the 1000K grain condensation temperature was reached at a radial distance of 1.27×10^{14} cm or 3.175 stellar radii from the photosphere, once again

Figure 4.6: Model fit to *IRAS* LRS spectrum of WX Ser, for model using composite dust parameters

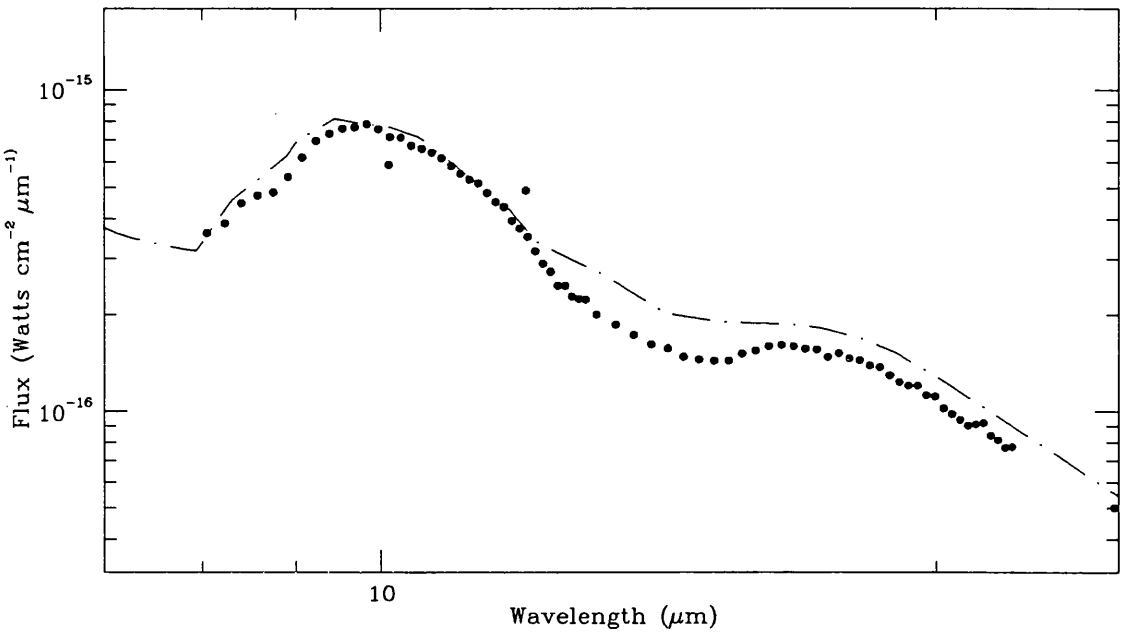

assuming a dust to gas ratio of 0.002 in the envelope. At this inner radius, the temperature difference between the largest and smallest dust grains was approximately 100K, with the larger grains having the warmer temperature.

In the model, the outer radius of the dust shell was assumed to be 1.27×10^{17}cm, where predicted grain temperatures had fallen to a value of $\approx$ 41 K for all grain radii, for a model where the far-IR emissivity of dust grains was allowed to fall off as λ^{-2} (see below for discussion). The temperature gradient through the dust shell for both largest and smallest grain sizes in the MRN size distribution used in the modelling procedure is plotted in Figure 4.8.

The 1000K condensation temperature used in the best fitting model is identical to that used by Rowan-Robinson & Harris (1983b) in their model for this object, and is also the same as that used by Skinner & Whitmore in their models for O-rich circumstellar shells. Models which utilised the higher condensation temperature, favoured by Volk & Kwok (1988) of 1500K for Silicate dust grains were found to exhibit too much absorption in the optical (0.5–1.0μm) spectroscopic region.

Figure 4.7: Dust optical depths in the 4–22μm spectral region for each of the three 'best' models for WX Ser

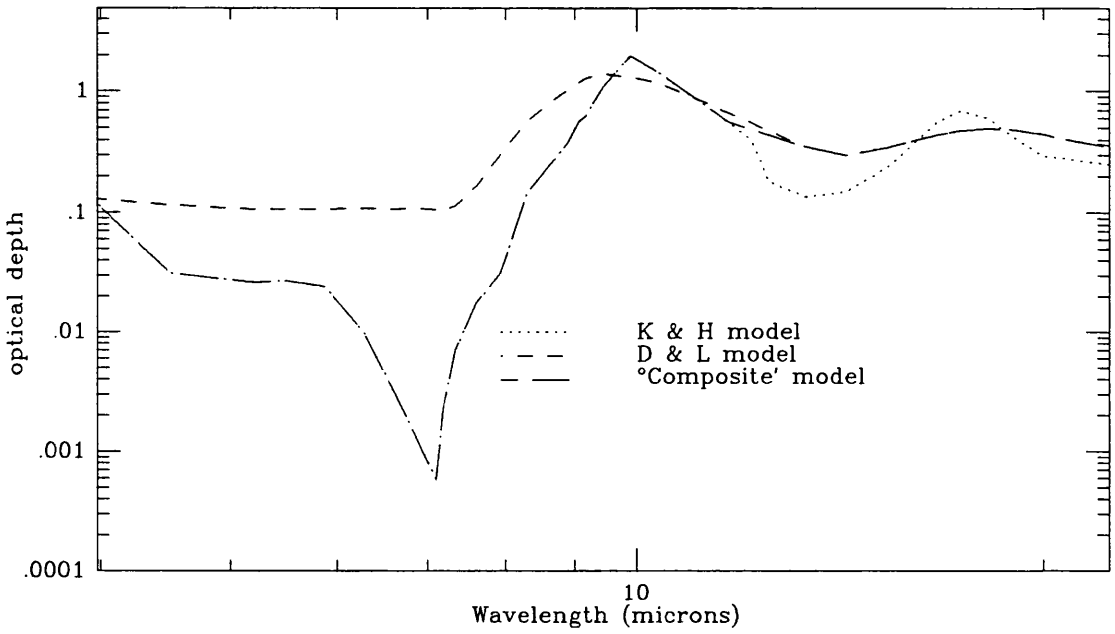

This can be explained by the fact that in that model, dust grains condensing at 1500K would be present in the inner and more dense regions of the envelope (condensation was predicted to occur at 2.3R$_*$) and hence a larger number of grains would exist, causing more obscuration in the optical than occurred in the model with condensation occuring at 1000K.

4.6.5 Far-IR emissivity of grains in the WX Ser circumstellar shell

As discussed earler in this Chapter, one of the key ways of assesing the physical structure of dust grains in circumstellar envelopes is to study how the grain emissivity varies as a function of wavelength. To this end, models were calculated with emissivity variation in proportion to λ^{-1} and λ^{-2} longwards of 22μm.

In Figure 4.9, two models with different grain emissivities are directly compared with the *IRAS* long wavelength photometry at 25, 60 and 100μm of WX Ser; it is easily apparent that the best fit to the long wavelength observations comes from a model with emissivity variation in proportion to λ^{-2}.

Figure 4.8: Dust temperatures as a function of radial distance through the WX Ser dust-shell for largest and smallest grains in the MRN size distribution.

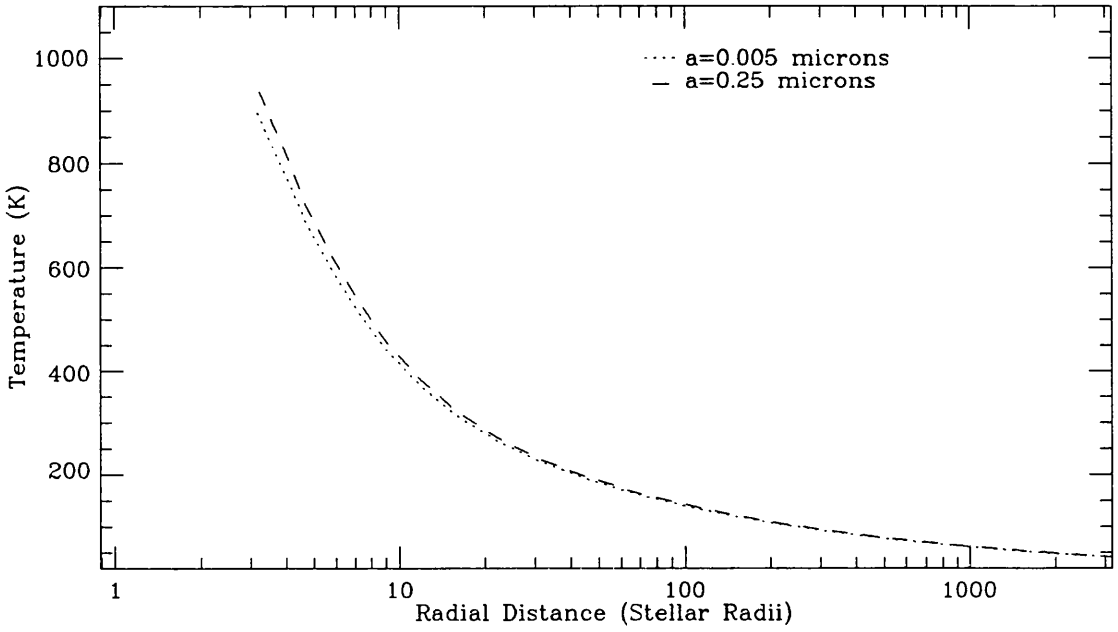

It is perhaps worthwhile at this point discussing how the *IRAS* photometric fluxes at 12, 25, 60 and 100μm were 'colour corrected' for direct comparison with the model spectra. The fluxes in the *IRAS* Point Source Catalogue were calculated by assuming that the intrinsic flux from the source $f_\nu \propto \nu^{-1}$. In order to compare the model spectra with the *IRAS* observations, it is necessary to calculate the observed fluxes at the effective wavelength of the photometric bands.

To perform this operation, the *IRAS* non-colour corrected flux was divided by a 'colour correction factor' (*IRAS* Explanatory Supplement, 1985) whose size required knowledge of the actual shape of the intrinsic spectrum of the source. One way to do this would be to approximate the shape by assuming a single temperature for the dust shell, and then using the slope of the Planck curve appropriate to that temperature as the shape However, this would not be appropriate if dust emission features were present in the bands. It was therefore decided to use the slope of the model spectrum to calculate the colour correction factor. In this case, the colour correction is given simply by the model band flux, divided by the model flux at the effective wavelength of the band. The model band

Figure 4.9: Model fit to complete WX Ser energy distribution, for model using composite dust parameters

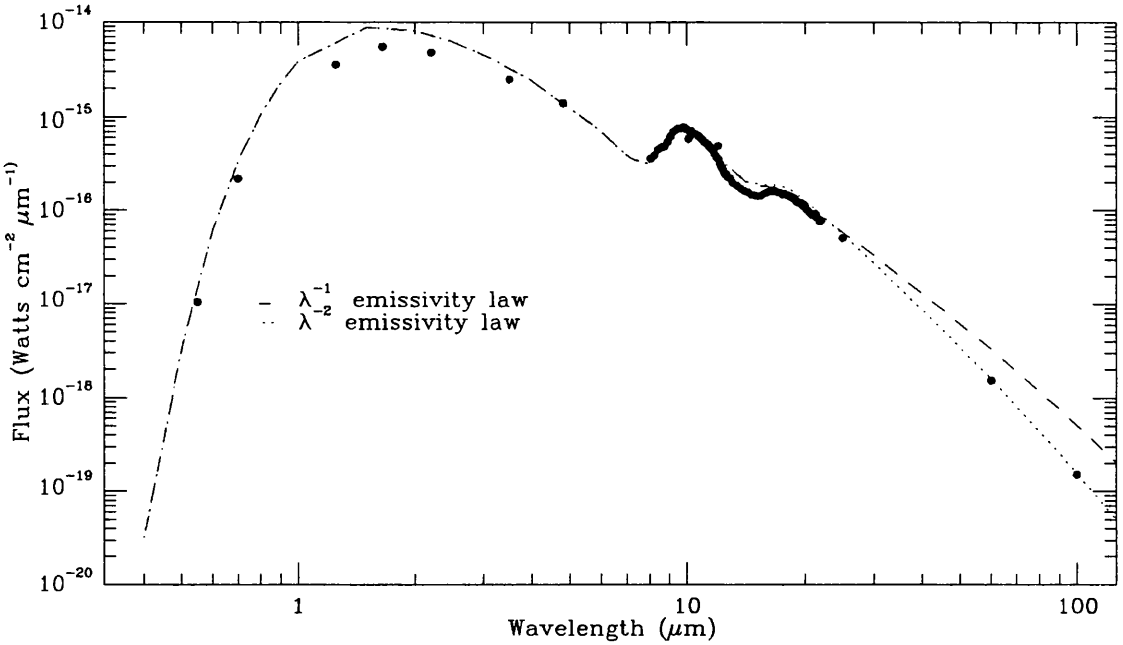

flux was calculated by convolving the model spectrum with the known responses of the *IRAS* filters, as tabulated in the *IRAS* Explanatory Supplement, 1985.

The best fitting model, with its fall off in emissivity proportional to λ^{-2} is in agreement with the models of Skinner & Whitmore, and does perhaps add weight to their suggestions that chromospheric emission may be responsible for the observed far-IR excesses observed in some M stars, where a fall off in emissivity less steep than λ^{-2} longwards of 20μm has been derived.

It is interesting to note that for this (admittedly single example) of an M type Mira, the λ^{-2} emissivity does provide a much better fit to the observations than the λ^{-1} law favoured by Rowan-Robinson & Harris and Volk & Kwok in their models for M stars in the 20-100μm region.

The difference is almost certainly due to both sets of authors utilisation of singly sized grains in their dust models. The superiority of the model proposed here over those suggested by previous workers is perhaps best supported by the fact that what laboratory observations and theoretical studies (e.g. Aanestad, 1975) there have been of silicate dust

grain emissivity longwards of 20μm are suggestive of a λ^{-2} emissivity law for the dust grains. It seems therefore that a grain size distribution must be incorporated into grain models if realistic properties of circumstellar dust, and indeed circumstellar dust shells are to be derived.

However, the extension of this work to the sample of stars examined by Skinner & Whitmore is required before this can be positively stated. Of particular interest also would be an investigation as to whether the λ^{-2} slope required to fit the observations of WX Ser in the 20-100μm region continues further into the mm and radio region of the spectrum. This will have to await the availability of observations at the longer wavelengths, which, given the recent advances in sensitivity of mm and sub-mm astronomical instrumentation, should be forthcoming in the not too distant future.

4.7 Conclusions

A detailed radiative transfer model for the observed energy distribution for the M type Mira star WX Ser at maximum light has been presented which can successfully match observations of the star in the wavelength range 0.55–100μm. Dust is found to play the dominant rôle in determining the observed spectrum of this source throughout the wavelength range modelled. A dust shell composed of silicate dust grains with radii in the range $0.005 \leq a \leq 0.25$ μm (whose distribution in sizes was identical to that proposed by Mathis, Rumpl & Nordsieck, 1977) was found to give an excellent fit to photometric observations of the star at maximum light.

A new 'composite' dielectric function has been proposed which gives a better fit to the observations of WX Ser in the 8–23μm region of the spectrum than that given by dielectric functions in the same spectroscopic region proposed by Draine & Lee (1984, 1987) and Krätschmer & Huffmann (1979). A dust condensation of 1000K for silicate grains was found to provide the optimum fit to the observed spectrum, and a λ^{-2} fall off in grain emissivity was found to provide the best fit to the colour corrected *IRAS* photometric fluxes for the source.

The best fitting model assumed a stellar temperature of 1960K, and a dust-to-gas ratio of 0.002 throughout the shell, implying a gas mass loss rate of $4.0 \times 10^{-6} M_{\odot} y^{-1}$.

Chapter 5

A Model for the Infrared and Radio Spectral Energy Distribution for IRC+10°216

In this chapter, a model is presented for the infrared, millimetre and radio continuum emission from the mass losing Carbon star IRC+10°216 at maximum IR brightness. The model is based upon a comprehensive analysis of the transfer of radiation through the star's circumstellar dust envelope. It is shown that recent observations of centimetre continuum radio emission may be understood in terms of the sum of thermal dust emission from amorphous carbon dust grains in the circumstellar envelope, plus the emission from the stellar photosphere, which in the models, becomes important at long ($\lambda \geq 100\mu$m) wavelengths, where the dust shell becomes optically thin to the underlying stellar photosphere. The dust to gas ratios for amorphous carbon and silicon carbide dust components in the circumstellar envelope are found to be 2.5×10^{-3} and 5.0×10^{-4} by mass respectively. Recent sub-millimetre and radio observations of the flux distribution from IRC+10°216 may be explained if the far infrared emissivity of dust grains is allowed to vary as λ^{-1}, though at the longest wavelengths, the observations require another emission component, which is suggested to be free-free emission from an optically thick chromosphere whose temperature is of the order 10,000K.

5.1 Introduction

Since its discovery in the 2 μm sky survey (Neugebauer and Leighton 1969) , IRC +10°216 has been observed at a variety of wavelengths spanning the range from visible to millimetre. Recently this wide wavelength coverage has been extended to centimetre radio wavelengths by the work of Spergel *et al.*(1983) and Sahai *et al.*(1989). As the prototype for the class of highly obscured carbon stars, and because it is the only object of this class to have been observed at the longer wavelengths, IRC+10°216 offers an unique opportunity to test the emissivity of dust grains in carbon rich envelopes over the entire range from optical to radio.

A number of different condensates are predicted to form in C-rich environments. Both graphite (Hoyle & Wickramasinghe 1962) and amorphous carbon (AC) grains (Draine 1981) have been suggested as the chief sources of dust emission in C-rich conditions, though the non-detection of the predicted 11.52μm emission feature of crystalline graphite in IRC+10°216 by Treffers and Cohen (1974) and by Glasse *et al.* (1986) in the circumstellar shell of the Wolf-Rayet star Ve 2-45 has been used as evidence against graphite being a major constituent of grains in carbon rich environments, and most recent models for the observed spectrum of IRC+10°216 (for example Martin and Rogers 1987; Le Bertre 1987, 1988b; Orofino *et al.* 1987, 1990) have relied upon single sized AC grains to represent the principal dust condensate.

Other condensates are also expected to form in C-rich circumstellar dust shells, and spectral emission features seen at 11.4μm and 30μm are generally ascribed to silicon carbide (SiC) (Treffers and Cohen 1974) and magnesium sulphide (MgS) (Goebel & Moseley 1985), respectively. To date, most workers have ignored these 'minor' constituents of C-rich circumstellar envelopes, when attempting to model emergent spectra, since outside the regions of their spectral emission, they are thought to be irrelevant in determining the overall characteristics of the emergent spectrum. However, Skinner and Whitmore (1988) have shown how the strength of the SiC feature may be used as a mass loss diagnostic for cool carbon stars, thereby implying that the dust to gas ratio for the SiC component is the same wherever the SiC emission feature is observed in C star spectra. In order to test their relationship, it becomes necessary to include SiC as a component in full multi-component radiative transfer models for a large number of stars; this work reports a first step towards achieving this goal.

Table 5.1: The adopted Stellar Parameters for IRC+10216.

Parameter	Value	Reference
Distance	200 pc	Kwan & Hill(1977)
R_*	7.25×10^{13} cm	This work
T_{eff}	2330 K	Ridgeway & Keady(1988)
v_∞	14.4 km s^{-1}	Schönberg (1989)
$\dot{M}$	3.0×10^{-5} $M_\odot$ yr^{-1}	Schönberg (1989)
R_{in}	1.4×10^{14} cm	This Work
R_{out}	6.0×10^{17} cm	This Work

5.2 The Model Code

The modelling utilises a code originally due to Haisch (1979) and modified by Hoare (1988) in which a generalised two stream Eddington approximation is applied to the problem of radiative transfer in a spherically symmetric extended dust shell. The code fully takes into account the effects of non-isotropic scattering, absorption and thermal re-emission and calculates the radiative equilibrium temperature distributions consistent with the radiation field for a multiple grain size, multiple grain component dust distribution. The code is used to calculate the temperature distribution for 20 grain sizes at 175 depth points through the dust shell and hence the emergent spectrum at 75 wavelength points from 0.5μm–10cm.

The model code requires a number of input parameters which may be usefully divided into those relevant to the star and those relevant to the dust grains. These will be discussed in turn.

5.2.1 Stellar Parameters

Table 5.1 lists the adopted stellar parameters. It is assumed that the stellar energy distribution may be adequately represented by a Planck blackbody function appropriate to the adopted T_{eff}.

5.2.2 Grain Size Distribution

The code allows for a power law distribution of grain sizes whereby the number density of grains of radius a, per unit grain radius interval at a distance r from the central star is:

$$n_d(a,r) = n_d(r)a^{-p}, \qquad a_1 \leq a \leq a_2. \tag{5.1}$$

As a starting point, the Mathis, Rumple and Nordsiek (MRN) (1977) grain size distribution is adopted, in which p=3.5, a_1=0.005μm and a_2=0.25μm. This has been shown by Biermann and Harwit (1980) to be a plausible description of the dust grain size distribution resulting from grain-grain collisions in red giant winds.

A value for n_d the number density of the dust grains at the inner (condensation) radius may be derived from a knowledge of the velocity of the stellar wind and the dust to gas ratio of the outflow. Hoare and Clegg (1988) give:

$$n_d(r) = \frac{3m_H}{4\pi}\frac{(4-p)}{(a_2^{4-p}-a_1^{4-p})}\frac{Rn_H(r)}{\rho_d} \tag{5.2}$$

where R is the dust to hydrogen ratio by mass, n_H is the number density of hydrogen nuclei, m_H is the mass of the hydrogen atom and ρ_d is the density of the grain material. Values for the grain density of 1.8 g cm^{-3}, 3.2 g cm^{-3} and 2.0 g cm^{-3} are adopted for the AC, SiC and graphite components respectively .

If the gas mass loss rate ($\dot{M}$) has been measured then $n_H(r)$ is given by:

$$n_H = \frac{\dot{M}}{4\pi r^2 \mu m_H v(r)} \tag{5.3}$$

where $v(r)$ is the outflow velocity at radial distance r from the star. Integrating equation (5.1) over the grain size distribution, and combining this result with (5.2) and (5.3) a relationship is obtained for the dust grain number density at radial distance r:

$$n_d(r) = \frac{3M_d/M_g}{(4\pi)^2}\frac{(4-p)}{(a_2^{4-p}-a_1^{4-p})}\frac{\dot{M}}{r^2 v(r)\rho_d}\frac{(a_2^{1-p}-a_1^{1-p})}{1-p} \tag{5.4}$$

Note that in equation (5.4) M_d/M_g is used to denote the more familiar dust to gas ratio, which is the dust to hydrogen mass ratio divided by μ =1.4 for a helium abundance of 0.1 by number relative to hydrogen.

The modelling process assumes that by the time dust grains condense out of the stellar outflow, it has reached its terminal velocity (i.e. $v(r) = v_\infty$). This is not necessarily a

valid assumption since in one of the few cases where a wind velocity has been traced as a function of distance from the central red giant, that of VX Sgr (Chapman and Cohen 1986), the gas is still being accelerated at distances of 2–5 stellar radii which is where the models predict temperatures to be such that dust grains can begin to condense, and in fact the gas in the envelope of VX Sgr only reaches terminal velocity at several hundred stellar radii. However, Keady, Hall and Ridgeway (1988) found that gas velocities in the envelope of IRC+10°216, derived from observations of the CO first overtone bands at 2μm, reached values close to terminal at around 10 stellar radii.

The lack of any realistic velocity law for red giant winds and the ready availability of published values for v_∞ led to the adoption of v_∞ as the velocity of gas everywhere in the outflow with the awareness of the possible inaccuracies this assumption introduces into the results. Thus the density of dust in the outflow is assumed to fall-off as the inverse of the square of the distance from the star.

5.2.3 Dust Optical Constants

Values for the dust absorption efficiency ($Q(a,\lambda)$), albedo ($\tilde{\omega}(a,\lambda)$) and the dust scattering asymmetry parameter ($g(a,\lambda)$) were calculated assuming spherical grains, for 20 grain radii spanning the MRN size distribution, using Mie theory (van de Hulst 1957) and dielectric functions tabulated in the literature for a variety of proposed condensates.

For graphite the dielectric functions given by Draine and Lee (1984) were used (noting the errata in Draine & Lee, 1987), and a temperature of 100K was assumed when calculating the free electron contribution to the opacity. Due to the anisotropic nature of graphite, it was assumed that the total grain efficiency factors for absorption and extinction, Q_{abs} and Q_{ext} could be approximated by assuming the grains to be composed of a collection of randomly orientated crystals such that;

$$Q(a,\nu) = \frac{2}{3}Q_{\perp}(a,\nu) + \frac{1}{3}Q_{||}(a,\nu) \tag{5.5}$$

where $Q_{\perp}(a,\nu)$ and $Q_{||}(a,\nu)$ are the efficiency factors calculated for the cases where the E vector is perpendicular or parallel to the c plane (itself perpendicular to the basal plane).

For AC grains, two runs of synthesized constants were compared; those tabulated in Hoare (1990) (and used to model the dust emission from the C-rich planetary nebulae IC 418 and NGC 7662) and those given by Mathis and Whiffen (1989 preprint) for AC

grains in the interstellar medium were compared. It is important to note that both of these runs of AC optical constants were derived essentially from *laboratory* measurements. Those tabulated by Hoare were based on the measurements of Borghesi *et al.* (1985a) in the wavelength range under study, whilst those listed by Mathis & Whiffen are derived from the measurements of Bussoletti *et al.* (1987) at the longer wavelengths, and Duley (1985) for the optical region.

Finally, the optical constants derived by Pégourié (1988) for α-SiC, were used to investigate the effect that varying the mass loss rate and dust to gas ratio had upon the observed strength of the 11.4μm feature in IRC+10°216. At wavelengths longwards of those tabulated by the authors for all grain types, Q(a,λ) was calculated for two power laws, Q(a,λ)$\propto \lambda^{-1.0}$ for the AC, and Q(a,λ)$\propto \lambda^{-2.0}$ for the crystalline graphite and SiC. The λ^{-1} power law was selected as most recent laboratory measurements of the extinction efficiencies for various types of submicron AC grains (eg Koike *et al.* (1979), Bussoletti *et al.* (1987)) have found values close to this out to wavelengths as long as 300μm, with no apparent falling off in the power law at the longer wavelengths.

The lack of any published optical constants for MgS, observed in IRC+10°216 by Forrest *et al.* (1979), precluded its inclusion as a component in the models for the dust envelope of IRC+10°216.

5.2.4 Dust Shell Inner Radius

The dust shell inner radius is determined by the dust grain condensation temperature. Individual grain components have different condensation temperatures and therefore in the multi-component models, the dust shell inner radius is defined to be the point where the ambient temperature of the warmest dust grains reaches the temperature of the grain component with the highest condensation temperature. The density of the second dust component is set to zero until a point is reached within the dust shell where the hottest dust grains reach their designated condensation temperature, at which stage this component is 'allowed' to condense, and its effect on the transport of radiation through the dust shell is calculated at all grid points outside this condensation radius.

Due to their more refractory nature, SiC grains are predicted to condense closer to the star than do the AC grains. The precise temperature of SiC grain condensation is not absolutely clear. McCabe (1982) constructed a chemical model of carbon star envelopes

in which SiC grains were found to condense from the outflow at temperatures of 1500K. More recent laboratory work by Frenklach *et al.* (1989) suggests that the SiC component may condense from the gas phase at temperatures as high as 2000K, and may already have begun to condense within the photosphere itself. In order to investigate the effect of SiC condensation temperature upon the emergent spectrum, models were run using both 1500K and 2000K condensation temperatures.

There is a much better consensus as to the condensation temperature of the AC or graphitic component. Both McCabe and Frenklach *et al.* have these grains condensing at temperatures of around 1000K. One important difference that should be noted in the models presented here, and that proposed for the circumstellar envelopes of carbon stars by Frenklach *et al.* is that these have discrete dust components, whereas Frenklach*et al.* suggest that the SiC grains act as nucleation sites for the AC component. The lack of any published dielectric functions for the 'amorphous Carbon/SiC' composite grains precluded the detailed testing of this model. In principle, an approach similar to that used by Aannestad (1974) for silicate core grains with ice mantles could have been adopted, where the grains were assumed to be composite spheres, enabling use of the formulae of Güttler as described by Wickramasinghe (1975), to calculate dielectric functions for these composite grains, which would presumably have SiC cores with AC mantles. At this stage in the modelling though, it was felt that such a move would lead to an unnecessary increase in the (already) large number of free parameters needed to model the grains, and should only be attempted, if multi-component grain models prove unable to give good fits to the observations.

5.2.5 Dust Shell Outer Radius

If a realistic model is to be constructed for the millimetre and radio fluxes from the dust shell, then the choice of dust shell outer radius becomes quite important, since most of the flux at millimetre wavelengths will have its origin in the cool outer regions of the shell. Previous authors have adopted a variety of outer radii: Rowan-Robinson *et al.* (1986) used a value of $1000R_{in}$, where R_{in} is the inner radius of the dustshell, to model the emergent spectrum from IRC+10°216, whereas Le Bertre (1987,1988b) adopts a value of $10000R_{in}$, and Martin and Rogers (1987) quoted the outer boundary of their model dust shell as occurring at $10000R_*$ Observations of the size of the CO molecular envelope

(Huggins *et al.* 1988) may also be used as an indication of the extent of the shell, since at the outer radius of the CO emitting shell, the CO molecules located within the dusty stellar outflow are presumably being dissociated by the interstellar radiation field. In the case of IRC+10°216, Huggins *et al.* found that the CO emission was coming from a region whose radius was less than 6.7×10^{17}cm ($9240R_*$). assuming a distance of 200pc for the object. This was adopted as a realistic starting value for the model's outer radius, since the lack of emission from CO molecules beyond this radius observed by Huggins *et al.* , is presumably due to the CO molecules having been dissociated. If this is true, then the dust shell may be taken to have become optically thin to the interstellar radiation field at this radius, with the dust grains coming into thermal equilibrium with the interstellar radiation field beyond this point. For this reason, the Huggins *et al.* outer radius was selected as the starting point for the modelling procedure; however, in order to investigate the effect that variation of the outer radius of the dustshell has upon emergent far-IR fluxes, model spectra were calculated for all of the above values for R_{out}, and the best value for it was determined by comparison with the available photometry.

5.3 Observations

Since IRC+10°216 is known to be variable with a period of ≈640 days (Witteborn *et al.* 1980, Ridgeway and Keady (1988)) it is necessary to select observations made at a similar phase in the light curve, if the star's energy distribution is to be modelled in a self consistent way. In making the selection of photometry from the literature, no allowance was made for the 'light travel time' whereby there is a phase lag between near-IR and far-IR variations in brightness. The non-inclusion of this effect in the selection of the observations was due to the relative scarcity of published multi-epoch photometry at wavelengths longer than 30μm.

The ephemeris given by Ridgeway and Keady (1988) was utilised to select observations from the literature that were made within ±0.2 period of IRC+10°216's peak 2μm brightness. Due to its importance in constraining the derived dust to gas ratio for SiC, the *IRAS* LRS spectrum of the object, obtained in 1983 has also been included. The *IRAS* 12, 25, 60 and 100μm photometry have been colour corrected by convolving the model spectra with the filter responses tabulated in the *IRAS* explanatory supplement (Beichman *et al.*

1984).

At far-IR and radio wavelengths, beam-size effects become important, since the beam used to observe the source may be smaller than the angular extent of the source on the sky, leading to a reduction in the flux observed from the object. To compare the models with the observations, the model spectra were convolved with circular gaussian beams whose diameters match those given by the observers. The beam-size corrected model fluxes may then be compared directly with the observations. Fluxes calculated in this way must be regarded with some caution, since the beam convolution takes no account of the spectral sensitivity of individual observers instrumentation, but this should hopefully be taken out by the calibration process used during the original observations.

The best fitting model is compared with long wavelength observations in this way in Table 5.2. In all the figures, the observed fluxes are plotted uncorrected for beam size effects.

5.4 Results

5.4.1 Grain size distribution

The standard MRN size distribution gives a remarkably poor fit to the data. In Figure 5.1, it is shown how, for both types of AC and for graphite dust models using the standard MRN size

distribution, the model spectra fall significantly below the observations at shorter wavelengths. This diagram further illustrates how, in the far-infrared and longer wavelength regions, the λ^{-1} fall-off in grain emissivity used in the Hoare AC dust models gives a superior fit to the observations than that given by the Mathis and Whiffen or by the graphite dust models, where the steeper fall-off in dust emissivity leads to a progressively larger difference between observations and model fluxes with increasing wavelength. The optical depth of the dust shell is given for the same models in Figure 5.2.

After some investigation, it was found that by reducing the upper limit of the grain size—distribution, such that $0.005 \leq a \leq 0.05 \mu m$, a far better fit to the observed spectral shape in the near-IR could be obtained, implying that large dust grains with $a \geq 0.05 \mu m$ are not present in large quantities in the outflow around IRC+10°216. This confirms a similar finding by Martin and Rogers. The effect that large grains in the outflow have on the

Table 5.2: Model fluxes corrected for the finite beam size used for the observations.

		1.5cm (mJy)	3.3mm (mJy)	1.0mm (Jy)	450μm (Jy)	350μm (Jy)	100μm (Jy)
	Observed Flux	6±1	145±39	4±1	29±8	73±19	2009±730
	(reference)	(1)	(1)	(2)	(3)	(2)	(2)
Model Emissivity Law	Outer Radius (cm)						
$\lambda^{-1.0}$	6.7×10^{17}	2.3	140.0	3.9	33.2	96.1	1977.3
$\lambda^{-1.1}$	6.7×10^{17}	1.4	83.0	2.5	22.7	67.7	1642.9
$\lambda^{-1.2}$	6.7×10^{17}	1.1	51.0	1.6	15.5	47.6	1348.4
$\lambda^{-1.3}$	6.7×10^{17}	0.9	37.0	1.1	11.0	34.3	1106.1
$\lambda^{-1.0}$	1.4×10^{17}	1.4	69.0	1.9	16.5	49.3	1448.8
$\lambda^{-1.0}$	1.4×10^{18}	2.9	196.0	5.4	44.7	127.1	2175.2

References: 1. Sahai *et al.* (1989), 2. Fazio *et al.* (1980), 3 Sopka *et al.*(1985).

emergent energy distribution may be demonstrated by assuming the circumstellar dust to be composed of single sized grains, and running models in which mass outflow from the star is composed of grains of these discrete sizes. Figure 5.3 indicates how, for the Hoare AC, grains larger than 0.05μm absorb too efficiently in the optical and near-IR region, and the model spectra fall beneath the observations.

Similar behaviour is found for the Mathis and Whiffen AC grains, and also for pure graphite grains, where better fits to the observed optical and near-IR energy distribution came from models with grains smaller than 0.05μm.

The AC grain models gave a superior fit to the observed photometry than did the graphite models, over the entire range of wavelengths at which the object was being modelled. It was therefore concluded that graphite grains are not a major opacity source

Figure 5.1: A comparison of model spectra calculated for 3 grain types (plus SiC grains) with a standard MRN grain size distribution.

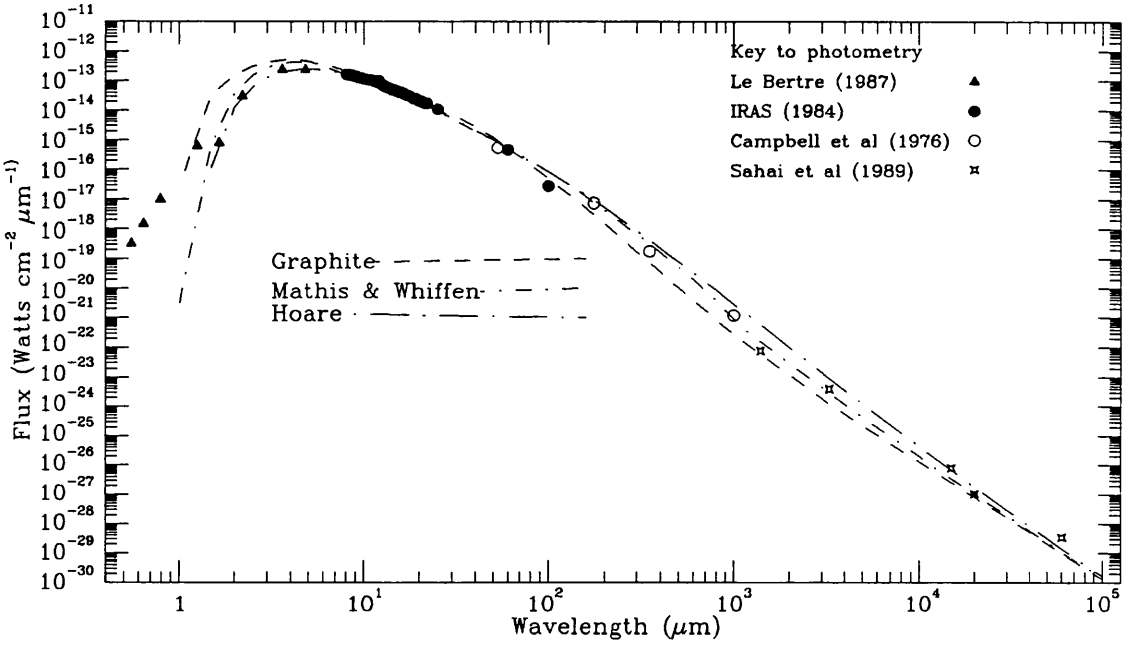

in the circumstellar environment of IRC+10°216.

The Mathis and Whiffen AC dust gives an inferior fit to the far-IR observations when compared to dust whose far-IR emissivity falls off as $\lambda^{-1.0}$, as suggested by Hoare (1990). The fit to the observations of models calculated using the Mathis and Whiffen AC dust was markedly poorer compared to the $\lambda^{-1.0}$ emissivity fall-off, at wavelengths longwards of 0.7mm.

At this stage it was decided that since the Hoare AC optical constant synthesis gave the best fit to the observations, they should therefore be used in all further investigations.

Figure 5.4 presents the best model fit to the photometry, calculated using the Hoare (1990) optical constants. With the adopted stellar and dust parameters, a gas to dust mass ratio of 400 for AC grains gives a good fit to most observations longwards of 0.5μm with the exception of the 1.5cm and 6cm data. This value is in excellent agreement with those derived by Knapp (1985) and Sopka *et al.* (1985) whose values for this ratio were 400 and 330 respectively. The value also agrees (within the errors) with the value of 350±200 found by Olofsson *et al.* (1987) from a survey of optically bright Carbon stars.

Figure 5.2: Dust optical depths for the models shown in Figure 5.1

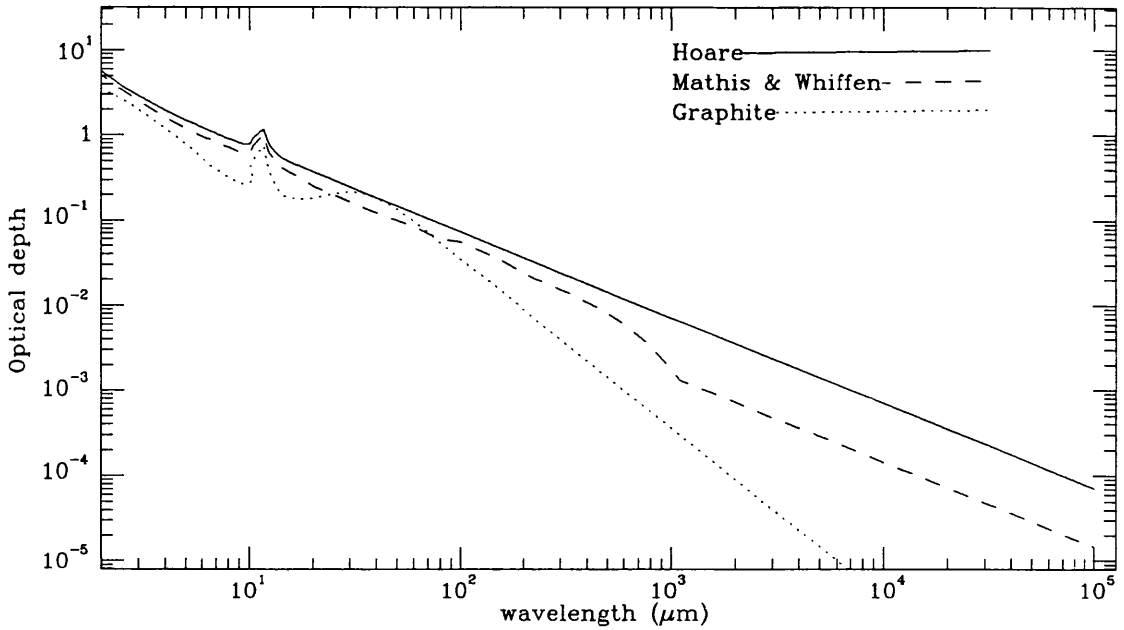

Examination of the optical depth of the dust shell, as predicted by the best fitting model (Figure 5.5) reveals that even at wavelengths longwards of 1 mm, the shell is still of sufficient optical depth that dust emission is an important contributor to the emergent spectrum. This is contrary to the findings of Sahai *et al.* (1989) who using a less detailed analysis, in conjunction with a steeper fall of in dust emissivity in the far-IR, found that the photosphere dominated dust emission in the radio region of the spectrum.

The relative importance of the contributions of the (reddened) photosphere and thermal emission from dust in the circumstellar envelope for the best fitting model are shown in Figure 5.6.

5.4.2 The Amount of Carbon in Dust grains

The best fitting model gives a dust to gas ratio for the AC component of the dust envelope of 2.5×10^{-3} by mass. This converts to a value of $\approx2.1\times10^{-4}$ by number relative to hydrogen. Adopting the cosmic abundance presented by Grevesse & Anders (1989) for C relative to H of 3.63×10^{-4} by number then one finds that $\approx$60% of the available Carbon is locked up in the AC grains. Of course, the abundance of C relative to H in a carbon

Figure 5.3: A comparison of model spectra calculated for AC dust grains using single sized dust grains of the indicated radii. The optical constants used to calculate the grain parameters come from Hoare (1990).

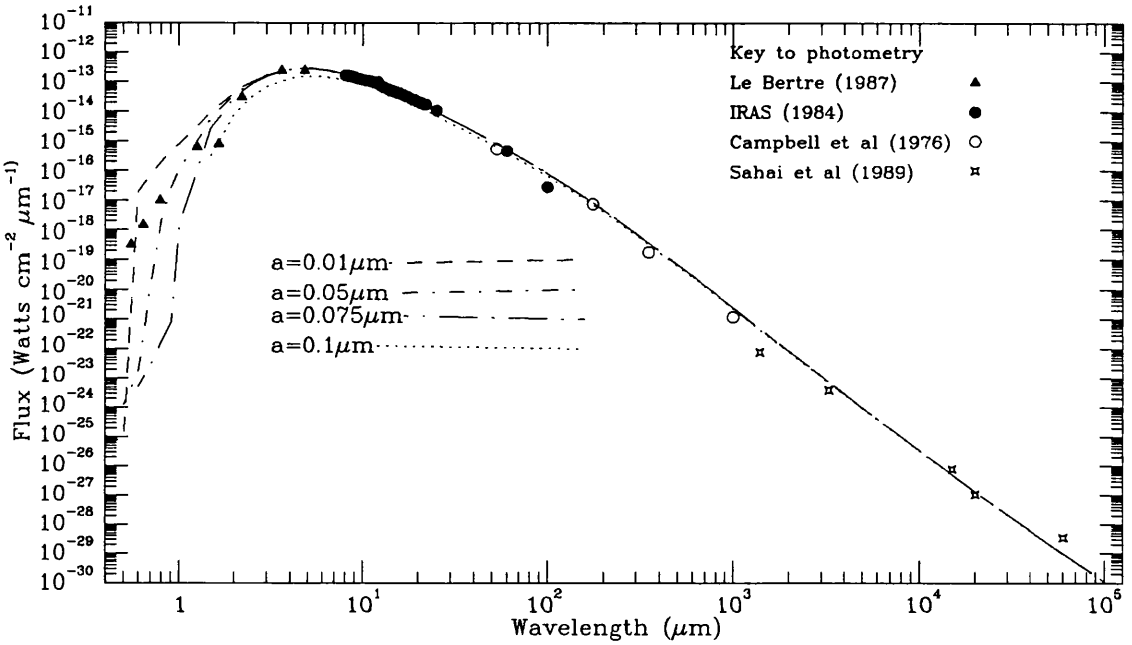

star envelope is by no means cosmic; Lambert *et al.* found that for a sample of 30 C stars, the C/H ratio was enhanced, relative to the solar photospheric value, by a mean value of 0.05±0.1 dex. Adopting this value for the C abundance, the fraction of carbon in AC grains lies somewhere in the range 0.4—0.64, assuming the photospheric abundances for IRC+10°216 to be similar to the sample of Lambert *et al.* .

5.4.3 Dust Temperature Distribution

The condensation temperature for the AC grains was found to be an important constraint in matching the optical and near-IR photometry. A condensation temperature of 1000K was found to give the optimum fit to the photometry, with the adopted grain size distribution. The effect on the model spectra of allowing the AC grains to condense at temperatures of 1500K, 1000K and 500K is illustrated in Figure 5.7. Temperatures larger than 1000K were found to give models with too much extinction in the optical, whereas, lower condensation temperatures gave progressively less extinction, due to the absence of

Figure 5.4: The model providing the best fit to the observed photometry. Note that the model fluxes have not, in this figure, been corrected for the finite beam-sizes of the observations. Beam-size corrected fluxes are compared directly with the observations in Table 5.2

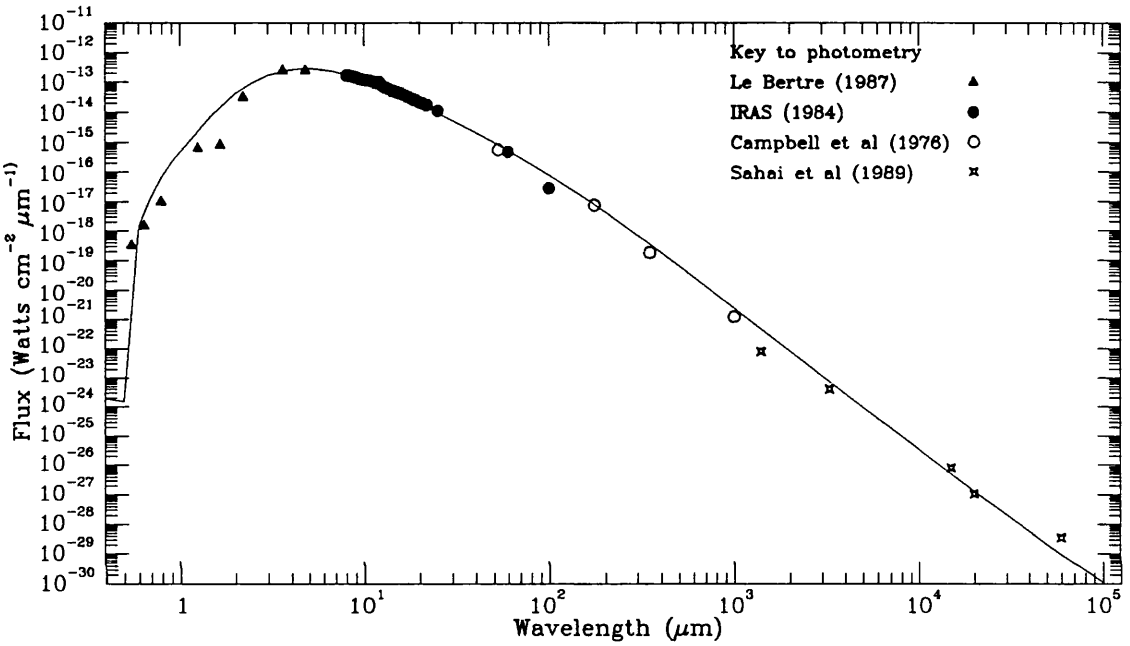

the AC grains from the dense inner regions of the outflow. The models described above imply that AC condensation must occur at temperatures lower than ≈1000K, though precisely how much lower is difficult to determine, until accurate model atmosphere fluxes for cool C stars become available enabling account to be taken of the line blanketing in the underlying cool stellar photosphere, which would reduce the stellar fluxes when compared to those of a black body in the optical and near-IR regions of the spectrum.

The condensation temperature for the SiC dust grains was found to be of little importance in determining the properties of the model spectra. Increasing the condensation temperature from 1500K to 2000K did make a small difference to the total dust opacity at shorter wavelengths as can be seen in Figure 5.8. For the adopted AC condensation temperature of 1000K, the best fit to the observations was given by the lower SiC condensation temperature of 1500K, though within the observational and modelling uncertainties, the certainty of this better fit must be questionable, and no firm conclusions can be drawn

Figure 5.5: Dust optical depth as a function of wavelength for the best fitting model

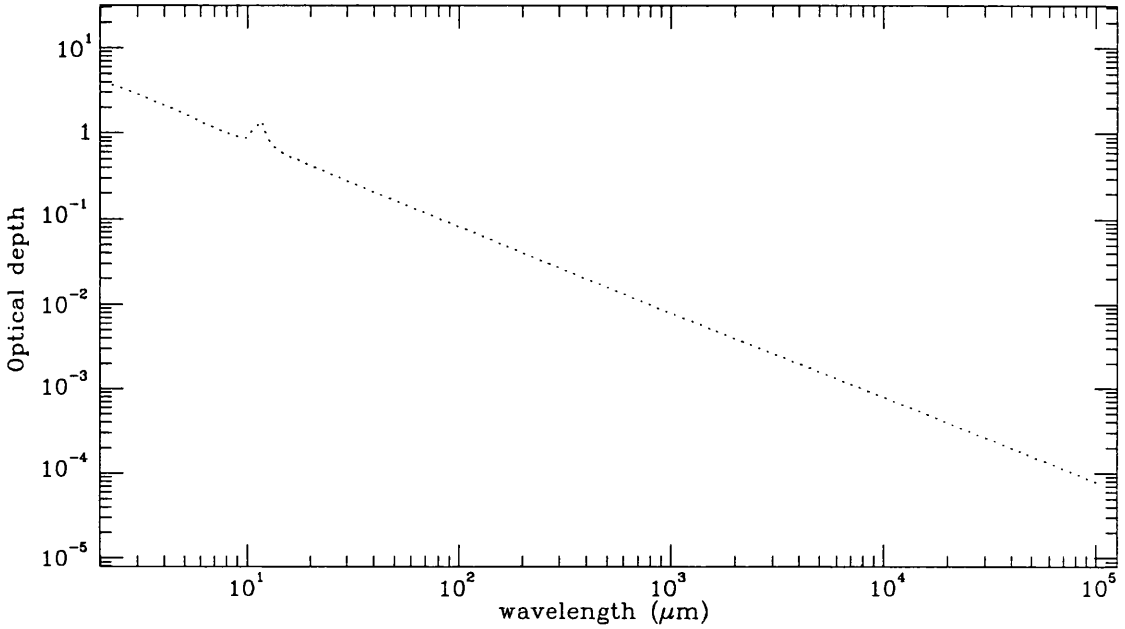

Figure 5.6: A comparison of the relative importance of the contributions to the model energy distribution of reddened photospheric and thermal dust emission components.

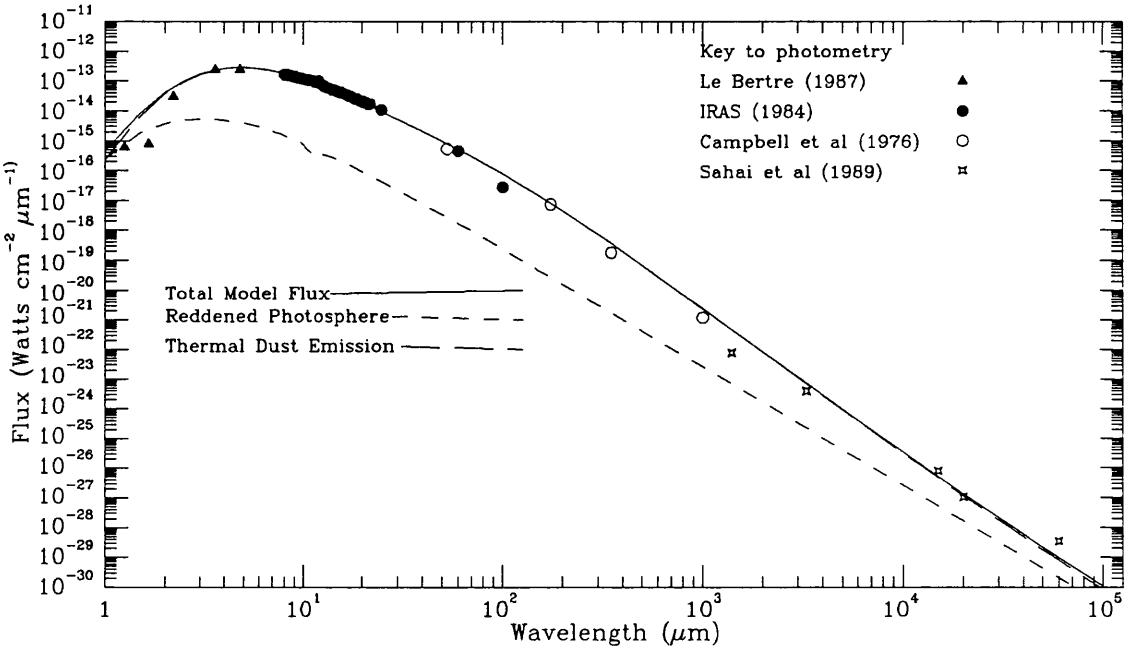

Figure 5.7: The effect of changing the condensation temperature of AC grains upon the emergent model spectrum. All other parameters are identical to those of the best fitting model.

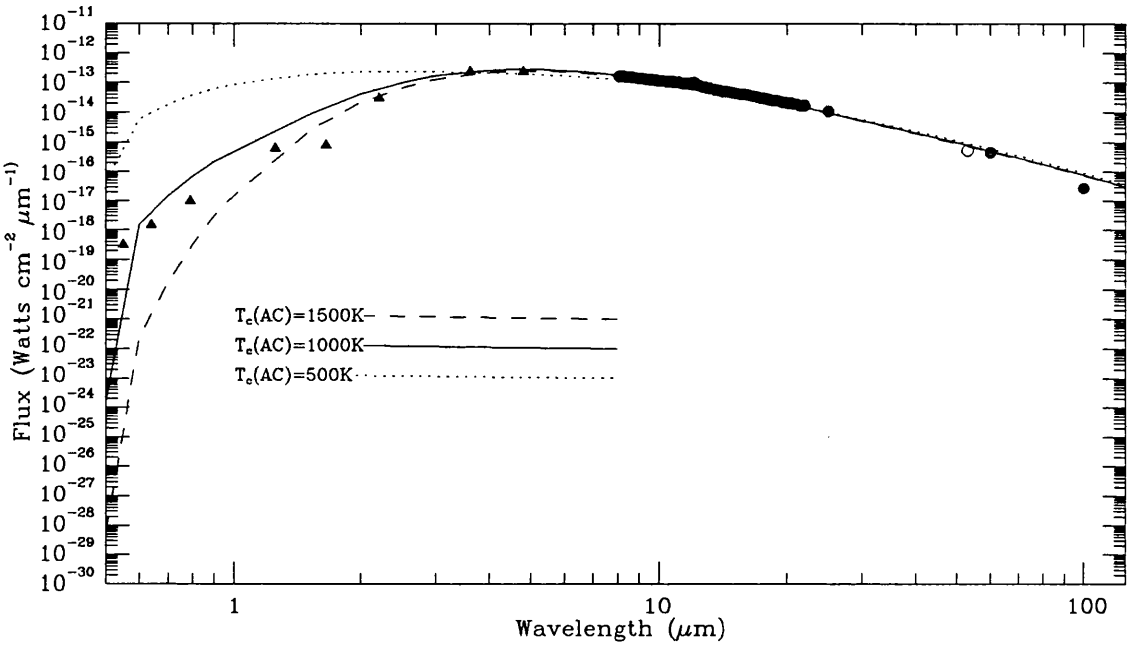

as to the accuracy of either the McCabe or the Frenklach *et al.* models.

The temperature distribution for the largest grains (0.05μm) is shown for both AC and SiC components in Figure 5.9, as a function of radial distance from the star. It can be seen that at the adopted outer radius of 6.0×10^{17}cm (which equates to 8275R$_*$ or 4786r$_{in}$), dust temperatures are of the order 35K. This is a factor 3 higher than the gas kinetic temperatures calculated by Huggins *et al.* for the CO molecules at this distance from the star; these authors finding that temperatures approached 10K at this point in the shell.

Increasing the outer radius to the values suggested by Martin and Rogers, or Le Bertre of around 10,000R$_{in}$ increases the model fluxes in the sub-mm and radio regions since emission from cooler dust in the outer regions contributes mainly at the longest wavelengths. In Figure 5.10, the effect of altering the adopted outer dustshell radius to the values proposed by a number of different authors is investigated. Increasing the dustshell outer radius to the value of 10,000R$_{in}$ increases the model fluxes in the far-IR and radio regions

Figure 5.8: The effect of increasing the condensation temperature of the SiC grains from the 1500K used in the best fitting model to the 2000K value suggested by Frenklach *et al.* has upon the emergent spectrum.

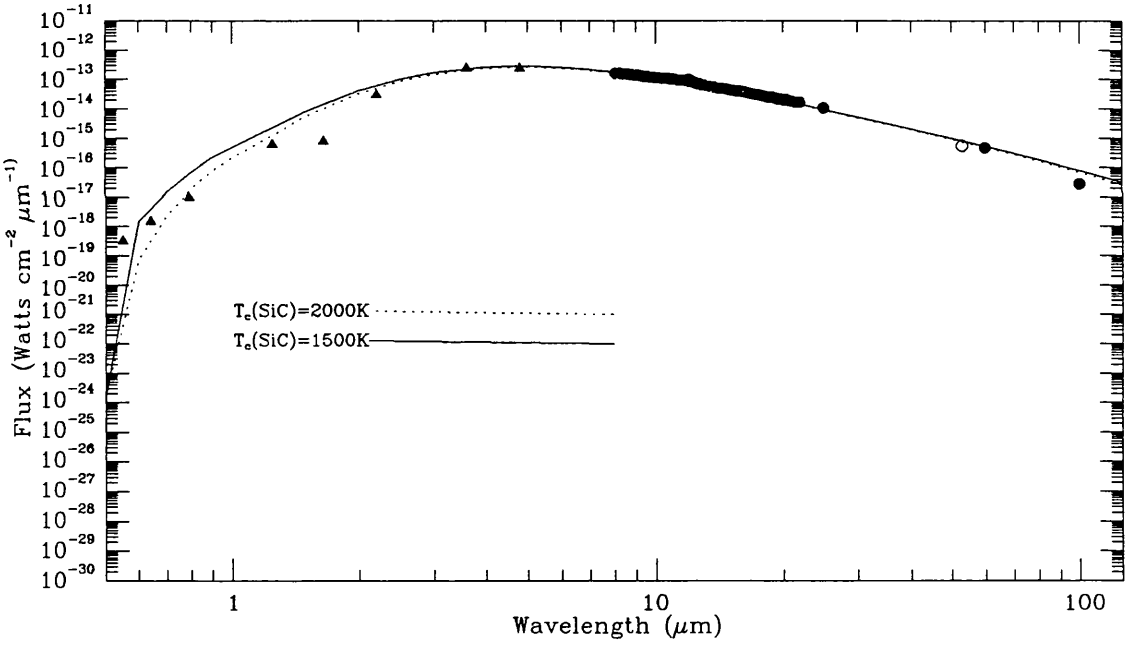

Figure 5.9: The temperature distributions of the largest (a=0.05μm) grains in the AC and SiC components for the best fitting model.

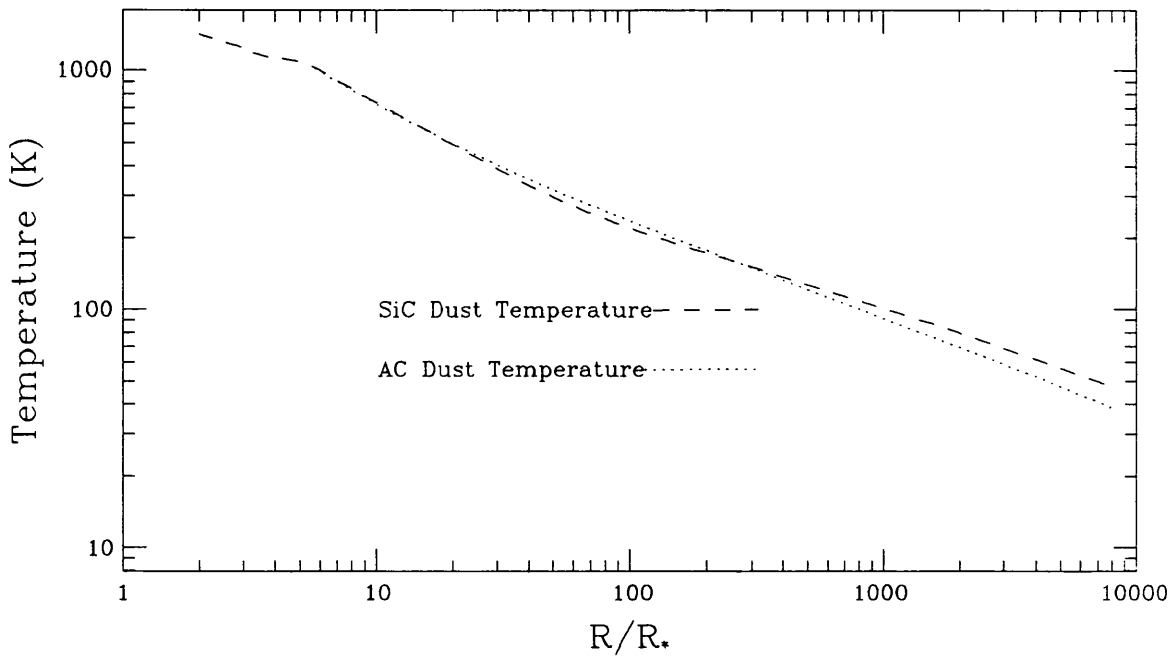

to such an extent, that when convolved with the beams used by individual observers, the predicted fluxes are greater than those observed. The excess however is generally within the errors of the original observations, and therefore no clear conclusions may be drawn as to the actual extent of the outer radius of the dustshell on this basis.

It will be shown however in Section 4.5, that adopting a power law dust emissivity whose fall-off is steeper than λ^{-1} necessitates a large outer radius if the observed far-IR and radio energy distribution of IRC+10°216 is to be matched. The modelling predicts grain temperatures of around 20K at this large outer radius of $10000R_{in}$

Decreasing the outer radius to the value of $1000R_{in}$ suggested by Rowan-Robinson *et al.* decreases the far-IR model fluxes to a level which is below the observations longwards of 350μm. Dust temperatures predicted by the models at this outer radius are of the order of 60K, which seems high when compared to 'standard' interstellar values of 10–30K. The convolved fluxes for models run with both Rowan-Robinson *et al.* 's and Le Bertre's adopted outer radii are presented in Table 2, whilst the models are compared directly with the observations (uncorrected for finite aperture size) in Figure 5.10.

Figure 5.10: The effect that variation of the outer radius of the dust shell has upon the emergent fluxes, for a model comprising dust grains in the 'modified' MRN distribution whose emissivity is assumed to fall off as $\lambda^{-1.0}$.

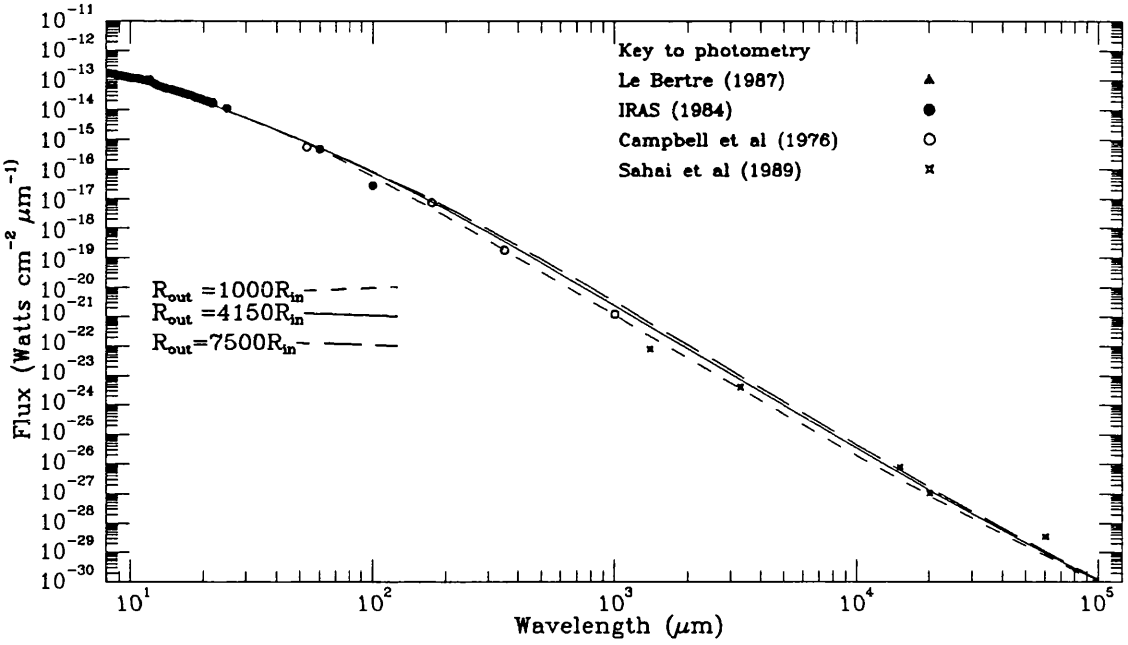

5.4.4 The SiC/AC Ratio

SiC dust grains are unimportant in determining the gross properties of the energy distribution, their effect being concentrated within the 11.4μm resonance feature. Assuming that the optical constants for α-SiC used in this study, derived by Pégourié from the laboratory measurements of Phillip and Taft (1960) in the UV and optical and by Borghesi *et al.* (1985a,1985b) in the IR, are valid for SiC grains in circumstellar dust shells, then this result must cast much doubt upon Le Bertre's suggestion (1988a) that SiC dust could be a dominant source of opacity in carbon rich circumstellar dust shells.

The weak SiC feature exhibited by the *IRAS* LRS spectrum of IRC+10°216 required a dust to gas mass ratio of 5×10^{-4} in the SiC grain component for a good fit to be obtained. For the best model, this implied a SiC:AC ratio of 1:5 by mass, or 1:17 by number, its value being relatively insensitive to the other adopted model parameters. Figure 5.11 illustrates the sensitivity of the SiC feature strength to the adopted dust to gas ratio for SiC by comparing models run with different SiC:AC ratios with the *IRAS* LRS spectrum of the

Figure 5.11: A comparison of a model calculated with different dust to gas (D/G) ratios for the SiC model component, with the *IRAS* LRS spectrum of IRC+10°216. The best fit to the observed SiC feature occurs when D(SiC)/G$\approx 5.0 \times 10^{-4}$.

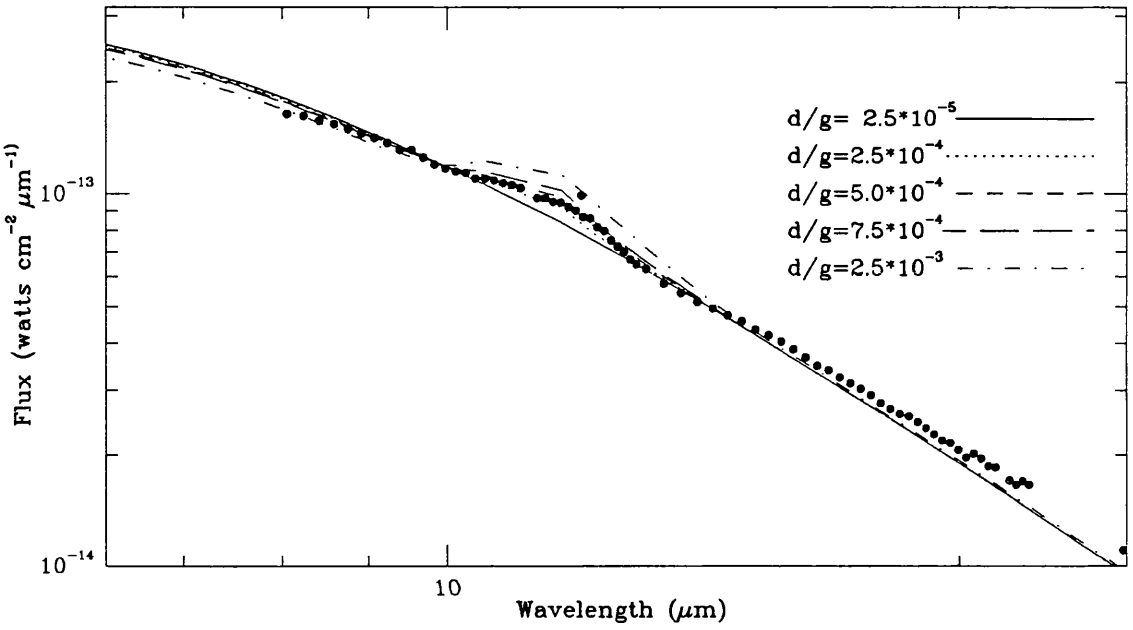

object. It is noted in passing, that though the dust optical constants derived by Pégourié give a feature whose profile is somewhat narrower than that suggested by the observations, the fit, which assumes spherical grains, is in fair agreement with the observations.

The derived dust to gas ratio for SiC implies a derived abundance of Si locked up in SiC in the circumstellar dust shell of IRC+10°216 corresponding to 1.25×10^{-5} by number relative to H. This implies, assuming a cosmic abundance for Si of 3.55×10^{-5} (Grevesse & Anders, 1989) that ≈ 0.35 of the available Si is tied up in the SiC grains. For their sample of 30 carbon stars, Lambert *et al.* found that $-0.3 \leq [M/H] \leq 0.0$, where [M/H] is the metal abundance relative to the cosmic (solar) value. If [Si/H] for IRC+10°216 is as low as −0.3 relative to the cosmic value, then the fraction of Si in dust rises to 0.70. Thus using the calculated dust-to-gas ratio for SiC, the fraction of Si in dust lies somewhere in the range 0.35—0.70 depending on the adopted Si abundance, though the likely errors associated with this determination of the dust to gas ratio for SiC probably increases this range to 0.20—0.80.

The figure of 35% for the fraction of Si in dust grains is in moderate agreement with that quoted by Sahai, Wootten & Clegg (1984), who found that to explain the observed upper limit to the amount of SiS molecules in the IRC+10°216 circumstellar envelope, it became necessary to invoke a scenario where most of the Si was locked up in dust grains.

The value derived for the ratio of SiC to AC dust also compares favourably with those found empirically by Baron *et al.* (1987) for their sub-class 1 objects (i.e. those C stars with weak 11.4μm features) but is somewhat higher than the value quoted by Martin and Rogers, who assuming just a single grain size, and using the (Q/a) values of Borghesi *et al.* (1985a), found that only a small fraction of the total number of Si atoms were in the dust.

The calculated SiC:AC ratio is within a factor of 2 of that derived by Hoare (1990) for the C-rich planetary nebulae IC 418 and NGC 7662. The fact that the ratio is higher than that found by Hoare may be evidence for preferential destruction of the AC or indeed preferential formation of a SiC component in the PN environment; though the errors involved in both models must make this conclusion very uncertain.

Whittet *et al.* (1990) have recently estimated the abundance of Si in SiC dust, in the interstellar medium, as being no more than ~5 per cent of that in silicates, using the sightline to the galactic centre as the basis for their argument. This value is at least a factor 2 lower than the value calculated for the best model of IRC+10°216 presented above, and if the abundance calculated by Whittet *et al.* is true for all sightlines, then it seems that circumstellar dust composition (at least in the case of IRC+10°216) is very different to that observed in the ISM, and that grain destruction mechanisms are particularly effective. It should be noted that the qualitative discussion, by Whittet *et al.* , of the general absence of an 11.4μm SiC absorption feature in the spectra of C stars (not necessarily meaning that SiC is underabundant) is bourne out by the quantitative models for the envelope of IRC+10°216 presented in Figure 5.9; the different grain species do have slightly different radial temperature gradients. It is clear that the lack of apparent SiC absorption in the thickest C rich shells (of which IRC+10°216 is surely the best example!) need not necessarily imply a low abundance of SiC.

5.4.5 Far-IR Dust Emissivity

The best model assumes that the dust emissivity falls off as λ^{-p}, with p=1, for wavelengths longer than 5μm, and gives a fair match to the observed energy distribution for IRC+10°216 in the range 0.5μm to 1cm. The emissivity law in the far-IR for AC dust is far from certain though, and published values for p lie in the range 1-1.5.

Le Bertre (1987, 1988b), in his models for IRC+10°216 adopted a value for p of 1.3, as suggested by Jura (1983) and managed to model the energy distribution of IRC+10°216 in the range 0.7μm to 3mm. Other values suggested for p are 1.2 by Sopka *et al.* (1985) and 1.1 by Zuckerman & Dyck (1986). In order to compare the adoption of p=1.0 with other published values, models were calculated in which dust emissivity varied as $\lambda^{-1.1}$, $\lambda^{-1.2}$ and $\lambda^{-1.3}$ longwards of 5μm. The results of these calculations are presented as Figure 5.12. The models indicate that, assuming a dustshell outer radius of 6×10^{17}cm, p=1.0 gives the best fit to the observed energy distribution, just as measured for AC grains in the laboratory (Koike *et al.* (1980), Bussoletti *et al.* (1987)). Of course, increasing the adopted outer radius would (as described in Section 4.3) increase the long wavelength model fluxes for the other values of p, but since the emissivity of the dust grains is also falling off faster than for p=1.0, so for the higher values of p, the dust shell outer radius has to be increased more to match the observed fluxes. With the adoption of p=1 the agreement between model and observations remains fair out to 3.3mm. Orofino *et al.* (1987, 1990) have also used laboratory derived optical constants for AC to model the circumstellar environment of IRC+10°216, as well as a number of other C-star envelopes. In their most recent (1990) model for the envelope, a stellar temperature of 1400K was found to provide the best fit to the observations near maximum light; this appears a rather low value, especially when recent observations (Ridgeway & Keady, 1988) of the CO band heads in the near-IR FTS spectra of IRC+10°216 at phase 0.01 (near maximum light) indicate an excitation temperature in excess of 2000K for the stellar photosphere. Orofino *et al.* criticise the use by Martin & Rogers (1987) of bulk optical constants derived from amorphous carbon film by Mie theory, as introducing considerable inaccuracies into the values of the derived cross sections. In practice, a direct comparison between the Martin & Rogers optical constants (essentially the same as those tabulated by Hoare) and those used by Orofino (which are similar to those used by Mathis and Whiffen) shows that there appear to be no large differences in the far-IR spectral region (Figure 5.1). In any case, the

Figure 5.12: Models calculated using various power laws for the far-IR emissivity of the AC grains with the 'modified' MRN grain size distribution.

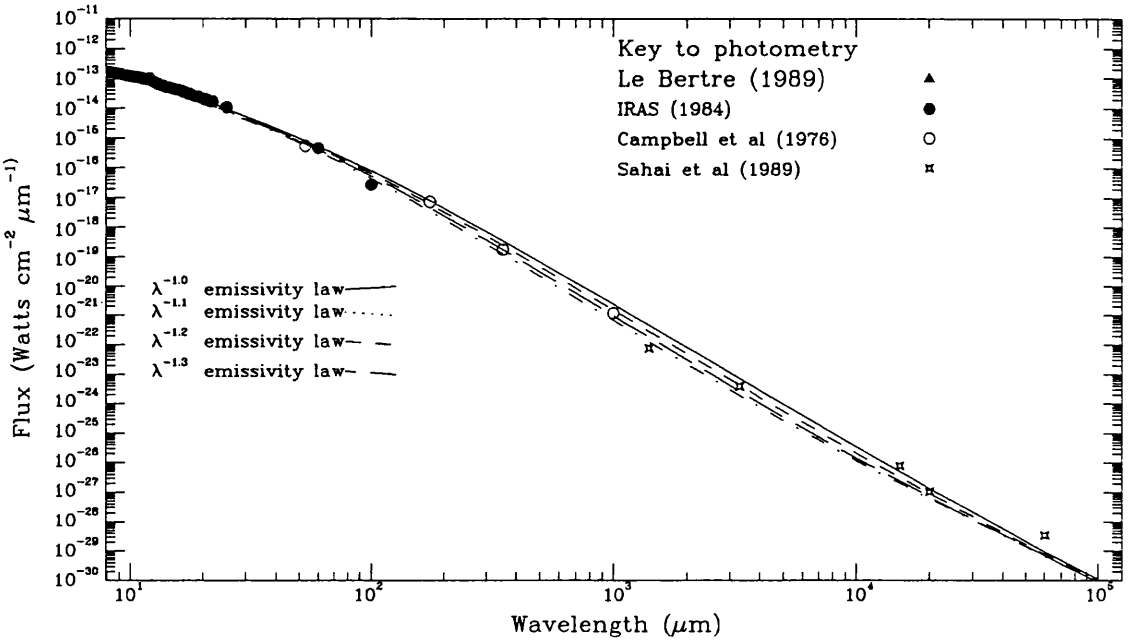

best fit to the data, in the models presented here comes from the Hoare optical constant synthesis, and since the models presented by Orofino *et al.* in both papers (Orofino *et al.* 1987, 1990) are based on a less comprehensive method of radiative transfer calculation that neglects scattering and the heating of inner dust by IR radiation from the outer grains, it is felt that inaccuracies in the modelling process adopted by Orofino *et al.* , in conjunction with the single grain size approach adopted in their models lead to the differences between their best model and that presented herein.

The fact that the adopted far-IR AC dust emissivity agrees well with the laboratory derived values is very encouraging, and perhaps indicates the superiority of using a grain size distribution rather than a single grain size, in the modelling process. At the longest wavelengths however, the model fit becomes inadequate, and possible reasons for the poorness of fit at wavelengths longer than 3mm will now be discussed.

Inspection of Table 2 reveals how, for the best model, when beam size effects are taken into account, the model flux lies below the 1.5cm flux detected by Sahai *et al.* (1989) even when account is taken of the finite beam-size of the observation. The same model

lies well above the measured 2cm flux, which, as pointed out by Sahai *et al.* (1989) was not obtained at an epoch close to visual maximum, and should therefore have a reduced photospheric contribution. Since at 2cm, the best model predicts that approximately 50% of the observed flux is blackbody emission from the stellar photosphere, then the model excess over the observations may understood.

Even with p=1 though, the predicted model fluxes are well below both the observed 1.5cm and 6cm fluxes of 6±1 mJy (Sahai *et al.*, 1989)) and 0.42±0.10 mJy (Spergel *et al.*, 1983) from IRC+10°216 suggesting that at these radio wavelengths at least, another emission component, in addition to the sum of thermal emission from dust and blackbody emission from the stellar photosphere, is required to increase model fluxes to the level suggested by the observations. In order to investigate the nature of this additional component, the excesses of observations over model were calculated at both 1.5cm (20Ghz) and 6cm (5Ghz), and found to be 3.75 mJy and 0.3 mJy respectively. The excess is proportional to $\nu^{1.8}$ and is therefore close to the ν^2 proportionality that would be indicative of free-free emission from an optically thick medium. The most likely candidate for the source of this excess would be a warm circumstellar chromosphere. Of course, if the excess emission of observation over model is optically thick, then the actual excess over the optically thin dust emission at 1.5 and 6cm is greater than that given above, by an amount equal to the photospheric contribution at each wavelength, which for the best model is 1.2 mJy at 1.5cm and 0.08 mJy at 6cm. The 'corrected' excesses therefore becomes ≈5 mJy at 1.5cm and 0.38 mJy at 6cm. If it is now assumed that the excess is coming from a region close to the stellar surface (i.e. R≈ R_*) then at the adopted distance of 200 parsecs, with a stellar radius of 7.25×10^{13}cm, the region must have a temperature of 9020K to sustain the observed excess, if it is assumed to be a blackbody radiating in the Rayleigh-Jeans tail. Interestingly, this is reasonably close to the 10000K value assigned to the chromospheric temperature of the C star TX Psc by Luttermoser *et al.* (1989), the only C star whose chromosphere has been studied in detail to date, using UV data from the IUE. It is therefore suggested that there is definite evidence for an optically thick chromospheric emission component from IRC+10°216 at 1.5cm and 6cm.

Figure 5.13: Normalised (to peak value) surface brightness profiles for the best fitting model, at a selection of wavelengths, for offsets of up to one arcsecond from the star.

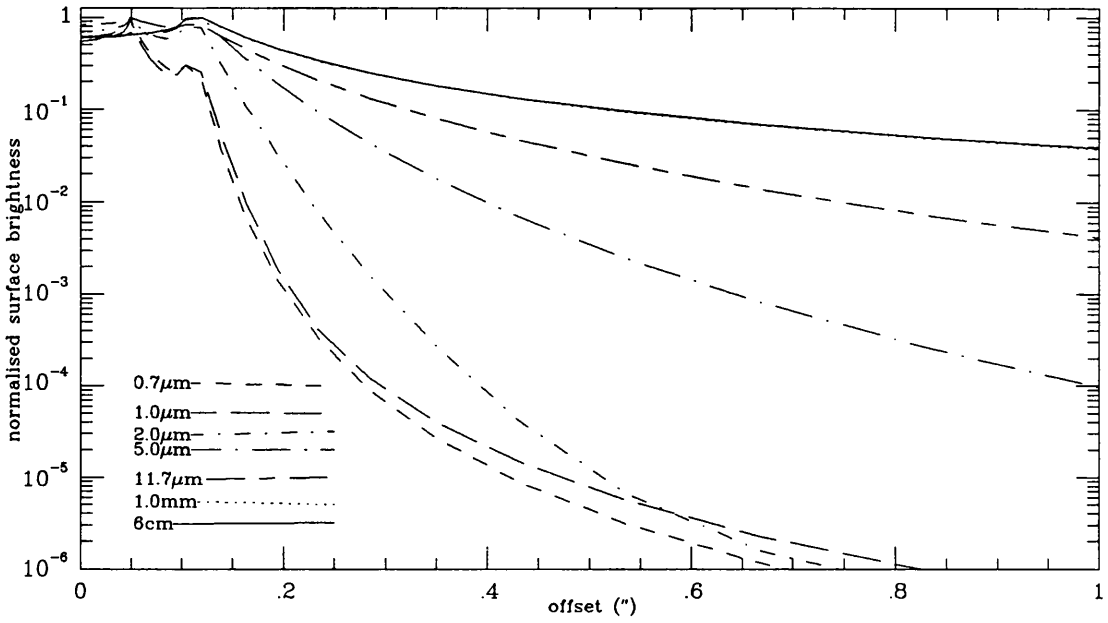

5.4.6 Surface Brightness Distributions

One of the key tests for any circumstellar dust model for IRC+10°216 is its ability to reproduce spatially resolved observations of the object, at a number of different wavelengths. Figure 5.13 presents normalised surface brightness profiles, calculated for the best fitting model, at a number of wavelengths, at distances up to one arcsecond from the star. The behaviour of the selected profiles within the central arcsecond may be seen to be relatively complex, and the observed profiles are worthy of some discussion.

The first point to note is that there are two apparent 'peaks' in the surface brightness profiles at the shorter wavelengths. Each discontinuity is due to a limb brightening effect at the point in the shell where a dust component is condensing. The inner peak arises as the SiC dust condenses at a temperature of 1500K, whilst the second occurring further from the central star is due to the condensation of the AC component. At the longer wavelengths ($\lambda \geq 100\mu$m) the inner peak is missing, due to the negligible contribution of the hot SiC grains to the flux at these long wavelengths (the emissivity of SiC grains in the far-IR has been assumed to decline as $\lambda^{-2.0}$ due to their crystalline structure, and

hence will always be dominated in these multi component models by the AC grains, whose fall-off in emissivity is less steep than λ^{-2} in these models).

The effect of scattering at shorter wavelengths for the AC dust used in the modelling may be seen by the broadening of the 0.7μm and 1.0μm profiles when they are compared with the 2.0μm profile. It should be noted however that when these model profiles are compared with those calculated by Mitchell and Robinson (1980) for a dust shell composed of graphite grains, the effect of scattering is relatively unimportant at large angular offsets for AC grains at the wavelengths under consideration here. To test whether this deduction is true, the predicted surface brightness profiles are now compared with observations made at a number of wavelengths, obtained from the literature.

In the optical and near-IR region, Le Bertre (1988b) obtained CCD frames of IRC+10°216 through Gunn g, r, i and z filters, and derived an intrinsic width of the IRC+10°216 central core region at each of these wavelengths by deconvolving the instrumental profile as measured by observing a nearby point source, from the observed surface brightness profile of IRC+10°216. In Table 5.3 the calculated FWHM's are compared with those measured by Le Bertre; in general, the calculated FWHM's are much narrower than the deconvolved observations, indicating that though at these shortest wavelengths the best model is predicting the fluxes fairly accurately, the scattering effects of the dust are not being reproduced as well as one might desire, though the signal to noise ratio of the Le Bertre observations, and indeed the spatial resolution are not high enough for any detailed conclusions to be drawn by comparing the models with them. It is noted that Le Bertre himself, using his single sized grains was unable to find an unique model able to match the observed FWHM's at all wavelengths; this probably reflects poor knowledge of the grain albedo's in the optical.

At longer wavelengths, direct images are more difficult to obtain due to the relative scarcity of IR array detectors. Instead, most workers have used interferometric techniques to derive information as to the spatial extent of IRC+10°216. Ridgeway and Keady (1988) used both lunar occultation and speckle interferometry to derive the half intensity radius of the source profile (assumed to be gaussian) at wavelengths of 1.66, 2.22, 3.05 and 4.64μm. The resolution of their interferometric beam was 0″.084, whilst the estimated resolution limit of the occultation data was 0″.06. To compare a model with the observations the model surface brightness profiles were convolved at these wavelengths with gaussian beams

Table 5.3: The FWHM's of the model surface brightness profiles, are compared with the measured FWHM's for IRC+10°216 by Le Bertre (1988b) and Ridgeway & Keady(1988).

Filter	Deconvolved FWHM (″)	Calculated FWHM (″)
Gunn g	1.4±0.2	0.10
Gunn r	1.3±0.1	0.14
Gunn i	1.3±0.2	0.12
Gunn z	1.29±0.07	0.13
1.64μm	0.1	0.095
2.22μm	0.15	0.15
4.64μm	0.15	0.16

with diameters matching the quoted resolutions, and then measured the FWHM of the resultant profile. These results are also given in Table 3; there is good agreement between the calculated FWHM's and those obtained from the observations.

Sutton *et al.* (1979) used a spatial interferometer with a maximum spatial resolution of 0″.2 to measure the surface brightness of IRC+10°216 at a wavelength of 11μm. Their interferometer passband was wide enough to include the 11.4μm SiC emission feature, and thus these observations are of use in constraining the inner radius of the circumstellar dust shell. They interpreted their observations in terms of two gaussian components, the first of diameter $\leq$ 0″.2, assumed to be due to stellar emission, the second having a 1/e diameter of 0″.90, which was thought to be due to dust emission. The two components contributed $\leq$ 14% and $\geq$86% to the total flux respectively. The result of convolving the best fitting model's surface brightness profile with a gaussian beam of FWHM 0″.2, is a profile that has a full width to 1/e diameter of 0″.6 which is a little narrower than that measured by Sutton *et al.*. That model does not however predict the unresolved central component, which Sutton *et al.* assumed to be due to the star, since the optical depth

in the SiC feature is greater than unity (Figure 5.5), and therefore dust emission should dominate at this wavelength; the star should be invisible, as it contributes $\leq$1% of the flux at this wavelength.

At a longer wavelength of 61μm, Fazio *et al.* (1980) used a gaussian beam of diameter 0'.92 to observe IRC+10°216. Convolving the best fitting model's surface brightness profile at 61μm with a gaussian beam of this diameter results in a predicted observed size for the best model of 1'.03. This is slightly smaller than the size as measured by Fazio *et al.* of 1'.3$\pm$0'.1, but since bandpass of the photometer used by Fazio *et al.* covered the wavelength range 40-250μm, and the observed size will be an 'average' of the source size in the quoted region of spectral sensitivity. It is therefore felt that the agreement between model and observations is reasonable.

It has been assumed throughout the modelling process that the mass loss from IRC+10°216 is uniform and that the dust envelope is spherically symmetrical. Observations show that for the outer envelope this assumption is fairly safe; the CO emission mapped by Wannier *et al.* (1979) presents very little evidence for large (angular) scale asymmetry. On smaller scales, the evidence for asymmetry has been reviewed by Martin & Rogers who surmised that the asymmetry was most pronounced within the central 20" of the object, and that this reflected the fact that the region of most recent mass loss was being studied at these scales. Recently, Le Bertre (1988b) has obtained a series of images, which he suggests give direct evidence of non-uniform mass mass loss, where the departure from circular symmetry was interpreted as being due to random radial inhomogeneities in the mass loss on large time scales (which he puts at longer than 20 years). It is interesting to note that though the models presented in this paper do not attempt to take into account the observed departures from spherical symmetry in the inner envelope, the model fluxes do agree fairly well with those measured by the observers, though at the shortest wavelengths, where the most notable asymmetries have been observed, the fit of model to observation could be improved. Although as pointed out above, better knowledge of the dust grain albedoes via improved optical constants may well improve the fit, particularly with regards to matching the spatial data. To summarize; the observed asymmetries in the envelope occur at the shortest wavelengths where knowledge of dust optical constants is not good, and also, as the asymmetries are observed on relatively small scales in the hotter, inner regions of the dust envelope then the properties of the outer envelope derived in preceding

Sections remain unchanged.

5.5 Conclusions

In the range $0.5\mu m \leq \lambda \leq 1.5cm$ the observed energy distribution of IRC+10°216 may be understood in terms of a multiple component optically thick dust shell comprised of AC and SiC dust grains with radii spanning the range $0.005\mu m \leq 0.05\mu m$ in a modified MRN size distribution, surrounding a 2300K stellar photosphere. The best fit to the far-IR observations occurs if the grain emissivity is allowed to vary as $\lambda^{-1.0}$. The best fitting model has dust to gas ratios by mass of 2.5×10^{-3} and 5.0×10^{-4} for the amorphous carbon and SiC components respectively. Within the adopted parameter space, graphite dust grains are unimportant in determining the character of the emergent spectrum of IRC+10°216, since models calculated for the object using pure graphite grains give an unacceptable fit to the observations.

At wavelengths longer than 3mm, it is suggested that optically thick free-free emission from a chromosphere with a temperature of $\leq$10000K is needed to explain the observed continuum emission from IRC+10°216.

Chapter 6

Anomalous Dust Envelopes

6.1 Introduction

Mass loss, typified by cool and dusty winds, is a dominant feature in the lives of AGB red giant stars. Dust that condenses in outflows around these objects should reflect the chemical composition of the underlying photosphere, since that is presumably the source of any mass outflow. Around 'oxygen-rich' (C/O$\leq$ 1.0) stars, silicate dust with its characteristic solid state spectral features at 9.7μm and 18μm is expected to condense. In 'carbon-rich' outflows (C/O$\geq$ 1), dust composed of amorphous carbon and/or graphite, together with silicon carbide (SiC) should condense, and the 11.4μm SiC emission feature should be visible. Thus the winds from most M giants and most S stars are characterised by silicate dust features and those from C stars by SiC dust features. Strong S stars (so called because their carbon and oxygen abundances are almost exactly equal) sometimes show a mixture of both silicate and SiC dust in the same spectum (Whitmore, 1986; Little *et al.*, 1988; Skinner *et al.*, 1990). Observations of most red giant stars have generally confirmed this scenario. In this chapter, an attempt is made to apply the lessons learned in modelling O and C-rich circumstellar envelopes around these 'normal' red giants to two recently discovered classes of star which appear to have abnormal dust shells.

Previously published observations of, and models for, stars with anomalous dust are reviewed. In the succeeding sections, details of a multi-wavelength investigation of a number of the 'oddball' stars are given, and in the resulting analysis a comparison is made between these observations and published models for these objects.

6.1.1 C Stars with Oxygen-rich Dust

One of the most unexpected discoveries, made as a result of post-mission analysis of the *IRAS* LRS database of 7–23μm spectra of point sources, was that a number of objects that had been classified as C stars on the basis of their optical spectra, exhibited 9.7μm and 18μm emission features, normally associated with O-rich circumstellar envelopes.

The precise number of C stars with apparently oxygen rich circumstellar envelopes is a topic of much debate. Initially, Little-Marenin (1986) listed just 3 C stars as having anomalous dust shells, whilst later discussions by Willems & de Jong (1986); Vardya (1989); Skinner *et al.* (1990) and Lloyd Evans (1990, 1991) have raised the number of candidate objects to between 7 and 20. It appears that most of the stronger candidate objects have a further observational characteristic in common, in that as well as having silicate dust shells they all appear to be 'J' type C stars (Lloyd Evans 1990, 1991; Lambert *et al.* 1990) (J stars are objects with enhanced ^{13}C lines in their spectra). Confirmation that at least some of these objects have unusual circumstellar envelopes has come from the detection of a number of OH or H_2O maser sources (Benson & Little-Marenin 1987; Nakada *et al.* 1987; Nakada, Deguchi & Forster 1988; Little-Marenin *et al.* 1988) coincident with the optical positions of the C stars (these masers are also a diagnostic of oxygen-rich environments).

A number of models have been suggested to explain the unusual nature of these objects. Willems & de Jong (1986,1988) have suggested that these stars are transition objects that have recently and rapidly evolved from oxygen-rich stars to carbon-rich stars; in this model the observed silicate dust shell is a 'fossil' remnant of mass loss during a previous O-rich phase. A similar model has been quantitatively applied to a few objects by Chan & Kwok (1988) who attempted to match the observed energy distributions for two 'oddball' stars using a detached shell model, in which mass loss had ceased from the C star, with the IR emission coming from the dust that condensed in the stellar wind during the previously O-rich epoch of mass loss.

An alternative binary model has been proposed (Benson & Little-Marenin 1987) to explain the observed energy distributions of these stars. In this qualitative model, the objects are assumed to be spectroscopic binary systems containing a C star and an M star. The C star has a very low mass loss rate; in consequence its dust shell has a low optical depth, and the star is relatively unobscured in the optical, whilst the low mass loss

rate means that the star has relatively little IR emission, and a weak SiC feature. The companion star is assumed to have a very high mass loss rate; it is therefore surrounded by a high optical depth of dust which is opaque to the underlying O-rich stellar photosphere in the visible region of the spectrum, whilst the thermal re-emission of the absorbed stellar radiation makes the dust envelope a bright mid IR object. Thus, Benson & Little-Marenin suggest that the observed spectrum is a composite one, dominated in the optical by the relatively unobscured C star, and in the mid and far-IR by dust emission from the circumstellar envelope of the (optically invisible) companion M star. A variation on this model, again qualitative in nature, designed to overcome some of the problems associated with the original, was proposed by Lloyd Evans (1990) and also favoured by Lambert *et al.* (1990) in which the objects are still assumed to be binaries, but the dust emission originates in an accretion disk surrounding a main sequence companion, rather than an M star.

Vardya (1989) has offered a different qualitative model for these objects, in which it is suggested that an unusual chemical equilibrium exists in the circumstellar matter such that an O-rich environment is produced out of C-rich material due to an interaction between graphite and SiC grain formation, with CO molecules in the circumstellar envelope. This model is largely derived from the work of Sharp (1989) whose theoretical studies of chemical reactions occuring in stellar envelopes first indicated that graphite could condense in marginally O-rich envelopes. A model involving dust grains forming out of thermodynamic and chemical equilibrium in the circumstellar envelopes of these objects is also favoured by Skinner *et al.* (1990), who also use it to explain a second type of star observed to have anomalous dust; M stars with apparently C-rich dust shells.

6.1.2 M Stars with SiC Dust

A further unexpected discovery of a search through the *IRAS* LRS catalogue was the apparent association of a number of (optically classified) O-rich M stars with C-rich circumstellar envelopes. The first two examples of this type of object were discussed by Skinner & Whitmore (1988a), and a further 8 candidates were presented by Skinner *et al.* (1990), who suggested the model described in the previous section, to explain the existence of both types of stars observed to have anomalous dust.

6.2 Observations

Before any detailed observing programme could be embarked upon, it was decided to re-examine the observational material for both types of 'oddball' star, and select for further study only those for which there was the strongest observational evidence of anomalous dust emission. In common with previous workers, the starting point for this re-examination was the *IRAS* catalogue of low resolution spectra (LRS). The procedure adopted for this work will now be described. It should be emphasised that for this project, all of the catalogues described were cross-correlated independantly of the work of Skinner *et al.* (1990), and that the work below is in fact more up to date than that presented therein.

The *IRAS* LRS catalogue (*IRAS* Science team 1986) contained 7-22μm spectra of 5425 sources, and is only one of a number of catalogues available to astronomers in machine readable form on the UK Starlink computer network. By cross-correlating the contents of the LRS catalogue with other catalogues also available in machine readable form, a database of available catalogued information on stars with spectral types M, S and C was created. The cross correlation, performed using the Starlink data manipulation package SCAR (Software Catalogue Access and Reporting System) developed at the Rutherford Appleton Laboratory, involved data drawn from the *Michigan Spectral Catalogue* (Houck & Cowley 1975, hereafter MSC), the *General Catalogue of Variable Stars* (Kukarkin *et al.* 1969, hereafter GCVS), the *Yale Bright Star Catalogue* (Hoffleit & Jaschek 1984, hereafter YBSC), *A General Catalogue of Cool Carbon Stars* (Stephenson 1978,1989), as well as data from the LRS. The final database gave a compilation of spectral types, photometry, variable types and periods and, of course the 7-22μm LRS spectra for each object. Particular care had to be taken over the positional associations between the *IRAS* and other catalogues, since the accuracy to which the *IRAS* source positions were known was low, and some spurious associations could have arisen.

Each *IRAS* LRS spectrum had been automatically classified by computer according to a 2 digit scheme, in which the digits characterised the shape and also gave some quantitative indication as to the strength of any significant feature present in the observed spectral window (Beichmann *et al.* 1988). Of particular interest for this project were the classes 2n and 4n, since these correspond to either silicate (class 2) or silicon carbide (class 4) dust emission of strength n, where n is an integer in the range 1 to 9. Candidate stars with anomalous dust emission were therefore defined as either stars flagged with spectral

type C as having LRS spectra of class 2n, or M Stars having 4n class LRS spectra. In practice, owing to the low signal to noise ratio for some sources, and owing also to the inability of the *IRAS* classification algorithm to cope with weak silicate or silicon carbide dust emission (if the strength of the emission band is less than 10% of the local continuum, then a.. classification into class 2 or 4 is arbitrary, *IRAS* Science team 1986), all candidate spectra were inspected by eye to determine the nature of the dust associated with them

It is not surprising that since the method employed here is similar to that used by the earlier workers, particularly Skinner *et al.* (1990), the final list of candidate sources differs little from those already published. Table 6.1 lists physical parameters, derived from the cross-correlations with the other catalogues for the 8 C stars for which there is strongest evidence for an association with silicate dust, whilst Table 6.2 lists the same parameters for 11 M stars that appear to be associated with silicon carbide dust emission. Figure 6.1 presents the *IRAS* LRS spectra of the 7 best candidate C stars with O rich circumstellar dust; the dust features associated with the stars may be directly compared with those associated with the 'normal' red giants R Lep (C star with C rich circumstellar envelope as exemplified by the 11.4μm SiC emission feature) and WX Ser (M Star with O rich circumstellar envelope exhibiting 9.7μm and 18μm silicate emission features), both of which are included in the diagram. The *IRAS* LRS spectra for the 10 candidate M stars with apparently C-rich circumstellar envelopes are given as Figure 6.2; once again the LRS spectra for WX Ser and R Lep are given for comparison.

The final lists of candidate objects given in Tables 6.1 and 6.2 do differ a little from those previously published, most recently by Skinner *et al.* and Lloyd Evans. Specifically, the objects C1633 and C2123 listed by Skinner *et al.* are not included, as they are now generally recognised as being mis-identifications or mis-classifications (Lloyd Evans, 1990; Le Bertre *et al.*, 1990), whilst the star RV Cen, present in the C star list presented by Skinner *et al.*, has been left out of Table 6.1, as a close inspection of the *IRAS* LRS spectrum revealed that the dust emission from this star was in fact due to SiC rather than to silicates. Note also the misprint in Skinner *et al.*; FJF270 is incorrectly labelled FJF272 throughout the paper.

Figure 6.1: *IRAS* LRS Spectra for C Stars with Silicate Dust. Spectra of WX Ser and R Lep are given for comparison

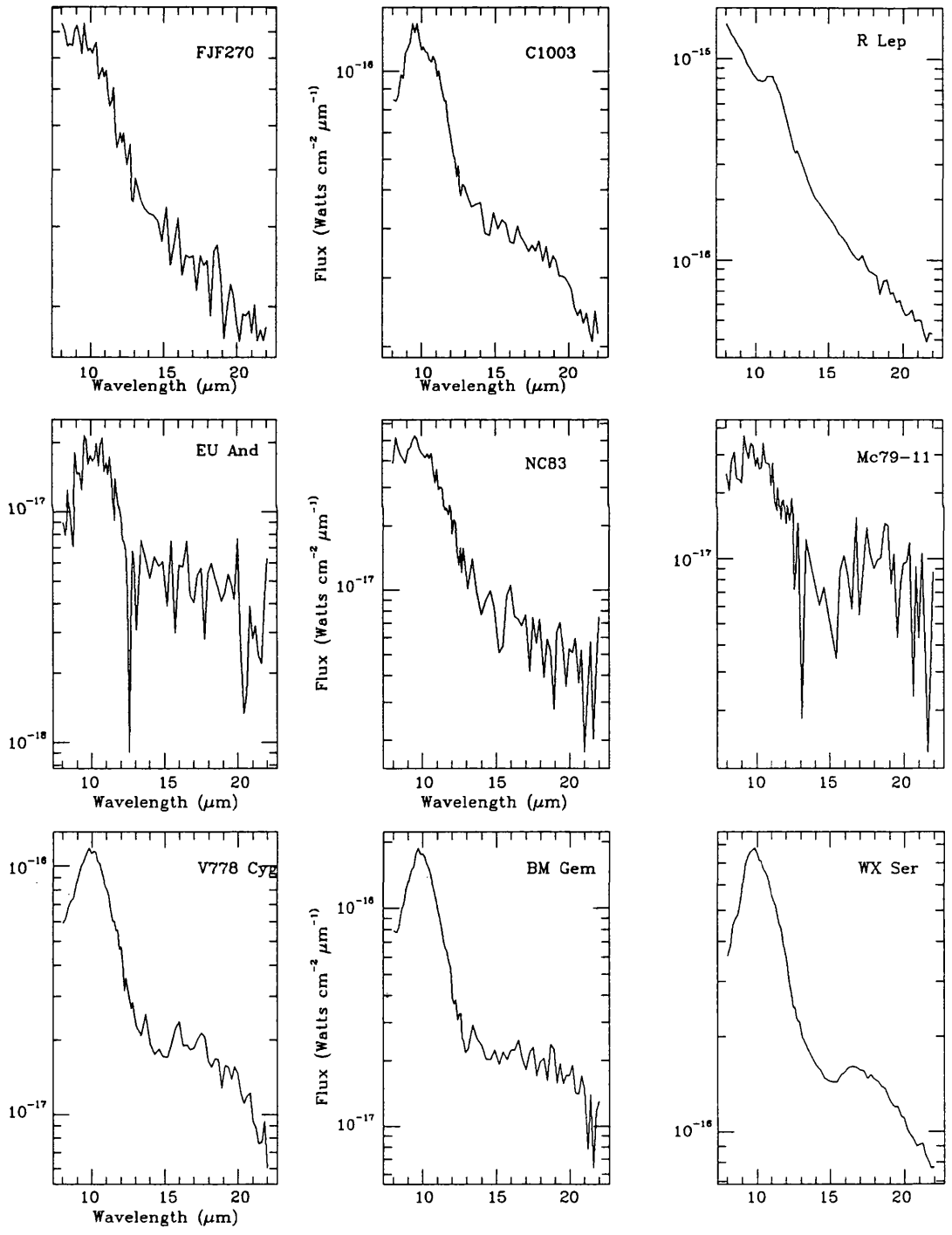

Figure 6.2: *IRAS* LRS Spectra for M Stars exhibiting SiC emission. Spectra of WX Ser and R Lep are given for comparison

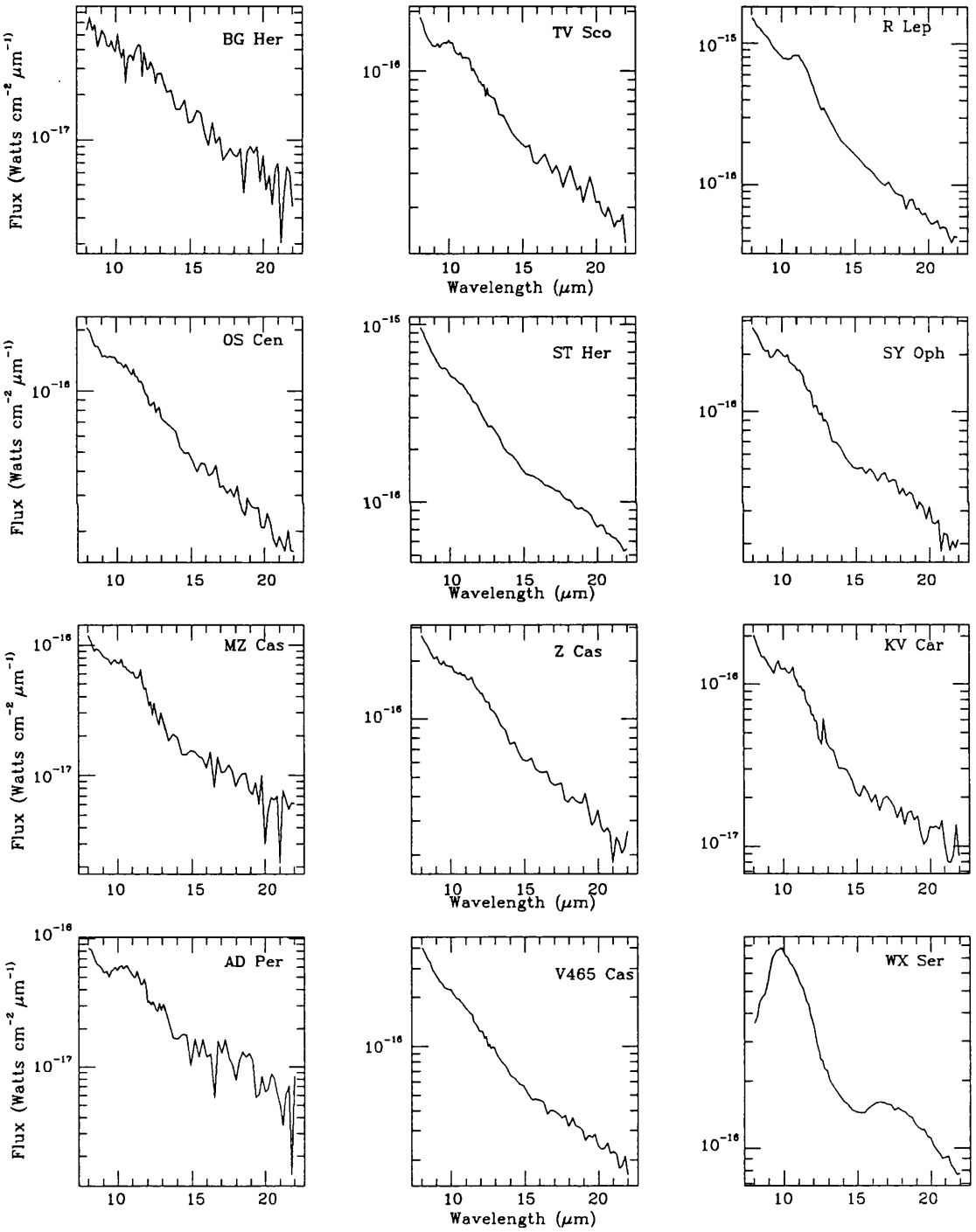

Table 6.1: **Physical properties of C stars with silicate dust**

Star Name	Spectral Type	Variable Type	Stellar v_r (kms^{-1})	Reference
BM Gem	C5,4J	Lb	85.3±0.3	1,2
C1003	C3,5J	-	+40±1	1,3
MC79-11	C4,5J	-	-	1
RV Cen	Nb	M	-	4
FJF270	C5,5J	-	-	1
NC83	C	-	-20.81±0.35	1,2
V778 Cyg	C4,5J	Lb	-33.01±0.35	1,2
EU And	C4,4J	SR	-43.69±0.25	1,2

References

1. Lloyd Evans (1990)
2. Lambert *et al.* (1990)
3. Lindgren Private communication
4. Skinner *et al.* (1990)

6.2.1 Visual and Photographic Photometry

The variability types and periods have been very well defined for the sample of M stars with SiC features, as may be seen in Table 6.2. The C star sample though has not been well observed; the GCVS lists variability types for only three of the stars, and no periods are given. In an attempt to improve knowledge of the light curves of these objects and better define the periods and amplitudes of any light variations in the optical, a collaboration was begun in May 1988 with amateur astronomers in the British Astronomical Association Variable Star Section (BAAVSS) whereby the three brightest Northern members of the C star sample; EU And, BM Gem and V778 Cygni and another J type C star, VX And, whose *IRAS* LRS spectrum did not exhibit anomalous dust emission (observed as a control with which any derived periods for the oddball stars could be compared), were observed visually by a number of BAAVSS members on a regular basis during the period 1988–1990.

Unfortunately, visual photometry of red stars is fraught with difficulties, and great care

Table 6.2: **Physical properties of M stars with silicon carbide dust**

Star Name	Spectral Type	Variable Type	Period (days)
MZ Cas	M2 Iab	SRb	-
V465 Cas	M3	Lb	-
AD Per	M3Iab	SRc	320
Z Cas	M7e	M	497
KV Car	M4 III	-	-
OS Cen	M	M	433
ST Her	M6–7S	SRb	148
SY Oph	M4	SRb	132
BG Her	M3	M	348
TV Sco	MS	SRb	200

must be used in interpreting results from a visual photometric observing campaign involving C stars, which owing to the combination of cool surface temperature, and enshrouding dust envelopes are amongst the reddest objects that a visual observer can study. There are several physiological reasons as to why these difficulties arise, and if full value is to be obtained from any results obtained from any observations, then these reasons must be understood, and attempts made to circumvent their effects. If this is not done, the work of a single observer may show considerable internal scatter, and when the work of several observers is compared it is not uncommon to find that one is systematically brighter than another by as much as a magnitude.

The main physiological cause of scatter in visual photometry of red stars is the 'Purkinje effect' which arises because of the different spectral responses of the rods and cones in the human eye. At low light levels, only the rods whose spectral sensitivity peaks at 5100Å are triggered by radiation, whereas at higher light levels, vision is mainly via the cones whose spectral sensitivity peaks at 5500Å. Thus, if R and W are the intensities of a red and a white star as viewed by the naked eye, R will appear up to 0.5 magnitudes brighter than W when observed by a telescope of moderate aperture, due to the increased

intensities of the telescopic images.

In principle, problems associated with the Purkinje effect may be avoided by using a filter to isolate light of a particular colour. The use of filters in visual photometry of stars does however introduce other problems though; particularly the loss of light, greatest in the narrow passband filters that would be most useful; and the need to determine a new set of comparison star magnitudes as seen through the filter. Nevertheless these problems may be less troublesome than that of analysing observations contaminated by the Purkinje effect, and it was therefore decided to attempt an experiment in visual photometry using a set of filters for these stars. The experiment, described by Isles (1989), meant that as well as observations obtained with unfiltered equipment, a small number of filtered observations were available to evaluate the errors in the unfiltered observations due to the Purkinje effect. The filters selected for use in this study were gelatine filters manufactured by Rosco Laboratories Ltd for use in stage lighting. These had the advantage of a well defined spectral response, and (important where amateur observations are concerned) were supplied free of charge to the observers by the manufacturer. Two gelatine filters were sent to observers. The first selected filter was Rosco filter number 15 which had an equivalent wavelength of 5370Å, and a transmission of 22%, selected because visual estimates made with this filter would closely match photoelectric observations made with the standard V filter (Isles, 1989). The other filter selected was Rosco filter 67, having an equivalent wavelength of 4630Å, and a transmission of 44%. The spectral response of this filter, when convolved with that of the human eye, was such that for stars with a wide range of colours, provided their spectra approximated those of blackbodies, the visual estimates made with the filter had a spectral response peaking 76% of the way between that of the V and B filters (Isles, 1989).

In addition to the programme of observations of C stars with unusual dust, the BAAVSS analysis of observations for two M stars with apparent SiC features was obtained (Isles 1989 private communication) spanning the years 1971-1988 in order to compare with the GCVS derived light curve for each star.

Finally, during the process of arranging the observing collaboration with the BAAVSS, serendipitous photographic observations of one of the target stars, V778 Cygni came to light. In 1980, a supernova (SN 1980K) appeared in a nearby galaxy NGC 6946, and for a period of time V778 Cygni was used as a comparison star for the supernova, as it

Table 6.3: **Summary of INT observations**

Object	date	U.T. Start	Exposure (S)	Z.D.	λ_c(Å)
V778 Cyg	9/10/88	23:56	60.0	46.2	7500
V778 Cyg	10/10/88	00:01	100.0	46.8	8500
ST Her	10/10/88	19:44	1.0	49.6	8500
ST Her	10/10/88	19:46	2.0	49.8	7500
AD Per	11/10/88	05:29	10.0	44.6	7500
AD Per	11/10/88	05:31	10.0	44.8	8500
BM Gem	11/10/88	05:45	60.0	19.5	7500
BM Gem	11/10/88	05:47	60.0	19.0	8500

was close enough to the supernova's position that it appeared in around 50 photographic observations of the supernova, obtained by a number of amatuer astronomers. Once the true identity of V778 Cygni was realised, these 50 observations, spanning the period October 1980 to January 1981 were analysed (Taylor 1981) and a photographic light curve constructed for the star for the 3 month period. The results of this analysis were obtained (Hurst 1989, private communication) and added into the database of visual observations for the star, in the hope that analysis would reveal any longer term periodicities in the light curve that analysis of the visual data from 1988–1990 alone would not.

6.2.2 Optical Spectroscopy

Low resolution spectra covering the wavelength range 6700Å–9800Å were obtained for 4 stars, BM Gem, V778 Cyg, AD Per and ST Her during a visit to the 2.5m Isaac Newton Telescope (INT) at the Roque de los Muchachos Observatory La Palma in October 1988. The spectra were obtained using the 500mm camera on the Intermediate Dispersion Spectrograph (IDS) with a GEC CCD. The R150V grating was used, giving a dispersion at the detector of 131.2Å mm^{-1}. The individual observations are summarised in Table 6.3. The spectra were extracted using the PAMELA optimal extraction algorithm (Horne, 1986) which has been incorporated into the FIGARO analysis package. This algorithm was used in place of the conventional FIGARO routine since it offered offered a gain in

Figure 6.3: INT IDS Spectra of V778 Cyg, BM Gem, AD Per and ST Her

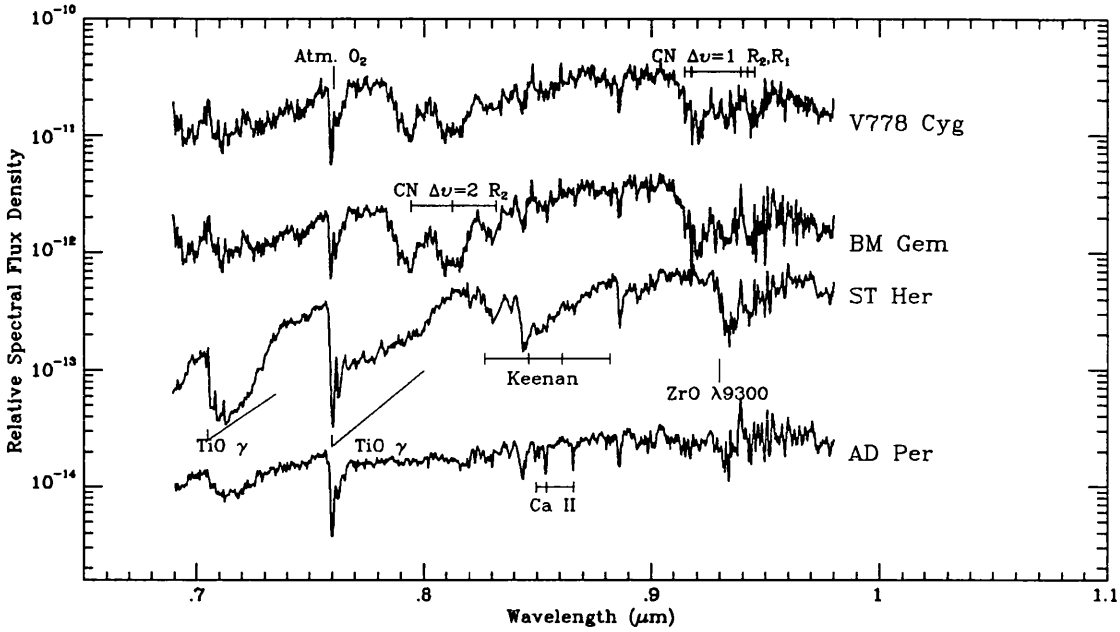

effective exposure time over it, whilst automatically accounting for the effects of moderate geometric distortion and cosmic ray hits.

Once extracted, the spectra were wavelength and flux calibrated, also using routines contained in the FIGARO package. The wavelength calibration was performed by applying a polynomial fit, derived from a similarly extracted CuNe arc spectrum, to the extracted stellar spectra. The flux calibration was based upon observations made on the same night of the spectrophotometric standard star EG247. The flux calibration procedure included a correction for extinction at the zenith of 0.13 and 0.10 magnitudes, as measured by the Carlsburg Meridian Circle at La Palma, on the nights of 10th and 11th October 1988 respectively (D. Monk, private communication). The observed spectra for the four stars are presented in Figure 6.3, which also indicates identifications for any spectral features present in the spectra.

6.2.3 Near-IR Spectroscopy and Photometry

Near IR spectra were obtained as service observations using the Fabry-Perot Infrared Grating Spectrometer (FIGS) (Bailey *et al.*, 1988) on the 3.9 metre Anglo Australian

Table 6.4: **Summary of AAT FIGS Observations, March 1988**

Object	Date	U.T. Start	Window
C1003	04/03/88	14:29	H,K,L
KV Car	04/03/88	14:54	H,K,L
OS Cen	04/03/88	15:14	H,K,L
TV Sco	08/03/88	19:42	H,K,L
SY Oph	08/03/88	19:53	H,K,L
BG Her	08/03/88	20:29	H,K,L

Telescope (AAT) for 6 stars during March 1988. The observations, summarised in Table 6.4, were made in the H (1.5–1.8μm), K (2.0–2.5μm) and L (3.0–4.1μm) atmospheric windows at a resolution ($\Delta\lambda/\lambda$) of 560 at H, falling to 480 at K and L. Wavelength and flux calibrated spectra were extracted from the raw FIGS data cubes using the FIGS reduction programmes in the FIGARO package. Wavelength calibration was performed using observations of a Xenon arc at H and K, whilst at L, the calibration was enacted using the telluric absorption line at 3.3109μm. Each spectrum was flux calibrated by ratioing the spectrum with that of a known near-IR standard from the list given by Allen & Cragg (1983) that had been observed shortly before or after it. Further flux calibrated near-IR spectra were obtained of MC79-11 and BM Gem using a 1.2–4.1μm Circular Variable Filter (CVF) spectrometer during a visit to SAAO in November 1988. These spectra were at relatively low resolution ($\Delta\lambda/\lambda \approx 50$) and covered the J (1.2–1.3μm) atmospheric window, as well as the H, K and L bands. The K- and L- band spectra obtained of these stars were of rather poor signal to noise, primarily due to the fact that the flux calibration process used at SAAO neccesitated division of the observed spectrum by that of a standard A type star; most standards proved to be faint at the longer wavelengths. The poor observing conditions encountered made it difficult to obtain standard spectra of particularly high S/N ratio, and consequently during the division additional noise was introduced into the spectrum of interest purely due to the inherent noisiness of the standard.

A near-IR spectrum was also obtained of the star V778 Cygni as a service observation using CGS2 (a 1–5μm Cooled Grating Spectrometer) on UKIRT during late 1987. This

Figure 6.4: Near-IR spectra of C stars with silicate dust. A spectrum of C1633, a normal C Star is included for comparison.

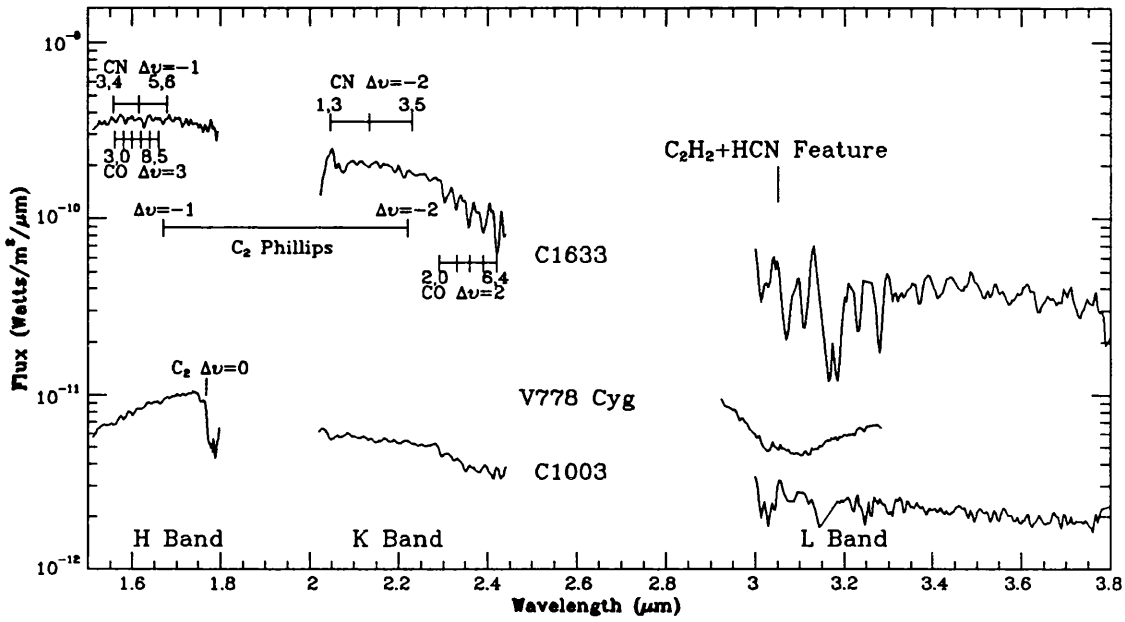

spectrum was of relatively high ($\Delta\lambda/\lambda \approx 300$) resolution and was centered on the 3.1μm C_2H_2 feature, which is often observed in the spectra of C stars.

A montage of the best near-IR flux calibrated spectra of C stars with silicate dust features are presented as Figure 6.4, whilst Figure 6.5 presents a similar montage for the best (i.e. highest S/N) observations of M stars with SiC dust. In both figures, identifications are offered for observed spectral features.

Finally, ground based 8–13μm spectra of the stars C1003 and TV Sco were obtained (C. Smith, private communication) with the UCL 10μm spectrometer on the AAT during December 1988. These spectra are presented as Figure 6.6, and provide the first independent evidence for the anomalous nature of the mid-IR emission from the circumstellar envelope of C1003. For TV Sco though, the spectrum presented in Figure 6.6 is fairly featureless, and there is certainly no conclusive evidence for either SiC or silicate emission. More recently, observations of the stars TV Sco and BG Her with the new common-user 10 & 20μm spectrometer on UKIRT (Skinner, private communication) show a broad emission feature, starting at $\approx$9μm, extending through to 12.5μm, with a small emission hump at

Figure 6.5: Near-IR spectra of M Stars with SiC emission features.

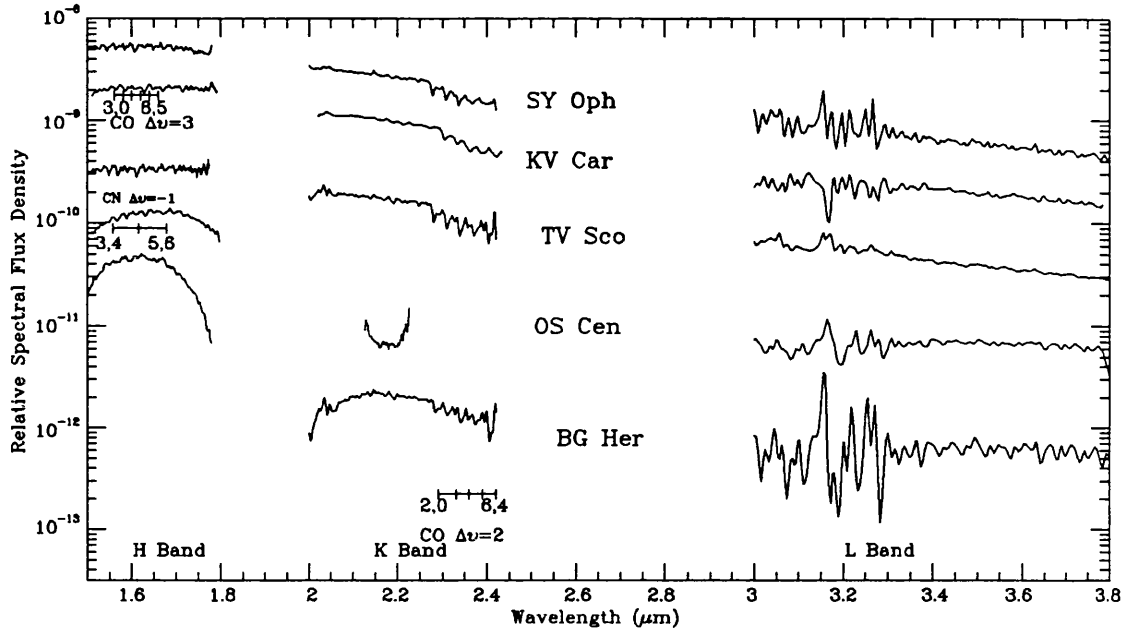

$\approx$11.2μm. The broad feature observed in these spectra is different to that observed for 'normal' O-rich stars, whose spectra were obtained using the same instrumentation. The 20μm spectrum of BG Her showed no excess at all, despite the prescence of significant excess in the 10μm spectrum. The CGS3 spectra of the unusual M stars do suggest that the spectra are unusual, but it is difficult to confirm that emission from SiC dust is the explanation for the broad spectral feature.

It is therefore apparent that for at least some of the M stars listed in Table 6.2, the SiC features are just artifacts of the low S/N ratio in the *IRAS* LRS Spectra. Further observations of the other stars listed in Table 6.2 are required to confirm the reality of the dust classifications.

6.2.4 OH Single Dish Maser Observations

Observations were obtained at 5 separate epochs in the case of V778 Cygni, and at two epochs for both BM Gem and EU And using the 76M MkIa Lovell telescope at Jodrell Bank, which has a halfpower beamwidth of 10′ at the frequencies of interest, which were the 1667.359 and 1665.402MHz mainline, and 1612.231MHz satellite OH maser line fre-

Figure 6.6: Ground based 8–13μm spectra for C1003 & TV Sco

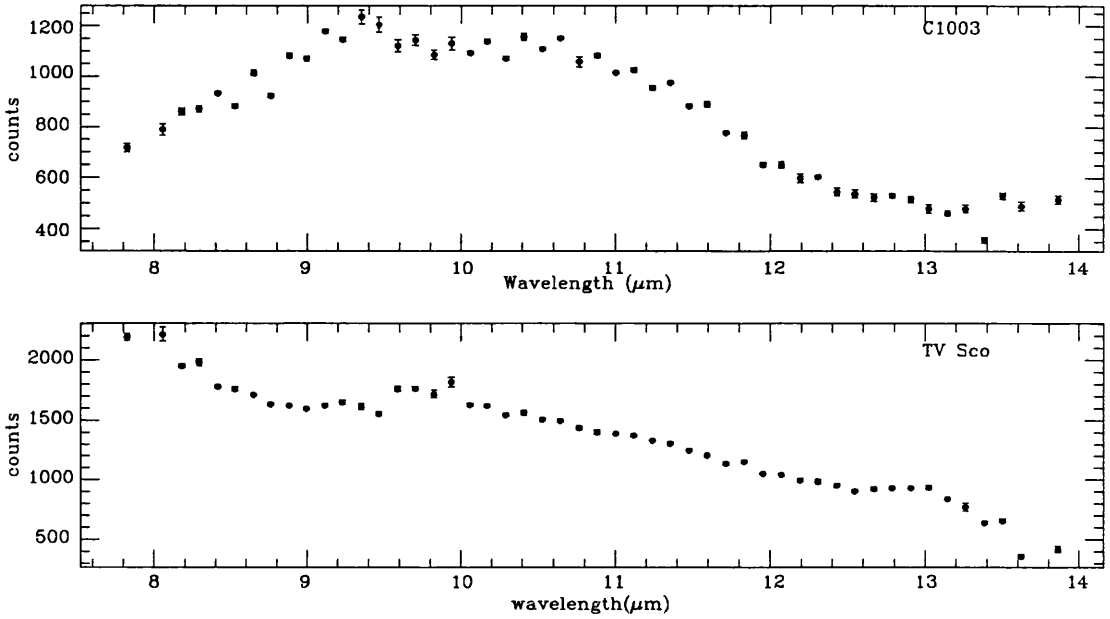

quencies. The sources were observed simultaneously in left- and right-hand circular polarisations using a dual-channel receiver system, identical to that described by Cohen *et al.* (1987), which used cooled Field Effect Transistor (FET) amplifiers and had system temperatures in the range 20–120K in both polarisations during the epochs in question. A frequency-switching mode was used to obtain spectra using a 1024 channel autocorrelation spectrometer, which was divided into two banks of 512 channels (one bank per polarisation) in order to make the observations. A bandwidth of 625kHz gave a channel spacing of 1.22kHz, and a frequency resolution of 2.16kHz (this is less than the channel spacing because of the triangular weighting of the autocorrelation function). The frequency resolution corresponded to a velocity resolution of 0.4 km s^{-1} over a total velocity range of 116 km s^{-1}. For each source, the frequency of the central channel was adjusted such that it corresponded to the radial velocity of the stellar photosphere relative to the local standard of rest at the epoch of observation, as derived from the literature. The adopted values for these photospheric radial velocities are indicated in Table 6.1.

Table 6.5 lists all observations made of the oddball stars during the period 1988 April to 1990 April. For all observations, the integration time listed in the table was split into

several shorter integrations, normally either 600 or 1000 seconds, but in some cases, as long as 3000 seconds. The raw observations were baseline subtracted, and the individual baseline subtracted spectra averaged to form mean spectra which could then be calibrated using the known calibrations (R. J. Cohen, private communication) in conjunction with the data manipulation routines contained within the Spectral Line Analysis Package (SLAP) on the Jodrell Bank Starlink node.

Note that in Table 6.5, the N, S, E and W suffixes to the April 1988 V778 Cyg data correspond to observations made at offsets of 5′ (half of one beamwidth at the frequencies of interest) from the stellar position. This was done in an attempt to investigate the angular extent of the maser region around V778 Cygni.

The individual baseline-subtracted and flux-calibrated OH maser spectra for all observed sources are given in Figures 6.7 through 6.10. In Figure 6.7 the multi-epoch spectra at each of the three frequencies are shown for the source V778 Cygni, whilst the 'map' of the 1667MHz emission made in April 1988, discussed above as a means of estimating the size of the masing region is presented as figure 6.8. Although observations were made in both polarisations at all positions, only the spectra obtained when observing in RHC polarisation are shown. This is because the emission from V778 Cyg is polarised, and as may be seen from the on-source spectra in Figure 6.7, in April 1988 the LHC on-source spectra showed very weak emission and as such were very noisy. The observations made in April 1988 and April 1990 of the sources BM Gem and EU And are given as Figures 6.9 and 6.10 respectively. Note that in all Figures containing OH spectra, unless explicitly stated, the X-axis is the radial velocity of the source relative to the local standard of rest (V_{LSR}) whilst the Y-axis represents the flux from the source in mJy.

6.2.5 MERLIN Observations of V778 Cygni

The star V778 Cygni was observed on 12th February 1989 using four telescopes of the Multiple Element Radio Linked Interferometer Network (MERLIN) which has been described by Thomasson (1986). The telescopes used to make the observations were the MkIA telescope at Jodrell Bank, and outstation telescopes at Knockin, Darnhall and Defford. The longest baseline (between the MkIA and Defford) was 127 km long, which corresponded to a lobe spacing on the sky of 0″.3. Observations were taken at the mainline frequency of 1667MHz in left-hand circular polarisation, and V778 Cyg was tracked by the telescope

Table 6.5: **Lovell Telescope Observations of OH Masers Associated with C Stars.**

Object	Date	U.T. Start	Integration (s)	Frequency (MHz)
V778 Cyg	1/4/88	23 56 19	6000	1667.359
V778 Cyg (N)	2/4/88	08 14 03	15000	1667.359
V778 Cyg (S)	2/4/88	13 13 29	6000	1667.359
V778 Cyg (E)	2/4/88	15 16 57	6000	1667.359
V778 Cyg (W)	2/4/88	17 13 45	6000	1667.359
V778 Cyg	2/4/88	19 10 45	6000	1667.359
V778 Cyg	2/4/88	21 07 42	15000	1665.402
V778 Cyg	3/4/88	21 36 13	9000	1612.231
BM Gem	5/4/88	16 14 25	6000	1612.231
BM Gem	5/4/88	18 10 28	6000	1665.402
BM Gem	5/4/88	20 07 35	6000	1667.359
EU And	6/4/88	13 52 28	6000	1612.231
EU And	6/4/88	15 49 47	6000	1665.402
V778 Cyg	26/6/88	12 58 00	6000	1665.402
V778 Cyg	26/6/88	14 57 42	6000	1667.359
V778 Cyg	26/6/88	16 56 35	6000	1612.231
V778 Cyg	19/7/88	02 49 29	6000	1667.359
V778 Cyg	19/7/88	03 49 08	6000	1665.402
V778 Cyg	25/8/88	09 08 20	3000	1667.359
V778 Cyg	25/9/88	10 07 56	1800	1665.402
BM Gem	22/04/90	16 40 00	2000	1612.231
BM Gem	22/04/90	17 08 24	2000	1665.402
BM Gem	22/04/90	17 45 56	2000	1667.359
V778 Cyg	22/04/90	18 44 27	2000	1612.231
V778 Cyg	22/04/90	19 21 40	2000	1665.402
V778 Cyg	22/04/90	19 58 56	2000	1667.359
EU And	22/04/90	20 40 41	2000	1612.231
EU And	22/04/90	21 17 55	2000	1665.402
EU And	22/04/90	21 55 11	2000	1667.359

Figure 6.7: Multi-Epoch OH Spectra of V778 Cygni

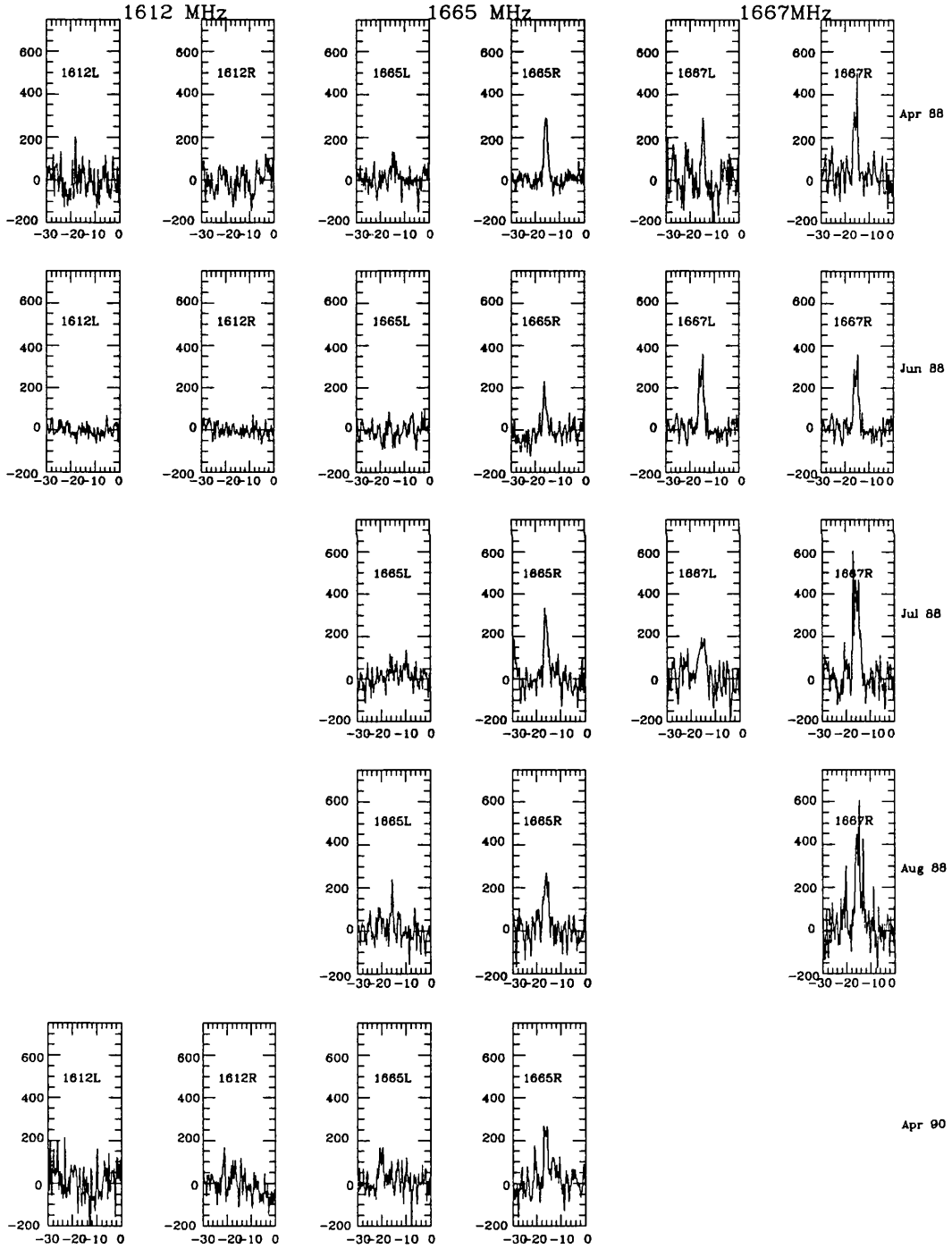

Figure 6.8: 1667MHz RHC polarisation observations at 5′ offsets from V778 Cyg in April 1988

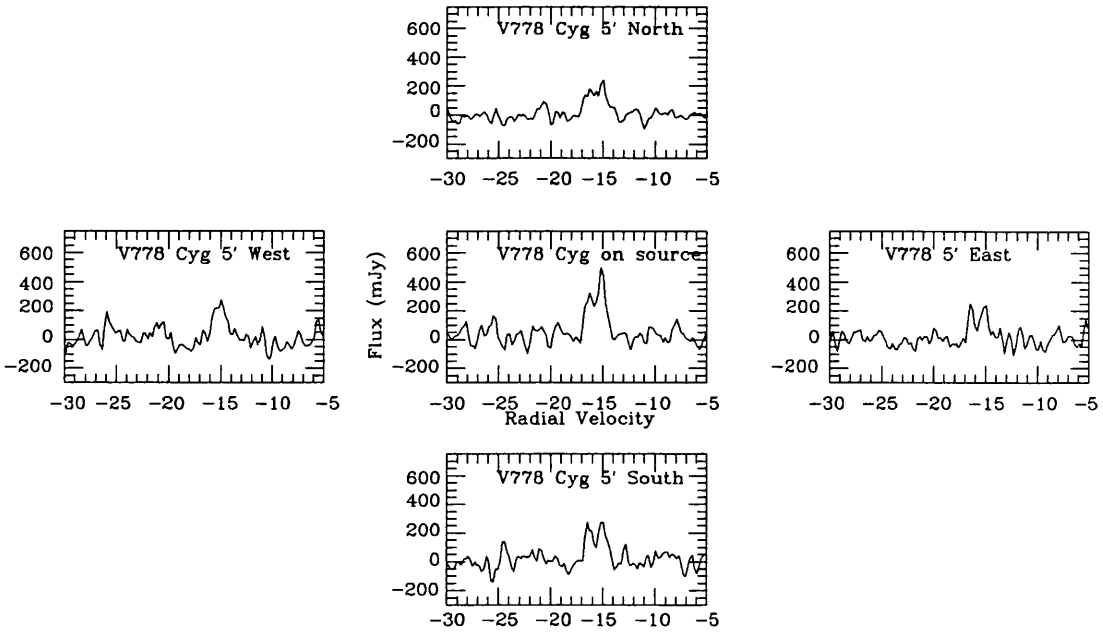

Figure 6.9: Multi-Epoch OH Spectra of BM Gem

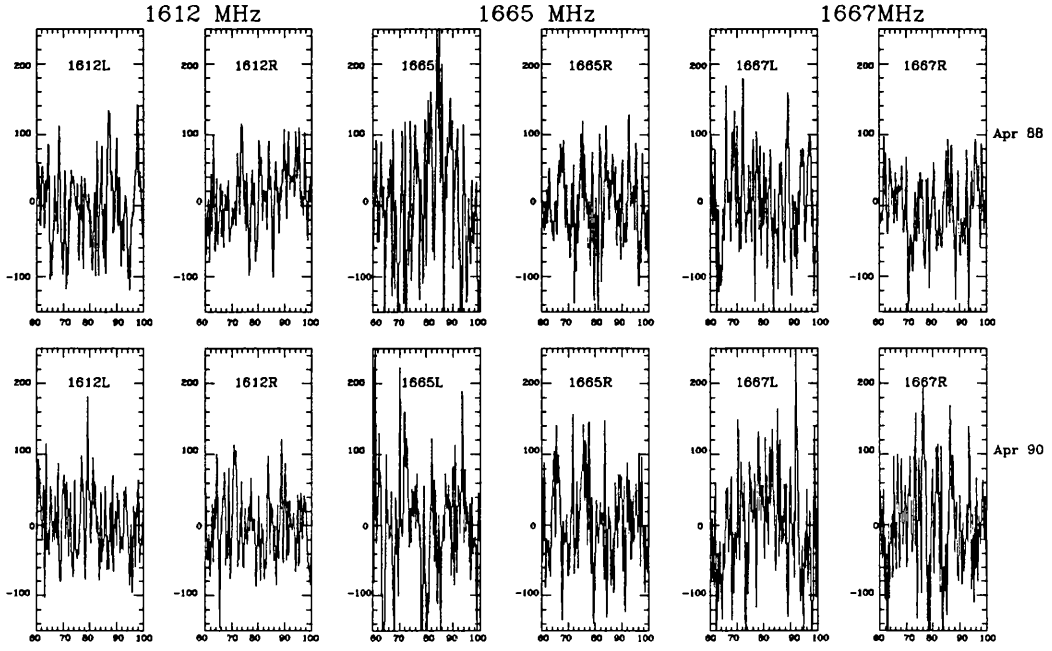

Figure 6.10: Multi-Epoch OH Spectra of EU And

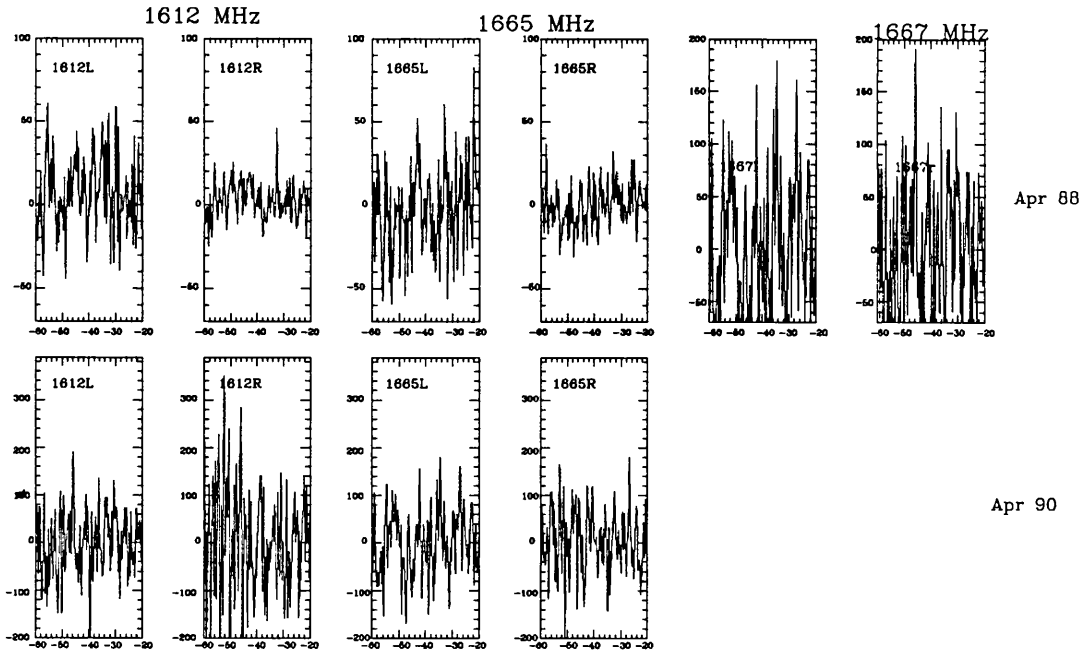

network for a period of 22 hours between 01:00 and 23:00.

As the radio flux density of V778 Cyg was low at the epoch of observation ($\leq$ 0.5Jy), the technique of 'phase-referencing' was adopted (Peckham 1973) to perform the observations. In this mode, the source observations were interrupted every 3 1/2 minutes and the MERLIN beam 'nodded' to a nearby phase reference source (in this case, 2021+614) which was observed for a further 1 1/2 minutes before the beam was nodded back to V778 Cyg and the cycle begun again. Observations of V778 Cyg were also interrupted to make regular observations of the source 3C84 which was used as an amplitude calibrator, with an assumed flux density of 22.5 Jy at the 1667MHz observing frequency.

Cross-correlation functions for each baseline were obtained on-line during the observations using 128 channels of a digital autocorrelator; these were weighted off-line using a triangular weighting function and were then Fourier transformed to give 64 channel cross-correlation spectra for every integration. An observing bandwidth of 312.5kHz gave a total velocity range of 56 km s^{-1} at 1667MHz with a velocity resolution of $\approx$1.4 km s^{-1}.

The cross-correlation spectra were then edited, vector averaged and calibrated using the routines in the off-line analysis format (OLAF) package at the Jodrell Bank Starlink

node. The visibility data created during this process were then turned into an intensity map of the source using the astronomical image processing system (AIPS). Initially 2021+60.4 (the phase reference source) was mapped using a self- calibration technique (Schwab 1980). The telescope gain solutions found from this method were then applied to the V778 Cyg data which were then further processed by Fourier inversion and use of the CLEAN algorithm (Högbom, 1974) which accurately related the flux density and position of V778 Cyg to that of the reference source (2021+60.4). The S/N ratio of the phase reference calibrator was increased by averaging the data from all 64 channels into one, and it was this average that was used as the reference for each of the channels making up the data for V778 Cyg.

V778 Cyg is amongst the faintest objects ever observed by the MERLIN network, and was the first object for which phase referencing spectral line observations were attempted (R. J. Cohen private communication). Unfortunately, due to a clerical error at Jodrell Bank, the source was observed in LHC polarisation, which is far weaker than RHC in V778 Cyg., and the resulting maps failed to detect any maser emission, to an upper limit of 100 mJy within 5″ of the stellar position in the sampled velocity range.

6.3 Results

6.3.1 Analysis of the Visual Data

A periodogram analysis was made of the available visual photometry of each star, after first inspecting the 'raw' observations for any obvious systematic differences from observer to observer. If any differences were identified, then the data from separate observers were analysed separately. The analysis used the algorithm of Belserene (1988) which utilises the Discrete Fourier Transform (Deeming, 1975) to search for strong periodic phenomena in a dataset. The advantage of this algorithm for the purposes of this project was that it has been used with great success in identifying both amplitudes and periods in semi-regular variable stars at the Maria Mitchell Observatory for a number of years (Belserene, 1988). The original version of the code was written in BASIC and run on a small PC, but to take advantage of the increased speed available on a minicomputers such as the Vaxes used in the Starlink network, the code was rewritten in FORTRAN. In the version of the algorithm used in this study, the value of z, a statistic which is a measure of how strongly

a frequency is represented in the data (sometimes called its power) has values of around 1.0 for worthless periods, whilst it can have a maximum value of approximately half the total number of observations.

There are many pitfalls associated with periodogram analysis (for a review see Scargle, 1982), and it is important if full meaning is to be attached to any results that these are taken into account during the analysis. The main problem associated with the employment of a periodogram analysis is that of *spectral leakage*; for a sinusoidal signal at frequency ν_0, the power in the periodogram not only appears at ν_0, but also leaks to other frequencies. This problem occurs with frequency analyses confined to a finite data sample. Leakage to nearby frequencies (sidelobe leakage) is due to a finite total data sampling interval, whilst leakage to distant frequencies can also occur, due to the finite size of the distance between samples. A good example of spectral leakage is *aliasing* which is leakage of power from high frequencies to much lower frequencies. Aliasing is very sensitive to the evenness of sampling, and may therefore be reduced greatly if the data are sampled irregularly. However, alias frequencies are still present in the data, due to unavoidable regularities in the sampling interval; for example observers tend to observe stars as they cross the meridian since they then are at their highest elevation, and suffer the least atmospheric extinction. Taken to extreme, this regularity in observation can lead to a peak in the power spectrum, after periodogram analysis; in reality this is a 0.997 day alias corresponding to one sidereal day.

In an attempt to account for aliasing in the data, due to regularities in the sampling, a programme was written that randomly scrambled the dataset (i.e. the times of the observation were common to both scrambled and unscrambled data, but the data themselves were randomly assigned to these times of observation). The scrambled data were then subjected to the same Discrete Fourier Transform (DFT) periodogram analysis as the unscrambled data, and the powers contained in the resulting power spectrum compared to those in the unscrambled data. In practice, for each dataset, this procedure was repeated 100 times, and a statistical weight could thus be attached to any periods present in the original data, by comparing them with those occurring in the randomly scrambled datasets.

The results of this analysis for each of the four stars investigated during the collaboration with the BAAVSS will now be presented.

V778 Cygni

V778 Cyg was the faintest of the 4 stars under study (the GCVS gives a mean photographic magnitude of 11.0), and as such, proved to be too faint for study through narrow band filters by the visual observers involved in the project. Thus, for this star, no study could be made that the Purkinje effect had upon the observations.

However, as mentioned previously, the visual observers' data for this star were complimented by a set of photographic observations made during 1980–1981. The spectral response of photographic emulsions differs somewhat from that of the human eye, and thus, the magnitudes derived from these data could very well differ systematically from those derived from the later, visual dataset. Internally though, each dataset utilised a self-consistent magnitude system, and hence it should be safe to search for periodic phenomena *within each dataset* that are common to both.

The 1980–1981 dataset spanned a 76 day period, and could thus be usefully searched for periods in the range 0–38 days. The 1988–1990 data could also be searched for periods in the range 0–38 days, but also enabled longer periods, up to 280 days, to be searched for in the analysis. By combining the 2 datasets, the reality of any longer periods identified in the analysis of the 1988–1990 data could be further tested, with the proviso that there may be systematic differences between the photovisual magnitudes derived for the earlier dataset, and the visual magnitudes derived from the latter.

Figure 6.11 gives the derived photovisual magnitudes as a function of Julian date for the 1980–1981 data, whilst Figure 6.12 performs the same function for the 1988–1990 dataset. It is interesting to note that there is no strong evidence for systematic differences between the 4 observers who supplied data for Figure 6.12. In most cases, observations made (almost) coevally by different observers agree to within 0.5 magnitudes; given the large uncertainties in the use of visual data for red stars discussed previously, the agreement between observers was felt to be sufficient to warrant a periodogram analysis of the (visual) dataset as a whole.

The individual datasets for V778 Cygni were initially searched for periods ranging upwards from their pseudo-Nyquist frequencies (defined as the reciprocal of twice the mean data spacing) to half the total period spanned by the observations. For the photographic data the pseudo-Nyquist frequency converted to $\approx$1.5 days, whilst for the visual data it was $\approx$11 days.

Figure 6.11: Photographic Observations Of V778 Cyg 1980–1981

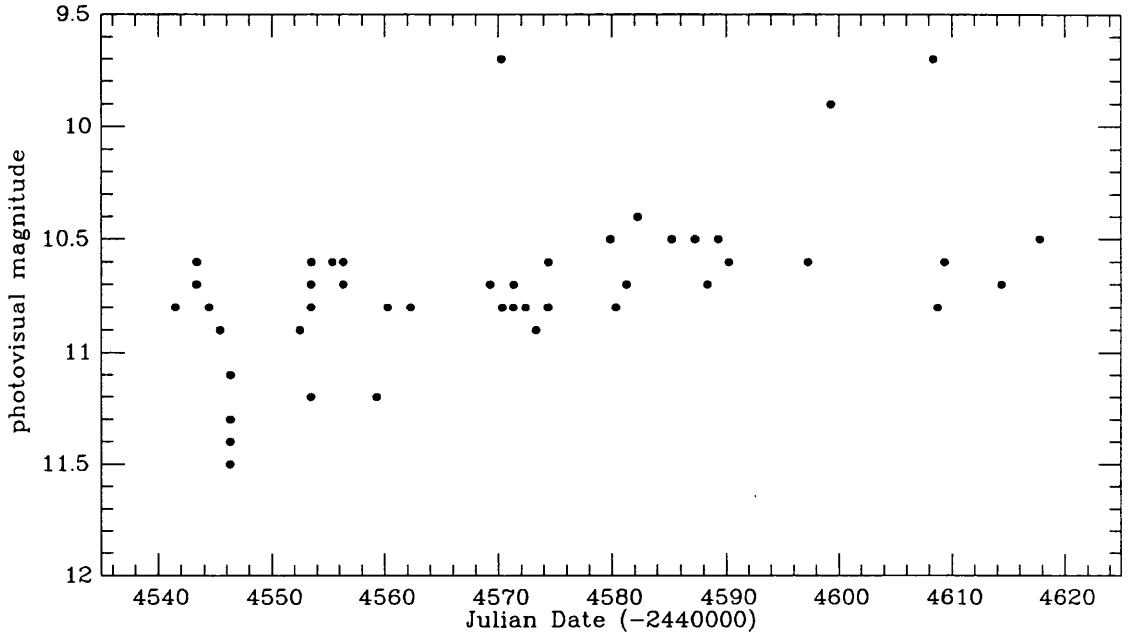

Figure 6.12: Visual Observations Of V778 Cyg 1988–1990

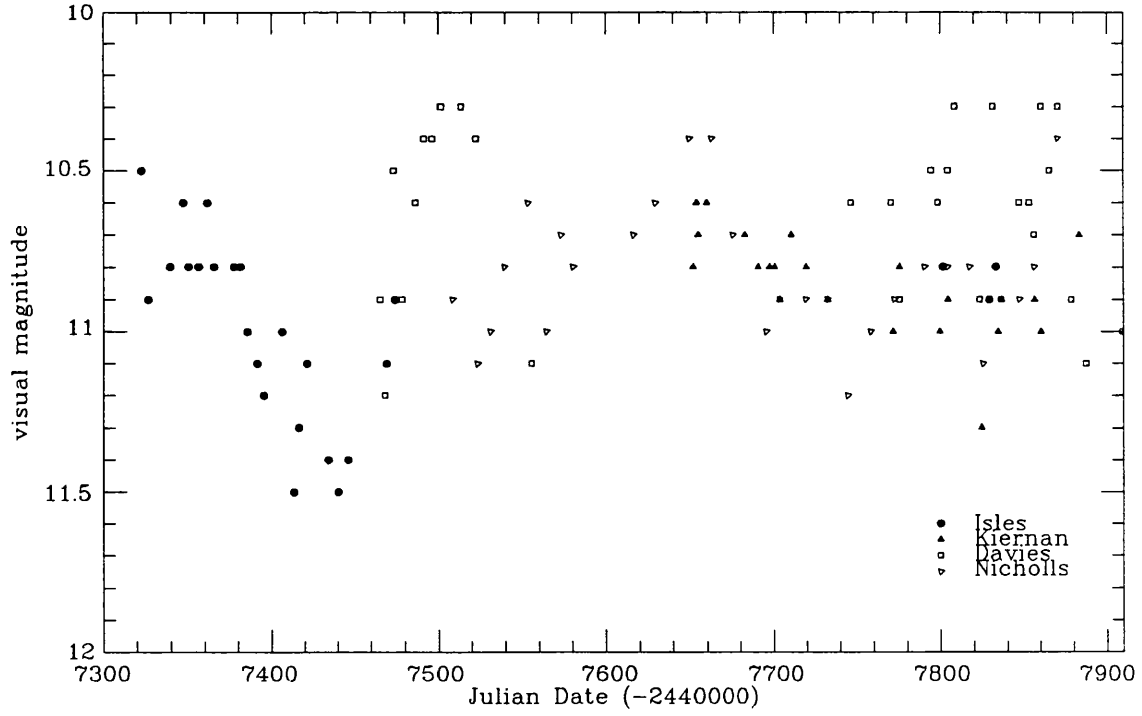

A DFT analysis of the photographic data revealed no evidence for periods in the range 1.5–38 days with powers in the power spectra greater than twice the minimum possible value; a similar analysis for the visual data gave an identical result in the range 11–38 days. It is therefore apparent that there is no evidence for recurrent short period variations in either dataset. This does not neccesarily rule out such variations in the star's optical brightness; indeed a dataset with a much higher frequency resolution (i.e. a higher rate of observations per interval sampled) than either of those presented here would be required to do that.

When the DFT analysis, was extended to search the full range of periods worthy of examination in the visual dataset (1000 frequencies in the range 11–280 days), three periods, the weakest one of ≈80days (actually 80.7±5d), one of ≈111 days (actually 111.2±5d) and one of ≈150 (actually 147.8±5) days did become evident. Figure 6.13 presents the full periodogram covering the range 11–280 days, and the 150 day period is obvious as the frequency with the strongest power statistic (z value) of 8 times the minimum value (or ≈0.1 the maximum possible value) whilst the 111 day period is present at approximately half the strength of the longer period. It should be noted though that the longer period is not an alias of the shorter ones, as it is not an integral multiple of either of the shorter periods. The amplitude of the 150 day period was found to be ≈0.3 magnitudes, whilst that of the 80 and 111 day periods were both ≈0.2 magnitudes.

In fact, due to noise in the data, a spread of periods in the range 65–80, 102–118 and 140–200 days are strongly represented in the data. The reality of all three periodicities, and their confinement to the observed dataset was confirmed by scrambling the data 100 times and repeating the DFT analysis on each of the scrambled datasets. In none of the randomly scrambled datasets did a peak in the power spectrum occur in the range 65–80, 102–118, or 140–200 days with a strength greater than 0.6 that observed with the unscrambled data. For the shortest period, in 12 out of the 100 scrambled datasets, a peak with power ≈0.5 that observed in the real data occurred, whilst for the longer periods, a peak corresponding to 0.5 the power contained in the real data at periods of 111 and 150 days was identified in only 4 and 1 respectively out of the 100 datasets generated. The confidence levels for the identified data are therefore 88% for the 80 day period, 96% for the 111 day period, and 99% for the one of 150 days.

Figure 6.14 indicates quite clearly how the 80, 111 and 150 day periods are confined

Figure 6.13: DFT Periodogram for 1988–1990 Visual observations of V778 Cyg

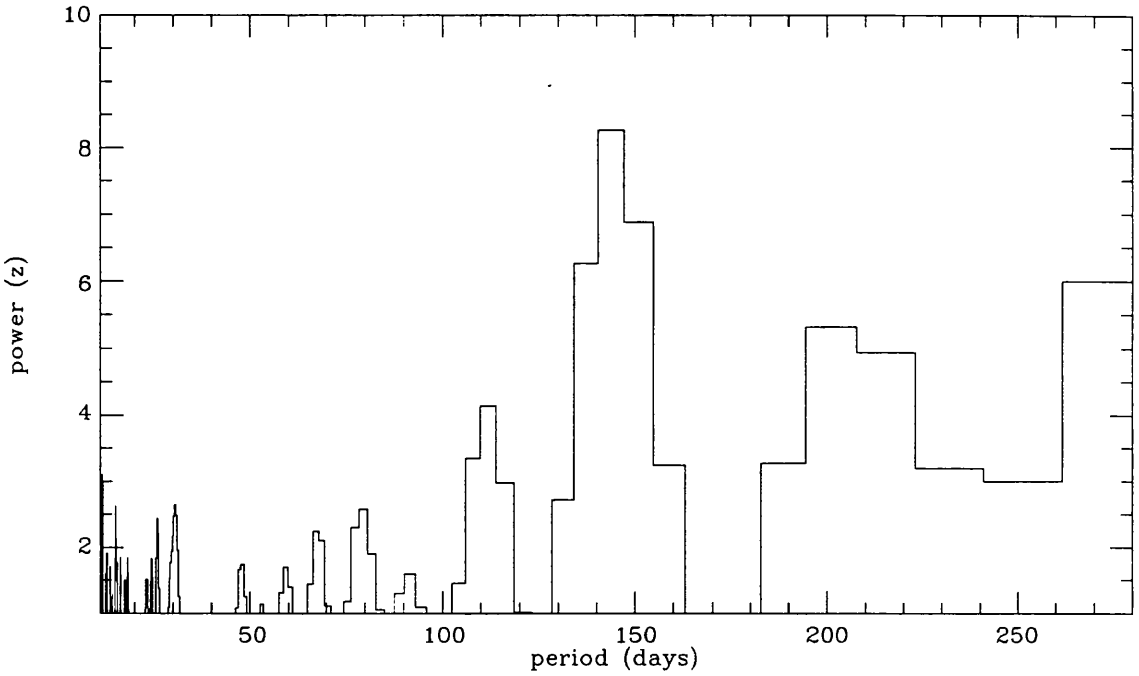

to the observed dataset by comparing the power spectrum calculated for the 'real' data with that for one of the randomly scrambled datasets; The only peaks not apparent in both spectra are those at 80, 111 and 150 days. The commonality of all other peaks to both power spectra is indicative of aliasing due to regularities in the data sampling rate.

As a final check on the three periods identified in the data above, the photographic data and the visual data were combined to form a single dataset covering some 10 years (with a long gap in the years 1981–1987!). The entire dataset was then subjected to periodogram analysis. The resultant power spectrum can be studied in Figure 6.15.

Once again the two periods at around 80 days and 150 days are strongly present in the data, although in the combined dataset, the values of these peaks have shifted slightly to 73 and 170 days. The 111 day period is however, almost completely absent from the combined dataset, and its reality therefore must be open to question. Note that in Figure 6.15, the individual components are better resolved as a higher number of frequencies were sampled (5000 rather than the 1000 used in Figures 6.13 and 6.14).

It is therefore concluded that there is strong evidence for a regular variation of period $\approx$170 days with an observed amplitude of $\approx$0.3 magnitudes in the visual magnitude of

Figure 6.14: Comparison of periodogram analysis for real and scrambled observations of V778 Cyg

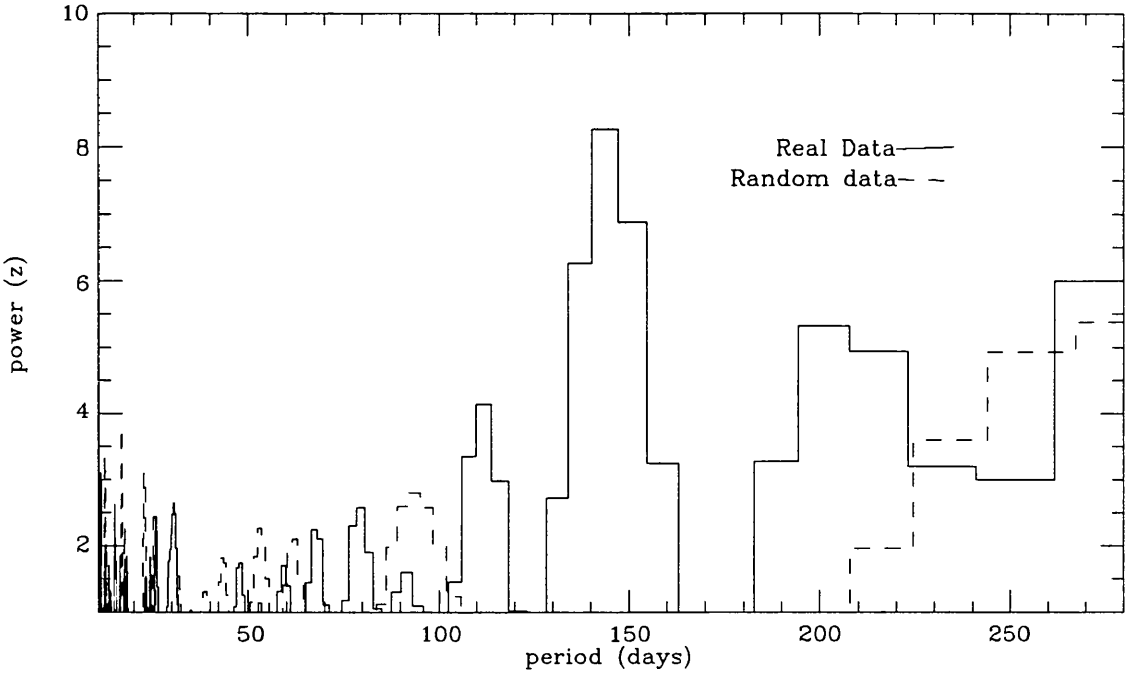

Figure 6.15: Periodogram analysis of all V778 Cyg observations 1980–1990

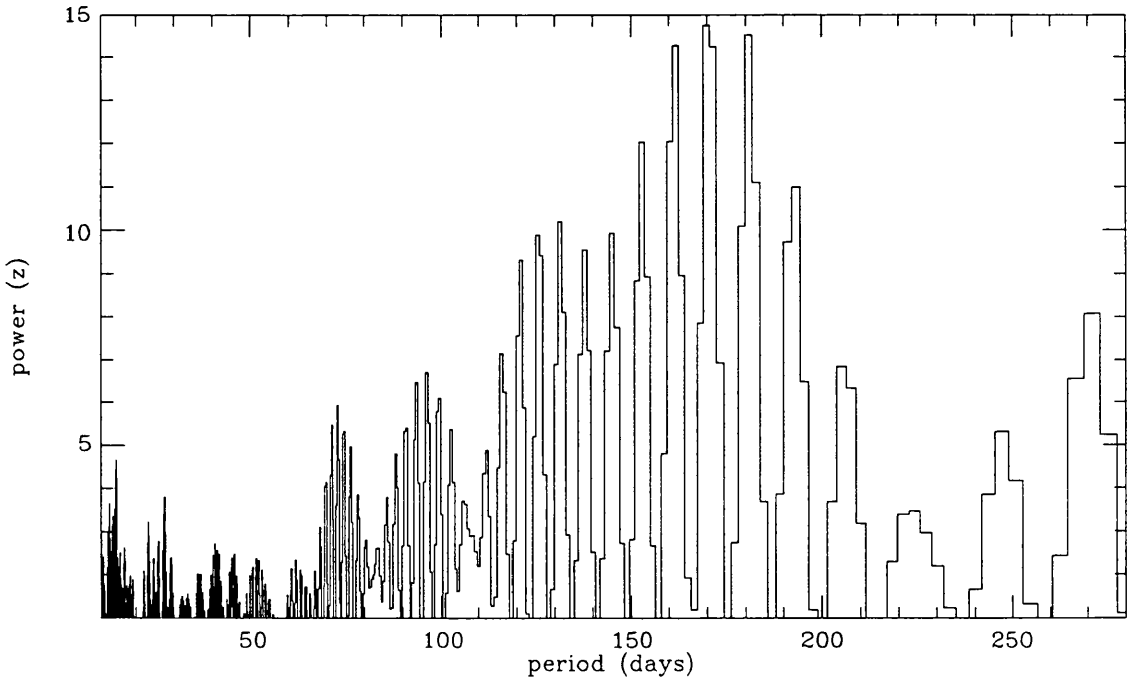

Figure 6.16: BAAVSS Visual Photometry of EU And 1988-1990

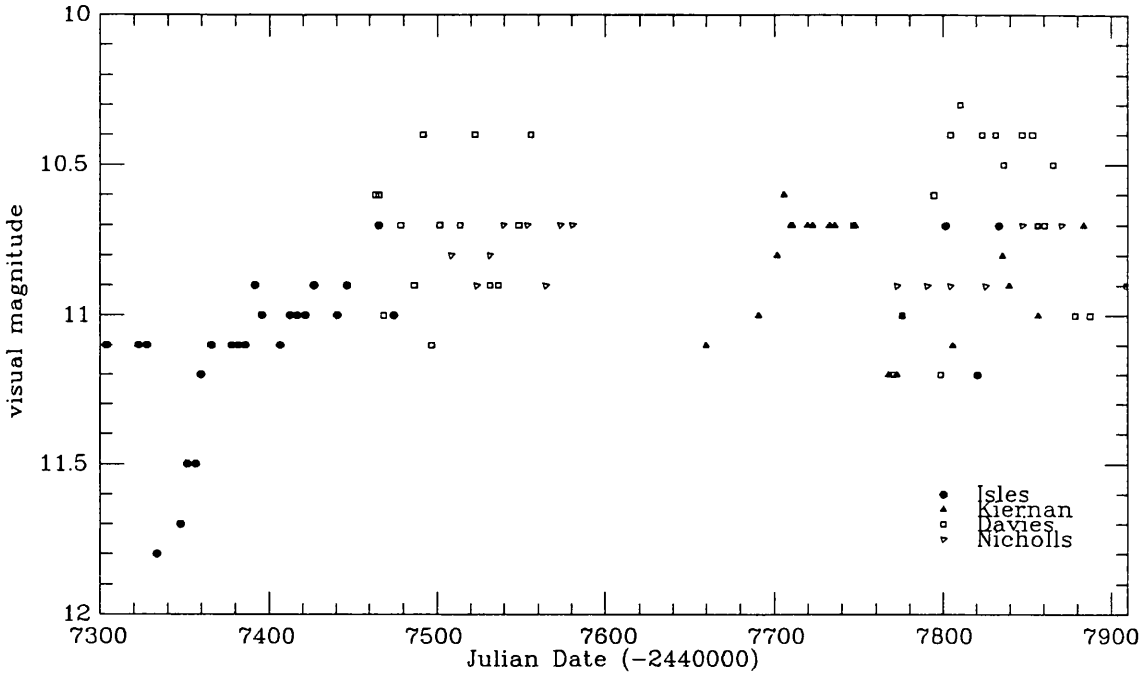

the star V778 Cyg. A variation with period ≈73 days and amplitude 0.2 magnitudes is also evident in the data. The reality of these variations must be somewhat open to question, as a 0.2–0.3 magnitude variation is right at the limits of detectability for a visual observer. Clearly, a long term observing campaign using either photoelectric or photographic photometry would be the best way of resolving this issue for V778 Cyg.

EU And

This star proved to be too faint for observers to employ filters whilst observing it, and hence, as for V778 Cygni, no analysis of the Purkinje effect upon the observations could be made. However, inspection of the collated BAAVSS photometry for this object (presented as Figure 6.16) reveals that once again, the agreement of the magnitude measurements from separate observers is good, and there appear no significant systematic differences between observers. A periodogram analysis was therefore performed upon the dataset as a whole.

The DFT analysis, combined with the data randomizing method (described above for V778 Cyg) identified 3 periods that did not appear to be due to spacings in the dataset.

The strongest peak in the power spectrum was for a 0.38 magnitude variation with period of 300±10 days (98% confidence) whilst the other two (in order of power in the DFT power spectrum) were a variation 0.33 magnitudes in 144±10d (95% confidence) and 0.26 magnitudes in 200±10 days (94% confidence). Since the dataset for this star spanned only the 2 years of BAAVSS visual photometry, the analysis was terminated at this point; clearly further observations are still required to better define which (if any) of the 3 periodicities best fits the data, though the best (as defined by having strongest peak in the DFT power spectrum and having least repetitions in the scrambled datasets) value of the 3 would currently appear to be the one at 300±10d.

BM Gem

BM Gem appeared on average to be $\approx$ 1 magnitude brighter than the other two oddball stars being investigated by the visual observers, and as such proved to be easily visible through the filters being used in the study. Figure 6.17 collates the observations made by visual observers using the two Rosco filters, together with observations made visually without the filters.

It can be seen from figure 6.17 that there is considerable scatter in the unfiltered observations of BM Gem; Unfortunately the scatter is also present in the filtered observations and therefore no conclusions may be drawn about systematic effects in the dataset. It may be seen that the extreme range of variation is less than one magnitude for BM Gem at visual wavelengths within the dataset, and no obvious variability trends may be gleaned from figure 6.17. A periodogram analysis of the unfiltered observations of BM Gem confirms that there are no strong periodicities in the dataset of amplitude greater than 0.2 magnitudes in the period range 11–300 days. Clearly, if there are periodicities present in the variations of this star, then more sensitive photoelectric techniques will have to be used to detect them.

VX And

This star was observed as a 'control object' as it has a similar spectral type as some of the 'oddball' C stars, is also a J type C star, and yet its *IRAS* LRS spectrum does not apparently show silicate emission. It was therefore observed by the BAAVSS observers to see whether its variations were significantly different to those of the 'oddball' stars to

Figure 6.17: BAAVSS Visual Photometry of BM Gem 1988-1900

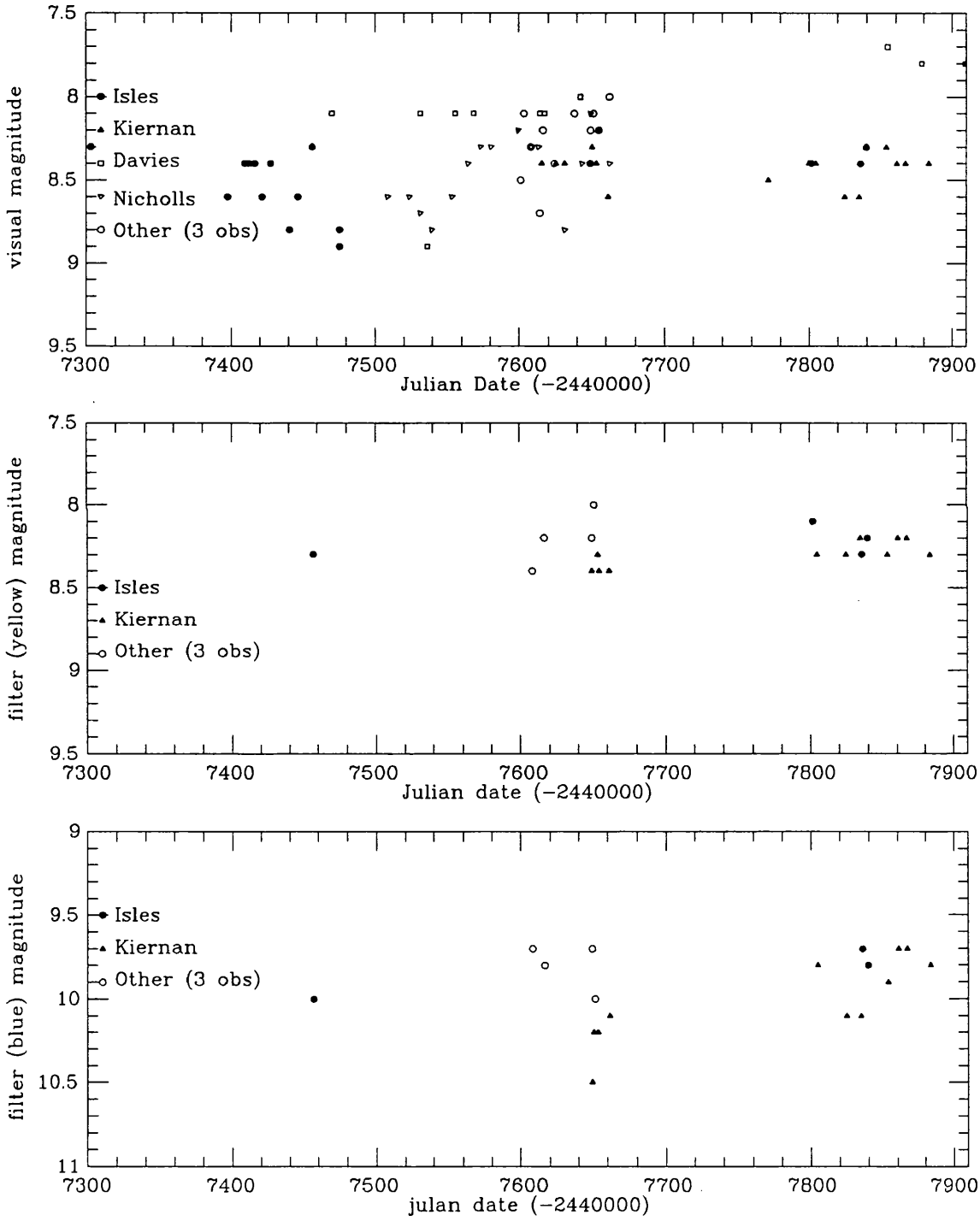

which its optical spectrum was identical.

Figure 6.18 presents the BAAVSS observations of this star (both filtered and unfiltered) made during 1988–1990. It appears that there are systematic differences between observers for this star, with magnitude estimates differing by as much as one magnitude for coeval observations. Unfortunately, filtered observations were received from only 2 observers and hence no estimate may be made of the Purkinje effect. It is encouraging though that the trend of the filtered observations is similar to that seen in the unfiltered observations, and that for the two observers who reported observations, the systematic difference between them has been reduced slightly in the filtered observations when compared to those made unfiltered. Despite the obvious systematic differences between observers though, a regularity is immediately obvious in the unfiltered observations, and a periodogram analysis suggested that the observations were best matched by an $\approx$188 day period with an amplitude of $\approx$1.0 magnitude. Interestingly, VX And has also been observed sporadically by the American Association of Variable Star Observers (AAVSO) (Mattei, private communication) and these observations suggest a period of $\approx$369 days, with an amplitude of 1.5 magnitudes; the period is almost exactly twice that found by the analysis in this work, and suggests that an aliasing is present either in the BAAVSS or in the AAVSO data. The BAAVSS data do not as yet span a sufficient timescale to resolve this aliasing problem, and the non-availability of the AAVSO data at the time of writing did not help the situation either. However, the BAAVSS observations of this star did serve the initial purpose in discovering a difference between the periodic behaviour between it, a 'normal' J star, and the 'oddball' C stars. Large ($\geq$0.5 magnitude) periodic variations were not observed to be present in any of the 3 stars investigated during the epoch of examination.

ST Her & AD Per

These stars have been on the BAAVSS monitoring programme since 1971, and the data are currently being analysed (Isles, private communication) for publication, but the pre-publication results of Fourier analysis of the light curve were made available for this study. For ST Her the analysis suggested irregular variations in a period of about 200 days, with an extreme range in magnitude from 7.0–8.6. The periodogram analysis of this star indicated possible periods of 149.0 days (peak to peak amplitude 0.23 magnitude), 268.7d (0.20 mag), 458.2d (0.20 mag), 969.0d (0.19 mag) and 2117d (0.29mag). The first

Figure 6.18: BAAVSS Visual Photometry of VX And 1988-1900

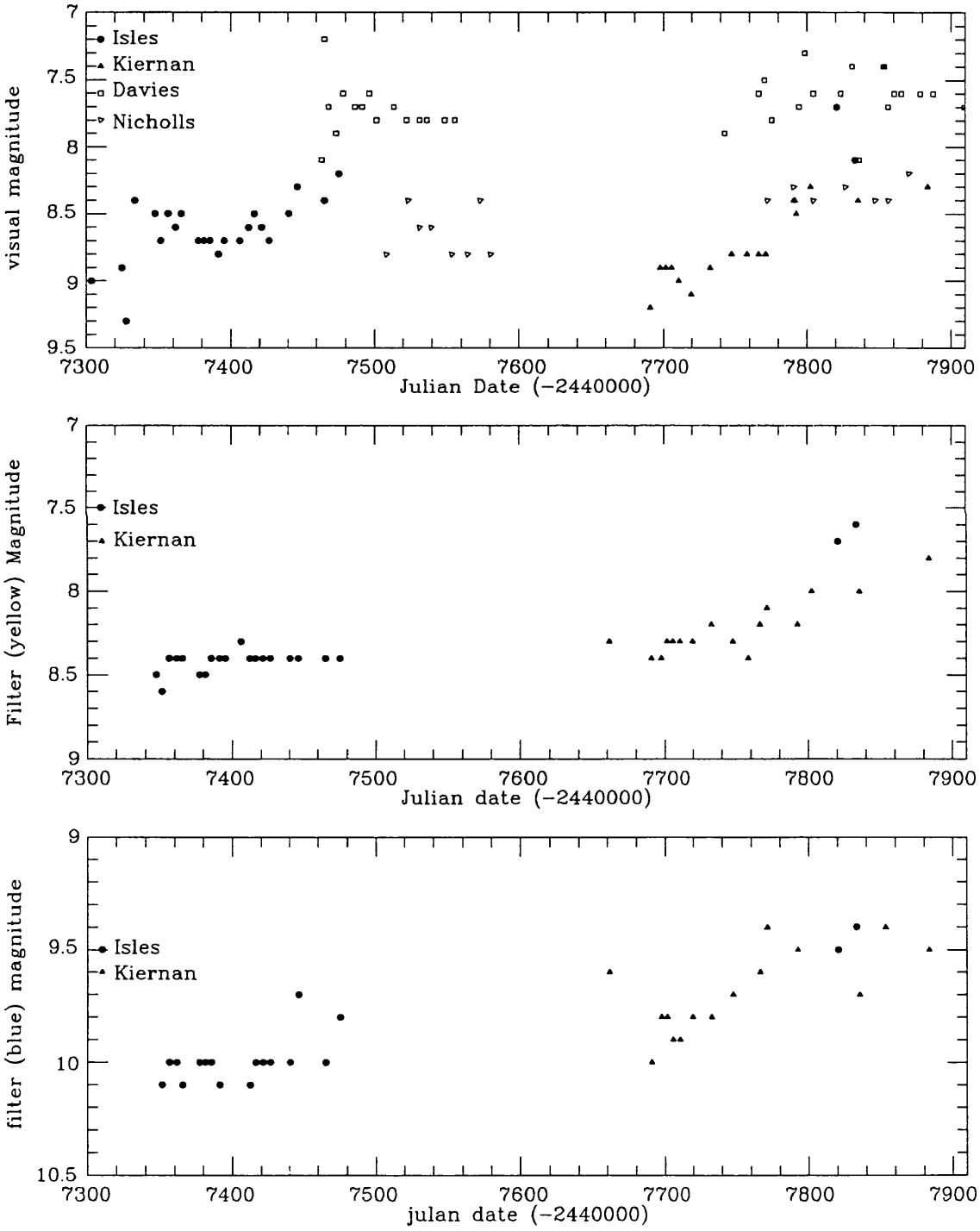

detected period (149d) agrees well with the 148d period listed in the GCVS.

For AD Per, the light curve suggests irregular variations with periods in the range 300-1600d, with an amplitude in the magnitude range 7.7–9.0. A periodogram analysis of the BAAVSS data fails to find the periods listed in the GCVS of 362.5 days and 2950 days, but instead gave possible periods of 314.2d (0.24 mag), 2167d (0.49 mag) and 3665d (0.27 mag).

It may thus be seen that the periods listed in the GCVS for variable stars, are not always present at all epochs, and if a full understanding of a star's temporal variations in light are to be understood, then a long term monitoring programme becomes very important, especially when one is attempting to correlate variations in a star's spectral appearance with those same temporal variations.

6.3.2 The Optical and Near-IR spectra

The rationale for obtaining the flux calibrated optical and near-IR spectra was to provide a twofold test of a binary model suggested for the C stars with silicate dust by Little-Marenin (1986) which implies that the energy distributions should be bimodal; at some point in the near-IR (with $1 \leq \lambda \leq 8\mu$m in Little-Marenin's favoured model) the spectra of the optically bright C star and optically obscured (but IR bright) M star should cross over. Thus, at some point in the predicted wavelength window, according to the Little-Marenin model, one should see 'the wrong' spectral features appearing in the stellar spectra (i.e. for the C stars, M star features should become visible). Assuming that the M stars with SiC dust are also a binary phenomenon, then an analogous explanation might be attempted to explain their composite spectra.

Unfortunately for the Little-Marenin model, in all cases where observations were obtained, the spectral features identified in the optical and near-IR spectra confirmed the spectral classifications for individual objects derived in the past by other workers; not one of the spectral identifications offered in Figures 6.3–6.5 is anomalous, given the optical stellar spectral classification.

Further evidence against the binary model comes from an examination of the stellar energy distributions of the candidate 'oddball' stars. In the previous section it has been shown that for 3 of the C stars with silicate dust features, the amplitudes of any long term variations in the optical magnitudes are small ($\leq$0.4 magnitudes in all cases). If we assume

the same to be true for all of the candidate (C star) objects, then spectrophotometric observations made at different epochs and wavelengths longer than the optical may safely be combined to provide a study of the objects spectral energy distribution, since the amplitude of variations will decrease at longer wavelengths (e.g. Sopka *et al.*, 1985).

Figure 6.19 presents a montage of the spectrophotometric observations described in Section 6.2 for 4 C stars, together with the *IRAS* LRS spectra and 12, 25, 60 and 100μm photometric fluxes, as given in the *IRAS* Point Source Catalogue (*IRAS* Science Team, 1988). It is immediately apparent from these plots that there is no obvious discontinuity or change in spectral slope for any of these 4 stars; the bimodal energy distribution predicted by the binary model is not at all obvious.

Though the amplitudes of magnitude variations for the M star sample are in general larger at visual wavelengths than is the case for the C stars, even for the most extreme case (δM $\leq$1.5 at V) the amplitude of variation is sufficiently small, that combining spectrophotometric observations at wavelengths longer than 1μm made at different epochs introduces errors that are generally smaller than those contained within the original flux calibration procedures at the various wavelengths. Therefore, as was done for the C stars, the available spectrophotometric observations were combined in an attempt to look for bimodal structure in the resulting energy distributions. These energy distributions, presented as Figure 6.20, also show a singular lack of evidence for binary nature in the source.

6.3.3 Analysis of the Radio data

The fluxes in the 1612, 1665 and 1667 MHz OH single dish maser spectra were measured using the trapezoidal integration routine INTEG in the SLAP software package. In cases where no OH emission was detected, upper limits to the maser flux were estimated from the observed noise at the expected maser velocity. The measured fluxes are presented in Table 6.6 (for observations of V778 Cyg) and Table 6.7 (for observations of BM Gem and EU And).

Inspection of Figure 6.7 and Table 6.6 reveals that the OH Maser emission from V778 Cyg is polarised, and highly variable in both flux and line profile as a function of time. At all epochs, the 1667 MHz emission is stronger than that at 1665 MHz by a factor greater than 2, and the stronger emission occurs in observations made in RHC polarisation. The

Figure 6.19: Combined Spectrophotometic Observations of C Stars with Silicate Dust

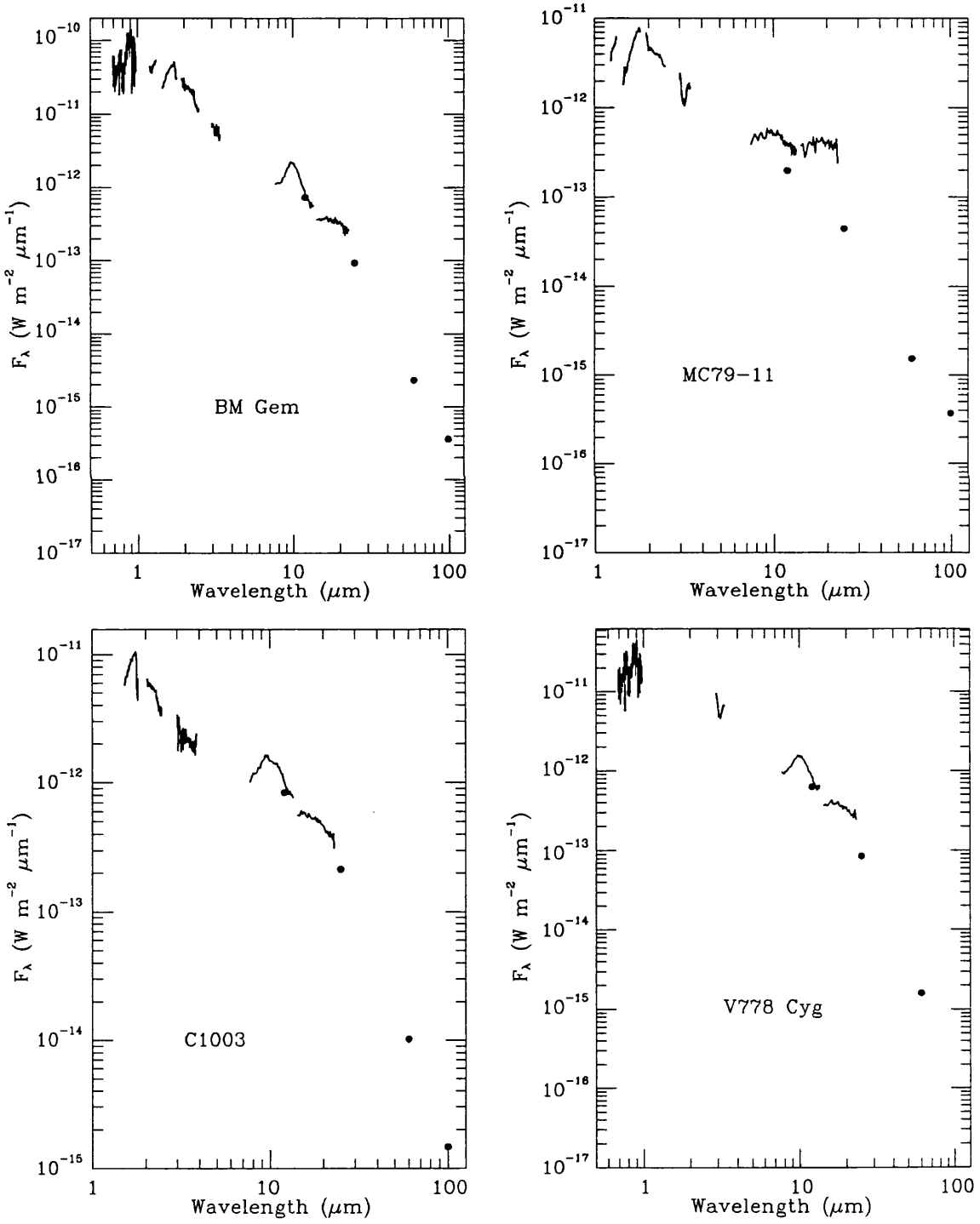

Figure 6.20: Combined Spectrophotometric observations of M stars with SiC dust

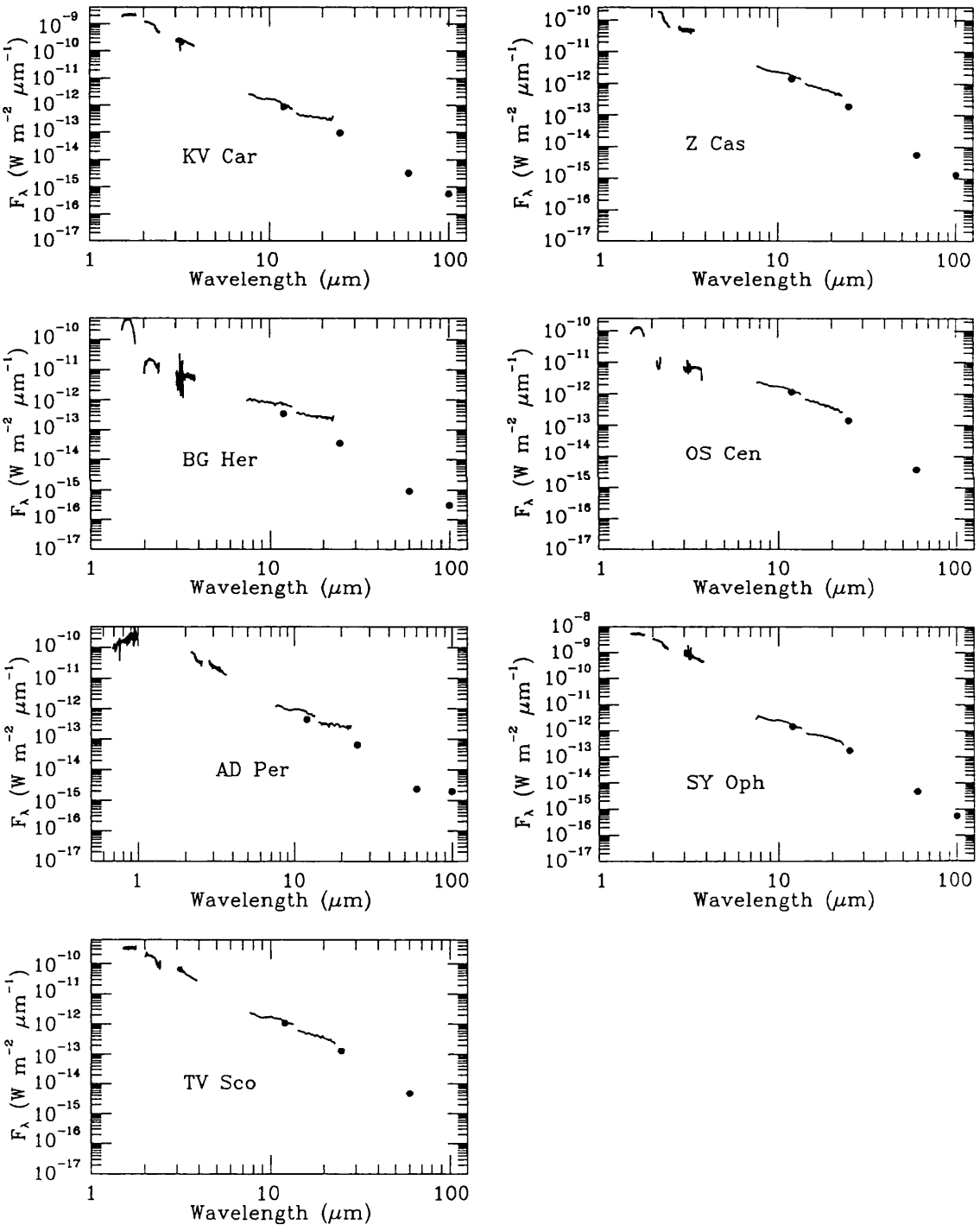

Table 6.6: OH maser flux measurements for V778 Cyg

Beam Position	Date	Freq (MHz)	Flux (Jy)	Velocity (km s^{-1})	FWHM (km s^{-1})
Onstar	Apr 1988	1667R	0.76	-15.3	2.1
"	"	1667L	$\leq$0.1	—	—
"	June 1988	1667R	0.70	-15.4	2.2
"	"	1667L	$\leq$0.1	—	—
"	July 1988	1667R	0.50	-15.8	3.4
"	"	1667L	0.25	-15.7	3.7
"	Aug 1988	1667R	0.56	-15.0	2.7
"	"	1667L	$\leq$0.1	—	—
"	Apr 1988	1665R	0.50	-16.3	1.5
"	"	1665L	0.23	-15.4	3.3
"	June 1988	1665R	0.61	-16.1	1.4
"	"	1665L	$\leq$0.1	—	—
"	July 1988	1665R	0.20	-16.0	2.2
"	"	1665L	$\leq$0.1	—	—
"	Aug 1988	1665R	0.25	-15.0	2.7
"	"	1665L	$\leq$ 0.1	—	—
"	Apr 1990	1665L	$\leq$0.3	—	—
"	"	1665R	0.72	-15.1	1.0
"	April 1988	1612R	$\leq$0.2	—	—
"	"	1612L	$\leq$0.2	—	—
"	Apr 1990	1612L	$\leq$0.1	—	—
"	"	1612R	$\leq$0.1	—	—
5′ N	April 1988	1667R	0.41	-15.4	2.4
5′ S	"	"	0.48	-15.4	2.3
5′ E	"	"	0.38	-15.4	2.0
5′ W	"	"	0.42	-14.9	1.6

Table 6.7: OH maser flux measurements for BM Gem & EU And

Star	Date	Freq (MHz)	Flux (Jy)	Velocity (km s^{-1})	FWHM (km s^{-1})
BM Gem	April 1988	1667R	$\leq$0.2	—	—
"	"	1667L	$\leq$0.2	—	—
"	"	1665R	$\leq$0.2	—	—
"	"	1665L	0.3	84.5	1.0
"	"	1612R	$\leq$0.2	—	—
"	"	1612L	$\leq$0.1	—	—
"	Apr 1990	1667R	$\leq$0.2	—	—
"	"	1667L	$\leq$0.1	—	—
"	"	1665R	$\leq$0.1	—	—
"	"	1665R	$\leq$0.15	—	—
"	"	1612R	$\leq$0.15	—	—
"	"	1612R	$\leq$0.1	—	—
EU And	Apr 1988	1667R	$\leq$0.2	—	—
"	"	1667L	$\leq$0.2	—	—
"	"	1665R	$\leq$0.2	—	—
"	"	1665L	$\leq$0.2	—	—
"	"	1612R	$\leq$0.2	—	—
"	"	1612L	$\leq$0.2	—	—
"	"	1665R	$\leq$0.1	—	—
"	"	1665L	$\leq$0.1	—	—
"	"	1612R	$\leq$0.1	—	—
"	"	1612L	$\leq$0.1	—	—

maser emission is concentrated in the velocity range -14 to -20 km s^{-1} with the mean velocity being -15±1 km s^{-1} having a FWHM of ≈3.0 km s^{-1}. During the 4 epochs of observation in mid-1988, the line flux in the stronger 1667 MHz RHC polarisation remained fairly constant at ≈0.7 Jy, b[illegible] made [illegible]; a similar behaviour was observed in the LHC 1667 spectra. The flux in the 1665 MHz lines did not show such extreme variation, and at all epochs, the RHC 1665 line flux was observed to lie in the range 0.1–0.7 Jy 1612 MHz maser emission was not detected from V778 Cyg at any epoch to an upper limit of ≈0.1 Jy in either LHC or in RHC polarisations. The velocity displacement between the OH masers and that measured for the stellar radial velocity of –33 km s^{-1} (Lambert *et al.*, 1990) remained constant at ≈17 km s^{-1} during the entire 2 year period spanning the maser observations.

Positive detections of OH maser emission at 1665/1667 MHz from V778 Cyg have previously been reported only by Little-Marenin *et al.* (1988), who found weak (≈0.1 Jy at 1665 MHz, ≈0.2 Jy at 1667 MHz) single lined emission features, at radial velocities of –15.3±1 and –16.5±1 km s^{-1} at 1665 MHz and 1667 MHz respectively. The Little-Marenin *et al.* observations were made simultaneously in both circular polarisations, and hence could not detect any intrinsic source polarisations.

For EU And, Table 6.7 confirms that within the given upper limits, no emission has been detected at any epoch. Little-Marenin *et al.* (1988) failed to detect OH emission at 1665/1667 MHz from EU And to an upper limit of 0.1 Jy, and the observations presented here as Figure 6.10 confirm that in April 1988 a similar upper limit could be placed upon the maser flux at these frequencies.

To date, with the exception of the one detection of V778 Cyg at 1665/1667 MHz discussed above, all observers have concentrated upon studying the 6_{16}–5_{23} H_2O maser emission line, at 22 GHz. Monitoring observations (Little-Marenin *et al.*, 1988, Benson & Little-Marenin, 1989) have shown this line to be highly variable for both V778 Cyg and for EU And on timescales as short as one day, with the fluxes ranging from ≤1.5–8.2 Jy for EU And, and 1.9–10.9 Jy in the case of V778 Cyg. Interferometric observations, made using the Nobeyama millimetre array (Deguchi *et al.*, 1988) have confirmed that the agreement between the measured optical photospheric and radio maser positions is better than 0″.5. The velocities measured for the H_2O maser emission features in V778 Cyg are in good agreement with those found above for the strongest components observed in the

OH masers, which perhaps suggests that maser activity is confined to a single region. The FWHM of the line profiles is also close to that measured above for the OH lines, i.e. 3 km s^{-1}. Unfortunately, the spectra published by Little-Marenin *et al.* (1988) and Nakada *et al.* (1987, 1988) for the 22 GHz H_2O emission around EU And do not extend to the −48.5 km s^{-1} value relative to the LSR at which the weak OH feature was identified in the April 1990 Jodrell Bank observations, and hence can not be used to investigate the reality of that feature.

6.3.4 Angular extent of OH emission from V778 Cyg

The flux measurements made at 5′ offsets N,S,E &W from the emission peak at 1667 MHz of V778 Cyg in April 1988 may be used to estimate the degree of any angular extension of the masing region. Ideally, to perform this task, the beam profile used to make the observations should be deconvolved from the data; however the simple 4 position map under examination here is far from the ideal case, and provides insufficient samples to use the deconvolution technique.

Instead, it was assumed that the source, as well as the beam profile was a gaussian. In this case, the FWHM of the source on the sky, $\theta_s = (\theta_o^2 + \theta_b^2)^{1/2}$, where θ_o is the FWHM of the observed profile, and θ_b is the FWHM of the beam profile. The beam profile of the MkIa telescope was assumed to be a gaussian with diameter 10′ at the zenith (R. J. Cohen, private communication)

The FWHM of the observed profile was calculated by finding the width of the best fitting gaussian profile to the measured flux at an offset of 5′, using a least squares method. The mean flux at an offset of 5′ was calculated to be 0.55±0.05 Jy, and in Figure 6.21 it may be seen that the best fit to the data is provided by a gaussian beam with a FWHM of 10′.4±0′.2. If due to real extension, this would correspond to an angular size of the source of 2′.8 on the sky.

However, it was assumed above that the angular size of the telescope beam on the sky was 10′. In practice, this is the value when observing at the zenith. When observing at other angles to the horizon, the telescope beam size can vary by up to 1′ (R. J. Cohen, private communication). Therefore it is highly likely that Figure 6.21 is really just showing the instrumental profile, and that the OH maser emission from v778 Cygni is not resolved by the MkIa telescope.

Figure 6.21: The fit of different gaussian beam models to the off source flux measurements for V778 Cyg

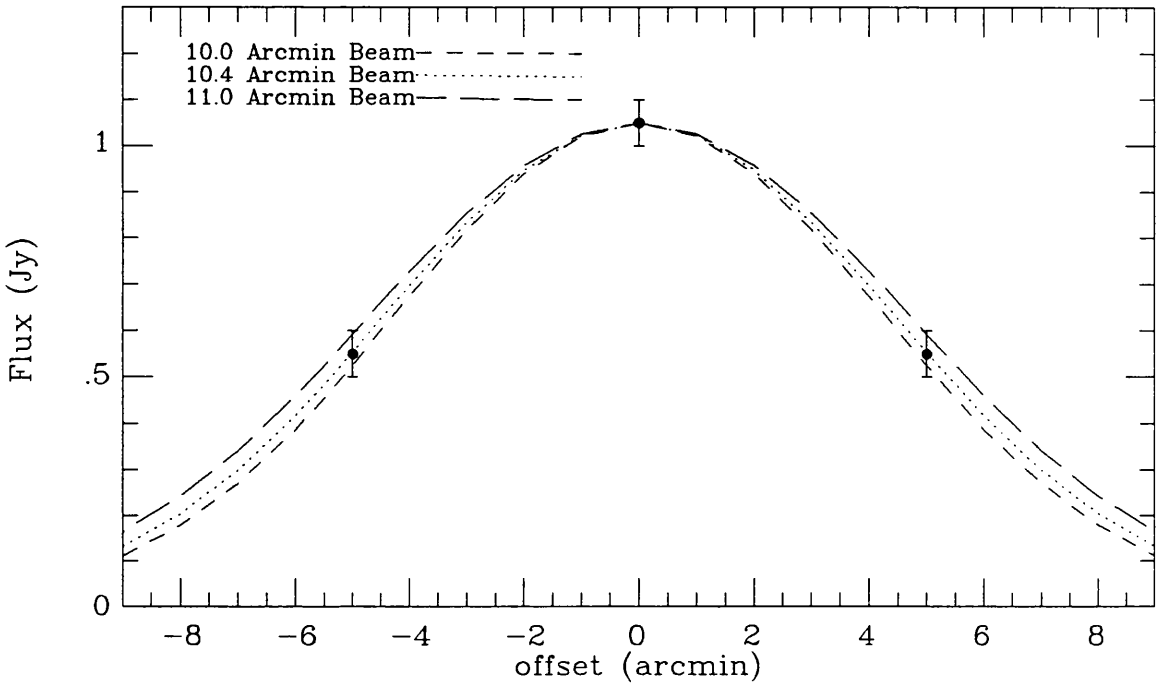

Peery (1975) has used a near-IR photometric data to estimate the distance to V778 Cygni as 1.4 kiloparsecs. If this distance is adopted, then an upper limit to the angular size of the circumstellar OH masing region may be inferred, if an upper limit to the linear diameter of the masing region at the source of 10^{16}–10^{17}cm is assumed as being typical of OH shell diameters for red giant stars (e.g. Reid & Moran, 1981; Cohen, 1989). A simple calculation then reveals that if the maser region associated with v778 Cyg is similar to that observed in other red giant circumstellar envelopes, and it is at a distance of 1.4 kpc, then one would expect it to be no larger than 7″ in diameter; in effect confirming that the MkIa beam would observe the region as being pointlike.

6.3.5 Correlation of Maser and Optical Variabilities

Observations indicate that maser emission, at OH and in H_2O maser frequencies is highly variable. Most accepted theories for H_2O and OH masers adopt some form of radiative pumping mechanism to prime the maser emission, either via far-IR radiation from dust (Elitzur, 1978) or IR radiation from the central star (Cimerman & Scoville, 1980). In either

case, as the ultimate source of the pumping mechanism is radiation from the central star, some correlation should exist between variations in stellar luminosity and observed maser strength.

Unfortunately, the sampling of published maser emission fluxes for EU And, and V778 Cyg at both OH and H_2O frequencies is far too sparse to perform a detailed analysis, and in any case, hardly overlaps at all with the BAAVSS photometry of the stars presented above. However, a fairly extensive database of observations of H_2O maser emission associated with the star V778 Cyg does exist (Little-Marenin *et al.*, 1988, Benson & Little-Marenin, 1988), which although not obtained coevally with the BAAVSS data, contains a sufficient number of observations made during 1987–1988.5 that a DFT analysis could usefully be employed to investigate any periods present. This analysis, performed identically to that done on the BAAVSS data, found that the period most strongly represented in the data was one of 143±20 days, with an amplitude of 7 Jy. The confinement of this period to the 'real' dataset was confirmed when the randomising procedure, described in the analysis of the visual data, found that similar periods in the range 120–160 days appeared in only 3% of the scrambled datasets at strengths compatible with that observed in the real data. The 143 day periodicity is, given the uncertainties involved in its derivation (small dataset, short period of observation), in fair agreement with the period of 148 days found in the visual dataset, although the amplitude of the maser variation, as a fraction of the mean maser flux from V778 Cyg, is greater than that observed in the visual data. It is also interesting to note that on the 2 occasions where H_2O maser measurements published by Benson & Little-Marenin were obtained within 1 day of OH measurements presented here, the trend in H_2O maser flux was followed by the OH masers (i.e. the increase in H_2O maser flux observed between JD 24447300 and JD 24447400 by Benson & Little Marenin was also observed in the OH observations (Table 6.7). This evidence is by no means conclusive though, since the H_2O flux was noted to be highly variable (factor 2 variations in 8 hours were observed by Benson & Little-Marenin, 1988) and to gain a real insight into correlations in OH and H_2O emission a coordinated observing campaign would be necessary. It is perhaps worth mentioning at this point that the factor 2 increase in brightness in a period of less than 8 hours reported by Benson & Little-Marenin is totally unprecedented for an astrophysical maser source; the fastest variability reported previously to this for an H_2O maser was a factor of 3 increase in a time period of 3 weeks

(Cohen, 1989). One possible explanation for the variation reported by Benson & Little-Marenin might be pointing errors in the observations, which, when coupled with the source being very close to the edge of the telescope beam might lead to the observed variations. This explanation, although purely speculative, is supported to some extent by the lack of information supplied about pointing checks by the authors.

At this stage, very little can be said about the 'phase lag' (caused by the light travel time across the circumstellar dustshell between stellar photosphere and the region of maser activity) between peaks in the H_2O maser fluxes and that shown by the star; however, it is notable that the peak flux recorded by Benson & Little Marenin (1988) of 17.5 Jy at ≈JD 2447400, occurred when the visual magnitude of the star was at around its lowest value. If it is assumed that this is due to a phase lag of one half the period of the visual light cycle, and that the period of variation for V778 Cyg is 170 days, then another estimate may be made as to the radius of the masing region of 85 light days, or $\approx 2.2 \times 10^{17}$cm.

It should be mentioned though, that Cohen (1989) reports values of 20–30 days for typical phase lags between optical and maser variation. In reality, a more extensive co-ordinated optical and radio dataset would be required before an accurate value could be assigned to the phase lag for v778 Cyg.

There are too few published maser observations available of EU And to attempt any form of periodogram analysis for that star, and at the time of writing the BAAVSS observations covering the period of the first OH detection of this source were not available, and hence nothing can be said relating the variation in visual magnitude of the photosphere to the observed maser flux from this star. No maser emission at either H_2O or OH frequencies has been detected towards BM Gem to limits of $\geq$0.1 Jy.

6.4 Radiative transfer models for stars with anomalous dust envelopes

6.4.1 C stars

The key assumption of the binary model for C stars with silicate dust that was proposed by Benson & Little-Marenin (1987) is that the silicate emission features associated with the stars arise in a dust cloud whose opacity is such that it totally hides the companion M star around which it is presumed to be situated. Even in the alternative binary model

proposed by Lloyd Evans (1990) the silicate emission, assumed to arise in a disk around a companion object to the C star, is frequently described as 'optically thick', particularly for the three stars with the highest S/N in the *IRAS* LRS spectra (BM Gem, C1003 and V778 Cygni). However, Chan & Kwok (1988), in the only quantitative model for a C star with silicate dust thus far published, found that the observed energy distribution for the stars BM Gem and C1003 could be understood in terms of a stellar photosphere illuminating a 'recently detached' dust shell composed of O-rich (silicate) dust grains.

The detached nature of the shell comes from the assumption in the Chan & Kwok model that BM Gem is a transition object, in which the stellar photosphere has recently changed from O-rich to C-rich, with mass loss terminating at the time of the transition; Chan & Kwok found that they could match the observed energy distribution of BM Gem by assuming the inner radius of the dust shell to be 6 times its original value at the time of dust grain condensation ($\approx 6.0 \times 10^{14}$cm , whilst for C1003 the inner radius of the dust shell needed to fit the observations has grown to $\approx 1.6 \times 10^{15}$cm, which, according to Chan & Kwok indicated that mass loss had terminated much earlier for that object. Of particular interest with regard to the binary model are the optical depths in the silicate features of the stars BM Gem and C1003. For BM Gem, Chan & Kwok give $\tau_{9.7}$ as 0.696, whilst for C1003 the value given for $\tau_{9.7}$ is 2.088. In both cases, the extinction caused by the circumstellar dust shell at optical ($\lambda \leq 1.0\mu$m) wavelengths is insufficient to hide the mooted M star binary companion for these objects, given the synthesis of optical constants adopted. For 2 of the 3 stars with the highest S/N in their LRS spectra, the energy distributions could be matched without recourse to a binary companion. The modelling procedure adopted by Chan & Kwok could not match the energy distribution of V778 Cyg, which they implied to be evidence for the binary nature of that source.

The models used by Chan & Kwok were not as comprehensive as those developed earlier in this thesis, since they assumed the circumstellar envelopes to be composed of only single sized grains, and also, the optical constant synthesis adopted by them (essentially those of Volk & Kwok, 1988) are not derived from laboratory measurements of real materials (e.g. Draine & Lee, 1984, Krätschmer & Huffman, 1979). It was therefore decided to re-model the sources BM Gem, V778 Cyg and C1003 using the same code, optical constants and grain size distribution that were used to model the circumstellar envelope of WX Ser in chapter 4, in the light of the observations of these three objects presented in this chapter.

Table 6.8: Parameters for model binary system

Parameter	O-star	C-star
T_*	2500K	2500K
D	0.75Kpc	0.75Kpc
v_∞	15 km s^{-1}	3 km s^{-1}
R_*	4.0×10^{13}cm	3.0×10^{13}cm
$\dot{M}$	$4.0\times10^{-6}M_\odot Y^{-1}$	$1.0\times10^{-7}M_\odot Y^{-1}$

Since it was shown in chapter 4 that a 'composite' silicate dust provided the best fit to the overall energy distribution for WX Ser, it was decided to utilise the same 'composite' dust parameters derived there to model the mooted silicate dust in the envelopes of the C stars observed in this chapter.

However, given the uncertainties in the physical parameters for each of the stars, the uniqueness of any of the presented fits must of course be open to question.

6.4.2 Testing a binary model for C stars with silicate dust

Before an attempt was made to model any real object, it was decided to utilise the radiative transfer code described in chapter 2 to test the qualitative binary model for EU And, first proposed by Benson & Little-Marenin (1987) in which an M star 'with a relatively thick circumstellar shell', analagous to that observed around WX Ser, and a C star, were responsible for the observed energy distribution.

The parameters adopted for the model of each star are given in Table 6.8; The binary system was located arbitarily at a distance of 0.75 Kpc for modelling purposes. The dust model parameters given for the 'O-rich' star in Table 6.8 are identical with those derived for the star WX Ser in Chapter 4; only the distance is different. A two component model was used for the circumstellar envelope of the C star, with the components assumed to be amorphous carbon and silicon carbide grains. Grains in the envelopes of both stars were assumed to be in an unmodified MRN size distribution.

The mass loss rate for the C star was set to the low value of $1.0 \times 10^{-7}M_\odot Y^{-1}$, again purely to fit in with the model of Benson & Little-Marenin, who suggested that the C star was not particularly obscured by its own circumstellar shell. The dust to gas ratio s in

the model C star's envelope are identical for those derived for IRC+10°216 in chapter 5.

The result of this attempt to present a quantitative version of the Benson & Little-Marenin model is given as Figure 6.22, where both the final 'composite' spectrum and its two components are indicated. In this model, the 'cross over' between the C-rich component and the O-rich component dominating the energy distribution occurs at $\approx$ 2μm. Thus, in this case, one might expect to see O-rich spectral lines in the spectrum of such a system longwards of 2μm, wheras at shorter wavelengths the C-rich lines from the C star should be apparent. One point to note also is that for this case where the mass loss rate for the carbon star is taken to be as low as $10^{-7}M_{\odot}Y^{-1}$ then the emissivity of the silicate grains determines the slope of the observed far-IR spectrum; this would not be the case were the C star mass loss rate to climb as high as $\approx 10^{-6}M_{\odot}Y^{-1}$ (assuming a circumstellar shell similar in nature to that found for IRC+10°216 in chapter 5) at which point the λ^{-1} slope of the amorphous carbon grains would determine the observed spectrum from the system. However, if the mass loss rate for the C star was as high as this value, the star would become less dominant in the optical and near-IR region, and the nature of the observed composite spectrum would become very confused indeed. The implications of this quantitative test for the Benson & Little-Marenin model will be discussed below.

6.4.3 Modelling real C stars with O-rich dust shells

Only fair model fits to the observed energy distributions for each of the three stars could be found (given the uncertainties in the absolute flux calibrations for the individual observations, as well as the ill defined stellar and dust parameters for the stars). The model parameters which gave the best fit to the observations are listed in Table 6.9, whilst the model fits to the observations for each of the three stars are presented as Figure 6.23.

In the modelling process, a dust condensation temperature of 1000K and density of 3.3 g cm^{-1} were assumed for the silicate dust grains, whilst the Mathis, Rumpl and Nordsieck (MRN, 1977) grain size distribution was used to represent the grain size distribution within the dust shell.

For all initial models, a dust to gas ratio of 2.0×10^{-3} by mass was assumed, for silicate dust in the circumstellar envelope. The expansion velocity of the V778 Cyg circumstellar shell was taken to be 3 km s^{-1}, as measured from the OH & H_2O maser lines; identical

Figure 6.22: Production of a composite model spectrum from model O-rich and C-rich envelopes

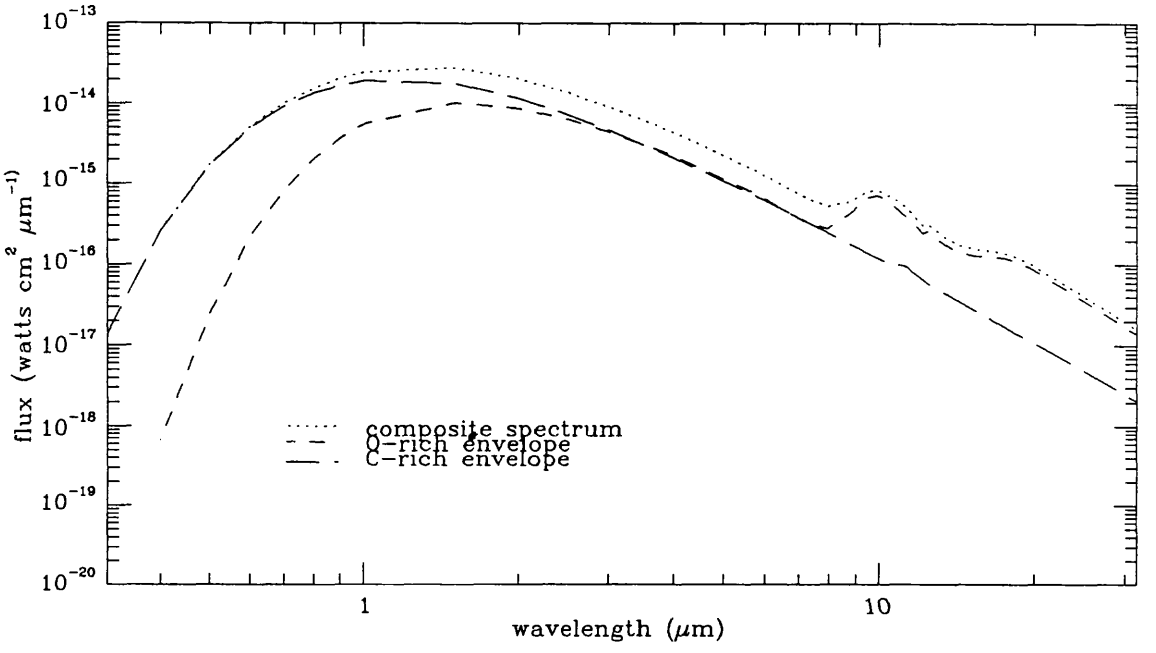

values for v_∞ were assumed for the shell of BM Gem and C1003. For V778 Cyg, the distance of 1.4 kpc given by Peery (1975) was adopted. In the cases of BM Gem and C1003, the distances quoted were those derived from the best fit to the observations, and as such rely on the assumed stellar radii. No account was taken of the effect of interstellar reddening upon the observed stellar energy distributions, once again due to the uncertainty in the accuracies of the quoted distances.

The individual models will now be discussed:

6.4.4 V778 Cyg

The best model for this star was obtained by adopting a dust condensation temperature of 1000K, which gave the inner radius of the stellar dust shell as 1.8×10^{14} cm. Thus, if this model is to be believed, silicate dust is required close (i.e. within 5 stellar radii) to the C star in order to obtain the observed energy distribution.

One obvious region where the model does not fit the observations of V778 Cyg very well is in the near-IR region of the spectrum; one reason for this may be an uncertain

Table 6.9: Model parameters for stars with anomalous dust emission

Star	Distance	T_*	R_*	$\dot{M}$	v_∞
	(kpc)	(K)	(cm)	($M_\odot$ yr^{-1})	(km s^{-1})
BM Gem	0.75	2500	3.0×10^{13}	2.5×10^{-7}	3.0
V778 Cyg	1.4	2500	3.5×10^{13}	7.5×10^{-7}	3.0
C1003	1.2	2350	3.0×10^{13}	1.5×10^{-6}	3.0
AD Per	2.1	3000	6.0×10^{13}	6.0×10^{-6}	15.0

calibration of the near-IR AAT spectra, which were obtained on a night of poor seeing. The model fit to the rest of the energy distributionios good however, as optical, mid-IR and far-IR observations are well matched.

6.4.5 BM Gem

Again the best fitting model assumed a dust condensation temperature of 1100K; With the adopted stellar parameters, this gave the inner radius of the dust shell as 1.25×10^{14}cm, or 4.1 stellar radii. As with V778 Cygni, the model fit is good in all except the near-IR spectral region, where again the plotted observations are derived from AAT FIGS spectra.

6.4.6 C1003

This star proved impossible to model using silicate dust alone. Models run assuming a dust shell composed only of silicate dust could only match the mid-IR spectral region; in the optical, they overestimated the observed flux by a factor ten or more, whilst in the far-IR, the obseved flux was underestimated.

The model plotted for C1003 is the best obtained to date, which assumes a dust shell composed of both silicate and amorphous carbon dust grains. A dust condensation temperature of 1000K was used for the AC dust component, whilst a temperature of 750K was adopted for the silicate dust in this model. For both components, a 'standard' MRN grain size distribution was assumed.

For the AC component a dust-to-gas ratio of 2.5×10^{-3} was used, whilst for the silicate component, the normal value of 2.0×10^{-3} was incorporated. It is obvious that the model shown in Figure 6.24 for this star is still not perfect, with the near-IR observations quite a little below the 60 and

Figure 6.23: Model fits to observed spectra of BM Gem, V778 Cyg & C1003

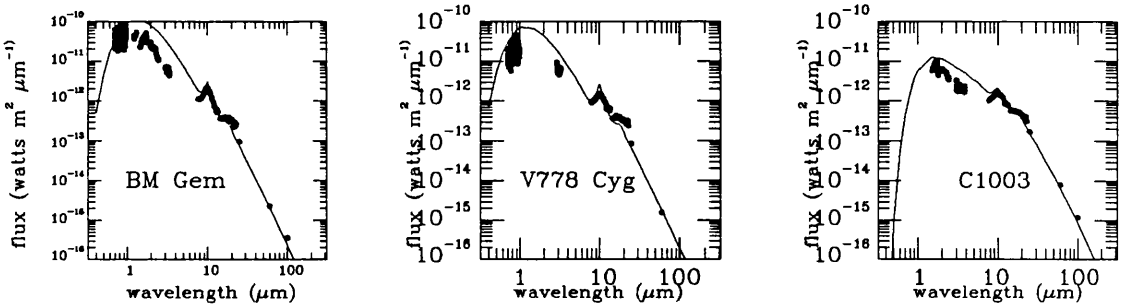

100μm photometry. However, it is felt that the model presented is at least as good a fit to the data as that presented by Chan & Kwok in their study of the system, and the fact that amorphous carbon dust was required to obtain a better match to the near-IR observations could perhaps be important if the true nature of this object is to be understood.

The models presented for BM Gem, V778 Cyg and C1003 indicate that the stars may be understood in terms of a single cool central star with a relatively low mass loss rate (in all three cases, $\leq 1.5\times10^{-6}$ $M_{\odot}$ yr^{-1}) illuminating a spherically symmetric expanding shell of oxygen-rich gas and dust. The optical depth in the 9.7μm feature is 0.4 for the best fitting model of V778 Cyg, whilst for BM Gem its value was 0.16. For all models, the optical depth of the circumstellar shell at optical wavelengths is consistent with the observed energy distribution of the underlying C star photosphere.

The adopted run of optical constants for silicate dust, used to successfully model the emergent spectrum of WX Ser in chapter 4, does not provide enough opacity at short wavelengths to hide the mooted companion around which the binary model suggests the silicate emission to arise. Thus the findings of Chan & Kwok that C1003 and BM Gem are probably single stars illuminating diffuse, if not detached, circumstellar shells are

confirmed by this work for BM Gem, and the single star model has been extended to V778 Cyg.

6.4.7 M Stars

The status of the M stars with apparently SiC features is open to question. All of the LRS spectra show weak emission features, but in all cases the S/N ratio for the individual spectra is relatively weak.

The energy distributions for all of the stars presented in Figure 6.20 appear similar, and show no obvious evidence of binarity. To test this, radiative transfer models were constructed for one of the better studied objects, AD Per, an M3Iab supergiant star, which had the advantage of a well defined distance, radius and T_{eff} on the basis of its membership of the h & χ Persei open cluster (Skinner & Whitmore, 1988; Tarafadar, 1988). Models were constructed for this star using the optical constants for SiC given by Pègouriè (1988), once again in a standard MRN size distribution. It was found that a good fit could not be obtained utilising these constants, and therefore the search for an adequate match to the observed energy distribution was extended to include models run utilising optical constants for silicate dust grains. The best fit model, shown in Figure 6.24, occurred with the parameters listed in Table 6.8. Also included in Figure 6.24 for reference purposes is the best fit to the energy distribution of AD Per that was obtained using the SiC optical constants; it was found that there was no way to get sufficient far-IR emission ($\lambda \geq 20\mu$m) from the SiC dust models without the resulting SiC feature at 11.4μm becoming too strong.

This best fit was obtained adopting a dust condensation temperature of 500K, implying that the dust shell is a detached one, similar to those modelled for the stars BM Gem and C1003 by Chan & Kwok. This is particularly interesting when one closely examines the optical spectrum of AD Per (Figure 6.3) since this does show some characteristics normally found in the spectra of S stars; for example the 9100Å ZrO feature may be present, and only the two strongest lines of the Ca II triplet are prominent which again is expected to be the case in S stars (Wing 1972). Although the case is far from certain, the fact that a good model for the dust shell could only be obtained with a detached shell for this object may indicate that AD Per is in the process of evolving from spectral type M to S, and its spectrum should be monitored carefully over the next few years. Given the low S/N ratios

Figure 6.24: Model fits to observed energy distribution of AD Per

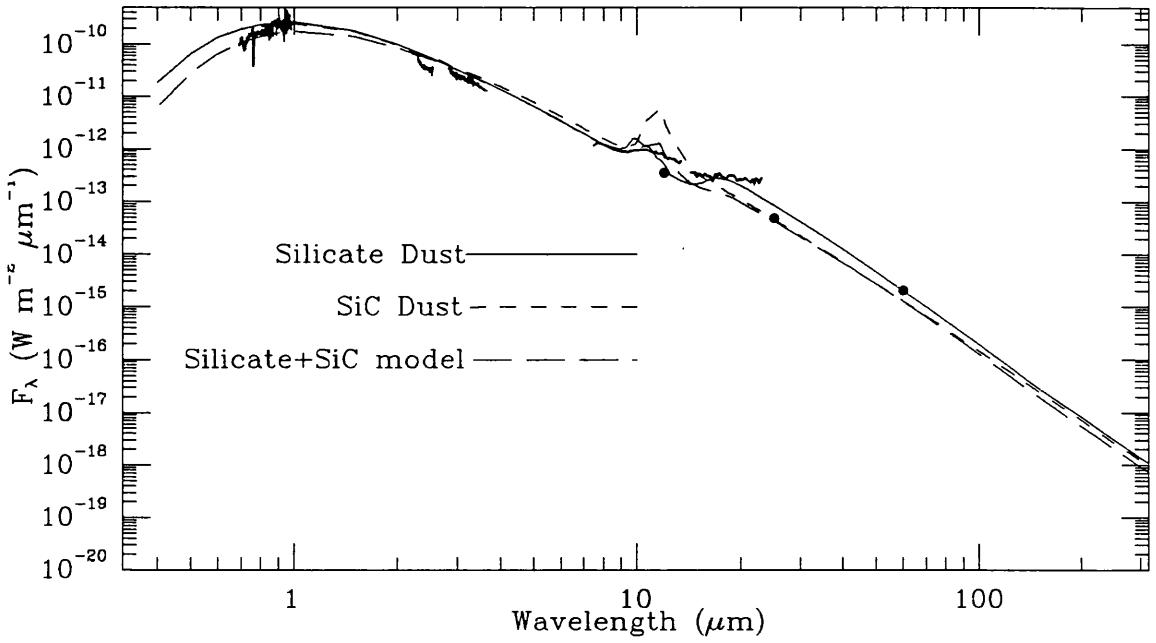

in the *IRAS* LRS spectra of the other M stars with apparent SiC features, and the growing evidence that at least some of the stars listed in Table 6.2 have been misclassified on the basis of these noisy spectra, and that such a good fit to the observations of AD Per had been achieved using silicate dust optical constants, it was decided that detailed radiative transfer modelling of all of the stars could wait until further 10μm spectra become available confirming the reality of the SiC features.

6.5 Discussion

The observations and models discussed above, when taken in conjunction with recent observational (e.g. Skinner *et al.*, 1990, Lambert *et al.*, 1990) and theoretical (Chan & Kwok, 1988) studies present difficulties for the standard binary model for C stars with silicate dust. Extensive searches for the spectroscopic signatures of M star companions, which according to the standard (Benson *et al.*, 1987) model should begin to dominate the energy distributions somewhere in the range 1–8μm, have been unsuccessful for all of the stars listed in Table 6.1; thus if the binary model is correct for all stars, the 'cross-over' region, where the M star spectral features become dominant over those of the C star, is

constrained to be in the region 4.5–7μm, which is completely inaccessible to ground-based observers. Thus, the observations alone cannot rule out either the standard binary model, or the modified binary model of Lloyd Evans, which in any case would not produce M star absorption features since the dust emission is assumed to come from O-rich dust associated with an accretion disk around the mooted companion object.

The radiative transfer models presented in the previous section for the three C stars with the strongest silicate features indicate that the observed energy distributions in the range 0.6–100μm for these stars may be understood without the need to invoke a binary companion, and also that the optical depth of the dust in the shells needed to reproduce the observed silicate features is too low in the optical to hide any reasonably luminous companion to the C Star, assuming a reasonable synthesis of silicate dust optical constants is adopted It is also notable that neither the H_2O nor the OH maser emission from V778 Cyg have shown any evidence for radial velocity variations, relative to the underlying stellar photospheric radial velocities, over the 2 years in which monitoring observations have been collected, which may also be used as evidence against orbital motion in a suspected binary system.

Given that there is strong evidence against the binary interpretation for C stars with silicate dust, the other models for the phenomenon will now be discussed, also in the light of the observations and models presented above.

Willems & de Jong (1986) suggestion that the observed silicate dust shells are fossil remnants of an earlier phase in the stars evolution, when its photosphere was O-rich, has been supported by radiative transfer models (Chan & Kwok, 1988) for the stars BM Gem and C1003. These models proposed that the inner radii of the dust shells needed to be $\approx 6.1\times10^{14}$cm (BM Gem) and $\approx 1.7\times10^{15}$cm (C1003) respectively in order to match the observed energy distributions for the two stars. With the adopted value of v_∞, the shell expansion velocity, being 10 km s^{-1} implied that the O-rich phase of mass loss terminated some 54 years ago in the case of C1003, whilst for BM Gem the smaller value of inner radius used by Chan & Kwok would imply that O-rich mass loss terminated within the last 19 years! The photosphere of BM Gem was first reported to be C rich by Sandford (1944), whilst Stephenson (1973) first reported the C-rich nature of C1003. For BM Gem at least then, there is observational evidence that its photosphere was carbon rich during a period when the Chan & Kwok model still required the condensate to be O-rich. This apparent

contradiction may perhaps be explained if the expansion velocity of the gas around BM Gem is as low as the 3 km s^{-1} value implied by the OH and H_2O maser spectra of the V778 Cyg circumstellar shell, although this would still require a fairly rapid evolution ($\approx$10–100y) of the stellar photosphere from O-rich to C-rich chemistry. There is then a problem if one wishes to identify the C stars with silicate dust as examples of transition objects whose photospheres have recently undergone a change in chemistry.

The models presented in Figure 6.23 were made by assuming that mass loss was still occurring at the rates given in Table 6.8; the dust shell inner radii for these models being determined by the adopted dust condensation temperature of 1000K. Thus, the model fits to the observed energy distributions were made assuming that the principal condensate from the stellar wind was O-rich. This would be the case if, as suggested by Vardya (1989) and Skinner *et al.* (1990), an unusual chemical equilibrium exists in the stellar wind such that an O-rich wind is produced following grain formation in a nominally C-rich shell. A scenario such as this was suggested by Thronson and Bally (1986) for the dust cocoon of the planetary nebula NGC 7027. Thronson and Bally suggested that silicate grains might form in a C-rich wind, if prior to their formation, graphite or silicon carbide grains had condensed in the C-rich wind at a temperature too high ($\approx$ 1500K) for significant quantities of CO molecules to form. If a significant proportion of the C available in the wind was condensed out of the wind in the C-rich dust grains, the speculation was that the wind could become O-rich, and consequently silicate grains could begin to condense. In this case, the stellar outflow would contain both C-rich and O-rich dust grains. The ideas of Thronson and Bally have been given support by theoretical calculations by Sharp (1989) who showed that graphite dust grains could condense out of stellar winds that were slightly O-rich.

There is both observational and theoretical evidence that for stars whose C/O ratios are close to unity ('S' stars) the type of dust that condenses in the circumstellar wind becomes quite unpredictable. In their survey of the dust associated with 84 S stars, Skinner *et al.* (1990) found that 20 appeared to have SiC dust, 20 to have silicate dust, 11 to have a mixture of silicate and SiC dust whilst the remaining 33 showed no evidence for dust emission features at all (though this did not rule out the presence of amorphous carbon or graphite as a source of opacity around these stars). There was apparently no correlation between any of the physical properties of the stars and the type of dust that

condensed around them. Thus, Skinner *et al.* suggested that the presence of silicate dust around the C stars implied a C/O ratio fairly close to (but not exactly) 1.0. (If the C/O ratio was extremely close to 1.0, the optical photospheric spectra would exhibit the characteristic S star features, e.g. ZrO bands, which are not apparent.) The Skinner *et al.* model would also similarly account for the identification of M stars with SiC features as being objects that had C/O ratios close to the window of unpredictability at $C/O \approx 1.0$.

Until fairly recently, chemical models of grain formation in circumstellar envelopes have assumed that chemical, as well as local thermodynamic, equilibria are maintained throughout a stellar wind. Gilman (1969) used these assumptions to predict that in winds with $C/O \geq 1$ the chief condensate should be SiC, whilst in cases where $C/O \leq 1$ silicate grains should condense preferentially. However, the assumption of chemical equilibrium holding in the wind has been shown to be violated, even for the case of an abundant diatomic molecule (Scalo & Slavsky, 1980) in the wind of a red giant star. The classical nucleation theory, upon which Gilman based his calculations has also been questioned in its applicability to cool stellar winds (Donn & Nuth, 1985). Thus, although the Gilman model for dust condensates may hold for environments which are very O or C-rich, it may well break down as the C/O ratio approaches unity. The assumption of LTE in the circumstellar envelope, assumed by Gilman, as well as by more recent dust condensation models such as that of Gail & Sedlmeyer (1987) must also be open to question, especially when there is observational evidence for cool molecular material existing cospatially with warm plasmas in the chromospheric regions of red giants.

The 'chemical equilibrium' models of Vardya, and Skinner *et al.* do not explain why all C stars with silicate dust features have enhanced ^{13}C (J stars). The majority of C stars are believed to be evolutionarily located on the asymptotic giant branch (AGB); the ^{12}C and s-process elements having been added to the envelope by dredge up from the He-burning shell. For these AGB C-stars, $^{12}C/^{13}C \approx 50$ (Lambert *et al.*, 1986) whilst for the J stars, the $^{12}C/^{13}C$ ratio approaches the equilibrium value of 3.4 for nuclear processed material that has undergone the CN cycle. The J stars also differ from the AGB C-stars since they show little evidence for the presence of s-process elements in their spectra (Utsumi, 1985; Dominy 1984).

The differences between the J stars and 'normal' C stars has led Lambert *et al.* (1990) to suggest that the two groups of stars have different origins; rather than assuming that

the J stars are resident upon the AGB (as suggested by Willems and de Jong 1986, 1988), Lambert *et al.* (1990) suggested that the progenitors of J-type C stars were early-R stars. These objects have identical surface temperatures and luminosities to those found for core He-burning K giants, whilst the analysis of Dominy (1984) found that they were similar to the J-type C stars (i.e. ^{13}C enhancement with little evidence for s-processed materials in the spectra). In the Lambert *et al.* (1990) evolutionary scenario, the origin of J type C stars with silicate dust is linked into the binary model of Lloyd Evans, since it is assumed that mass lost during the stage of the stars life when its photosphere was O-rich (i.e. during the K giant phase) condenses to form silicate grains that are stored in an accretion disk around a low mass main sequence companion nearby. After further evolution, the K star has become a J-type C star, whose mass loss rate is sufficiently low that emission from SiC grains condensing in its wind is negligible, whilst the luminosity of the star is sufficient to heat the silicate grains in the accretion disk giving rise to the observed emission. However, the scenario is tied to the binary model only by the need to explain the assumed optically thick dustshell, which, as shown above by the successful radiative transfer models, was found to be a fallacious assumption. It is interesting though that the mass loss rates derived by the modelling process are relatively low, which is in keeping with the Lambert *et al.* model, although of course the chemical composition of the grains in the outflow is different.

It seems then that there is, at present, no conclusive explanation for the phenomenon of C stars with silicate dust grains. However, I feel that there is fairly strong evidence that a model involving anomalous dust grain formation in environments where $C/O \approx 1.0$ may be successful in explaining the observations. The fact that all of the C stars with silicate dust shells are J stars is rather difficult to explain though; as pointed out by Lambert *et al.* (1990), the difference in chemical bond energies that affect the rate constants for chemical reactions involving ^{12}C and ^{13}C are small in relation to the thermal energy at the temperatures in the circumstellar dust shell.

A good test as to whether the envelopes associated with the C stars are derived from a current phase of mass loss would be to search for emission from $H^{12}CN$ and $H^{13}CN$ molecules in the envelope. This is not as surprising an idea as it seems, since 88.6 GHz emission from the $H^{12}CN$ J=1–0 transition has been identified with O-rich circumstellar shells associated with the OH/IR stars GK Tau and OH231.8+4.2 (Deguchi & Goldsmith,

1985). Since all of the C stars with silicate dust are known to be J stars, an observational search for $H^{12}CN$ and $H^{13}CN$ molecules might confirm a scenario in which O and C-rich species are present simultaneously in a stellar outflow.

The existence of M stars with Si-O dust features is by no means certain, and further observations are needed to confirm the nature of the dust associated with the candidate objects suggested by Skinner *et al.* (1990).

Chapter 7

Summary and future work

This thesis has presented the first stage of what it is hoped will lead to a much more extensive study of the circumstellar environments of late type stars.

A numerical method has been described by which the transfer of radiation through a circumstellar dust shell may be calculated in a general case where the shell is composed of multiple dust components within which grains are present with a distribution in sizes.

The method provides a large amount of information as to the physical conditions within the model dust shell, such as the temperature gradient and intensity distributions throughout the shell, as well as predicting the emergent fluxes.

The radiative transfer models presented for WX Ser and IRC+10°216 in chapters 4 and 5 respectively represent arguably the most detailed studies yet published for O-rich and C-rich circumstellar environments, and the models calculated for both objects suggest that a fair representation of their emergent spectra may be obtained by assuming that dust grains located within the circumstellar shell of each object bare a chemical affinity to materials whose optical properties have been studied in Earth-based laboratories. It has also been suggested that one of the reasons other workers have found Earth based materials to be poor analogues for circumstellar dust may have been due to their assumptions that the shells consisted of single sized dust grains, rather than a distribution of grain sizes.

In the case of O-rich circumstellar shell around WX Ser, grains with optical properties intermediate between those of olivines described by Krätschmer & Huffmann (1979) and Draine & Lee (1984, 1987) in a distribution of sizes identical to that proposed by Mathis, Rumpl & Nordsieck (1977) were found to provide a good match to the observed energy distribution for this star in the wavelength range $0.5 \leq \lambda \lesssim 100 \mu m$

The best match to the far-IR observations of the circumstellar shell of WX Ser was found to occur if the emissivity of the grains was allowed to fall off as λ^{-2} longwards of 20μm, whilst a dust to gas ratio of 0.002, similar to that found by Skinner & Whitmore (1987, 1988a,b) for the circumstellar envelopes of other late type stars with O-rich circumstellar shells was utilised for the adoped mass loss rate.

For the C-rich envelope around the star IRC+10°216 a multiple component dust shell had to be invoked to match the observed energy distribution. Amorphous carbon grains, with optical properties similar to those described by Hoare (1988) were found to account for the bulk of the dust opacity in the region 0.3$\leq$1μm whilst a component of silicon carbide grains proved necessary to match the 11.4μm emission feature observed in the *IRAS* LRS spectrum of this object. A modified MRN size distribution with lower and upper limits to the grain radii of 0.005μm and 0.1μm was found to give a superior fit to the observations than the standard MRN size distribution, whose lower and upper grain radii were 0.005μm and 0.25μm for the AC grains in the model.

The best match to the observations longwards of 20μm was provided by a λ^{-1} emissivity law for the amorphous carbon grains, although at the very longest wavelengths (i.e. $\lambda \geq 100\mu$m) neither emission from dust grains nor the stellar photosphere could match the observed flux from IRC+10°216, and it was suggested that free-free emission from a stellar chromosphere with a temperature of 10000K could be responsible for the excess over the predicted model flux.

Extensive new observations of carbon stars with apparently O-rich circumstellar shells, and of O stars with apparently C-rich circumstellar shells were presented in chapter 6. A number of proposed models for these objects were reviewed in the light of the new observations, and some initial radiative transfer models calculated using the methods described in chapter 2 were given.

It is not clear either from the new observations, or from the initial models presented for these objects in chapter 6 what their precise nature is, and further observations at a number of wavelengths, and over a relatively long timescale must be made before any real conclusions may be drawn. However, observations over a two year period, of the maser emission from one of the stars, V778 Cyg, shows no indication, within experimental accuracy, of radial velocity variations, which might be expected were it situated in a binary system.

It will also be necessary to gain a much more accurate idea as to the parameters of the individual systems (especially their distances) before any insights may be gained into what these 'oddball' stars are.

Of particular importance in deriving a distance to the stars from which maser emission has been detected will be trying to correlate the maser variations with observed variations in the optical brightness for each object; Although as pointed out in chapter 6, this will require a dedicated monitoring campaign at optical and radio wavelengths. Unfortunately, visual observations by amateur astronomers will not provide information of sufficient photometric accuracy for this, and the data must be obtained using electronic photometric methods, for the project to be a success.

One possible test for the latest binary model for the 'oddball' stars (that of Lloyd Evans, 1991) will be observations in the UV spectroscopic region either by the I.U.E. or by space telescope, since it is only there that a contribution to the energy distribution from a mooted compact companion might become visible.

7..1 Future work

It is believed that the models presented within this thesis for the circumstellar shells of WX Ser and IRC+10°216 are amongst the most detailed yet published for any late type stellar environments. However, as with any modelling technique, there are several ways in which the models presented could be improved to provide a better representation of the true nature of the circumstellar shells that they are being used to study.

Perhaps the most obvious way of improving the models presented would be to incorporate stellar atmospheric models, to represent the stellar energy distributions in the modelling process. Currently, the best stellar models for late type stars are those developed by Bessell & his co-workers for M stars (e.g. Bessell & Scholz, 1989), and those of Gustafsson and his collaborators (e.g. Lambert *et al.*, 1986, B. Gustafsson, private communication) for C stars.

As yet however, no accurate model atmosphere has been produced for stars of either O-rich or C-rich composition whose surface temperatures are lower than 2500K, and to some extent this has hampered their inclusion into radiative transfer analyses, since the central stars which provide the illumination for the dust shells are almost invariably cooler than 2500K.

Added to this is the problem that the atmospheres of nearly all late type stars are non-static, and consequently a static model atmosphere coupled with a static dust shell model can at best provide an accurate representation of the situation at only a single photometric phase; However, non static model atmospheres for Mira stars have recently become available, for warmer stellar atmospheres (e.g. Bessell & Scholz, 1989; Bowen, 1989), and the ultimate model for the circumstellar environment for a late type stellar atmosphere will certainly be derived from coupling the dynamics of the stellar photosphere with those in the circumstellar shell.

A further problem which has to be addressed before a model atmosphere can be incorporated into the dust models described in this thesis is the question of precisely how many flux points are required in the model to provide an accurate description of the stellar energy distribution; Obviously some form of smoothing must be introduced in order to reduce the number of wavelengths for which fluxes are calculated to a number which will produce an accurate representation of the emergent flux from a circumstellar dust model within a reasonable (i.e. $\approx$hours) computational timescale. At this stage, a quantitative analysis will become possible, as to the true disadvantages of utilising a 'black body' model for the energy distribution of the central star.

Some objects (e.g. α Ori, with an estimated surface temperature of $\approx$ 3000K) do have effective temperatures which fall within the range of presently available (and reasonably reliable) model atmospheres, and, although intrinsically variable stars, it would certainly be worthwhile studing these objects using the methods described in this thesis, now that a self consistent set of dust optical constants has been derived from models for the stars WX Ser and IRC+10°216. A model for α Ori, incorporating a model atmosphere, a stellar chromosphere, and using the radiative transfer method described within this thesis is currently possible, and will in fact be the next development of the work presented here.

Another way of expanding upon the results presented within this thesis will be to extend the modelling techniques presented here to a much larger sample of stars, in much the same way as was done (using inferior models) by Skinner & Whitmore (1987, 1988a, b) and Rowan-Robinson and his co-workers (Rowan-Robinson & Harris, 1983; Rowan Robinson *et al.*, 1986). Of particular interest will be to re-model some of the stars studied by Skinner & Whitmore (1987, 1988a,b) using the more realistic methods of this thesis to test their conclusions as to the number of M stars having warm chromospheres and

coronae contributing to their energy distributions in the far-IR regions of the spectrum.

If unique and good model fits can be derived for a large sample of O-rich late type stars, then it will also prove interesting to compare the results of that study with those of workers such as Hoare (1988) for planetary nebulae, which represent a stage of stellar evolution later than that exhibited by the late type stars modelled in this thesis.

Similarly, models should also be developed for a larger sample of C stars so that the conclusions drawn from the study of IRC+10°216 in chapter 5 may be tested on other C stars; It will prove interesting to study whether the ratio of AC/SiC dust remains constant from star to star, as is inferred from the work of Skinner & Whitmore, 1988b), or whether some C stars can be modelled on the basis of SiC grains being the sole opacity source in their circumstellar shells, as was implied by Le Bertre (1988b). Of particular interest will be the development of models for stars such as R Lep and V Cyg, whose photospheric compositions have been derived from optical and near-IR spectroscopy by Lambert *et al.* (1986). By using the techniques discussed in chapter 5, whereby information about the chemical composition of the circumstellar dust shell was derived from the observations, it will prove interesting to compare chemical compositions of photosphere and dustshell, albeit in a gross fashion.

A further group of objects which would repay study using the radiative transfer techniques developed in this thesis are the S stars, whose photospheric carbon to oxygen ratio is approximately unity. Some of these stars (as discussed in Skinner *et al.*, 1990) present emission features which appear to be 'blends' of 9.7μm silicate and 11.4μm SiC features, and interesting information as to the chemical composition of the circumstellar dust shells, compared with the stellar photospheres of these objects could be drawn from a modelling campaign for these objects too.

Finally, once the parameters of the 'oddball' stars have been better defined, perhaps with the availability of better and more extensive coeval multiple wavelength photometry, even the nature of these objects may be identified.

As mentioned in the very first line of this final chapter, this work must be regarded as the very initial part of what will eventually be a much larger study, which, when complete, will present a more reliable picture as to the nature of the circumstellar dust shells around late type stars.

The techniques and some of the problems associated with using them have been laid

down, discussed and, to some extent understood for single examples of bright and well studied O-rich and C-rich circumstellar shells, and it is in the extension of these models to more stars with which the next stages of this work will lie. Much work remains to be done, and it is felt that the methods described within this work may perhaps be amongst the best techniques thus far presented, by which the nature of dust grains and indeed the conditions within circumstellar envelopes in which they lie, may be studied.

References

Aannestad, P. A., 1975., *Astrophys. J.*, **200**, 30.

Admas, W. S. & MacCormack, E., 1935. *Astrophys. J.*, **81**, 119.

Aitken, D. K., Roache, P. F., Spenser, P. F., & Jones, B., 1979. *Astrophys. J.*, **233**, 925

Aitken, D. K., & Roache, P. F., 1982. *Mon. Not. R. ast. Soc.*, **200**, 217

Ake, T. B., 1979., *Astrophys. J.*, **234**, 538.

Allen, D. A. & Cragg, T. A. 1983. *Mon. Not. R. ast. Soc.*, **203**, 777.

Allen, C. W., 1973. *Astrophysical Quantities,* 3rd Edition, The Athlone Press, University of London.

Andriesse, C. D., 1974. *Astr. Astrophys.*, **27**, 257.

Bailey, J., Barton, J. R., Conroy, P., Davies, H., Hillier, D. J., Hyland, A. R., Jones, T. J., Shortridge, K & Whittard, D., 1988. *Publ. Astr. Soc. Pac.*, **100**. 1178.

Barnard, E. E., 1907. *Astrophys. J.*, **25**, 218.

Barnard, E. E., 1910. *Astrophys. J.*, **31**, 8.

Barnard, E. E., 1919. *Astrophys. J.*, **49**, 1.

Baron, Y., de Muizon, M., Papoular, R. & Pegourié, B. 1987., *Astr. Astrophys.*, ,186, 271.

Beichmann, C. A., Neugebauer, G., Habing, H. J., Clegg, P. E. & Chester, T. J., (Eds) 1984. *IRAS Catalogs and Atlases Explanatory Supplement, NASA*

Belcher, J. W. & Olbert, S., 1975. *Astrophys. J.*, **200**, 369.

Belserene, E. P. 1988. *Sky & Telescope.*, **Sept.**, 288.

Benson, P. J. & Little-Marenin, I. R., 1987. *Astrophys. J.*, **316**, L37.

Benson, P. J. & Little-Marenin, I. R., 1988. *Journal American Assoc. Var. Star. Obs.*, **17**, 111.

Allamandola, L.J., 1989. In Interstellar Dust. Eds. L.J. Allamandola + Tielens, A.G.G.M. (Dordrecht: Kluwer)

Bessell, M.S., Brett, J.M., Scholz, M. and Wood, P.R. 1989. Astr. Astrophys. 213 225.

Bessell, M.S., and Scholz, M., 1989. in Evolution of Peculiar Red Giant Stars. Eds Johnson, H.R. + Zuckerman, B. (Cambridge: CUP)

Biermann, P. & Harwit, M., 1980. *Astrophys. J.*, **241**, L105.

Bless, R. C., & Savage, B. D., 1972. *Astrophys. J.*, **171**, 293.

Bode, M. F., 1988. in *Dust in the Universe,* Eds. Bailey, M. E. & Williams, D. A. (Cambridge: CUP)

Bohren, C. F. & Huffmann, D. R., 1983. in: *Absorption and scattering of light by small particles* (New York: Wiley)

Borghesi, A., Bussoletti, E. & Colangeli, L., 1985a. *Astr. Astrophys.*, **142**, 225

Borghesi, A., Bussoletti, E., Colangeli, L. & De Blasi, C. 1985b. *Astr. Astrophys.*, **153**, 1.

Borghesi, A., Bussoletti, E., Colangeli, L., Minafra, A. & Rubini, F., 1983. *Infrared Phys.*, **23**, 85.

Borghesi, A., Bussoletti, E., Colangeli, L., Orofino & V., Guido, M. & Nunziante-Cesario, S. 1986. *Infrared Phys.*, **26**, 37.

Bowen, G. H., 1989. in *Evolution of Peculiar Red Giant Stars; Proc IAU Colloquium 106* Eds. Johnson, H. R. & Zuckerman, B. (Cambridge: CUP)

Bregman, J., 1989, in: *Interstellar Dust* Eds. Allamandola, L. J. & Tielens, A. G. G. M. (Dordrecht: Reidel)

Burstein, D. & Heiles, C., 1982. *Astron. J.*,**87), 165.**

Bussoletti, E., Colangeli, L., Borghesi, A., Orofino, V., 1987. *Astr. Astrophys. Suppl.*, **70**, 257.

Bussoletti, E., Colangeli, L. & Orofino, V. 1987. *Astrophys. J.*, **321**, L87

Campbell, M. F., Elias, J. H., Gezari, D. Y., Harvey, P. M., Hoffmann, W. F., Hudson, H. S., Neugebauer, G., Soifer, B. T., Werner, M. W. & Westbrook, W. E., 1976. *Astrophys. J.*, **208**, 396.

Carnochan, D. J., 1988. *Mon. Not. R. ast. Soc.*, **231**, 455

Chan, S. J., & Kwok, S., 1988. *Astrophys. J.*, **334**, 362.

Chandrasekhar, S., 1960. *Radiative Transfer*, Dover, New York.

Chapman, J. M. & Cohen, R. J., 1986. *Mon. Not. R. ast. Soc.*, **220**, 513.

Chini, R., Kreysa, E., Mezger, P. G. & Gemünd, H. P., 1986. *Astr. Astrophys.*, **154**, L8.

Cimerman, M. & Scoville, N., 1980. *Astrophys. J.*, **239**, 526.

Cohen, R. J., Downes, G., Emerson, R., Grimm, M., Gulkis, S., Stevens, G., & Tarter, J. 1987. *Mon. Not. R. ast. Soc.*, **225**, 491.

Cohen, R.J. 1989. Rep. Prog. Phys. 52, 881

Colangeli, L., Capozzi, V., Bussoletti, E., & Minafra, A., 1986. *Astr. Astrophys.*, **168**, 349.

Curtis, H. D., 1917. *Publ. Astr. Soc. Pac.*, **29**, 145.

Day, K. L., 1976. *Astrophys. J.*, **210**, 614.

Day, K. L., & Donn, B., 1978. *Astrophys. J.*, **222**, L45.

Day, K. L., 1979. *Astrophys. J.*, **234**, 158.

Day, K. L. 1981. *Astrophys. J.*, **246**, 110.

Deeming, T. J., 1975. *Astrophys. Space Sci.*,**36**, 137.

Deer, W. A., Howie, R. A. & Zussmann, J., 1976. in: *An Introduction to the Rock Forming Minerals* students' edn, 9th impression. (London: Longmans)

de Groot, M. S., van der Zwet, G. P., Jenniskens, P. M. M., Bauer, R., Baas, F., & Greenberg, J. M. 1988. in: *Dust in the Universe* Eds. Bailey, M. E. & Williams, D. A. (Cambridge: CUP)

Deguchi, S. & Goldsmith, P. F., 1985. *Nature.*, **317**, 336.

Deutsch, A. J., 1956. *Astrophys. J.*, **123**, 210.

Dominy, J. F., 1984. *Astrophys. J. Suppl.*, **55**, 27.

Dominy, J. F., 1985. *Publ. Astr. Soc. Pac.*, **97**, 1104.

Donn, B., 1968. *Astrophys. J.*, **152**, L129.

Donn, B. & Nuth, J. A., 1985. *Astrophys. J.*, **288**, 187.

Dorschner, J., Friedemann, C. Gürtler, J., 1977. *Astron. Nachr. Bd.*, **298**, H5.

Dorschner, J., Friedemann, C., Gürtler, J., Henning, T., & Wegener, H., 1986. *Mon. Not. R. ast. Soc.*, **218**, 37p.

Draine, B. T., & Anderson, N., 1985, *Astrophys. J.*, **292**, 494.

Draine, B. T., 1981. *Astrophys. J.*, **217**, 425.

Draine, B. T., 1985. *Astrophys. J. Suppl.*, **57**, 587.

Draine, B. T., 1987. *Astrophys. J. Suppl.*, **64**, 505.

Draine, B. T. & Lee, H. M., 1984. *Astrophys. J.*, **285**, 89.

Draine, B. T. & Lee, H. M., 1987. *Astrophys. J.*, **318**, 485.

Duley, W. W., 1985. *Astrophys. J.*, **287**, 694.

Duley, W. W., 1987. *Mon. Not. R. ast. Soc.*, **229**, 203.

Duley, W. W., & Najdowsky, I., 1983. *Astrophys. Space Sci.*,**95**, 187.

Efstathiou, A., & Rowan-Robinson, M., 1990. *Mon. Not. R. ast. Soc.*, **245**, 275.

Engels, D., 1979. *Astr. Astrophys. Suppl.*, **36**, 337.

Elitzur, M., Goldreich, P. & Schoville, N., 1976. *Astrophys. J.*, **205**, 384.

Elitzur, M., 1978., *Astr. Astrophys.*, **62**, 305.

Erikson, E. F., Knacke, R. F., Tokunaga, A. T., & Haas, M. R., 1981. *Astrophys. J.*, **245**, 148.

Fazio, G. G., McBreen, B., Stier, M. T. & Wright, E. L., 1980. *Astrophys. J.*, **237**, L39.

FitzGerald, P. M., Stephens, T. C. & Witt, A. N., 1976. *Astrophys. J.*, **208**, 709.

Fitzpatrick, E. L., & Massa, D., *Astrophys. J.*, **307**, 286

Fix, J. D. & Alexander, D. R., 1974. *Astrophys. J.*, **188**, L91.

Forrest, W. J., Gillett, F. C., & Stein, W. A., 1975. *Astrophys. J.*, **195**, 423.

Forrest, W. J., McCarthy, J. F., & Houck, J. R., 1979. *Astrophys. J.*, **233**, 611.

Forrest, W. J., Houck, J. R., & McCarthy, J. F., 1981. *Astrophys. J.*, **248**, 195.

Frenklach, M., Carmer, C. S. & Feigelson, E. D., 1989. *Nature.*, **339**, 196.

Friedemann, C., Gürtler, J. Schmidt, R. & Dorschner, J., 1981. *Astrophys. Space Sci.*,**79**, 405.

Gail, H. P., & Sedlmayer, E., 1987. *Astrophys. J.*, **177**, 186.

Gear, W. K., Robson, E. I., & Griffin, M. J., 1988. *Mon. Not. R. ast. Soc.*, **231**, 55p.

Gehrz, R. D., & Woolf, N. J., 1971. *Astrophys. J.*, **165**, 285.

Gillet, F. C., Low, F. J., & Stein, W. A., 1968. *Astrophys. J.*, **154**, 677

Gilman, R. C., 1969. *Astrophys. J.*, **155**, L185

Gilra, D. P., 1972. in: *The Scientific Results from the Orbiting Astronomical Observatory OAO-2* Ed. Code, A. D. (NASA SP-310)

Glasse, A. C. H., Towlson, W. A., Aitken, D. K. & Roche, P. F., 1986. *Mon. Not. R. ast. Soc.*, **220**, 185.

Goebel, J. H. & Moseley, H., 1985. *Astrophys. J.*, **290**, L35.

Goldberg, L., 1979. *Quart. Jou. Roy. Astr. Soc.*, **20**, 361.

Goldberg, L., 1984. in: *CNRS-NASA Monograph Series on Nonthermal Phenomena in the Stellar Atmosphere* (Washington D. C.: NASA)

Greenberg, J. M., & Chlewicki, G., 1983. *Astrophys. J.*, **272**, 563

Greenberg, J. M., 1986. *Astrophys. Space Sci. Lib.*, **124**, 177.

Grevesse, N. & Anders, E., 1989. In *Cosmic Abundances of Matter, AIP Conference Proceedings 183* AIP New York

Griffin, I. P., 1990. *Mon. Not. R. ast. Soc.*, **247**, 591.

Gundermann, E., 1965. *PhD. thesis, Harvard Univ. Cambridge Mass.*

Hakakawa, S., 1970. *Prog. Theor. Phys.*, **43**, 1224.

Haisch, B. M., 1979. *Astr. Astrophys.*, **72**, 161.

Hartmann, J.,1904. *Astrophys. J.*, **19**, 268.

Hartmann, L. & MacGregor, 1980. *Astrophys. J.*, **242**, 260.

Hecht, J. H., 1986. *Astrophys. J.*, **305**, 817

Hecht, J. H., Holm, A. V., Donn, B. & Wu, C. C., 1984. *Astrophys. J.*, **280**, 228.

Harwitt, M., 1973. *Astrophysical Concepts* Publ. Wiley

Herbig, G. H., 1975. *Astrophys. J.*, **196**, 129

Hoare, M. G. & Clegg, R. E. S., 1988. *Mon. Not. R. ast. Soc.*, **235**, 1049.

Hoare, M. G., 1988. *PhD. Thesis, University of London*

Hoare, M. G., 1990. *Mon. Not. R. ast. Soc.*, **244**, 193.

Hoffleit, D. R., & Jaschek, C., 1984. *Yale Catalogue of Bright Stars,* Yale University, New York.

Högbom, J. A., 1975. *Astr. Astrophys. Suppl.*, **15**, 417.

Holzer, T. E. & MacGregor, K. B., 1985. in *Mass Loss from Red Giants* Eds. Morris, M. & Zuckerman, B. (Dordrecht: Reidel)

Hong, S. S., & Greenberg, J. M., 1980. *Astr. Astrophys.*, **88**, 189

Horne, K., 1986. *Publ. Astr. Soc. Pac.*, **98**, 609.

Houck, N. & Cowley, A. P., 1975. *University of Michegan Catalogue of Two-Dimensional Spectral Types for the HD Stars,* Department of Astronomy, Univ. Michegan, Ann Arbor (vols 1-3)

Howarth, I. D., 1983. *Mon. Not. R. ast. Soc.*, **203**, 301.

Howarth, I. D. & Phillips, A. P., 1986. *Mon. Not. R. ast. Soc.*, **222**, 809.

Hoyle, F. & Wickramasinghe, N. C., 1977. *Nature.*, **266**, 241

Hoyle, F. & Wickramasinghe, N. C., 1962. *Mon. Not. R. ast. Soc.*, **124**, 417.

Hoyle, F. & Wickramasinghe, N. C., 1982. *Astrophys. Space Sci.*,**86**, 321.

Huggins, P. J., Olofsson, H. & Johansson, L. E. B., 1988. *Astrophys. J.*, **332**, 1009.

Hyland, A. R., Becklin, E. E., Frogel, J. A., & Neugebauer, G., 1972. *Astr. Astrophys.*, **16**, 204.

Iben, I. & Renzini, A., 1983. *Ann. Rev. Astron. Astrophys.*, **21**, 271.

Iben, I., 1985. in *Mass Loss from Red Giants* Eds. Morris, M. & Zuckerman, B. Publ. Reidel

IRAS Science Team, 1986. *Astr. Astrophys. Suppl.*, **65**, 607.

Isles, J., 1989. *Brit. Astron. Assoc. Var. Star. Circ.*, **68**, 2.

Jaki, S. L., 1970 *Journal for the History of Astronomy*, **1**, 53.

Johnson, H. L., 1968. in *Nebulae & Interstellar Matter,* Eds. Middlehurst, B. M. & Aller, L. H. (Chicago: University of Chigago Press)

Jones, T. W., & Merrill, K. M., 1976. *Astrophys. J.*, **209**, 509.

Jones, A. P., 1988. *Mon. Not. R. ast. Soc.*, **234**, 209

Jones, A. P., Duley, W. W., & Williams, D. A., 1988. in: *Dust in the Universe* Eds. Bailey, M. E. & Williams, D. A. (Cambridge: CUP)

Jones, T. J., Hyland, A. R., Fix, J. D., & Cobb, M. L., 1988. *Astron. J.*,**95**, 158.

Jourdain de Muizon, M., d' Hendecourt, L. B. & Geballe, T. R., 1989. in: *Proc. 22nd ESLAB Symposium on Infrared Spectroscopy in Astronomy* Ed. Kaldeich, B. H. (ESA SP-290)

Jura, M., 1983. *Astrophys. J.*, **267**, 647.

Jura, M., 1984. *Astrophys. J.*, **282**, 200.

Jura, M. & Zuckerman, B., 1985. *Astrophys. J.*, **294**, 242.

Keady, J. J., Hall, D. N. B. & Ridgeway, S. T., 1988. *Astrophys. J.*, **326**, 832.

Khare, B. N., & Sagan, C., 1979. *Astrophys. Space Sci.*,**65**, 309.

Keenan, P. C. & Boeshaar, P. C., 1980. *Astrophys. J. Suppl.*, **43**, 379.

Knapp, G. R., 1985. *Astrophys. J.*, **293**, 273.

Koike, C., Hasegawa, H. & Manabe, A., 1980. *Astrophys. Space Sci.*,**67**, 495.

Koike, C., Hasegawa, H. & Hattari, T., 1987. *Astrophys. Space Sci.*,**134**, 95.

Krätschmer, W. & Huffman, D. R., 1979. *Astrophys. Space Sci.*,**61**, 195

Krätschmer, W., 1980. in *Solid Particles in the Solar System* Eds. Halliday, I. & McIntosh, B. A. (Dordrecht: Reidel)

Koorneef, J., 1983. *Astr. Astrophys.*, **128**, 84

Kukarkin, B. V., Kholopov, P. N., & Efremov, Y. N., 1969. *General Catalogue of Variable Stars,* 3rd Edition, Publishing Office Nauka, Moscow.

Kwan, J. & Hill, F., 1977. *Astrophys. J.*, **215**, 781.

Kwok, S., 1975. *Astrophys. J.*, **198**, 583.

Kwok, S., 1987. *Physics Reports.*, **156**, 111.

Lambert, D. L., Gustafsson, B., Eriksson, K. & Hinkle, K. H., 1986. *Astrophys. J. Suppl.*, **62**, 373.

Lambert, D. L., Hinkle, K. H., & Smith, V. V. 1990. *Astron. J.*,**99**, 1612.

Lambert, D. L., 1989. in *Evolution of Peculiar Red Giant Stars; Proc. I.A.U. Colloquium 106* Eds. Johnson, H. R. & Zuckerman, B. (Cambridge: CUP)

Lattanzio, J. C., 1989. *Evolution of Peculiar Red Giant Stars; Proc. I.A.U. Colloquium 106.* Eds. Johnson, H. R. & Zuckerman, B. (Cambridge: CUP)

Le Bertre, T., 1987. *Astr. Astrophys.*, **176**, 107.

Le Bertre, T., 1988a. *Astr. Astrophys.*, **190**, 79.

Le Bertre, T., 1988b. *Astr. Astrophys.*, **203**, 85.

Le Bertre, T., Deguchi, S. & Nakada, Y., 1990. *Astr. Astrophys.*, **235**, L5

Lèger, A. & Puget, J. L., 1984. *Astr. Astrophys.*, **137**, L5.

Leung, C. M., 1975. *Astrophys. J.*, **199**, 340.

Little, S. J., Little-Marenin, I. R. & Price, S. D., 1988. in: *Proc 5th Cambridge Workshop on Cool Stars, Stellar Systems, and the Sun,* eds Linsky, J. L., & Stencel, R. E. (Berlin: Springer-Verlag)

Little-Marenin, I. R., 1986. *Astrophys. J.*, **307**, L15.

Little-Marenin, I. R., Benson, P. J., & Dickinson, D. F., 1988. *Astrophys. J.*, **330**, 828.

Little-Marenin, I. R., Benson, P. J., & Little, S. J., 1988. In: *Proc. 5th Cambridge Workshop on Cool Stars, Stellar Systems, and the Sun,* p. 396, eds Linsky, J. L. & Stencel, R. E., Springer Verlag, Berlin.

Lloyd Evans, T., 1990. *Mon. Not. R. ast. Soc.*, **243**, 346.

Lloyd Evans, T., 1991. *Mon. Not. R. ast. Soc.*, **249**, 409.

Low, F. J., Bientena, D. A., Gautier, T. N., Gillet, F. C., Beichmann, C. A., Habing, H. J., Hauser, M. G., Houck, J. R., Rowan-Robinson, M., Neugebauer, G., Young, E., Auman, H. H., Boggess, N., Emerson, J. P., Soifer, B. T., Walker, R. G., & Wesselius, P. R., 1984. *Astrophys. J.*, **278**, L19

Lucas, R., Omont, A., & Stora, R. (Eds.), 1985. *Birth and Infancy of Stars*, USMG/NATO ASI Session XLI. (Amsterdam: North Holland Publishing Co.)

Luttermoser, D. G., Johnson, H. R., Avrett, E. H. & Loeser, R., 1989. *Astrophys. J.*, **345**, 543.

Martin, P. G., 1978. *Cosmic Dust, Clarendon, Oxford*

Martin, P. G., Rogers, C. & Rybicki, G. B., 1984. *Astrophys. J.*, **284**, 317.

Martin, P. G. & Rogers, C., 1987. *Astrophys. J.*, **322**, 374.

Massa, D. & Savage, B. D., 1989. in *Interstellar Dust* Eds. Allamandola, L. J. & Tielens, A. G. G. M. (Cambridge: CUP)

Mathis, J. S., Rumpl, W. & Nordsieck, K. H., 1977. *Astrophys. J.*, **217**, 425

Mathis, J. S., 1988. *B. A. A. S.*, **20**, 732.

Mathis, J. S., 1986. in *Interrelationships Among Circumstellar, Interstellar and Interplanetary Dust* Eds. Nuth, J. & Stencel, R. (NASA CP2403)

Mathis, J. S., & Whiffen, G., 1989, *Astrophys. J.*, **341**, 808.

Mathis, J. S., Mezger, P. G. & Panagia, N., 1983. *Astr. Astrophys.*, **128**, 212.

Mauche, C. W., & Gorenstein, P., 1986. *Astrophys. J.*, **302**, 371.

McCabe, E. M., 1982. *Mon. Not. R. ast. Soc.*, **200**, 71.

Middlemass, D., 1990. *Mon. Not. R. ast. Soc.*, **244**, 294.

Mitchell, R. M. & Robinson, G., 1978. *Astrophys. J.*, **220**, 841.

Mitchell, R. M. & Robinson, G., 1980. *Mon. Not. R. ast. Soc.*, **190**, 669.

Morris, M., 1987. *Publ. Astr. Soc. Pac.*, **99**, 1115.

Nakada, Y., Deguchi, S. & Forster, J. S., 1988. *Astr. Astrophys.*, **193**, L13.

Nakada, Y., Izumiura, H., Onaka, T., Hashimoto, O., Ukita, N., Deguchi, S. & Tanabe, T., 1987. *Astrophys. J.*, **323**, L37.

Neugebauer, G. & Leighton, R. B., 1969. *Two Micron Sky Survey -a Preliminary Catalog* (NASA SP-3047 [Washington, D. C. Govt. Printing office])

Nuth, J. A., 1985. *Nature.*, **318**, 166

Nuth, J. A., Donn, B., & Nelson, R., 1986. *Astrophys. J.*, **310**, L83

Olofsson, H., Eriksson, K. & Gustafsson, B., 1987. *Astr. Astrophys.*, **183**, L13.

Onaka, T., de Jong, T. & Willems, F. J., 1989. *Astr. Astrophys.*, **218**, 169.

Orofino, V., Colangeli, L., Bussoletti, E. & Strafella, F., 1987. *Astrophys. Space Sci.*,**138**, 127.

Orofino, V., Colangeli, L., Bussoletti, E, Blanco, A. & Fonti, S., 1990. *Astr. Astrophys.*, **231**, 105.

Papoular, R. & Pègourie, B., 1983, *Astr. Astrophys.*, **128**, 335

Parenago, P. P., 1940. *Astron. zh.*, **17**, 3.

Parker, E. N., 1958. *Astrophys. J.*, **128**, 664.

Peckham, R. J., 1973. *Mon. Not. R. ast. Soc.*, **165**, 25.

Peery, B. F., 1975. *Astrophys. J.*, **199**, 135.

Pégourié, B., 1988. *Astr. Astrophys.*, **194**, 335.

Penman, J. M., 1976. *.PhD. Thesis, University of London*

Perry, C. H., Khanna, B. N. & Ruppracht, G. 1964. *Phys. Rev.*, **135**, A408.

Petrosian, V. & Dana, R. A., 1980. *Astrophys. J.*, **241**, 1094.

Phillip, H. R. & Taft, E. A., 1960. in *Proc. Conference on Silicon Carbide*, ed. O'Connor, J. Smiltens, Pergammon.

Reid, M. J. & Moran, J. M., 1981. *Ann. Rev. Astron. Astrophys.*, **19**, 231.

Ridgeway, S. T. & Keady, J. L., 1988. *Astrophys. J.*, **326**, 843.

Rieke, G. H., & Lebofsky, M. J., 1985. *Astrophys. J.*, **288**, 618.

Rogers, C. & Martin, P. G., 1984. *Astrophys. J.*, **284**, 327.

Rogers, C. & Martin, P. G., 1986. *Astrophys. J.*, **311**, 800.
Rogers, C., Martin, P.G. and Cantrell, D.R., 1973. Astrophys. J. 272, 175.
Rowan-Robinson, M., 1980. *Astrophys. J. Suppl.*, **44**, 403.

Rowan-Robinson, M., 1982. *Mon. Not. R. ast. Soc.*, **201**, 289.

Rowan-Robinson, M. & Harris, S., 1983a. *Mon. Not. R. ast. Soc.*, **202**, 767.

Rowan-Robinson, M. & Harris, S., 1983b. *Mon. Not. R. ast. Soc.*, **202**, 797.

Rowan–Robinson, M. Lock, T. D., Walker, D. W. & Harris, S., 1986. *Mon. Not. R. ast. Soc.*, **222**, 273.
Rybicki, G.B., 1971., J. Quant. Spectroc. and Rad. Transf., 11. 589.
Sahai, R., Claussen, M. J. & Masson, C. R., 1989. *Astr. Astrophys.*, **220**, 92.

Sahai, R., Wootten, A. & Clegg, R. E. S., 1984. *Astrophys. J.*, **284**, 184.

Sakata, A., Wada, S., Okutsu, Y., Shintani, H., & Nakada, Y., 1983. *Nature.*, **301**, 493

Sandford, R. F., 1944. *Publ. Astr. Soc. Pac.*, **56**, 122.

Sarazin, C. L., 1978. *Astrophys. J.*, **220**, 165.

Savage, B. D., & Mathis, J. S., 1979. *Ann. Rev. Astron. Astrophys.*, **17**, 73.

Scalo, J. & Slavsky, D., 1980. *Astrophys. J.*, **239**, L73.

Scargle, J. D., 1982., *Astrophys. J.*, **263**, 835.

Schönberg, K., 1989. *Astr. Astrophys.*, **208**, 219.

Schwarzchild, M., 1970. *Quart. Jou. Roy. Astr. Soc.*, **11**, 12.

Schönberner, D., 1983. *Astrophys. J.*, **272**, 708.

Schwab, F., 1980. *Proc. Soc. photo-opt. Instr. Engng.*, **231**, 18.

Seaton, M. J., 1979. *Mon. Not. R. ast. Soc.*, **187**, 73p

Seab, C. G., Snow, T. P. & Joseph, C. L., 1981. *Astrophys. J.*, **246**, 788.

Seab, C. G., & Snow, T. P., 1989. *Astrophys. J.*, **347**, 479.

Seeley, D. & Berendzen, R., 1972. *Journal for the History of Astronomy*, **3**, 52.

Seki, J. & Yamamoto, T., 1980. *Astrophys. Space Sci.*,**72**, 79.

Sharov, A. S., 1964. *Soviet Astronomy.*, **7**, 689.

Sharp, C. J., 1989. in *Evolution of Peculiar Red Giant Stars,* eds. Johnson, H. R. & Zuckerman, B. (Cambridge: CUP.)

Sitko, M. L., Savage, B. D. & Meade, M. R., 1981. *Astrophys. J.*, **246**, 161.

Skinner, C. J., Griffin, I & Whitmore, B., 1990. *Mon. Not. R. ast. Soc.*, **243**, 78.

Skinner, C. J., & Whitmore, B., 1987. *Mon. Not. R. ast. Soc.*, **224**, 335.

Skinner, C. J., & Whitmore, B., 1988a. *Mon. Not. R. ast. Soc.*, **235**, 603.

Skinner, C. J. & Whitmore, B., 1988b. *Mon. Not. R. ast. Soc.*, **234**, 79P.

Slipher, V. M., 1909. *Lowell Observatory Bulletin.*, **2**, 1.

Sopka, R. J., Hildebrand, R., Jaffe, D. T., Gatley, I, Roellig, T., Werner, M., Jura, M. & Zuckerman, B. 1985. *Astrophys. J.*, **294**, 242.

Snow, T. P., Buss, R. H., Gilra, D. P. & Swings, J. P., 1987. *Astrophys. J.*, **321**, 921.

Spergel, D. N., Giuliani, J. L. & Knapp, G. R., 1983. *Astrophys. J.*, **275**, 330.

Spitzer, W. G. & Kleinmann, D. A., 1961. *Phys. Rev.*, **121**, 1324.

Stephens, J. R., & Russell, R. W., 1979. *Astrophys. J.*, **228**, 780

Stephens, J. R., 1980. *Astrophys. J.*, **237**, 450.

Stephenson, C. B., 1973. *Publs. Warner & Swasey Obs.*, **1**, No. 4.

Stephenson, C. B., 1989. *Publs. Warner & Swasey Obs.*, **3**, No. 2.

Stecher, T. P., 1965. *Astrophys. J.*, **142**, 1683

Stecher, T. P., 1969. *Astrophys. J.*, **157**, L125

Steyer, T. R., Day, K. L., & Huffmann, D. R., 1974. *Appl. Optics.*, **13**, 1586.

Sutton, E. C., Betz, A. L., Storey, J. W. V. & Spears, D. L., 1979. *Astrophys. J.*, **230**, L105.

Tarafdar, S. P., 1988. *Astrophys. J.*, **331**, 932.

Taylor, M., 1981. *The Astronomer.*, **212**, 174.

Tayler, R. J., 1975. *The origin of the Chemical Elements* Publ. Wykeham

Thomasson, P., 1986. *Quart. Jou. Roy. Astr. Soc.*, **27**, 413.

Thronson, H. A., & Bally, 1986. *Astrophys. J.*, **300**, 749.

Tielens, A. G. G. & De Jong, T., 1979. *Astr. Astrophys.*, **75**, 326.

Treffers, R. R. & Cohen, M., 1974. *Astrophys. J.*, **188**, 545

Trumpler, R., 1930. *Lick Observatory Bulletin.*, **14**, 154.

Unno, W. & Kondo, M., 1976. *Publ. Astr. Soc. Japan.*, **28**, 347.

Utsumi, K., 1988. in *Atmospheric Diagnostics of Stellar Evolution: Chemical Peculiarity, Mass Loss and Explosion,* ed. Nomoto, K., (Berlin: Springer-Verlag.

Vardya, M. S., 1989. In: *The Evolution of Peculiar Red Giant Stars* p. 359. eds Johnson, H. R. & Zuckerman, B. Cambridge University Press. Cambridge.

van de Hulst, H. C., 1957. *Light Scattering by Small Particles*, Wiley

van de Hulst, H. C., 1946. *Recherches Astr. de l' Observatoire d' Utrecht.*, **11**, 1.

Verschur, G. L., 1989. *Interstellar Matters*, Springer-Verlag

Volk, K. & Kwok, S., 1988. *Astrophys. J.*, **331**, 435.

Wannier, P. G, Leighton, R. S., Knapp, G. R., Redman, R. O., Phillips, T. G. & Huggins, P. J., 1979. *Astrophys. J.*, **230**, 149.

Watanabe, T., 1981. *Publ. Astr. Soc. Japan.*, **33**, 679.

Weaver, H., Williams, D. R. W., Dieter, N. H. & Lum, W. T., 1965. *Nature.*, **208**, 29.

Whitmore, B., 1986. *PhD. Thesis, University of London.*

Whittet, D. C. B., 1984, *Mon. Not. R. ast. Soc.*, **210**, 479

Whittet, D. C. B., 1988, *Mon. Not. R. ast. Soc.*, **234**, 209.

Whittet, D. C. B., 1989, in *Interstellar Dust* Eds. Allamandola, L. J. & Tielens, A. G. G. M. (Dordrecht: Kluwer)

Whittet, D. C. B., Duley, W. W. & Martin, P. G., 1990. *Mon. Not. R. ast. Soc.*, **244**, 427.

Wickramasinghe, N. C., 1975. *Light Scattering Functions for Small Particles with Applications for Astronomy*, Adam Hilger

Wildt, R., 1933. *Z. Astrophys.*, **6**, 345.

Willems, F. J. & de Jong, T., 1986. *Astrophys. J.*, **309**, L39.

Willems, F. J. & de Jong, T., 1986. *Astr. Astrophys.*, **196**, 173.

Willner, S. P., Jones, B. Puetter, R. C., Russell, R. W. & Soifer, B. T., 1979. *Astrophys. J.*, **234**, 496.

Wilson, W. J. & Barrett, A. H., 1968. *Science.*, **161**, 778.

Wilson, W. J., Barrett, A. H. & Moran, J. M., 1970. *Astrophys. J.*, **160**, 545.

Willson, L. A., 1981. in *Physical Processes in Red Giants,* Eds. Iben, I. & Renzini, A. (Dordrecht: Reidel)

Willson, L. A., 1981., in *Physical Processes in Red Giants* Eds. Iben, I. & Renzini, A. (Dordrecht: Reidel)

Willson, L. A. & Bowen, G. H., 1986. *Irish Astronomical Journal.*, **17**, 249

Wing, R. F., 1972. *Mem. Soc. R. Sci. Liège, 6th Ser,* **III**, 123.

Witt, A. N., Schild, R. E., & Kraiman, J. B., 1984. *Astrophys. J.*, **281**, 708.

Witt, A. N., & Schild, R. E., 1985. *Astrophys. J.*, **294**, 225.

Witt, A. N., & Schild, R. E., 1986. *Astrophys. J. Suppl.*, **62**, 839.

Witt, A. N., 1988. in *Dust in the Universe* Eds. Bailey, M. E. & Williams, D. A. (Cambridge: CUP)

Wisniewski, W. Z., Wing, R. F., Spinrad, H., & Johnson, H. L., 1967. *Astrophys. J.*, **148**, L29.

Witteborn, F. C., Strecker, D. W., Erikson, E. F., Smith, S. M., Goebel, J. H. & Taylor, B. J., 1980. *Astrophys. J.*, **238**, 577.

Wolf, N. J. & Mey, E. P., 1969. *Astrophys. J.*, **155**, L181.

Wood, P. R., 1979. *Astrophys. J.*, **227**, 220.

Zuckerman, B. & Dyck, H. M., 1986. *Astrophys. J.*, **304** 394.

Publications

'Observations & Models for Red Giants with Unusual Dust Shells'

Griffin, I. P., Skinner, C. J. & Whitmore, B., 1989. *The Evolution of Peculiar Red Giant Stars*, eds. Johnson, H. & Zuckerman, B. (Cambridge: CUP)

'Unidentified *IRAS* Sources –I. Two New Extreme Carbon Stars'

Skinner, C. J. & Griffin, I. P., 1989. *Mon. Not. R. ast. Soc.*, **240**, 189.

'Red giants with unusual dust shells –I. The database'

Skinner, C. J., Griffin, I. & Whitmore, B. 1990. *Mon. Not. R. ast. Soc.*, **243**, 78.

'Red giants with unusual dust shells'

Skinner, C. J., Griffin, I. P. & Cohen, R. J., 1990. in *From miras to planetary nebulae: Which Path for stellar evolution?* Eds. Mennessier, M. O. & Omont, A. (Paris: Editions Frontiers)

'A model for the infrared and radio spectral energy distribution of IRC+10°216'

Griffin, I. P., 1990. *Mon. Not. R. ast. Soc.*, **247**, 591.

'Four Important Red Giant Stars'

Griffin, I. P., 1989. *Brit. Astron. Assoc. Var. Star. Circ.*, **68**, 7.

'Occultation of 27 Sagittarii by Titan'

Appleby, G., Brierley, D., Debehogne, H., Dekersgieter, A. Geyer, E. H., Hoffmann, M., Griffin, I., Smalley, B., Smith, K. C., Wonnacott, D., Hurst, G. M., Hurst, M. & Schlyter, P., 1989. *IAU Circular 4801.*